THE ROLE OF COFILIN IN GLIOBLASTOMA CELL BEHAVIOUR

BY CELESTIAL THERESE SUEN MEI YAP

Thesis submitted for the degree of Doctor of Philosophy at the University of Edinburgh

2002

The Cosmos extends, for all practical purposes, forever. After a brief sedentary hiatus, we are resuming our ancient nomadic way of life. Our remote descendents, safely arrayed on many worlds through the Solar System and beyond, will be unified by their common heritage, by their regard for their home planet, and by the knowledge that, whatever life may be, the only humans in all the Universe come from Earth.

They will gaze up and strain to find the pale blue dot in their skies. They will love it no less for its obscurity and fragility. They will marvel at how vulnerable the repository of all our potential once was, how perilous our infancy, how humble our beginnings, how many rivers we had to cross before we found our way.

Carl Sagan, Pale Blue Dot, 1994.

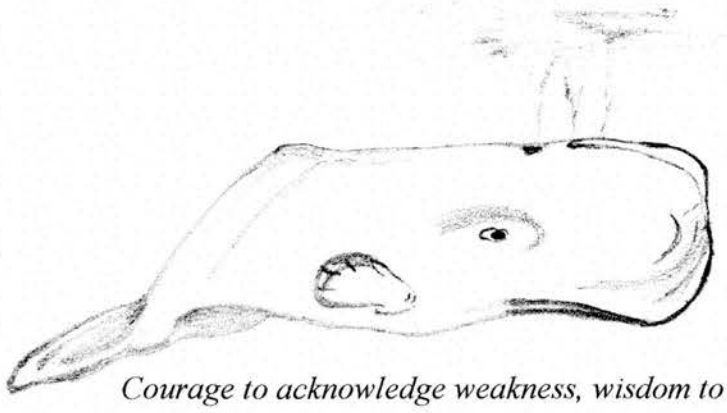

Courage to acknowledge weakness, wisdom to learn from ignorance and love to tread the ravines of the unexplored.

DISCLAIMER

I, Celestial Therese Suen Mei Yap, performed all the experiments presented in this thesis unless otherwise indicated in the text. No part of this work has been, or is being submitted for any other degree of qualification.

Signature:

Date: 5 DECEMBER 2002

ABSTRACT

The actin cytoskeleton is intimately involved in the mechanisms required for cell motility, being able to reorganise into dynamic structures such as cellular protrusions (lamellipodia) at the front edge of crawling cells. Several intracellular proteins associate with the actin cytoskeleton to change its structure, and this is necessary for a cell to respond to motility-inducing signals such as growth factors. Small actin-binding proteins, which include cofilin, actin-depolymerizing factor (ADF) and profilin, are known to synergise in accelerating actin turnover in moving cells.

Dysregulation of cell motility plays a pivotal role in conferring invasive behaviour in tumour cells. It is now evident that tumour progression is often associated with abnormal expression of genes that regulate cytoskeletal assembly, as well as genes involved in cytoskeletal turnover. My project focuses on exploring the role of cofilin in glioblastoma tumours of the brain, which frequently infiltrate into adjacent normal tissue. The hypothesis is that altered levels of cofilin expression in glioblastoma cells affect their motility, which may have a significant impact on invasiveness. Cofilin is ubiquitously expressed in eukaryotes and appears to be crucial to the formation of lamellipodia in a variety of motile cells, including metastatic tumour cells. It is likely that the motility observed in tumour cells might arise from disruptions in the activities of cofilin and other proteins that modify actin dynamics.

In vitro studies were performed on the human glioblastoma cell line U373 MG, originally derived from a patient. Reverse transcription-polymerase chain reaction (RT-PCR) showed that the actin-binding proteins cofilin, ADF and profilin are

expressed by these cells. Using immunochemistry, the distribution of cofilin was investigated in cells cultured under standard conditions and after serum stimulation. To test whether altered levels of cofilin expression in glioblastoma cells affects cell motility, cofilin was overexpressed in the glioblastoma cell line and changes in the motility of transfected cells were analysed and compared to untransfected cells. Overexpression was achieved by transient and stable transfections with a plasmid vector, pCofilin-IRES2-EGFP, which was constructed by subcloning the coding sequence of human cofilin into pIRES2-EGFP. Transfected cells were identified by the expression of EGFP (enhanced green fluorescent protein) in timelapse experiments using confocal microscopy. In order to quantify the relative levels of cofilin overexpression in stable transfectants, cells were immunostained for cofilin using fluorescent detection and analysed by flow cytometry. Western blots confirmed the specificity of the anti-cofilin primary antibody used. The timelapse analyses indicated that overexpression of cofilin increases the motility of glioblastoma cells.

The project was extended to investigate whether variable levels of cofilin overexpression might affect cell motility to different extents. An inducible gene expression system based on the Tet-Off system (Clontech laboratories Inc.) was developed in order to control the level of cofilin overexpression. The coding sequence for cofilin-IRES2-EGFP was subcloned into pTRE, so that cells with inducible expression of cofilin could be identified by green fluorescence. Stable cell lines potentially responsive to the effects of tetracycline or doxycycline antibiotics were cultured and flow sorted to select green fluorescent cells. This system would enable the correlation between cofilin expression and motility to be examined over a wide range of overexpression.

Abbreviations

ADF	Actin depolymerizing factor
ADP	Adenosine diphosphate
Arp 2/3	Actin-related proteins 2/3
ATP	Adenosine triphosphate
DAG	Diacylglycerol
DEPC	Diethylpyrocarbonate
DIG	Digoxigenin
DMSO	Dimethyl sulfoxide
DTT	Dithiothrietol
EGF	Epidermal growth factor
EGFP	Enhanced green fluorescent protein
EGFR	Epidermal growth factor receptor
FACS	Flourescence activated cell sorter
FGF	Fibroblast growth factor
GDP	Guanosine diphosphate
GTP	Guanosine triphosphate
IRES	Internal ribosome entry site
MARCKS	Myristoylated alanine rich C-kinase substrate
MLCK	Myosin light chain kinase
MTOC	Microtubule-organising centre
Pak1	p21-activated kinase 1
PCR	Polymerase chain reaction
PDGF	Platelet-derived growth factor

Pi	Inorganic phosphate
PIP_2	Phosphatidylinositol 4,5-biphosphate
ROCK	Rho-activated kinase
SCAR	Suppressor of cAMP receptor mutation
SDS	Sodium dodecyl sulphate
TESK	Testicular protein kinase
TESPA	Amino-propyltriethoxysilane
TRE	Tetracycline-responsive element
WASP	Wiskott-Aldrich syndrome protein

ACKNOWLEDGEMENTS

My supervisors Dr. David J. Price and Dr. Sutherland K. Maciver patiently and diligently guided me throughout the endeavour. Their professional advice, unremitting support and cheerful spirit have been indispensable to the completion of my PhD studies.

Dr. Paul McLaughlin, the chairperson of my thesis committee, has benefited me with his thoughtful and sensible counsel.

Dr. Thomas Pratt and Dr. Ian Simpson have played instrumental roles in teaching me laboratory techniques and many other necessary skills. Their generosity has contributed tremendously to making my PhD studies a most gratifying experience.

Ms. Linda Sharp (Biomedical Sciences) has provided invaluable expertise in confocal imaging and fluorescent microscopy. She has also been a wellspring of practical information on the techniques of microscopy and image analysis, which she never fails to offer wholeheartedly.

Ms. Shonna MacCall (Rayne laboratory) has introduced me to techniques in flow cytometry and given excellent suggestions which helped formulate my protocols for flow cytometric immunodetection.

Ms. Diane Ternent guided me in several biochemical techniques including the purification of cofilin, and has been a most willing and able teacher.

Thanks also to Dr. William Sellers (Bioinformatics) who developed the movement analysis program, MacGap Debug; Dr. David McLaughlin who imparted his knowledge in many techniques including *in situ* hybridization; Ms. Katy Gillies who provided reliable protocols and logistical support so that experiments could be performed with peace of mind; Dr. Peter Kind and Dr. John Mason for sharing their expertise; Dr. Paulette Zaki for an especially constructive role during the writing of the thesis; Ms. Vivian Allison and Ms. Grace Grant for their aid in tissue culture. I am grateful to all the members of the laboratory who have had a positive impact on my experience: Jonathan Butt, Benjamin Fenby, Jane Quinn, Martine Manuel, Catherine Naughton, Jennifer Pinson, David Tyas and Tania Vitalis. I also thank my family who lovingly endured the distance. Finally, my husband Yaw Chong Goh who has given me much encouragement, and occasionally a piece of scientific gem.

The studies have been realised with the Overseas Graduate Scholarship awarded by the National University of Singapore.

CONTENTS

CHAPTER 1

INTRODUCTION

I.I An introduction to the cytoskeleton

The cytoskeleton is a lattice of fibres within the cytoplasm of a cell that performs structural roles in maintaining cell morphology, and forming tracks along which organelles traffic. Dynamic rearrangements of this lattice is responsible for changes in cell morphology that accompany several cellular processes such as differentiation, cell division, movement, and phagocytosis. The cytoskeleton is composed of a network of three main types of fibres: microfilaments (7-9nm diameter), microtubules (25nm diameter) and intermediate filaments (10nm diameter). These fibres are essentially protein polymers, with microfilaments comprising polymers of actin subunits, and microtubules of tubulin subunits. Intermediate filaments are built from a variety of subunits in different cell types. Cytoskeletal filaments are also crosslinked into an interlacing network, and attach to the cell membrane. Linkage to the cell membrane provides support to maintain cell shape, and tissue integrity by stabilising intercellular and cell-matrix adhesions.

The actin cytoskeleton

Actin is often the most abundant protein in eukaryotic cells, comprising as much as 20% of total protein in muscle cells, and up to 15% in nonmuscle cells (reviewed by Lodish *et al.*, 1995; Maciver, 1995; Sheterline and Sparrow, 1994). Actin is a

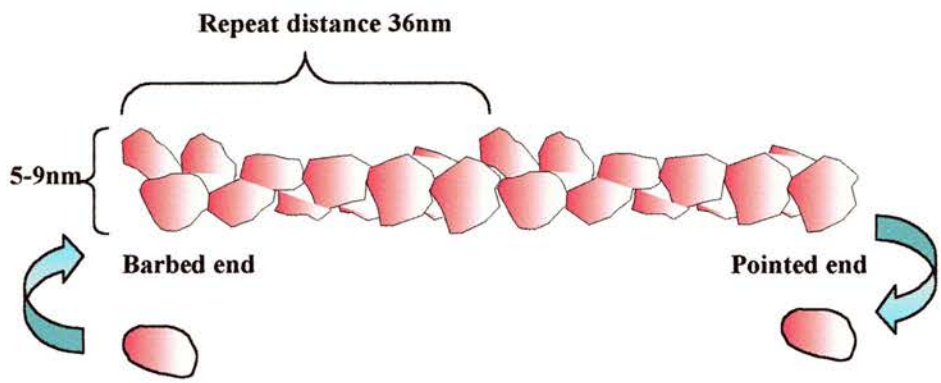

Fig. 1.1 The actin microfilament has a barbed (fast-growing) end and a pointed (slow-growing) end.

Actin monomers add to the barbed ends (polymerization), and leave at the pointed ends (depolymerization). Polymerization is accompanied by ATP hydrolysis. The microfilament is a single-stranded helix, with repeats spanning 36nm.

(modified from Maciver S. K., http://www.bms.ed.ac.uk/research/others/smaciver/lectures/Csl.htm)

moderate-sized protein with a molecular weight of 43kDa. Actin was first described in 1942 by Straub (Straub, 1942), and non-muscle actin was first isolated from the plasmodium of the myxomycete, *Physarum polycephalum* (Hatano and Oosawa, 1966). The amino acid sequence of actin is highly conserved in evolution (Sheterline and Sparrow, 1994). In vertebrates, three main groups of actin isoforms have been identified. α-actins are found in muscle and are part of the contractile apparatus. β- and γ-actins are present in most non-muscle cells.

The actin monomer is also called globular actin, or G-actin. It has four domains designated 1-to-4, with a central cleft that binds a nucleotide (ATP or ADP), and a divalent cation (Mg^{2+}) through ionic and hydrogen bonding (reviewed by Sheterline and Sparrow, 1994). This cleft possesses ATPase activity. Microfilaments are formed when actin monomers polymerize, and this is associated with ATP hydrolysis (Cooke, 1975). Microfilaments are polarised into a 'barbed' fast-growing end, and a 'pointed' slow-growing end (Figure 1.1), that can be visualised with an electron microscope especially if filaments are 'decorated' with the fragments that include the heads of myosin II (Wakabayashi *et al.*, 1975). Coating all the actin subunits with myosin heads results in the appearance of arrowheads that point opposite to the 'barbed' end, and towards the 'pointed' end. The microfilament is a single-stranded helix twisted in an angle that forms a repeat pattern across every 13 subunits, with each repeat spanning 38 nm. Within the microfilament, each actin subunit is in contact with four other subunits. The reorganisation of actin microfilaments necessary for cell movement and changes in morphology is achieved through polymerisation, breaking into shorter segments and depolymerisation. It is now known that this cycling of actin filaments is facilitated by several actin-binding proteins, such as actin-depolymerizing factor

(ADF)/cofilin and profilin. In addition, a pool of actin monomers exists in the cytoplasm, complexed with monomer-binding proteins, principally β-thymosin (Borisy and Svitkina, 2000).

Intracellular organisation of actin microfilaments

The cortex of the cell, which lies just below the cell membrane, often contains high concentrations of actin filaments. The cortical actin cytoskeleton is tethered to the cell membrane via linkages to transmembrane proteins, such as integrins, cadherins (Hynes, 1992; Takeichi, 1991) and a host of actin-binding proteins associated with the membrane such as the ERM (ezrin/radixin/moesin) family of proteins (Bretscher, 1999), annexins (Isenberg, 1991) and MARCKS (myristoylated alanine rich C-kinase substrate) (Hartwig *et al.*, 1992). Integral membrane proteins form part of adhesion complexes that anchor the cell to the extracellular matrix and to other cells. The supporting cytoskeleton thus serves to buttress the anchoring sites on the cell membrane, stabilising cell shape and matrix adhesion. Cortical actin filaments may be organised into bundles and networks by bundling and cross-linking proteins (reviewed by Maciver, 1995; 1996). Actin filaments are bundled together in parallel arrays by proteins such as fimbrin and α-actinin. Criss-crossing networks of actin are also formed by proteins that interlock the filaments. These cross-linking proteins possess binding sites for adjacent filaments, and include filamin, spectrin and dystrophin. In motile cells, the cortical actin cytoskeleton undergoes continuous rearrangements. At the front edge, the actin filaments are oriented radially and assemble to form protruding sheets (lamellipodia) or fingers (filopodia). At the trailing edge, filaments are rapidly disassembled as the membrane is pulled in towards the cell body. In contrast, the actin cytoskeleton around the nucleus is often thickly bundled and dense,

presenting as a highly ordered structure known as the cellular geodom. Cellular projections such as microvilli also contain a high density of polar actin filaments, with barbed ends abutting the plasma membrane.

Stress fibres are axial bundles of actin and myosin II (non-muscle myosin) filaments which can be observed to run along the ventral surface of a cell. These fibres are held under tension by attachments to focal adhesions at both ends. At focal adhesions, the cell binds to the matrix by the interaction of transmembranous integrins with fibronectin in the matrix (Hynes, 1992). The actin filaments are linked to the intracellular domains of integrins via adapter proteins such as talin (Horwitz *et al.*, 1986), vinculin (Ezzell *et al.*, 1997) and α-actinin (Otey *et al.*, 1990). Filaments may also bind integrins directly (Kieffer *et al.*, 1995). The presence of myosin II confers contractility to the stress fibres, which enables the cell to contract (Isenberg *et al.*, 1976). This appears to be important in processes such as wound contraction and healing by fibroblasts (Maciver, 1996).

A polarised pattern of contractile actin-myosin bundles is found in epithelial cells associated together in sheets. At the apical surface of the epithelial sheet, each cell has a circumferential belt of actin-myosin bundles linking its intercellular adhesions. Organised contraction at this apical surface is responsible for the closure of wounds in the embryonic epithelium, and the apical surface of each cell is tightened like a 'purse string' (Martin and Lewis, 1992). This mechanism operates in embryonic development, such as in the closure of the dorsal epidermis in *Drosophila melanogaster* (Young *et al.*, 1993).

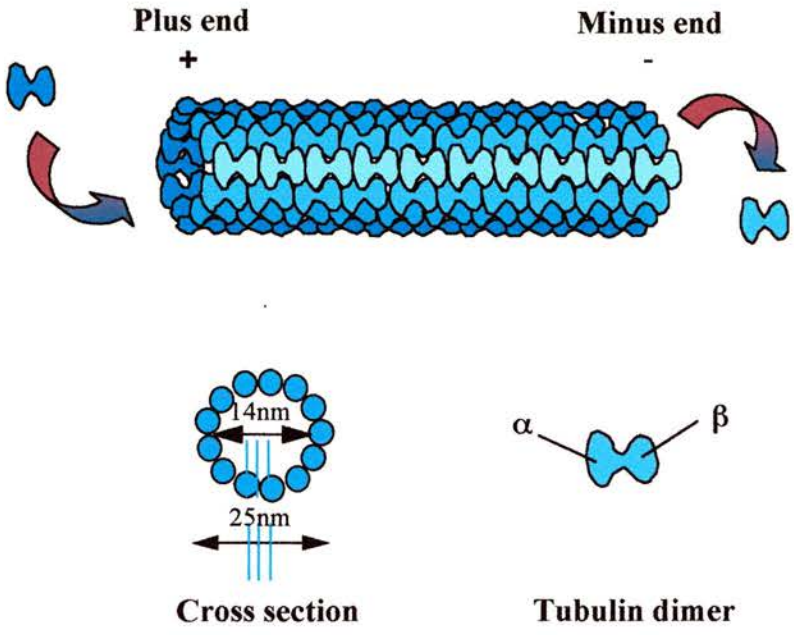

Fig. 1.2 The microtubule is polarised into a plus (fast-growing) end and a minus (slow-growing) end.

The microtubule subunit is a tubulin dimer composed of α-tubulin and β-tubulin. Dimers add to the plus end, and are lost from the minus end. In cross section, the microtubule measures 25nm in external diameter, and 14nm in internal diameter.

(modified from Maciver S. K., http://www.bms.ed.ac.uk/research/others/smaciver/lectures/Csl.htm)

The tubulin cytoskeleton

The microtubular cytoskeleton plays a major role in the transport of vesicles and organelles, formation of cellular structures such as flagella, cilia, neuronal axons and dendrites, and in mitosis forming the spindle that separates chromosomes (Downing and Nogales, 1998). It is assembled from microtubules, which are polymers of α- and β-tubulin (Figure 1.2). The subunit is therefore a heterodimer composed of a 55kDa α-tubulin molecule and a 55kDa β-tubulin molecule. A typical microtubule measures 25nm in external diameter, with a hollow core of 14nm diameter. Generally, the circumference of the microtubule is built from 13 tubulin molecules. Microtubules are also polarised, with α-tubulin exposed at the fast-growing 'plus' end, and β-tubulin at the slow-growing 'minus' end (Margolis and Wilson, 1978). Tubulins are highly conserved proteins, present in eukaryotes from yeasts and fungi, to insects, birds and mammals. Isoforms of both α- and β-tubulins exist, which can undergo post-translational modifications such as acetylation (reviewed by Luduena, 1998).

Intracellular organisation of microtubules

A unique feature of microtubule organisation is the presence of a microtubule-organising centre (MTOC) within the cytoplasm, which controls microtubule assembly (Joshi, 1998). Electron microscopy reveals this centre as a darkly staining point close to the nucleus, from which microtubules radiate to the periphery to occupy the entire cytoplasm. The MTOC nucleates microtubule polymerisation, so that it contains the 'minus' ends of microtubules, whilst 'plus' ends polymerize away from it. In the dividing cell, the MTOC duplicates and migrates to opposite poles to organise the assembly of microtubules into the mitotic spindle. Microtubules in some cellular

structures do not appear to be organised from a discernable centre. The dendrites of neurons provide such an example, containing microtubules in a mixture of orientations, with 'plus' or 'minus' ends towards the cell body. Microtubules in axons are orientated with 'plus' ends distal to the cell body, many of which do not emerge from an MTOC.

In highly motile cells such as leukocytes and macrophages, microtubules are important in determining the polarity of movement, as microtubule disruption causes them to move randomly despite a chemotactic gradient (Mareel and De Mets, 1984). However not all cells require microtubules for movement and directionality. In fish keratinocytes, fragments of the leading lamellae can move directionally without microtubules (Euteneuer and Schliwa, 1984). The amoeba *Naegleria gruberi* lacks microtubules but is capable of rapid locomotion (Walsh, 1984). Peripheral microtubules grow towards the advancing lamellipodia, where they associate transiently with newly formed focal adhesions, or form stable connections with larger, more mature adhesions (Kaverina *et al.*, 1998), or target the disassembly of the adhesion sites (Kaverina *et al.*, 1999). These adhesion sites are capable of acting like the MTOC to nucleate microtubule assembly at the cell periphery. The function of microtubules at focal adhesions is not clearly understood. It is postulated that microtubules might guide signalling molecules to influence the stability and lifetime of contacts with the matrix, which then determines directionality in movement (Kaverina *et al.*, 1998).

The intermediate filament cytoskeleton

Intermediate filaments (IF) are found in most eukaryotic cells, and perform mainly structural roles, providing mechanical support in cells and physical integrity in tissues (Coulombe *et al.*, 2001). They form stable structures such as hair, nail and the outermost layer of skin. A biochemical characteristic is their extreme stability, remaining polymerized in the presence of strong detergents and high ionic concentrations which solubilise actin filaments and microtubules. Different cell types express distinct intermediate filament proteins, and more than forty IF proteins have been identified in mammals. All have a similar structure, consisting of a central helix with more variable amino- and carboxy-terminal domains. Based on similarities in amino acid sequence, the IF proteins are divided into five major classes:

Class	Type	Predominant tissue location
I	Acidic keratins	Epithelia
II	Basic keratins	Epithelia
III	Desmin	Muscle
	Glial fibrillary acidic protein	Glia
	Peripherin	Peripheral neurones
	Vimentin	Mesenchyme
IV	Neurofilaments	Neurons
V	Lamins	Nuclear envelope

Intracellular organisation of intermediate filaments

Intermediate filaments form networks that fill the cytoplasm and stable cellular protrusions such as neuronal axons. However, unlike microfilaments and microtubules, they are excluded from actively protruding sites such as the lamellipodia of moving cells, and are not thought to generate forces necessary for locomotion (Maciver, 1996). In epithelial cells, keratin intermediate filaments link to the cell membrane at sites of matrix and intercellular adhesions, giving structural support to the epithelium. Organelles such as the nucleus may also derive support by being caged within intermediate filament networks. The nucleus itself is kept intact by intermediate filaments that are a component of the nuclear envelope (Wilson *et al.*, 2001). The lipid bilayer of the inner membrane of the envelope associates with a lamin filament mesh, and depolymerisation of this lamin mesh causes breakdown of the nuclear envelope during mitosis.

Motor systems associated with the cytoskeleton

Microfilaments and microtubules can be found in association with motor proteins that can transduce biochemical energy derived from nucleotide hydrolysis to mechanical movement. The motor system of microfilaments is based on myosin, and that of microtubules is based on kinesin and dynein. The coupling of motor proteins to microfilaments and microtubules generates power to transport 'cargo' along cytoskeletal networks. The interaction of myosin with actin filaments is necessary for contraction of muscles and cells.

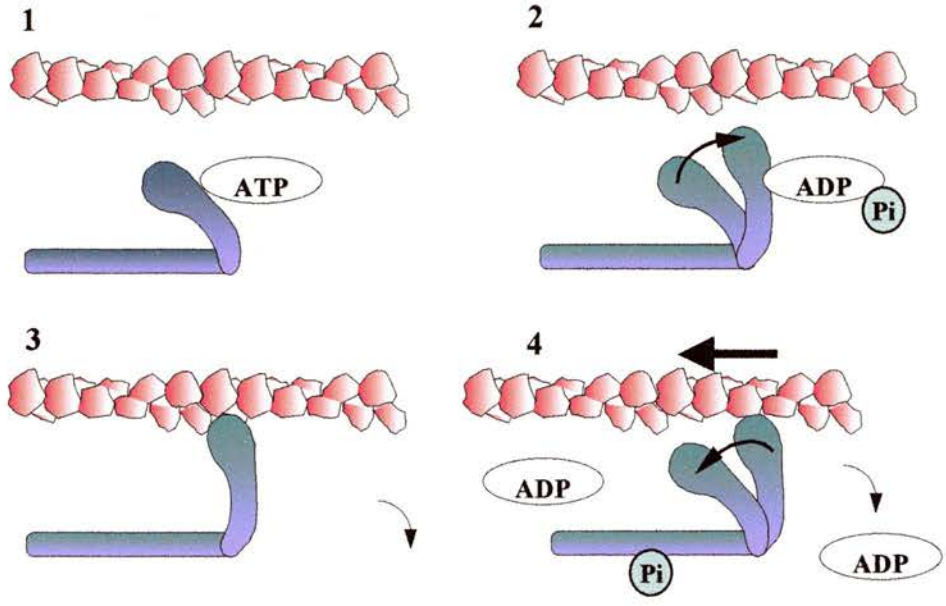

Fig. 1.3 Force generation by interactions between myosin and actin.

1.ATP binds the myosin head and induces a conformation which is unable to bind actin.

2.As ATP hydrolyses, the myosin head springs into position, ready to bind actin. Myosin is bound to both ADP and Pi at this point.

3.The release of Pi allows myosin to bind strongly to actin.

4.Force is generated as the myosin head binds actin, and this 'power stroke' causes the actin filament to slide on myosin. ADP is released. In the absence of ATP, myosin remains tightly bound to actin in a state of 'rigor'.

(modified from Maciver S. K.,
http://www.bms.ed.ac.uk/research/others/smaciver/Myosin%20II.htm)

Myosins and the actin cytoskeleton

Myosins belong to a family of motor proteins which produce movement in actin filaments, of which myosins I, II and V are best known (Berg *et al.*, 2001). Myosin II, first identified in muscle cells, is now known to be present also in non-muscle cells, and is implicated in muscle and cell contraction, and cytokinesis (Maciver, 1996). Myosin I and V bind actin filaments to the plasma membrane and membranes of organelles respectively, and function to move these structures. Myosins may exist as monomers, such as myosin I, or heterodimers which are formed by assembling heavy and light polypeptide chains. Monomers and heterodimers can polymerize to form filaments. Each myosin molecule is further organised into head and tail regions. In many myosins, the head binds actin and has ATPase activity, whilst the tail associates with others into a filament. However, The tail region of myosin I does not participate in filament assembly but has binding sites for actin and phospholipid membranes (Becker, 1996).

The basic motor effect of myosins is to cause movement of an actin filament over the attached myosin heads, and this is powered by ATP hydrolysis (Figure 1.3) (Sheterline, 1983). This sliding filament theory was first proposed by Huxley and Hanson (1954). The head of each myosin molecule initially binds the actin filament loosely. Its ATPase activity then allows it to achieve a tighter bond, leading to a conformational change that causes it to pull on the actin filament. The coordinated pull by several myosin heads along the length of the actin filament causes actin to slide on the myosin filament. Finally, myosin dissociates from actin in the presence of ATP, ready to initiate another cycle. Since actin filaments are anchored to the cell

membrane, and to the ends of each contractile subunit (sarcomere) in skeletal muscle, successive cycles of pulling results in contraction of the cell or sarcomere.

The activation pathway of actin-myosin contraction in skeletal muscles is distinct from that in smooth muscles and non-muscle cells, although both are calcium-dependent (Becker, 1996; Ganong, 1999). In skeletal muscles, influx of calcium into cells removes the inhibition on actin-myosin interaction, by exposing binding sites on actin previously concealed by a complex of proteins (tropomyosin and troponin). In smooth muscles and non-muscle cells, a rise in intracellular calcium activates myosin light chain kinase (MLCK) via binding of calcium to calmodulin, a small cytosolic protein. A regulatory myosin light chain is phosphorylated by MLCK, triggering actin-myosin interaction.

The roles of myosin II in non-muscle cells offer a fascinating insight into the variety of processes utilising this contractile mechanism (Maciver, 1996). Myosin II is implicated in cytokinesis, where it is essential in the formation of the contractile cleavage, and causes cells to 'round up' prior to this event. It does not appear to be crucial in locomotion, as its absence in *Dictyostelium* does not impede motility (De Lozanne and Spudich, 1987). However, there are suggestions that myosin II might aid locomotion by causing contraction at the rear of the cell, hence removing excess matrix adhesions there (Sinard and Pollard, 1989). Myosin II also appears to facilitate secretion, perhaps by contracting around vesicles and causing their contents to be expelled under high pressure. Inhibiting myosin II activity by functional antibodies hinders secretion (Neco *et al.*, 2002). As mentioned earlier (see the Actin

Cytoskeleton), epithelial wounds have been observed to heal by contraction of cells along the margins, closing the gaps between cells (Martin and Lewis, 1992).

Kinesins, dynein and the microtubular cytoskeleton

Microtubular transport is recognised as 'long range' trafficking of vesicles and organelles, travelling in a bidirectional manner towards the 'plus' and 'minus' ends (Goode *et al.*, 2000). Motor proteins bind these membrane-bound intracellular entities, 'walk' them along the microtubules, and are responsible in determining which direction they head. 'Conventional' kinesins are directed towards the 'plus' ends of microtubules, and dynein towards the 'minus' end, although some kinesins more recently identified hold exceptions to this generalisation, such as the 'minus' end-directed kinesin Ncd in *Drosophila* (Sablin *et al.*, 1998).

Interactions between the microfilament, microtubule and intermediate filament cytoskeletons

Although the three cytoskeleton systems appear to occupy distinct locations in cells, co-localisations are observed in certain structures. Neuronal axons contain microfilaments, microtubules and neurofilaments. Focal contacts with the matrix appear to be convergence points for microfilaments, microtubules and intermediate filaments. The cytoskeleton coordinates several functions, facilitated by proteins that connect the networks (Fuchs and Yang, 1999; Goode *et al.*, 2000; Waterman-Storer and Salmon, 1999). Many of the proteins that were initially thought to bind microtubules, called microtubule-associated proteins (MAPs), have been found also to bind actin microfilaments.

Cooperation between microtubules and microfilaments has been established to occur during vesicle trafficking in neurons and melanocytes. Vesicles are transported along central microtubular 'highways' and utilise microfilament routes at the cell cortex. In neurons, secretory vesicles move along microtubules in axons, then 'hop' onto microfilaments on reaching the growth cones (Kuznetsov *et al.*, 1992). Distal parts of axons are enriched in MAP1B, which is thought to bridge the intersections between the two cytoskeletal highways. Melanophores are specialised pigmented cells in the skin of fish, amphibians and mammals. The pigment granules in these cells aggregate centrally by latching onto microtubules. Cues leading to darkening of colours in fish and frogs cause pigments granules to move to the periphery along microtubules, then disperse throughout the cytoplasm by actin-myosin transport (Allan and Schroer, 1999; Rodionov *et al.*, 1998). Mammalian melanocytes utilise a similar system to transfer the pigment granules from microtubule tracks to the actin cytoskeleton at their tips. It is not known how vesicles pass from one track to the other, but it probably involves coordinated activation of motor systems driving transport by microtubules and microfilaments. Indeed, there is evidence that the microtubule-based kinesin motor potentially interacts with the actin-based myosin motor, via molecular binding between a class V myosin (MyoVA) and the ubiquitous kinesin heavy chain (KhcU) (Huang *et al.*, 1999).

I.II The actin cytoskeleton in cell motility

Cell motility involves the mechanistic steps of membrane extension, formation of new adhesions, cell body contraction, and rear detachment. The actin cytoskeleton is central to all these mechanisms required for locomotion. In order to move on a substrate, a cell forms protrusions (lamellipodia) at the leading edge, stabilised by focal points of adhesions. The cell body contracts via actin-myosin interactions, adhesions to the substrate are released at the rear, and the whole cell thus translocates forward.

The lamellipodium is essential for motility

A thin layer of cytoplasm at the front edge of migrating cells was first proposed to be the primary 'organelle' for movement by M. Abercrombie (Abercrombie, 1980). This region, about 0.2μm thick, is labelled the 'leading lamella', the 'leading edge', or the 'lamellipodium', where it protrudes parallel to the substrate. Where the edge curls upwards, it is referred to as 'ruffles'. The structure of the lamellipodium has been revealed to consist of actin microfilaments in largely polarised arrays, in a constant flux of reorganisation as cells crawl (Small *et al.*, 2002). This is a major site of microfilament activity, where the molecular bustle includes incorporation of actin monomers into filaments (polymerization), breakdown of filaments (depolymerization), and crosslinkage of the actin network. Here, the actin cytoskeleton is coupled to cell surface receptors that enable cells to regulate activity in response to external cues, such as chemoattractants.

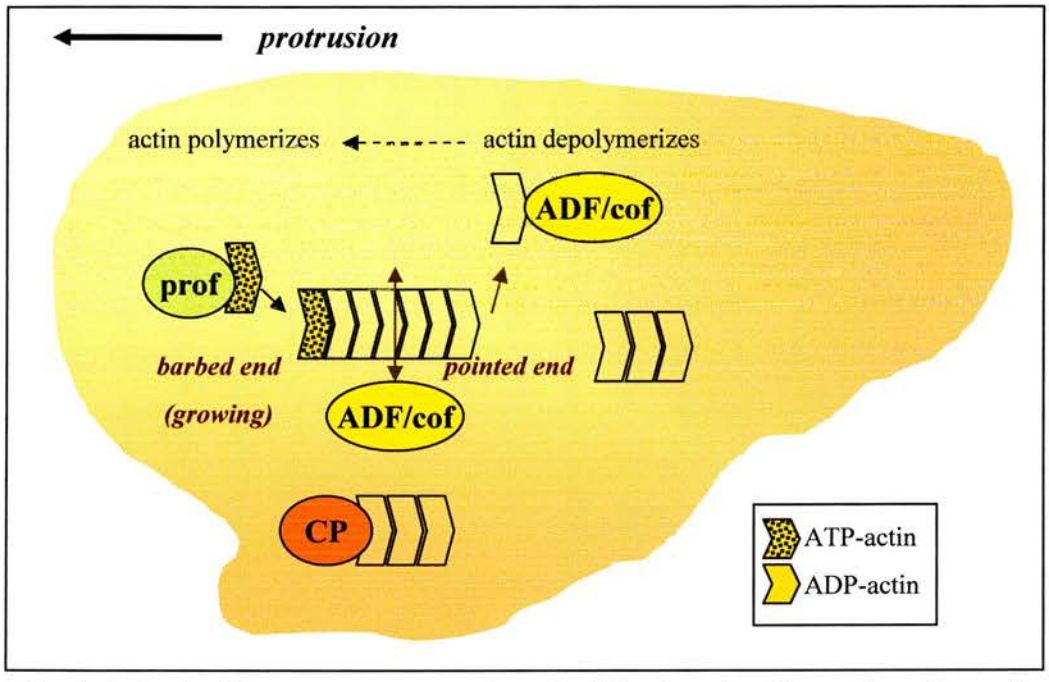

Fig. 1.4 Actin filament turnover (treadmilling) at leading edge of motile cells.

Actin filaments at the leading edge undergo continuous polymerization by incorporation of ATP-bound G-actin at the barbed ends, enhanced by profilin.Towards the pointed ends at the interior of the cell, ATP hydrolyses to ADP and actin becomes associated with ADP. Depolymerization and severing of filaments occurs, catalysed by ADF/cofilin. Subunits are recycled for a new round of polymerization by nucleotide exchange of ADP for ATP, catalysed by profilin. Capping protein blocks polymerization at the barbed ends of filaments outwith the leading edge.

ADF/cof: Actin depolymerizing factor / cofilin; prof: profilin; CP: capping protein.

The forces generated within the lamellipodium drive protrusive activity, and is dependent on actin polymerization. In order for cells to move, actin polymerization has to be localised to the leading edge. Proteins involved in polymerization and depolymerization of actin, as well as the regulation of these activities, have been found to be concentrated here. These include the actin monomer-binding proteins of the ADF (actin depolymerizing factor)/cofilin family and profilin; actin filament-associated proteins such as the Arp 2/3 complex (actin-related proteins 2 and 3), gelsolin and capping protein; and proteins participating in signalling events to the actin cytoskeleton, such as proteins of the Ena/VASP family and WASP (Wiskott-Aldrich syndrome protein).

Actin filaments generate forces to push the lamellipodium

The turnover of actin filaments at the leading edge of moving cells generates forces that push the membrane forward, by a process known as treadmilling (Borisy and Svitkina, 2000). The barbed ends of actin filaments abutting the plasma membrane grow by addition of ATP-bound actin monomers (polymerization), accompanied by ATP hydrolysis. Actin subunits are lost from the pointed ends enriched in ADP-bound actin, orientated towards the interior of the cell (depolymerization). Nucleotide exchange occurs so that ATP-bound monomers are generated from ADP-bound monomers and recycled back to the barbed ends (Figure 1.4). Filaments are thus transposed forward, in the direction of protrusion. Definitive evidence that actin filament treadmilling provides a mechanism for movement comes from observations on bacterial motility, in media reconstituted from pure proteins involved in actin dynamics (Loisel *et al.*, 1999). *Listeria* and *Shigella* bacteria are intracellular

pathogens which can harness cellular proteins for propulsion, riding on an 'actin tail'. These bacteria are able to move in artificially created cell-free media containing actin and the actin-binding proteins ADF, profilin, capping protein and Arp2/3 complex, by initiating actin polymerization at their surfaces, forming 'actin tails'. Treadmilling occurs as the opposite (pointed) ends of the tails depolymerize and actin monomers recycle to the polymerizing (barbed) ends. This argues for a primary role of actin treadmilling in driving movement, without an absolute need to recruit the myosin motor. However, myosins are undoubtedly involved in other aspects of cell locomotion, such as de-adhesion of the rear end of moving cells (discussed in Part I, Myosins and the Actin Cytoskeleton).

Several models have been proposed to explain how actin treadmilling pushes the plasma membrane. A basic requirement is that the actin cytoskeleton has to be anchored to the substratum at the leading edge, or crosslinked to a relatively static structure, to prevent the membrane from slipping backwards. The addition of monomers is accompanied by hydrolysis of ATP, releasing energy that powers protrusion. The molecular events that physically engineer protrusion are, however, complex and less well understood. In the 'elastic Brownian ratchet' model, the actin filament is like an elastic wire that is constantly bending due to thermal fluctuations (Mogilner and Oster, 1996). When bent away from the membrane, the space created allows a monomer to insert into the barbed end, lengthening the filament. As the filament straightens by elastic forces, the elongated filament springs against the membrane and pushes it forward. An alternative model proposes that the osmotic forces created by actin polymerization are responsible (Condeelis, 1992). Perhaps

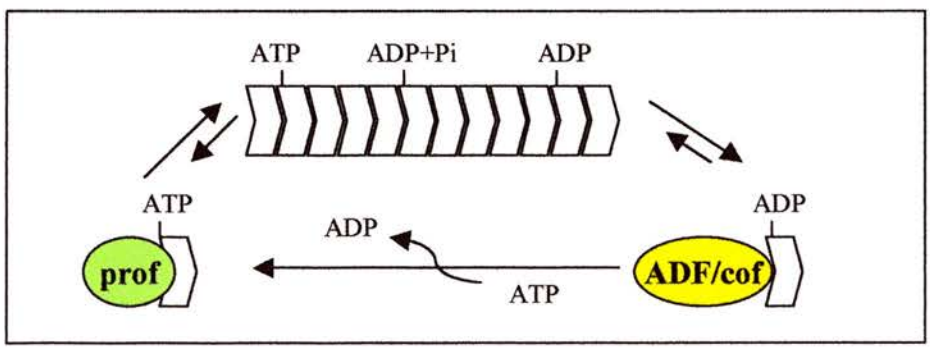

Fig. 1.5 ADF/cofilin and profilin synergise to increase actin filament turnover.

The cytoplasmic pool of unassembled actin exists as ATP- and ADP-bound G-actin, preferentially bound to profilin and ADF/cofilin respectively. ADF/cofilin enhance the dissociation rate of monomers at the pointed ends of actin filaments (ADP-bound). The profilin-ATP-G actin complex contributes to assembly at the barbed ends.

polymerization releases bound ions, increasing osmolar concentration in its vicinity, causing the membrane to swell outwards due to influx of water.

Actin filaments undergo dynamic rearrangements at the lamellipodium

Actin filaments at the lamellipodium are in a constant state of flux (Cooper and Schafer, 2000). New filaments are continually generated by severing old filaments, or by nucleation, a process in which a few actin monomers associate to form a short filament. In addition, actin filaments here can be observed to arrange in a branching network, due to polymerization being initiated from the sides of pre-existing filaments. This is mediated mainly by the Arp 2/3 complex of proteins (Actin-related proteins), which has been localised to the branch points of filaments (Svitkina and Borisy, 1999).

ADF/cofilin and profilin accelerate actin treadmilling at the leading edge

ADF(actin depolymerizing factor)/cofilin and profilin are low molecular weight proteins that bind actin, and synergise to accelerate treadmilling at the leading edge (Figure 1.5). Synergy of activity has been observed by measuring rates of actin treadmilling in biochemical assays (Didry *et al.*, 1998), and actin-based motility of bacteria in reconstituted media containing ADF/cofilin and profilin (Loisel *et al.*, 1999). ADF/cofilin has a higher affinity for free ADP-actin monomers (Carlier *et al.*, 1997; Maciver and Weeds, 1994), whilst profilin binds mainly free ATP-actin monomers (Pantaloni and Carlier, 1993). The binding of filaments by ADF/cofilin causes an increase in the dissociation of monomers from the pointed ends (Carlier *et al.*, 1997; Maciver *et al.*, 1998), and severing of filaments (Maciver *et al.*, 1991). Profilin shuttles the recycled actin monomers to the fast-growing barbed ends

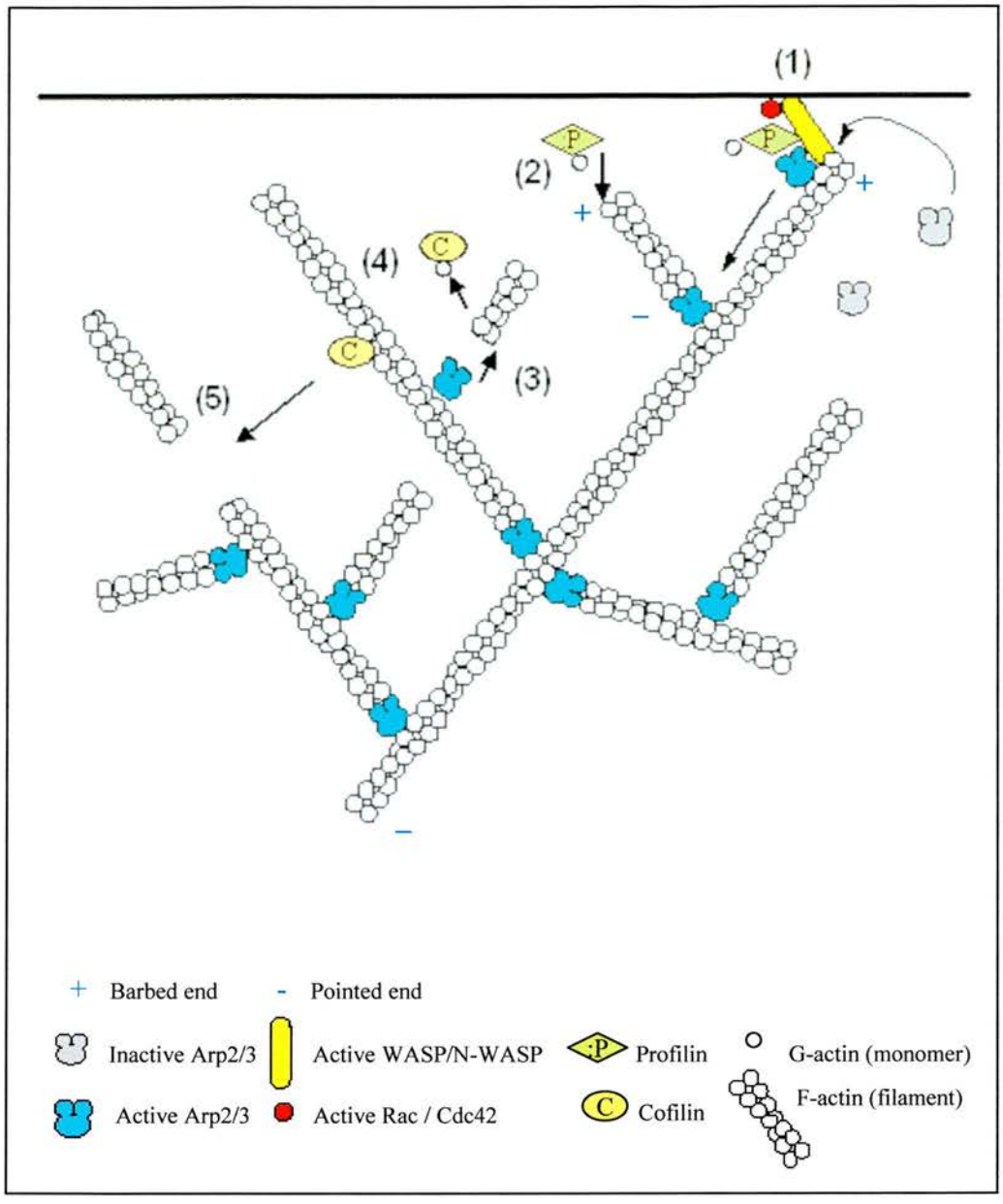

Fig. 1.6 The activity of Arp2/3, ADF/cofilin and profilin in branched actin filaments at the lamellipodium.

(modified from Welch M.D., 1999)

(1)Transmembrane signaling activates the Rho GTPases (Rac or Cdc42), which recruits and activates WASP. Actin nucleation is initiated by Arp2/3 complex bound to a pre-existing filament, and brought into close proximity with profilin and actin.

(2)The newly nucleated branch grows by addition of ATP-G actin at the barbed ends, catalysed by profilin.

(3)ADF/cofilin binds to older filaments, with several consequences. ADF/cofilin encourages formation of ADP-bound F actin, which detaches from Arp2/3 complex.

(4)ADF/cofilin depolymerizes the exposed pointed end, forming a 1:1 complex with monomeric ADP-bound actin.

(5)ADF/cofilin severs longer, older branches associated with ADP, producing shorter filaments with free ends, and potentially able to act as new foci for treadmilling.

(Blanchoin and Pollard, 1998; Didry *et al.*, 1998). In addition, profilin promotes the rate at which nucleotides are exchanged on actin monomers (Nishida, 1985), so that ATP-bound actin is regenerated from ADP-bound actin and participates in polymerization. Thus, ADF/cofilin generates ADP-actin monomers, and profilin enhances the recycling of monomers to ATP-actin and addition to the barbed ends. In addition, ADF/cofilin creates new nuclei for filament assembly by severing filaments, whilst profilin harbours a pool of ATP-actin in readiness for polymerization.

The Arp2/3 complex localises to the leading edge to nucleate actin polymers and create a branching network of filaments

The Arp2/3 complex is a stable complex of seven subunits and is conserved in eukaryotes (Machesky *et al.*, 1994; Welch *et al.*, 1997). It is formed from two actin-related proteins, Arp2 and Arp3, and five novel proteins p40, p35, p19, p18, p14. Arp2/3 functions to nucleate actin filaments at the cell membrane and to the sides of other filaments, by binding to the pointed (slow-growing) ends of filaments, leaving the barbed ends free for polymerization. Arp2/3 also caps the pointed ends of filaments and possibly blocks depolymerization (Mullins *et al.*, 1998). New filaments are thus anchored to and sprout from the sides of existing filaments, organising the actin cytoskeleton into a branched pattern at the lamellipodium (Welch, 1999) (Figure 1.6).

Arp2/3 localises predominantly to the actin-rich leading edge, being maximally activated in the presence of signals that induce polymerization. Biochemical evidence favours the model in which signalling and effector molecules interact to cause highly localised actin polymerization, perhaps by initiating an intracellular gradient of

activated molecules which declines away from the stimulated membrane. Activation of transducer G-proteins, linked to transmembrane receptors, are required for maximal activation of the downstream effector WASP/N-WASP (Wiskott-Aldrich syndrome protein) (Rohatgi *et al.*, 1999). Activated WASP is in turn consequential to maximising Arp2/3 activity (Machesky *et al.*, 1999). These interlocking requirements for activation perhaps aid to focus the actin machinery to the leading edge.

Interactions between ADF/cofilin, profilin and Arp2/3 complex

An intriguing question arises as to how ADF/cofilin and profilin interact with the Arp2/3 complex at the lamellipodium. ADF/cofilin has been shown to be excluded from the most peripheral zone of the lamellipodial network, whilst Arp2/3 localises mainly to the peripheral network and less towards the cellular interior (Svitkina and Borisy, 1999). Arp2/3 is found at the branch points of the actin network, consistent with its ability to nucleate actin polymerization by binding to the sides of pre-existing filaments. It appears that Arp2/3 protects the peripheral filaments at the lamellipodium from depolymerization by ADF/cofilin, possibly by capping their pointed ends. In contrast, the inner actin network is subjected to depolymerization by ADF/cofilin, suggesting that ADF/cofilin gains access to the pointed ends here. This might be explained by the different affinities of Arp2/3 and ADF/cofilin for nucleotide-bound actin. The lag of ATP hydrolysis and phosphate (Pi) release following actin polymerization implies that within the lamellipodium, inner regions of actin filaments are enriched in ADP-bound actin, whilst outer filaments are mainly associated with ATP (Pollard and Weeds, 1984). The Arp2/3 complex has a lower affinity for ADP-bound actin filaments, compared to ATP-bound filaments (Blanchoin *et al.*, 2000b). On the other hand, ADF/cofilin binds ADP-actin with greater affinity (Maciver and

Weeds, 1994). In addition, actophorin (*Acanthamoeba* ADF/cofilin) promotes the loss of phosphate from ADP-Pi-actin in filaments, leaving pointed ends bound to ADP (Blanchoin *et al.*, 2000b). Thus filaments in the inner lamellipodium become associated with ADP and dissociate from the Arp2/3 complex as the bonds weaken, creating free pointed ends which are exposed to the activity of ADF/cofilin. Visualisation of branched actin filaments in biochemical assays using fluorescence microscopy shows that debranching is accelerated by actophorin.

The Arp2/3 complex is brought into close association with profilin and actin by WASP/N-WASP, which has binding sites for these proteins (Welch, 1999). When WASP/N-WASP is activated by G-protein signalling, polymerization of actin monomers is inititiated by Arp2/3 (ie. nucleation), and enhanced in the presence of profilin which adds ATP-actin monomers preferentially to the barbed ends (Blanchoin and Pollard, 1998; Didry *et al.*, 1998). In this manner, Arp2/3 and profilin focus actin polymerization close to the surface of the lamellipodium, and ADF/cofilin supplies the building blocks from the rear to accelerate treadmilling.

Actin filament treadmilling is funnelled to the leading edge

Further distant from the vicinity of the leading edge, actin filaments are prevented from growing by capping protein. This protein binds or 'caps' their barbed ends and blocks the addition of monomers, a property which is essential for the actin-based propulsion of bacteria in reconstituted media (Loisel *et al.*, 1999), as well as motility in *Dictyostelium* (Hug *et al.*, 1995). *Dictyostelium* was observed to move slower with decreasing levels of capping protein, indicating the importance of differential actin polymerization in cell motility. The free pointed ends of capped filaments undergo

depolymerization, generating actin monomers which can join barbed ends at the leading edge. Gelsolin is another actin-binding protein that severs filaments and caps their barbed ends to prevent elongation of polymers (Sun *et al.*, 1999). ADF/cofilin has been shown to bind gelsolin-capped filaments with higher affinity (Ressad *et al.*, 1998), hence potentially interacting with gelsolin to enhance the disassembly of actin filaments away from the polymerizing front. Simultaneously, profilin and thymosin β4 sequester a pool of ATP-bound actin monomers (Pantaloni and Carlier, 1993). The concentration of actin treadmilling to the leading edge is further reinforced by inhibiting spontaneous nucleation of actin filaments elsewhere, attributed to the activity of profilin. By funnelling actin polymerization to a localised site on the cell membrane, polarity and hence directional movement can be established.

Signalling to the actin cytoskeleton

Cells can change shape or move in response to a variety of stimuli, such as extracellular cues arising from secreted factors, contact with neighbouring cells or with the extracellular matrix. Not unexpectedly, several signalling pathways converge onto the actin cytoskeleton, which include tyrosine kinase receptor signalling involving EGF (epidermal growth factor), PDGF (platelet-derived growth factor) and insulin; and integrin receptor signalling activated by matrix glycoproteins such as fibronectin and laminin. A myriad of intracellular second messengers exist, including small G-proteins, phospholipids, and protein kinase C. The small G-proteins, Rho GTPases, have generated much interest because they appear to have specific effects on the actin cytoskeleton (Ridley, 2001).

Rho GTPases

The Rho GTPases play important roles in coordinating cellular responses to motility-inducing signals (Ridley, 2001). The Rho family is a subgroup of the Ras superfamily of GTP-binding proteins. These small proteins, 20 to 30kDa, are coupled to cell surface receptors, and function as signal transducers linking the actin cytoskeleton to extracellular stimuli. They are conserved in evolution, with Rho family members identified in mammals, *Drosophila melanogaster, Caenorhabditis elegans, Dictyostelium discoideum,* yeasts and plants. In humans, the Rho family comprises at least 20 Rho proteins. Of these, Rho, Rac and Cdc42 proteins have been the most avidly studied in their effects on cell motility. The diverse functions of the Rho GTPases also include cell cycle regulation, membrane trafficking and transcriptional regulation.

Rho GTPases are activated by receptor stimulation

The Rho proteins cycle between an active GTP-bound state, and an inactive GDP-bound state (Figure 1.7). The active GTP-bound Rho targets downstream signalling cascades. Rho proteins can exchange guanine nucleotides (GTP and GDP), catalysed by guanine nucleotide exchange factors (GEFs). Rho also hydrolyses GTP, and this is catalysed by GTPase-activating proteins (GAPs). In the cytoplasm of inactive cells, Rho GTPase is in the inactive GDP-bound form, complexed with Rho-GDI (guanine nucleotide dissociation inhibitors). Rho-GDI prevents interaction with the cell membrane. On receipt of specific extracellular signals, Rho dissociates from GDI and is converted into the active GTP-bound form by GEF, which allows it to be recruited to the cell membrane.

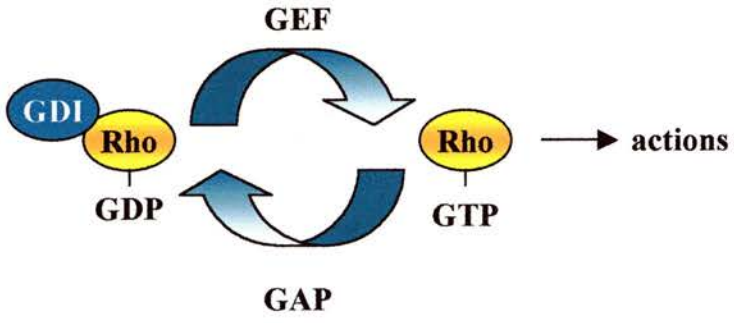

Fig. 1.7 Rho GTPases cycle between an active GTP-bound state and an inactive GDP-bound state.

GAP: GTPase-activating protein; GEF: Guanine nucleotide exchange factor; GDI: Guanine nucleotide dissociation inhibitor.

In the absence of signalling, the inactive Rho-GDP predominates, and GDI prevents assocation with the cell membrane. Rho is activated by binding to GTP, in the presence of GEF, and targets downstream molecules. Hydrolysis of GTP, enhanced by GAP, returns Rho to the inactive state.

Stimulation of tyrosine kinase receptors (EGF, PDGF and insulin) and integrin receptors activate Rho GTPases, enabling the actin cytoskeleton to be restructured in response to motility-inducing growth factors, as well as matrix attachment. When cells are plated on fibronectin, Rac and Cdc42 are activated via integrin signalling, and cell spreading occurs (Price *et al.*, 1998).

Rho GTPases are involved in actin dynamics

Activation of Rho GTPases leads to specific alterations in the actin cytoskeleton. Actin stress fibres form in response to microinjection of activated Rho (Ridley and Hall, 1992), activated Rac causes membrane ruffling (Ridley *et al.*, 1992), whilst activated Cdc-42 stimulates formation of microspikes at the cell membrane (Kozma *et al.*, 1995). Whilst the actin cytoskeleton adopts specific patterns when stimulated by different Rho GTPases, observations on moving cells indicate that they cooperate to establish a defined direction of movement. When a gap or 'wound' is introduced in a confluent monolayer of rat embryo fibroblasts, cells move into the wound to completely obliterate it over time. The contributions of Rho, Rac and Cdc42 in polarised movement can be dissected by microinjecting the cells lining the wound edges with specific function-blocking antibodies (Nobes and Hall, 1999). It appears that Rho anchors cells to the substratum, Rac induces lamellipodial protrusions, and Cdc42 establishes polarity of movement by limiting protrusions to the leading edge.

Downstream of Rho GTPases

The downstream effectors of Rho GTPases regulate proteins controlling the assembly of actin filaments (Figure 1.8). One such effector is a family of proteins that determine actin polymerization, the WASP family of proteins, which is altered in the genetic

immunodeficiency disorder, impairing motility in lymphoid immune cells. This family comprises WASP in haemopoietic cells, the ubiquitous N-WASP, and SCAR (Suppressor of cAMP Receptor mutation, also called WAVE). WASP (Blanchoin *et al.*, 2000a) and SCAR (Machesky *et al.*, 1999) proteins couple Rho GTPase signalling to actin polymerization via recruitment of the Arp2/3 complex to the cell membrane, stimulating its nucleation activity. WASP and N-WASP are responsible for Cdc42-induced actin assembly, and SCAR mediates Rac activity (Mullins, 2000).

Rac, Rho and Cdc42 stimulate the activity of LIM kinases, responsible for inhibiting the depolymerizing activity of cofilin. Rac and Cdc42 achieve this by activating p-21 activated kinase (PAK) (Edwards *et al.*, 1999), and Rho acts via ROCK (Rho-kinases), leading to the accumulation of actin filaments due to actin polymerization (Maekawa *et al.*, 1999; Sumi *et al.*, 1999).

Cofilin

Mammalian cofilin is a small molecular weight (20kDa) protein that belongs to the ADF/cofilin family of actin-binding proteins. ADF (actin depolymerizing factor, also called destrin) was first isolated in chick embryo brains as a 19kDa protein that promoted the disassembly of actin filaments (Bamburg *et al.*, 1980). Distribution of ADF was found to be widespread in adult mammalian and avian tissues, with even higher expression levels in embryonic tissues (Abe *et al.*, 1989; Bamburg and Bray, 1987). Representatives of this family have been identified in a spectrum of eukaryotes. These include depactin from starfish (Mabuchi, 1983), yeast cofilin (Iida *et al.*, 1993; Moon *et al.*, 1993), actophorin from *Acanthamoeba castellanii* (Cooper *et al.*, 1986),

ADF and cofilin from chick skeletal muscle (Abe *et al.*, 1990), porcine destrin (ADF) (Moriyama *et al.*, 1990) and cofilin (Matsuzaki *et al.*, 1988). The *unc-60* gene in *Caenorhabditis elegans* also encodes two ADF/cofilin homologues (McKim *et al.*, 1994). The amino acid sequences of porcine ADF (destrin) and cofilin have been found to be highly similar, with 70% identity (Matsuzaki *et al.*, 1988; Moriyama *et al.*, 1990). Most vertebrates have one ADF and two isoforms of cofilin: the ubiquitous cofilin 1, and cofilin 2 (m-cofilin) in skeletal muscle.

ADF/cofilin proteins bind actin filaments and monomers. Their enzymatic activity is targeted primarily to the slow-growing (pointed) ends of actin filaments, where they destabilise the filaments by severing (Maciver *et al.*, 1991), and enhance the loss of actin monomers. They also exhibit actin monomer-sequestering properties, forming 1:1 complexes with monomeric actin. Together with other monomer-sequestering proteins including profilin and thymosin β4, they contribute to a pool of unpolymerized actin in cells. This is important in regulating the availability of monomeric actin for polymerization at the leading edge of moving cells.

Molecular structure of ADF/cofilins

ADF/cofilins share a common ADF homology domain, which is a folded domain (Lappalainen et al., 1998; Maciver and Hussey, 2002). This domain is conserved in the proteins isolated from eukaryotes examined so far, despite the variabilities in sequence and size. The main actin-binding region in the ADF domain is a long α-helix, which in human ADF spans amino acids Leu111 to Phe128. A short sequence that binds both phosphatidylinositol-4,5-biphosphate (PIP_2) and actin has also been identified, from

Trp104 to Met115 (Yonezawa *et al.*, 1991). ADF/cofilin is known to enter the nucleus when cells are subjected to stress, and at least one nuclear-localization signal is present in most ADF/cofilins, close to the amino terminal.

Intracellular localisation of ADF/cofilins

ADF/cofilins localise to sites where there is high turnover of actin filaments, such as the leading edge of motile cells (Bamburg and Bray, 1987; Quirk *et al.*, 1993), and the contractile ring between daughter cells undergoing cytokinesis (Nagaoka *et al.*, 1995). Here, ADF/cofilins depolymerize actin filaments, and cooperate with other actin-associated proteins in enhancing actin filament dynamics in motile and dividing cells. ADF/cofilins also localise to actin-rich rods that form in the cytoplasm and nucleus of cells exposed to stress, such as heat shock or treatment with 10% dimethylsulfoxide (Nishida *et al.*, 1987). It is unclear what function ADF/cofilins play by translocating to the nucleus, but could be related to the observation that ADF can inhibit actin denaturation (Hayden *et al.*, 1993). Perhaps it is a cell survival mechanism that ensures the integrity of actin protected within the nucleus, which will be crucial in recovery when cells resume normal activity.

ADF/cofilins depolymerize actin filaments

The depolymerizing activity of ADF/cofilin has been proposed to be the result of two mechanisms: increasing the rate at which actin monomers leave the filament (the 'off rate'), and actin filament severing. There is evidence that both mechanisms operate to explain the observed effects on actin filaments *in vitro* (Maciver, 1998; Theriot, 1997).

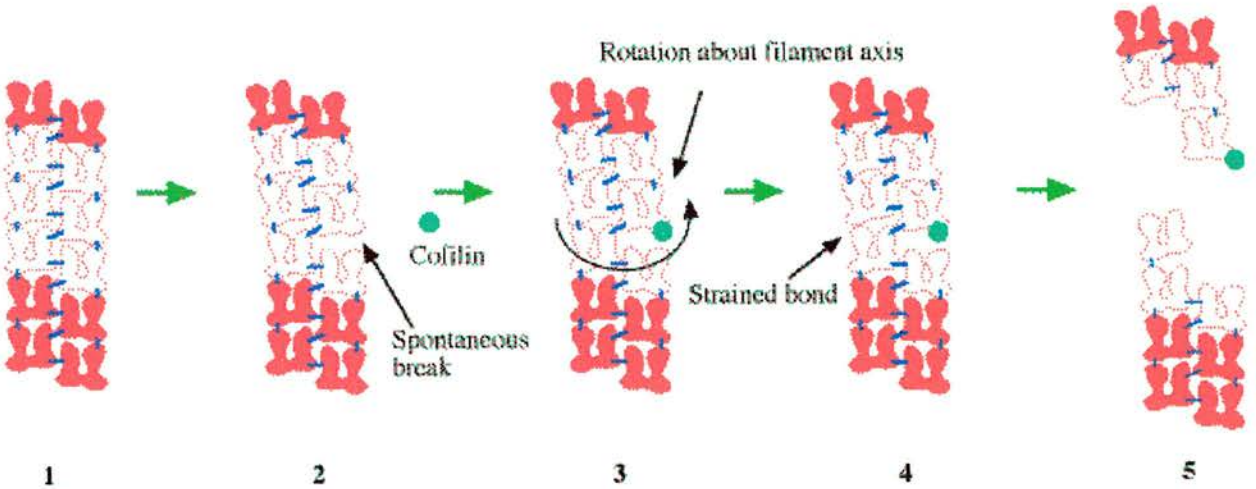

Fig. 1. 9 ADF/Cofilin severs actin filaments.

(Maciver S.K., 1998)

1. The actin filament is held together by stronger longitudinal bonds and weaker diagonal bonds between actin subunits (indicated by bars). 2. In the presence of thermal stress, spontaneous but reversible breaks occur between the longitudinal bonds. 3. ADF/cofilin binds in the cleft created at the break, preventing the bond from reforming and introduces torsion into the filament. 4. Torsion strains the surrounding bonds. 5. The filament is severed as adjacent bonds are broken.

Actin hydrolyses ATP as it polymerizes, so that whilst the fast-growing (barbed) ends of actin filaments are composed of ATP-actin, the central portions and slow-growing (pointed) ends are enriched in ADP-actin (Pollard and Weeds, 1984). ADF/cofilin has a higher binding affinity for ADP-bound than ATP-bound actin filaments and monomers (Maciver and Weeds, 1994). This preferential binding is thought to be crucial to the activity of ADF/cofilin on actin filaments. Possibly ADF/cofilin facilitates the dissociation rate by binding actin filaments at the pointed ends. The last monomer is either severed off, or detaches due to strain introduced in the bonds between the monomer and filament.

The severing of actin filaments by actophorin (amoebic cofilin) can be followed by fluorescence microscopy (Maciver *et al.*, 1991). Actin filaments appear to be preferentially severed at the central regions, and less at filament ends. It is postulated that ADF/cofilin interacts centrally with actin filaments where ADP-actin is exposed, due to spontaneous partial breaks that occur in the presence of thermal stress. Once it binds, torsion in the filaments is exacerbated, eventually resulting in complete severing (Figure 1.9). Severing of actin filaments by ADF/cofilin generates shorter filaments with free barbed ends which can repolymerize.

Regulation of ADF/cofilin activity

Phosphorylation status

The phosphorylation status of cofilin in a major regulator of its activity, as phosphorylated cofilin is unable to bind actin (Figure 1.10). Phosphorylation of human non-muscle cofilin at its third serine residue (Ser3) by LIM kinases 1 and 2 inhibits its

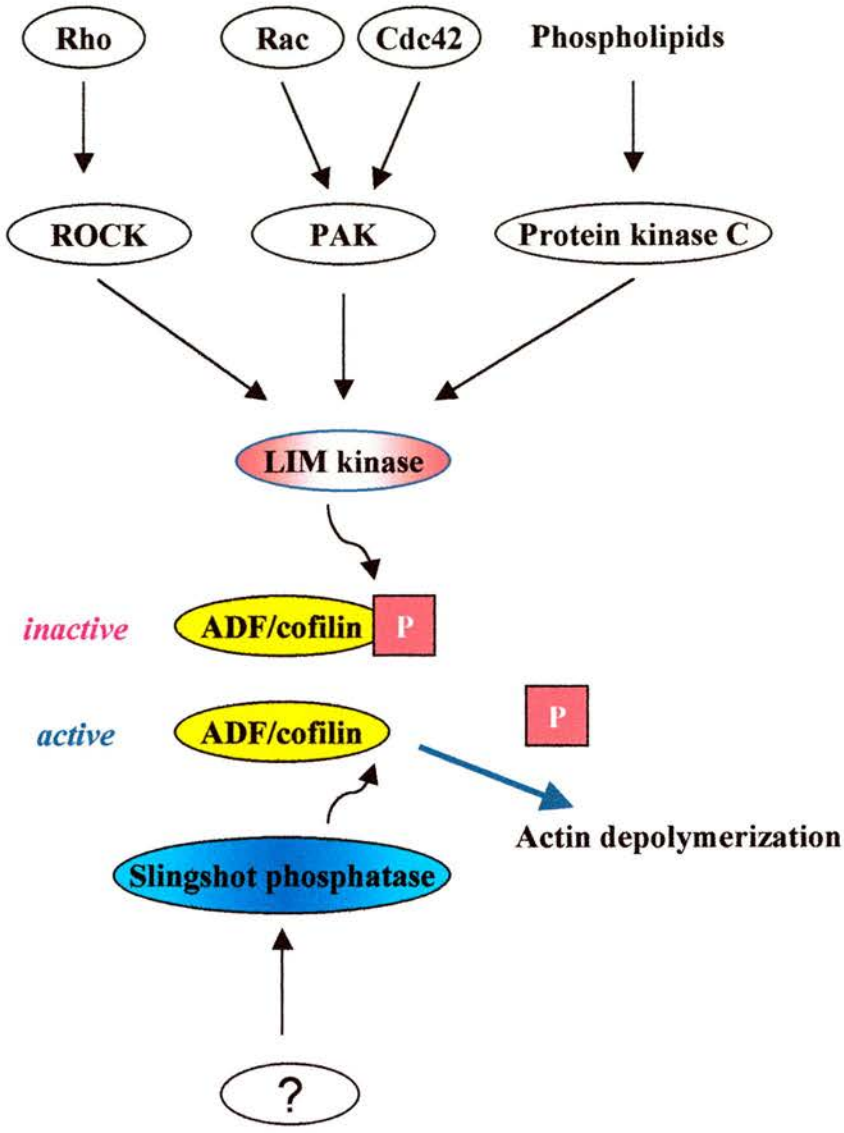

Fig. 1.10 Regulation of ADF/cofilin activity by phosphorylation.

PAK: p21-activated kinase; ROCK: Rho kinase.

Signalling through the Rho GTPases and phospholipids such as diacylglycerol (DAG) activates LIM kinase, which phosphorylates ADF/cofilin and prevents it from binding actin filaments. ADF/cofilin activity is restored with dephosphorylation by Singshot phosphatase. The pathways leading to activation of Slingshot phosphatase are unknown.

actin depolymerizing activities (Yang *et al.*, 1998), as does phosphorylation by testicular protein kinases 1 and 2 (TESKs) (Toshima *et al.*, 2001a; Toshima *et al.*, 2001b). In HeLa cells cotransfected with cofilin, the overexpression of LIM kinase 1 represses depolymerization of actin filaments and results in accumulation of actin filaments at the cell periphery. LIM kinases are activated by p21-activated kinase 1 (Pak1) (Edwards *et al.*, 1999), Rho-activated kinase (ROCK), and protein kinase C, which lie downstream of signalling pathways involving Rho GTPases, or the phospholipid diacylglycerol (DAG).

The search for proteins that dephosphorylate ADF/cofilin has yielded the Slingshot family of phosphatases as a possible candidate (Niwa *et al.*, 2002). The *slingshot* (*ssh*) gene encodes a phosphatase of 1045 amino acids in *Drosophila*, and is named after the bristle bifurcation phenotype in mutants. The protein appears to be conserved in several species, and human homologues have been identified (hSSHs). Slingshot phosphatase colocalises with actin filaments in *Drosophila* cells. Cell-free assays reveal its ability to bind actin filaments as well as dephosphorylate cofilin. Although the control of Slingshot phosphatases is unknown, it is conceivable that Slingshot and LIM kinases coordinate in the regulation of ADF/cofilin activity.

Phosphoinositides

Vertebrate ADF/cofilins (Yonezawa *et al.*, 1990), *Acanthamoeba* actophorin (Quirk *et al.*, 1993), *Saccharomyces cerevisiae* cofilin1 (Iida *et al.*, 1993), and *Zea mays* ADF3 (Gungabissoon *et al*, 1998) all possess binding sites for the membrane-derived phospholipid PIP_2 (phosphatidylinositol 4,5-bisphosphate). PIP_2 causes ADF/cofilins to dissociate from actin, perhaps as a result of overlap between PIP_2 and actin-binding

sites (Van Troys *et al.*, 2000). Binding of the phospholipid to ADF/cofilins may help localise these proteins close to the cell membrane, where they are required for actin filament turnover. The metabolism of PIP_2 is also linked to ADF/cofilins, which prevent its hydrolysis by phospholipase C (Yonezawa *et al.*, 1991).

pH sensitivity

Cofilin acts in a pH-sensitive, calcium-independent manner *in vitro*. Lowering the pH below 7.3 decreases severing activity, whilst increasing pH above 7.3 allows complete severing of actin filaments. Moreover, below pH 7.3, cofilin cosediments with F(filamentous)-actin, but cannot bind F-actin stably at higher pH (Yonezawa *et al.*, 1985). Thus cofilin switches from an F-actin binding state, to favour monomeric actin-binding and actin depolymerization at more alkaline pH.

ADF shows pH-dependent actin severing similar to cofilin, although a discrepancy remains as to whether ADF binds actin filaments significantly at low pH. Work on porcine ADF indicate no filament binding (Moriyama *et al.*, 1990). This contrasts with observations on human ADF (Hawkins *et al.*, 1993), which binds mainly actin filaments at pH below 7.0. At pH above 7.5, ADF binds preferentially with actin monomers, and rapidly disassembles actin filaments.

The pH sensitivity of cofilin and ADF established *in vitro* may have important physiological outcomes in cells. A change in intracellular pH has been reported in fibroblasts, where motility was associated with an increase in pH from 7.1 to 7.4 (Bright *et al.*, 1987). Localised pH changes might be of higher magnitude, in which case motility might be associated with enhanced depolymerization by cofilin and

ADF. Presumably a rise in intracellular pH in response to motility signals induces rapid disassembly of actin filaments to which ADF and cofilin are already bound.

Effects of ADF/cofilin in cells

Cell movement

Cell-free studies indicate that ADF/cofilin synergise with other actin-binding proteins, like profilin and capping protein, to accelerate actin filament treadmilling necessary for cell movement. The force generated from treadmilling appears to be sufficient to power movement. However the regulation of ADF/cofilin activity in effecting movement appears to be complex. There is evidence that lamellipodia formation requires ADF/cofilin to be inactivated to some extent by LIM kinases. Rac GTPase induces lamellipodia, which fail to form in the presence of inactive LIM kinase (Yang *et al.*, 1998). However, there is also supportive evidence arguing for an active role of cofilin in promoting movement. In *Dictyostelium discoideum*, the overexpression of cofilin stimulates membrane ruffling and movement (Aizawa *et al.*, 1996). Cofilin is recruited to the lamellipodia, and its severing activity increases in tumour cells which are stimulated to move by epidermal growth factor (Chan *et al.*, 2000). Transfection of cells with the active kinase domain of LIM kinase inactivates a large proportion of the intracellular pool of cofilin. Treatment of metastatic rat mammary adenocarcinoma cells in this manner inhibits lamellipodial extensions in response to epidermal growth factor stimulation, indicating the need for cofilin activity (Zebda *et al.*, 2000). A plausible explanation for these divergent observations would be that cells require both the active and inactive forms of cofilin. Perhaps the depolymerizing and monomer-sequestering functions of cofilin have to be balanced against polymerization for

effective filament treadmilling to occur. Hence, it is probably not surprising that cells are immotile when the bulk of cofilin is biased towards either the active or inactive mutant form. In contrast, overexpression of wild type cofilin *Dictyostelium* and other cells may circumvent the 'bias', being subject to regulation by endogenous LIM kinases and phosphatases. One indication that this might be the case is that the actin monomer:filament ratio is not altered by overexpression of wild type ADF/cofilin in neurites (Meberg and Bamburg, 2000), suggesting that the degree of depolymerization and generation of monomers are kept in check. It is unknown if cofilin overexpression induces an altered expression or activity of its regulatory proteins, or proteins that promote polymerization.

Cell division

In dividing cells, the contractile ring is depolymerized as daughter cells separate (Nagaoka *et al*, 1995). Cofilin mutations in several organisms, including yeast and *Drosophila*, leads to impaired cytokinesis, abnormal development and lethality (see under Development). Mitotic divisions of somatic cells as well as meiotic divisions of germ cells are disrupted in *Drosophila melanogaster* which carry mutations in *twinstar*, an essential gene that encodes its ADF/cofilin (Gunsalus *et al.*, 1995). Mutant larval neuroblasts exhibit polyploidy, presumably arising from failure of cytokinesis after nuclear division. Spermatids derived from abnormal cytokinesis during meiosis each have more than one nucleus, and an enlarged mitochondrial component, reflecting unequal subdivisions of chromosomal and mitochondrial elements.

Besides embryonic development, cofilin also plays a role in the expansion of lymphoid immune cells. Proliferative signals in T-lymphocytes stimulate dephosphorylation and translocation of cofilin from the cytoplasm to the nucleus (Samstag *et al.*, 1994). The nuclear translocation of cofilin appears to be important for lymphocytic cell division, although the reasons remain unclear. Furthermore, cofilin is implicated in tumour growth, as several tumorigenic cell lines appear to harbour an excess of the dephosphorylated, active form of cofilin, compared to untransformed cells (Nebl *et al.*, 1996). This suggests that the deregulation of cofilin activity may be a contributory factor in tumour proliferation.

Development

ADF/cofilin have pivotal roles in development. Knocking out ADF/cofilin is lethal in a variety of organisms, such as yeast (Moon *et al.*, 1993), *Dictyostelium discoideum* (Aizawa *et al.*, 1995), and *Drosophila melanogaster* (Gunsalus *et al.*, 1995), attributable to abnormalities in cytokinesis. Yeast cells with complete loss of cofilin fail to divide, and truncation of the last 19 amino acids severely limits divisive ability. There is also evidence that tipping the balance in favour of an excess of inactive ADF/cofilin could disrupt the development of tissues. Loss of Slingshot phosphatase function in homozygous *ssh* mutants of *Drosophila* leads to increases in levels of phosphorylated (inactive) cofilin, coincident with accumulation of actin filaments. s*sh* mutants develop thickened bristles and wing hairs with terminal bifurcations, and lose many interommatidial bristles. This abnormal phenotype possibly arises from overaccumulation of actin filaments in the apical cellular protrusions that normally form hairs and bristles.

In *Xenopus laevis*, both the inhibition of cofilin and excess cofilin activity block division at early embryonic stage (Abe *et al.*, 1996). When blastomeres at the 2-cell stage are injected with constitutively active cofilin, or an inhibitory antibody, cleavage of the injected cell is repressed. The cleavage furrow can be observed to regress when constitutively active cofilin is introduced into fertilised eggs undergoing the first cleavage. Hence, a regulated balance between active and inactive cofilin appears to be integral to proper cellular function, as echoed in the requirements for cell movement and cell division.

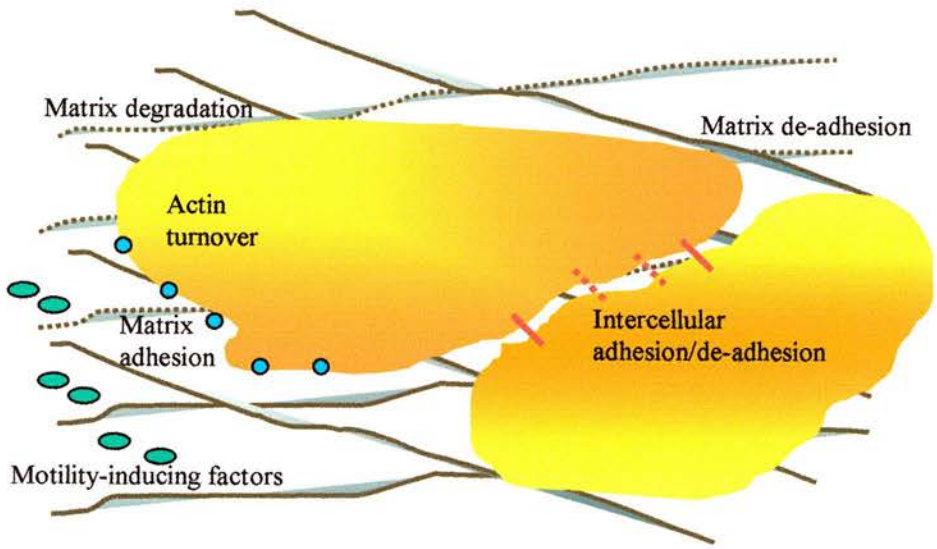

Fig. 1.11 Interplay of factors required for a migratory phenotype in tumours.

I.III Motility as a crucial factor in tumour invasion

Progression of tumours to a malignant phenotype is associated with an increased ability of cells to migrate and invade surrounding tissue, and sometimes disseminate to distant sites (metastasis). Interaction of the tumour cell with the extracellular matrix and remodelling of its cytoskeleton are required to attain a migratory phenotype. There is a complex interplay of factors that might predispose to invasive behaviour (Figure 1.11). This includes increased tumour cell motility, reduced intercellular adhesion, and degradation of the extracellular matrix to create planes for tumour spread (Van Roys and Mareel, 1992). The tendency to disperse has to be balanced against the maintenance of cellular integrity, which relies on mechanical anchorage of cells to the matrix or neighbouring cells.

Dysregulation of cell motility has emerged as a key issue in the transition from a benign and constrained tumour to one which is malignant and invasive (Grimstad, 1987). This is thought to stem from an altered control of cytoskeletal remodelling (involvement of the cytoskeleton in brain tumour migation is reviewed by Maidment, 1997). Cells move by directional rearrangements of its cytoskeleton, mainly composed of actin microfilaments, microtubules and intermediate filaments. The actin cytoskeleton is of paramount importance in generating forces that drive cell movement, via actin filament turnover and actin-myosin contraction. The cytoskeleton is also tethered to sites of contact with the matrix (focal adhesions), as well as to intercellular cadherin-mediated adhesions. There is dynamic turnover of the cytoskeleton at these sites as well, enabling motile cells to form new contacts at the leading edge and lose those at the trailing end. It is becoming evident that tumour

progression is often associated with abnormal expression of genes that regulate cytoskeletal assembly, such as the Rho GTPases, as well as genes that directly influence the mechanics of cytoskeletal turnover. These alterations generate potential changes in motile behaviour.

Altered expression of Rho GTPases in migratory tumours

The Rho GTPases are involved in the induction of tumour formation and metastatic behaviour (Frame and Brunton, 2002; Hernandez-Alcoceba *et al.*, 2000). Rho GTPases coordinate components of the actin cytoskeleton necessary for motility, such as actin polymerization at the lamellipodia, actin-myosin contraction of the cell body, and turnover of integrin-actin adhesions. RhoC, a member of this family, is expressed at higher levels in overtly metastatic melanomas (Clark *et al.*, 2000) and pancreatic adenocarcinomas (Suwa *et al.*, 1998). Inducing its overexpression in poorly metastatic melanomas augments metastatic capacity, whilst inhibiting it with a dominant-negative Rho GTPase suppresses the generation of metastases in nude mice (Clark *et al.*, 2000). The main phenotypic change associated with RhoC-induced metastasis appears to involve enhanced migration.

There is evidence that supports the suspicion that cytoskeletal events targeted by Rho GTPase might be implicated in tumour migration. Manipulating the activity of its downstream effector, ROCK (Rho kinase), alters invasive and metastatic capacity in rat hepatic tumour (Itoh *et al.*, 1999). Tumour cells expressing constitutively active ROCK exhibit heightened adhesion and invasion in vitrio, and increased dissemination when injected into the peritoneal cavities of normal rats. In contrast,

when ROCK is inhibited using a specific pharmacological agent, Y-27632, invasion and tumour dissemination are reduced. Since ROCK stimulates both actin assembly and cell body contraction via actin-myosin interactions, the observations suggest these processes operate in invasion.

Actin polymerization is disrupted in invasive and metastatic tumours

Proteins that directly impact actin polymerization have also been implicated in tumour invasion and metastasis. Expression of thymosin β4, an actin-binding protein, is correlated with invasiveness of renal tumours (Hall, 1991), and metastasis in melanomas (Clark *et al.*, 2000). In normal cells, thymosin β4 sequesters the bulk of unpolymerized actin by binding to monomers in a 1:1 complex, and inhibits polymerization of these monomers (Safer *et al.*, 1990; 1991). It remains to be established why thymosin β4 confers malignant behaviour in some tumours. Perhaps it enables a large reservoir of actin monomers to be harboured in readiness for actin polymerization. The complexity is highlighted by the contrasting finding that thymosin β4 is reduced in the invasive glioma tumour compared to normal astrocytes in rat brain (Gunnersen *et al.*, 2000).

N-WASP (neuronal Wiskott-Aldrich syndrome protein), a ubiquitous protein that couples Rho GTPase signalling to actin polymerization, is upregulated in metastatic colon cancer cell lines (Yanagawa *et al.*, 2001). The EMS1 gene that encodes cortactin, another protein that binds actin filaments, is commonly upregulated in breast cancer (Hui *et al.*, 1997). Cortactin promotes actin polymerization by activating the Arp2/3 complex (Uruno *et al.*, 2001), and is also thought to stabilise

new actin filaments at the penetrating edge of invading cells by crosslinking actin filaments in a network (Weaver *et al.*, 2001). Cofilin, an actin-binding protein that depolymerizes actin filaments and sequesters actin monomers, is expressed at higher levels in invasive glioma tumours when compared to normal astrocytes in rats (Gunnersen *et al.*, 2000). When tumour cells are stimulated to move by growth factors, their extending lamellipodia can be observed to recruit several of these actin-interacting proteins, including WASP, cortactin, the Arp2/3 complex and cofilin. Changing the levels of these factors at the lamellipodia could have a substantial impact on the actin machinery that drives motility, and affect the ability for invasion.

Many of the proteins that have been implicated as contributory to tumour invasion are crucial in the cytoskeletal dynamics of untransformed cells, which are required for normal processes of growth and maintenance of a multicellular organism. Cell motility, cell division, the morphological changes that accompany cellular differentiation, and phagocytosis of bacteria by immune cells are all effected by remodelling the cytoskeleton. Cell migration is a normal feature of fibroblasts and leukocytes in wound healing, and is necessary in embryonic development. The transition from controlled to aberrant motility can therefore be viewed as representing an extreme deviation from 'normal' movement, made possible by operating different permutations of regulatory elements.

I.IV Glioma tumours of the brain

Gliomas are tumours of neuroepithelial origin, and constitute the major forms of primary tumours arising in the brain. The classification of gliomas is complex, due to

the considerable number of cell types involved, the heterogeneity within the major classes, and often within each tumour. Most classifications are based on that set out by Bailey and Cushing (1926), who observed the morphological stages through which the cells evolved. In general, the identification of cytological features reflective of those found in normal mature and developing brain guides the assignment of a tumour to a particular group. Even so, the distinction is based on the prevalent cell type, and does not describe other cell types that often reside in a heterogeneous tumour. Cellular diversity is a common denominator in neoplastic transformation, compounded by the propensity of tumour cells to dedifferentiate. (A detailed description of the classification and pathology of gliomas has been written by Russell and Rubinstein, 1989).

Glioblastoma

Glioblastomas are believed to derive from neoplastic transformation of astrocytes (Russell and Rubinstein, 1989). Astrocytes, together with oligodendrocytes, constitute the glial population of cells which perform supportive roles in the central nervous system. Histologically, astrocytic tumours (astrocytomas) range in their degree of differentiation, and increased malignancy is often associated with loss of differentiation in tumours . The poorly differentiated glioblastoma multiforme is thought to derive from progressive transformation of an initially more benign counterpart.

Grossly, the poorly differentiated and highly malignant glioblastoma tumour presents as an unencapsulated mass in the brain, with an infiltrating periphery. Areas of

necrosis and vascular haemorrhage can be identified in its cut surface. Microscopic examination reveals a high density of small, undifferentiated cells, mixed with spindle-shaped astrocytes. There may be marked polymorphism of tumour cells, with the presence of giant mutinucleated cells, as well as mitotic cells. A characteristic feature is vascular proliferation within and adjacent to the tumour.

Glioblastomas are capable of progressive and infiltrative growth, penetrating and often destroying the architecture of the normal brain tissue. Dissemination may sometimes occur along paths of circulation of the cerebrospinal fluid, when tumours invade the ependymal lining of the ventricles. Metastatic spread to distant sites outside the central nervous system is very rare, even for highly malignant tumours.

Protein expression is altered in glioblastomas

Glioblastomas have altered expression of several genes involved in cell growth and migration. Mutations have been identified in p53, a transcription factor that induces apoptosis and cell cycle arrest; in p14 and p16 proteins that control retinoblastoma protein acivity; and in PTEN (phosphatase and tensin homologue deleted on chromosome ten), a phosphatase that inhibits the activity of tyrosine kinase and PI3-kinase (phosphoinositide-3-kinase) proteins. These mutations are thought to render an uncontrolled state of cell cycle progression, and cellular proliferation (Ishii *et al.*, 1999).

The EGF (epidermal growth factor) receptor gene is amplified and overexpressed at high frequency in malignant human gliomas (Bigner *et al.*, 1988; Fuller and Bigner,

1992). Fibroblast growth factor and platelet-derived growth factors are also often expressed in gliomas (Rasheed and Bigner, 1991). Overexpression of growth factors and their receptors foster the development and progression of tumours by inducing invasion, proliferation and angiogenesis. Growth factor signalling can stimulate motility by causing cytoskeletal changes, loss of focal adhesions and reduced adhesion. *In vitro* experiments using gliomas derived from patients indicate that these tumours respond to the presence of growth factors by increased proliferation, migration and invasion (Engebraaten *et al.*, 1993).

Several other proteins associated with the extracellular matrix and cytoskeleton have been found to be altered in expression, including cofilin and thymosin β4 in rat gliomas (Gunnersen *et al.*, 2000). In addition, tumour cells can elaborate matrix proteins *in vitro*, such as fibronectin and collagen, which are also present in normal brain (Bouterfa *et al.*, 1999).

I.V Aims of the project

The project aims to study the effects of the actin-binding protein, cofilin, on the motility of human glioblastoma tumour cells. There has been substantial data suggesting that the mediation of actin-based motility might be important in inducing migration of tumour cells. The inherently invasive nature of the glioblastoma tumour makes it a good candidate to investigate how actin filament dynamics influence its motile behaviour. Cofilin is a crucial component in the motility of eukaryotic cells, and has a direct impact on the actin machinery. The outcome of tumour motility when expression levels of cofilin are altered might afford an insight into some of the

fundamental issues in the mechanics of invasion. The main experimental approach was to examine the locomotion of glioblastoma cells which overexpressed cofilin. Overexpression was achieved by transfecting the U373 MG cell line with an overexpression vector, and motility assays performed using both transient and stable transfectants.

The methods employed in the project and the construction of the recombinant plasmid vectors are explained in Chapter 2 (Materials and Methods). These plasmids were used to induce cofilin overexpression, as well as for the in vivo detection of ADF/cofilin by in situ hybridization. In Chapter 3, investigations into the expression of ADF/cofilin in the mouse embryo offers a window into possible roles in brain development. In addition, the activity of cofilin in glioblastoma cells is characterised using immunochemistry to study its distribution under normal and altered culture conditions. Chapter 4 explains how levels of cofilin are determined in untransfected and stably-transfected cells by flow cytometry and Western blot analysis. The results of cofilin overexpression on the movement of glioblastoma cells are reported in Chapter 5, which also includes a discussion on the design of the motility studies. Chapter 6 concerns the development of an inducible system of cofilin expression (Tet-Off system) which attempts to explore in greater detail the nature of the relationship between motility and the intracellular levels of cofilin. The final chapter highlights the hypotheses that might account for the altered locomotion observed in cofilin-overexpressing glioblastoma cells.

Fig. 2.1 Experimental design for inducing overexpression of cofilin in U373 MG glioma cells and motility analysis

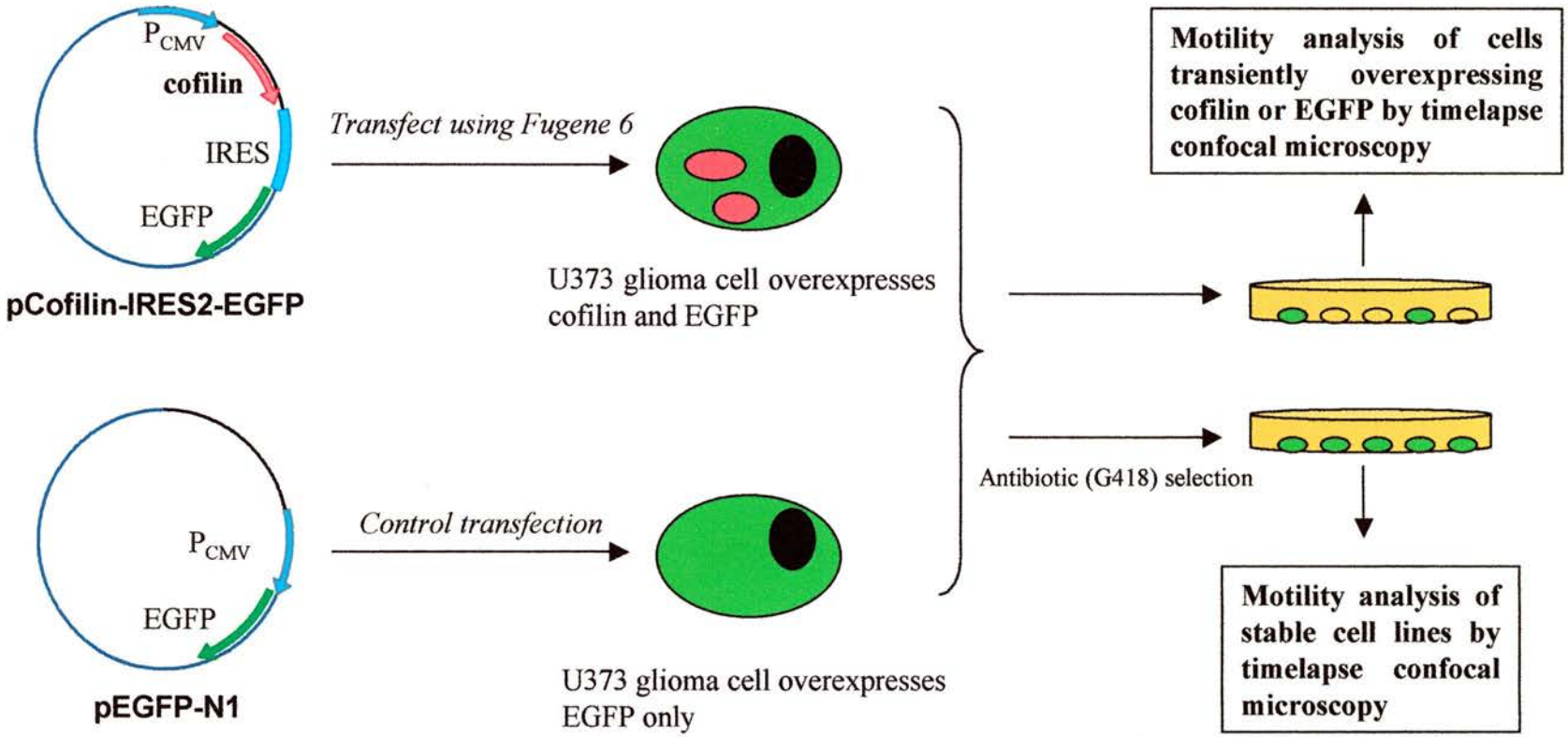

CHAPTER 2

MATERIALS AND METHODS

INTRODUCTION

This chapter records the materials and methods used in the project, and the results of molecular biology experiments that constructed the necessary plasmid vectors. The plasmid vectors encoded the cDNA of cofilin 1, actin depolymerizing factor (ADF) and profilin 1. The pCofilin-IRES2-EGFP vector was used to induce overexpression of cofilin in the glioblastoma cell line, U373 MG. U373 MG cells that were transfected with this vector were analysed for changes in motility, by imaging them over a period of time in a controlled environment with confocal microscopy. This main experiment is summarised in Figure 2.1. Levels of cofilin expression in untransfected and transfected U373 MG cells were determined by flow cytometric analysis of immunofluorescence, and confirmed with Western blots. An inducible system of cofilin overexpression using the Tet-Off Gene Expression system was also developed. This potentially allows a closer examination at the relationship between cofilin expression and motility, as variable levels of overexpression can be induced. Expression of cofilin, ADF and profilin in U373 MG cells were characterised by reverse transcription-PCR and immunochemistry. Cofilin expression in embryonic mouse brain was also determined using *in situ* hybridization. The materials are listed in detail in Appendix A – E.

METHODS

The methods described were modified mainly from Current Protocols in Molecular Biology, edited by Ausubel F.M. et al (2001). The materials used are listed in Appendix A - E.

II.I MOLECULAR BIOLOGY

The coding sequences of human cofilin, ADF (actin depolymerizing factor), and profilin in pMW 172 vectors (developed by Michael Way) were subcloned into the plasmid vectors pBluescript II KS (-) (Stratagene), pIRES2-EGFP (Clontech laboratories Inc.) and pTRE (Clontech laboratories Inc.). Recombinant plasmids were amplified in *E. coli* strains.

Preparation of chemically competent *Escherichia coli* (*E. coli*)

Competent *E. coli* bacteria were prepared by harvesting an exponentially proliferating culture grown in 500ml of LB or 2XTY medium, which had reached an absorbance of 0.5 – 0.6 at 600nm (A_{600}), measured with a Jenway spectrophotometer. The bacteria was chilled on ice and washed twice by centrifuging at $2000g_{av}$ for 10 minutes at 4°C. Cells were resuspended in ice-cold 50mM $CaCl_2$, then in competent cell freezing mix and stored in 0.5ml aliquots at -70°C.

Preparation of electro-competent *E. coli*

E.coli from frozen stock was plated onto an LB-agar plate and grown overnight at 37°C. A single colony was picked to innoculate 5ml of LB or 2XTY medium in a

vented universal tube, which was incubated at 37°C overnight at 200rpm in a Gallenkamp shaking incubator. The 5ml culture was split into two 5L flasks each containing 250ml of medium, with continued growth at 37°C in the shaking incubator, and harvested when exponentially proliferating at A_{600} 0.5 – 0.6. The bacteria were chilled on ice, pelleted by centrifuging at $4000g_{av}$ for 15 minutes at 4°C, and washed twice in 200ml of ice-cold sterile ddH_2O. The bacteria were resuspended in 20ml of 10% glycerol (v/v) (ice-cold), and finally concentrated in 2-3ml of 10% glycerol (v/v) (ice-cold). They were stored as 55µl aliquots in thin-walled 0.5ml microfuge tubes at -70°C.

Transformation of chemically competent *E.coli* by heat shock

The ligation mix containing 10-100ng of plasmid DNA in a volume of 5µl was added to 200-400µl of competent E.coli bacteria that had been thawed on ice, and the mixture was incubated on ice for 30 minutes. The bacteria were heat shocked for exactly 2 minutes in a water bath set at 42°C, and recovered in twice the volume of LB or 2XTY medium (400-800µl). The transformed bacteria were grown for 1 hour in a vented universal tube at 37°C in a shaking incubator, then plated onto selective LB-agar plates in different amounts (eg. 25 and 250µl) and grown overnight at 37°C.

Transformation of electro-competent *E.coli* by electroporation

A 55ml aliquot of electro-competent E.coli was thawed on ice, and an electroporation cuvette chilled on ice prior to use. 10-100ng of plasmid DNA was added to the bacteria, mixed by tapping, and incubated on ice for 1 minute. The mixture was transferred to the chilled electroporator cuvette, and the cuvette introduced into the electroporator after drying its outer walls. Transformation was effected at 2.5kV, 25µF

capacitance, and 200Ω resistance with a 5ms pulse time. Bacteria were recovered in 400µl of SOC medium, incubated for 1 hour in a shaking incubator at 37°C, then plated onto selective LB-agar and grown overnight at 37°C.

Selection of transformed bacteria on LB agar plates

The appropriate antibiotic for selection was dictated by the antibiotic resistance gene carried by the plasmid, in this case ampicillin or kanamycin. The antibiotic was added to the liquid LB agar after it had cooled to 50°C or lower, to a concentration of 50-100µg/ml. To make X-gal-coated LB agar, 30µl of the 30mg/ml stock was pipetted and spread onto the solid agar and left to dry before bacteria were plated.

Storage of frozen bacterial stock

A saturated overnight culture of 0.5ml grown to turbidity was added to 0.5ml of glycerol freezing storage medium, and mixed by pipetting. The bacterial stock was frozen immediately on dry ice, and stored at -70°C.

Plasmid DNA extraction

Plasmid DNA was amplified in *E.coli*, and the DNA extracted using either the Ultraclean Mini Plasmid Prep kit (Mo Bio) or QIAprep Spin Miniprep kit (Qiagen) for minipreps, or the Plasmid Midi kit (Qiagen) for midipreps. For the miniprep, a single colony of transformed bacteria was grown in 2-3 ml of selective LB or 2XTY medium overnight at 37°C in a shaking incubator. For the midiprep, the colony was first grown in 2ml of selective medium for 6-8 hours, then expanded in 100ml of selective medium overnight.

Genomic DNA extraction

U373 MG cells were harvested by trypsinization, and washed twice in phosphate buffered saline. Cells were then lysed by incubating at 37°C overnight with 1ml of tail tip lysis buffer containing Proteinase K (at 0.1 – 1 mg/ml). Protein was extracted using first an equal volume of re-distilled phenol, then phenol/chloroform/isoamyl alcohol (PCIA). DNA was retrieved in the upper aqueous phase, and RNA contaminants were removed by adding heat-treated RNAse at 50μg/ml, incubating at 37°C for 1-2 hours. (The RNase had been heat-treated at 100°C for 10 – 30 minutes to inactivate contaminating DNase). A third round of protein extraction was repeated using PCIA. DNA was then precipitated in the presence of 2 – 2.5 volumes of cold 100% ethanol (v/v), and pelleted by centrifuging at $13{,}000g_{av}$ on the benchtop Biofuge pico centrifuge. The pellet was washed in 70% ethanol (v/v) to remove salts and small organic molecules, air-dried briefly and finally resuspended in 10mM Tris-Cl (pH 8.0).

Restriction digest of DNA

Plasmid DNA was digested with restriction enzymes (1-5 units/μg DNA) using the appropriate buffers at 1X concentration, in a total volume ranging 10-20μl. The volume of restriction enzymes used did not exceed 10% of the final volume. DNA was incubated for 1-2 hours at temperatures recommended by the manufacturer.

Synthesis of primers for PCR

Primers were designed using the Primer3 Output program (Whitehead Institute, MIT), and synthesized by MWG-Biotech AG.

Polymerase chain reaction (PCR)

Taq polymerase (5U/μl) and its 10X buffer containing 15mM $MgCl_2$ (Promega, M2661) was used to polymerize nucleotides from double-stranded DNA. The PCR mixture was made to a final volume of 25μl, and consisted of PCR buffer at 1X concentration with 1.5mM $MgCl_2$, 200μM of dNTP mix (dTTP, dATP, dGTP, dCTP, each stocked at 10mM), 0.5μM each of the forward and reverse primers (stocked at 10mM), and 0.2μl of *Taq* polymerase. 35 cycles of PCR were performed on the PTC-225 Peltier Thermal Cycler following a 'hot' start at 94 - 96°C for 2 minutes, using the following conditions: denaturation at 94 - 96°C for 30 seconds, annealing for 15 – 30 seconds at 1 - 2°C below the lower melting temperature (Tm) of the primers, and extension at 72°C for 1 minute (1 minute/kb PCR product). The PCR products were retrieved on ice and loaded onto agarose gel for electrophoresis.

Reverse-transcription PCR (RT-PCR) to detect expression of cofilin, ADF and profilin in U373 MG glioma cells

RT-PCR was performed on U373 MG cells using the Superscript Preamplification System for first strand cDNA synthesis (GibcoBrl), according the manufacturer's instructions. RNA was extracted from cells by the RNeasy Mini kit (Qiagen) and treated with DNase I (Roche) to remove contaminating DNA. cDNA was synthesized using Superscript II RT (reverse transcriptase) and Oligo$(dT)_{12\text{-}18}$ primers provided in the kit. PCR by *Taq* polymerase was then performed using primers specific for cofilin, ADF and profilin, under conditions as described above. PCR controls included samples that lacked the reverse transcriptase.

Agarose gel electrophoresis

DNA fragments were separated in 0.8 – 2.0% (w/v) agarose gels, by electrophoresis at 4V/cm (3 – 8V/cm). 1X TBE buffer was used to dissolve agarose (Sigma), and was also the running buffer for electrophoresis. NuSieve GTG agarose (FMC Bioproducts) was used for gel extraction of DNA fragments. Ethidium bromide was added to gels to a final concentration of 0.1μg/ml, from a 10mg/ml stock. DNA samples and molecular weight ladders were mixed with 1X Orange G loading buffer before loading into the gel. DNA fragments were visualized with the dual intensity ultraviolet transilluminator (Ultra-Violet Products), and gels recorded and analysed using the Alphaimager 1220 program (Alpha Innotech Corporation).

Gel extraction of DNA fragments

Specific DNA bands obtained by gel electrophoresis in NuSieve GTG agarose were excised with a blade under direct visualization by ultraviolet illumination, wearing protective headgear. DNA was extracted using the Qiaex II gel extraction kit (Qiagen) or QIAquick gel extraction kit (Qiagen), and resuspended in 10mM Tris-Cl, pH 8.0 for long term storage at -20°C.

Ethanol precipitation of DNA

DNA was concentrated by precipitating with ethanol and resuspending in a smaller volume of solvent. This protocol was also used to remove salts from a ligation mix prior to electroporation, when the precipitated DNA was resuspended in water. $1/10^{th}$ volume of sodium acetate (pH 5.2) and 2 volumes of cold absolute ethanol were added to DNA and mixed by inverting the tube. DNA was precipitated by incubating on ice or at -20°C for 30 minutes to overnight, and pelleted by centrifuging at maximum

speed on a benchtop centrifuge for 15 minutes. The pellet was washed with 75% ethanol (v/v), then air-dried briefly before resuspending in 10mM Tris-Cl (pH 8.0), TE buffer or water.

Dephosphorylation of 5' ends of plasmid vectors

Restriction digests of vector plasmids with a single enzyme generated complementary 5' ends. In order to prevent self-ligation of vectors, 5' ends were dephosphorylated by calf intestinal phosphatase (CIP, Roche). The plasmid DNA digest was incubated with 1X CIP reaction buffer, CIP (0.01U/pmol of ends) and water to a final volume of 100µl.

Digests resulting in 5' recessed ends (eg. *Xba*1 digests) were incubated at 37°C for 15 minutes, then at 56°C for 15 minutes. A second aliquot of the same volume of CIP was added, and incubations at 37°C and 56°C repeated. Digests resulting in 5' protruding ends were incubated at 37°C for 30 minutes at a time, but otherwise treated similarly. To stop the reaction, 2ml of 0.5M EDTA (pH 8.0) was added and heated to 65°C for 20 minutes. The dephosphorylated plasmid DNA was then purified using the QIAquick gel extraction kit.

(A general formula for calculating the picomoles of ends of linear double-stranded DNA is: (µg DNA/kb size of DNA) X 3.04 = pmol of ends. [Protocols and Applications Guide, 3rd edition, Promega])

Ligation of vector plasmid and DNA restriction fragment

Complementary ends were generated in the DNA insert and vector plasmid by restriction digest, and the digested DNA purified by gel extraction. The extracted insert and plasmid were quantified by running aliquots on a 1% agarose gel (w/v), alongside a known amount of the 500bp Molecular Weight marker XVII (Roche), and band intensities compared using the Alphaimager 1220 program. The ligation mix was set up with 1X ligase reaction buffer, 20ng of cut vector, insert in adequate amount for a insert:vector ratio of 3 (see below), 1mM ATP, T4 DNA ligase (Roche) and water to a final volume of 10µl. A control ligation mix excluded the insert. The ligation reaction was performed at 16°C for 2 hours or at 4°C overnight. This was then used directly to transform *E.coli*, or purified by ethanol precipitation if a large amount was required to transform by electroporation.

The amount of insert DNA required was calculated by the following formula:

$$\frac{\text{ng vector} \times \text{kb insert size}}{\text{kb vector size}} \times \text{molar ratio of insert:vector (eg. 3)}$$

Fluorescence-based cycle sequencing of DNA

Fluorescence-based cycle sequencing of DNA was performed on DNA plasmid inserts which had been cloned by PCR of the sequences in the original plasmids. The ABI PRISM BigDye Terminator Cycle Sequencing Ready Reaction kit (Perkin-Elmer), which contains AmpliTaq DNA polymerase and dye terminators, was used for sequencing. This method provides a high signal intensity so that a lower quantity of starting template (200 – 500ng of plasmid template) is required. Only one of the primers could be incorporated into the sequencing reaction at a time, hence two sequencing reactions were set up for each plasmid for forward and reverse sequencing.

The plasmid template was introduced into a 0.5ml microfuge tube in a volume not greater than 5µl. 1µl of a 10mM primer, 4µl of ready reaction mix and water were added to a final volume of 10µl, mixed and centrifuged briefly to deposit the contents. The following program was run on a thermal cycler: 96°C for 1 minute, followed by 25 cycles of 96°C for 30 seconds (denaturation), 50°C for 15 seconds (annealing), 60°C for 4 minutes (extension), finally holding at 4°C. The product was then precipitated by adding 2µl of 3M sodium acetate/EDTA (pH 4.6) and 50µl of ice-cold absolute ethanol, mixed and placed on ice for 10 minutes. The precipitate was pelleted by centrifuging for 20 - 30 minutes, rinsed in 250µl of 75% ethanol (v/v) and air-dried. This product was sent to the DNA Sequence Facility at the Department of Biochemistry, University of Oxford, for sequence analysis.

Cloning the coding sequences of cofilin, ADF (actin depolymerizing factor) and profilin into the plasmid vectors pBluescript KS II (-), pIRES2-EGFP and pTRE

Detailed information on the construction of the specific vectors is found in the Results section of this chapter. In general, directional cloning was effected by using two distinct restriction enzymes to excise each coding sequence, as well as cut the multiple cloning site of the plasmid into which the sequence would be inserted. This created complementary ends between the excised fragment and plasmid, allowing the coding sequence to be ligated into the plasmid with T4 DNA ligase. Restriction digests that generated compatible 5' ends within the plasmid vector were treated with calf intestinal alkaline phosphatase (Roche) to dephosphorylate the 5' ends. This prevented the cut plasmid from ligating within itself.

The ligation mix was then introduced into competent E. coli by heat shock or electroporation, and transformed bacteria was isolated by growth on selective LB agar containing the appropriate antibiotic. After overnight culture at 37°C, single colonies were picked and streaked onto selective LB agar to incubate for 6 – 8 hours. Each of these was expanded in 3ml of LB or 2XTY medium overnight, and a plasmid miniprep was obtained for each selected colony. The identity of the inserted DNA was checked by restriction mapping, using a combination of restriction enzymes to cleave specific sites in the coding sequence. Inserts which had been cloned by PCR of coding sequences in the original plasmids were checked by fluorescence-based sequencing using the ABI PRISM BigDye Terminator Cycle Sequencing Ready Reaction kit (Perkin-Elmer). Finally, recombinant plasmid stocks were made from minipreps and midipreps and stored at -20°C.

II.II *IN SITU* HYBRIDIZATION

mRNA expression of cofilin, ADF and profilin in wax-embedded sagittal sections of mouse embryos at embryonic day 17 were analysed by *in situ* hybridization. Digoxigenin (DIG)-labeled RNA probes were generated from pBluescript KS II (-) vectors encoding these genes. Chromogenic detection of hybridization was performed using anti-DIG antibody conjugated to alkaline phosphatase, and NBT/BCIP substrate. 0.01% DEPC (v/v) (Diethylpyrocarbonate) in double-distilled water was used for diluting solutions to inhibit endogenous RNase activity of cells.

Slide and glassware preparation

Slides were treated with TESPA (amino-propyltriethoxysilane, Sigma) to promote cell adherence. Slides were first polished by soaking in sulphuric/chromic acid (0.3M potassium dichromate, 1.84M sulphuric acid) overnight in a fume cupboard, and washed in running tap water for 2 hours. They were dried at 37°C overnight and sterilized by baking at 180°C overnight. Slides were then subbed in 2% TESPA (v/v) diluted in acetone for 2 minutes, followed by two 30-second treatments with acetone, and washed with double-distilled water for 1 minute. They were dried at 37°C before storage. Glassware was baked at 180°C overnight to sterilise before use.

Making riboprobes (single –stranded RNA probes)

DIG-labeled riboprobes were made using pBluescript KS II (-) plasmids encoding cofilin, ADF and profilin. These were first linearised by single restriction digests with

*Not*1 to generate the antisense probes, and *Eco*R1 to generate the control sense probes. The linearised plasmids were electrophoresed on 1% agarose gel (w/v), and gel extracted using the Qiaex II Gel Extraction kit (Qiagen). DIG-labeled RNA probes were made using DIG RNA labeling kit (Roche), by incubating 1 – 2μg of linearised plasmid with 1X transcription buffer, 1X NTP labeling mixture, 2μl of RNA polymerase (20units/μl) to a final volume of 20μl, at 37°C for 2 hours. The *Not*1-digested plasmids were incubated with T3 RNA polymerase (antisense probes), and the *Eco*R1-digested plasmids with T7 RNA polymerase (sense probes). 2μl of 0.5M EDTA (pH 8.0) was added to stop transcription, and the riboprobe precipitated with 4μl of 3M sodium acetate (pH 5.5) and 36μl of 100% ethanol (v/v). Riboprobe was pelleted by centrifuging at 13,000g_{av} for 15 minutes at 4°C, washed with 50μl of 70% ethanol (v/v), air-dried and resuspended in 100μl of DEPC-water. This was stored at -20°C when not used immediately. The concentration of the riboprobe could be estimated by running an aliquot on 1% agarose gel (w/v) alongside a known amount of quantitation DNA ladder (eg. Molecular weight marker XII, Roche).

***In situ* hybridization**

The principles of the protocol are reviewed by Wilkinson (1998).

Prehybridization

The following protocol was performed at room temperature. Slides on which embryonic sections had been mounted were treated twice with 100% xylene (v/v) for 10 minutes each to dewax the sections. This was followed by an ethanol series of 100% (2 times), 95%, 85%, 70%, 50%, 30% (v/v) at 1 minute each, to permeabilize

and further dewax the sections. The slides were transferred into 2X SSPE buffer for 5 minutes, 1X phosphate buffer with 15μg/ml Proteinase K for 7.5 minutes to permeabilize tissues and inactivate endogenous RNases, then washed twice with 2X SSPE for 30 seconds each. Tissues were fixed in cold 4% paraformadehyde (v/v) for 15 minutes, then washed with 2X SSPE for 5 minutes. Slides were arranged into a rack and placed into 400 ml of 0.1M triethanolamine with 2ml acetic anhydride, with stirring for 10 minutes, followed by washing with 2X SSPE for 5 minutes. The acetic anhydride acetylates positively charged amino residues and reduces non-specific binding of the probe.

Hybridization

Approximately 100ng of riboprobe was used for each slide. This was diluted in a total volume of 60μl with hybridization mix, denatured at 80°C for 5 minutes, quenched on ice and centrifuged to collect. Slides were incubated with the riboprobe mix at 65°C overnight.

Post-hybridization washes

Slides were washed at 50°C for 10 minutes with 2X SSC which had been pre-warmed, then treated with 50% formamide (v/v) in 2X SSC for 45 minutes at 65°C. This was washed off with 4X SSPE for 5 minutes at 50°C, and treated with RNase A in 4X SSPE (75μl of 10mg/ml RNase A in 100ml 4X SSPE) at 37°C for 20 – 30 minutes. A second treatment with 50% formamide (v/v) in 2X SSC followed, then washed with 2X SSC at 50°C for 30 minutes, and cooled to room temperature before replacing with PBS-0.1% Tween (v/v). After 10 minutes, slides were incubated with blocking buffer for 30 minutes. Finally, anti-DIG antibody conjugated to alkaline phosphatase (Anti-

Digoxigenin-AP, Roche) was used in a 1:5000 dilution in anti-DIG immunoreaction buffer, and the immunoreaction was performed overnight at 4°C.

Detection of hybridization by chromogenic assay

Detection of DIG-labeled riboprobe which had hybridized to mRNA was detected using an alkaline phosphatase substrate, NBI/BCIP (Nitroblue tetrazolium chloride/5-bromo-4-chloro-3-indoyl-phosphate, Roche). After immunoreacting with anti-DIG-AP antibody, slides were washed three times in PBS-0.1% Tween (v/v) for 20 minutes each, and placed in alkaline phosphatase (AP) buffer for 5 minutes. Colour reaction was obtained by incubating in the dark with 1:500 dilution of NBT/BCIP in AP buffer. The buffer containing NBT/BCIP was refreshed every 12 hours, and slides were monitered daily for colour development.

Counterstain and mounting

To process slides for mounting, the chromogenic substrate was washed off with AP buffer for 5 minutes. Slides could be counterstained at this point, for example, with Nuclear Fast Red stain. They were then rinsed with double-distilled water, then dehydrated through an ethanol series of 70%, 90%, 95% 99% (v/v) for 10 minutes each, followed by two 10 minute immersions in 30% xylene. Slides were mounted with coverslips using DPX mountant (BDH).

II.III CELL BIOLOGY

Cell culture

Growth and maintenance of cells

The U373 MG human glioblastoma-astrocytoma cell line was cultured at 37°C, 5% CO_2, in a humidified incubator. Cells were maintained in Dulbecco's Modified Eagle medium / Nutrient Mix F12 (1:1), supplemented with 10% fetal bovine serum (v/v), 2mM L-glutamine, 100units/ml penicillin and 100μg/ml streptomycin. Confluent cultures were passaged by washing with phosphate buffered saline, treating with 0.25% trypsin (v/v) at 37°C for 5 minutes, and then recovered in culture medium.

Frozen stocks of cells were prepared by centrifuging at $160g_{av}$ for 5 minutes in the Heraeus Biofuge primo centrifuge to pellet and resuspending the pellet in 0.5ml of freezing medium in cryotubes. Cells in cryotubes were stored at -70°C. To regrow frozen stock, cells were thawed rapidly in a 37°C water-bath, and transferred to culture medium. The culture medium was refreshed 24 hours later, after cells had plated down, to minimise contact with DMSO.

Transfection of cells

U373 MG cells were plated at approximately 5 X 10^4 cells per well of a 6-well (35mm diameter) plate, and grown using standard conditions. Cells reached 50-80% confluence a day later, when transfection was performed, according to the manufacturer's recommendations. Fugene™ 6 was diluted in 100μl serum-free DMEM/F12 for 1 minute, 1-2μg of plasmid was added to the mixture, and incubated

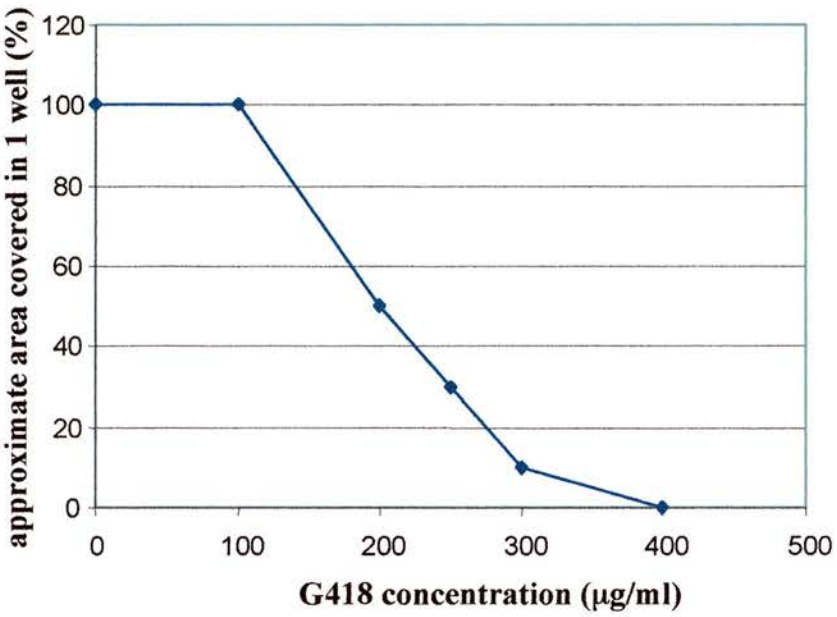

Fig. 2.2 Kill curve for untransfected U373 in G-418

for 15 minutes at room temperature. This final mixture containing the plasmid was then pipetted directly into the cell cultures, and cells were returned to incubate as normal. Fugene™ 6 (volume):plasmid (μg) ratios of 3:2, 3:1 and 6:1 were used for each of the plasmids.

Fluorescence microscopy was performed 24 - 72 hours after transfection with pCofilin-IRES2-EGFP and pEGFP-N1 to detect EGFP expression, and ascertain the proportion of transfected cells. The highest transfection efficiency obtained was estimated at 20% of total cell population.

Selection of stable cell lines

A. Determination of antibiotic concentration for selection

G-418 (geneticin sulphate)

Untransfected U373 MG cells were plated on 6-well plates (approximately 100,000 cells/well) and grown for 72 hours. The toxicity of G-418 was tested by adding a different concentration of the antibiotic to each well, with final concentrations ranging from 0 – 400 μg/ml. 5 days after antibiotic treatment, the effect on growth was determined by counting the number of dead cells aspirated, as well as estimating the extent of growth in each well. Almost all the cells were dead at 400μg/ml. The average area occupied by cells visualised in 3 different fields using a 20X lens was estimated to be 30% at 250μg/ml, whilst below 200μg/ml, cells were confluent (Figure 2.2). Stable cells transfected with pCofilin-IRES2-EGFP, pEGFP-N1 and pTet-Off were subsequently selected at G-418 concentration of 250 – 400 μg/ml.

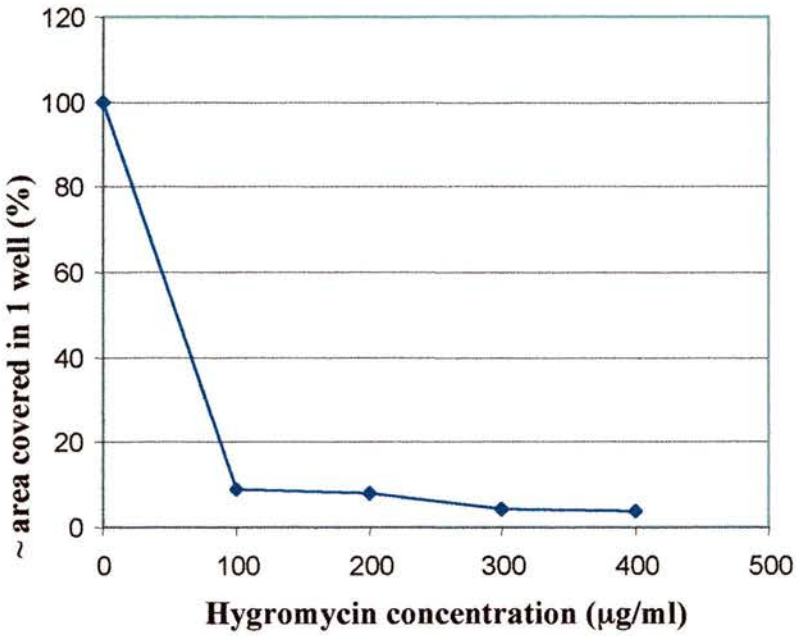

Fig. 2.3 Hygromycin kill curve for U373

Hygromycin

The lethal dose for U373 MG cells for hygromycin was determined in a similar manner to G-418. Hygromycin concentrations tested ranged from 0 – 400 μg/ml. At concentrations at and above 100 μg/ml, less than 10% confluent growth was achieved five days later (Figure 2.3). Cells transfected with pTK-Hyg were subsequently selected at 100 μg/ml.

B. Clonal selection of stable cell lines transfected with pCofilin-IRES2-EGFP, pEGFP-N1 and pTRE

U373 MG cells that had been transfected with pCofilin-IRES2-EGFP, pEGFP-N1 or pTet-Off were selected using G-418 added to standard culture medium, at least 48 hours after transfection. Massive cell death was usually observed about 5 -7 days after antibiotic selection. The surviving cells were allowed to grow up in colonies, and maintained in G-418. Once the colonies had grown to sizes that could be visualised by the naked eye, they were picked using a pipette with 10-15 μl 0.25% trypsin, and transferred to 24-well (16 mm diameter) plates. G-418 was re-introduced to the newly-picked cultures 24-48 hours after transfer. Colonies derived from cells transfected with pCofilin-IRES2-EGFP and pEGFP-N1 were checked for green fluorescence before picking, to ensure stable expression of genes cloned into the plasmids. The process of colony selection was repeated more than once: 6-8 times for cells stably transfected with pCofilin-IRES2-EGFP and pEGFP-N1; twice for cells transfected with pTRE. Resultant colonies were finally expanded by growing in T-25 and T-75 flasks, passaged when confluent, and frozen stocks obtained.

C. Selection of stable pTet-Off cells cotransfected with pTRE vectors and pTK-Hyg using fluorescence activated cell sorter (FACS)

Stable transfections of U373 MG cells with pTet-Off were obtained as described. These cells, which express the tet-controlled transcriptional activator, were cotransfected with pTRE-Cofilin-IRES2-EGFP and pTK-Hyg, or pEGFP-N1 and pTK-Hyg as controls. Cells were grown in Hygromycin 100μg/ml, and a mixture of green and non-green fluorescent cells resulted from the selective culture. In order to select the EGFP-expressing cells, the populations were expanded in T75 flasks, grown to confluence, and harvested by trypsinization. Cells were suspended in PBS-1% fetal calf serum with prophylactic antibiotics 5μg/ml plasmocin^{TM} (Invivogen), 100units/ml penicillin and 100μg/ml streptomycin. In order to obtain single-cell suspensions, they were filtered through cell strainers of 70nm nylon mesh (BD Falcon) before introduction into the Beckson Dickinson FACS Vantage SE flow sorter.

EGFP was excited by an argon laser at 488nm, and detected in the FL1 channel using a 530/30 bandpass filter (detection range 515 – 545nm). Simultaneously, background red fluorescence was detected in the FL3 channel using the 675/20 bandpass filter (detection range 665 – 685nm). Green fluorescent cells were collected into standard culture medium containing prophylactic antibiotics, and transferred to 6-well plates to grow under standard culture conditions.

Immunocytochemistry

A. Immunostaining U373 MG cells on slides to detect expression of cofilin and actin

Preparation of 4% paraformaldehyde (w/v) for fixation

10% paraformaldehyde stock (w/v) was made by dissolving paraformaldehyde in water in a 60°C water-bath, with a drop of 10M NaOH, and occasional agitation till dissolved. This was stored in aliquots at -20°C, which was thawed and diluted to 4% (w/v) with PBS when needed.

Moviol aqueous mountant

This was prepared by mixing 2.4g of moviol with 6g of glycerol in 12ml of double distilled water, and dissolving by continuous stirring overnight. 12ml of 0.2M Tris (pH 8.5) was added, and the solution was heated at 50°C for 1-2 hours, with an occasional vortex to help dissolve the components. The solution was clarified by centrifuging at 5000g for 15 minutes, and stored in aliquots at -20°C. On thawing, this was centrifuged at maximum speed for 5 minutes to remove trapped air bubbles before use.

Immunocytochemistry

Cells were plated onto chamber slides and grown in monolayers in standard medium. For immunostaining, cells were first washed twice in PBS, then fixed in 4% paraformaldehyde (w/v) for 15-20 minutes at room temperature. Cells were again washed twice in PBS, then permeabilised in PBS-0.1% Triton X-100 for a total duration of 6 minutes (3 X 2 minutes). Cells were then blocked for a minimum of 30

minutes in 20% blocking serum, at room temperature. Thereafter, they were incubated overnight at 4°C with the primary antibody diluted in 20% blocking serum, to final concentrations ranging from 1:100 to 1:250. Control experiments were run in parallel in the absence of the primary antibody. This was followed with washes with PBS-0.1% Triton X-100 before incubation with the fluorescent secondary antibody, performed at room temperature and in the dark for 1-2 hours. The secondary antibodies (TRITC or Alexa Fluor 546) were used at concentrations ranging from 1:20 to 1:50 (TRITC) and 1:200 to 1:300 (Alexa Fluor 546), diluted in 20% blocking serum (v/v). Finally, the secondary antibody reaction was terminated by washing with PBS-0.1% Triton X-100 (v/v) for 6 minutes (3 X 2 minutes). The chamber partitions were moved, and the slide mounted in diluted Vectashield (1-2 drops in 50% glycerol, v/v) or Moviol aqueous mountant.

Visualisation of fluorescent immunostaining on slides

Fluorescence was visualised using both UV illumination and confocal microscopy. Under UV illumination, the TRITC filter was used to detect positive immunostaining, and the FITC filter to detect EGFP expression in transfected cells. The Leica DMRB upright microscope used was connected to the Leica DC 200 digital camera. Digital camera images were obtained by running the Leica QWin program.

Confocal imaging of immunostained slides were performed using the Leica TCS NT confocal system attached to the Leica DMRE Upright microscope. Red fluorescence was by excitation at 568nm, with emission collected by the LP 590 filter. Green fluorescence was by excitation at 488nm, with emission collected by the BP 525/50 filter.

B. Immunostaining U373 MG cells for detection of cofilin expression by flow cytometry

Cells were harvested by trypsinization, recovered in 10 ml of standard culture medium in a polystyrene 30ml skirted universal tube, and counted using a haemocytometer. Cells were then pelleted by centrifuging at $160g_{av}$ (1000rpm) for 5 minutes in the Heraeus Biofuge primo centrifuge, and washed in PBS-1% BSA (w/v), pipetting up and down to break up cell clumps. Cells were fixed in 4% paraformaldehyde (w/v) for 20 minutes at room temperature, then washed in PBS-1% BSA (w/v) and transferred to 1.5ml eppendorfs. Permeabilisation was achieved by treating with 70% ethanol (v/v) on ice for 1 hour. Cells were then washed in PBS-1% BSA (w/v) before blocking in 20% blocking serum (v/v) (goat serum in PBS) at room temperature for 1 hour, using ~ 100µl per million cells. The primary antibody (rabbit anti-human cofilin IgG, Cytoskeleton Inc.) was added to a final concentration of 1:100 (~2.5mg/L) and incubated at 4°C overnight. Two sets of controls were set up in parallel: the first excluded the primary antibody; the second replaced the anti-cofilin IgG with an isotype control IgG (rabbit anti-mouse, Dako), used at 1:100 dilution (~2.8mg/L).

After washes in PBS-1% BSA (w/v), the fluorescent secondary antibody (goat anti-rabbit (H+L specific) Spectral Red conjugate, Southern Biotechnology Associates) was added at a dilution of 1:100 in 20% blocking serum (v/v), using a volume of ~100µl per million cells. The cells were incubated in the dark at room temperature for 1-2 hours, followed by PBS-1% BSA (w/v) washes. Finally, cells were suspended in PBS-1% BSA (w/v) or PBS-1% BSA (w/v)-1% formalin (v/v), and stored in the dark

at 4°C before flow cytometry. The suspension was agitated gently before application to the flow cytometer to prevent clumping.

Cells were analysed by the Coulter EPICS XL Cytometer using the Expo^{TM} 32 ADC Analysis program (operated by Ms. Shonna MacCall). EGFP and Spectral Red were excited by a 15mW argon laser at 488nm. EGFP was detected in the FL1 channel using a 525 bandpass filter with a detection range of 505 – 545nm. Spectral Red was detected in the FL4 channel using a 675nm bandpass filter with a detection range of 660 – 700nm. Fluorescent emission was collected into a photomultiplier tube with a spectral range of 200 – 800nm. (For a detailed discussion on flow cytometry analysis, refer to Chapter 5).

Protein electrophoresis and Western blotting

Protein extraction

U373 MG cells were grown to confluence in T75 flasks. To harvest total cellular proteins, they were washed twice in cold PBS, then 1 ml of cold PBS was added to each T75 flask. Cells were dislodged by scraping with a Nunclon^{TM} cell scraper, then collected with a glass pipette into a 1.5ml eppendorf and kept on ice. Cells were pelleted by centrifuging at $1000g_{av}$ for 10 minutes, and lysed in 50-100 µl of TENT buffer for 20 minutes at 4°C. The lysate was clarified by centrifuging at $10,000g_{av}$ for 10 minutes at 4°C. Protein content was determined using the BCA Protein Assay Reagent kit (Pierce), with protein samples loaded onto a 96-well microplate. The absorbance at 590nm was measured by the Dynatech MR7000 plate reader, and a regression line obtained for the absorbance of bovine serum albumin (BSA) standards,

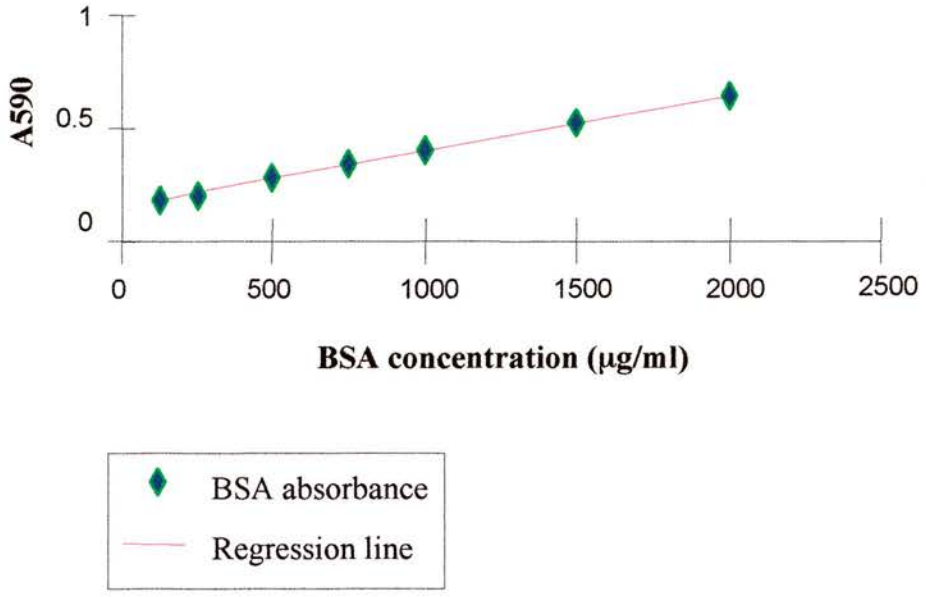

Fig. 2.4 Regression line for absorbance of BSA standards (125-2000 mg/ml) at 590nm in 1 experiment

Equation of regression line: y= 0.000247X + 0.152511
(y: A590; x: protein concentration (µg/ml)

Unknown protein concentrations are determined by substituting their absorbances at 590nm in 'y'.

Microsoft Excel program (Figure 2.4). The unknown protein concentrations were derived from the standard regression line. Proteins were stored at 4°C.

Protein electrophoresis under reducing and denaturing conditions using the NuPAGE system

Total cellular protein measuring 10 µg was loaded into each well of a NuPAGE 10% Bis-Tris gel (acrylamide/Bis-acrylamide), with 10% volume of NuPAGE 10X sample reducing agent (0.5M dithiothrietol (DTT)), and 25% volume of NuPAGE 4X sample buffer (Invitrogen Life Technologies). The final volume of each sample was 25 µl (adjusted with water), and volumes of sample reducing agent and sample buffer were standardised. O.5M DTT was introduced in order to reduce the protein samples. Immediately before electrophoresis, samples were denatured by heating at 90°C for 10 minutes, then loaded using 1-100 microliter filter tips (Alpha laboratories). Samples were run alongside 15 µl of Multimark multi-coloured molecular weight standard (Invitrogen Life Technologies), under denaturing conditions with 200 ml of NuPAGE MOPS SDS running buffer (diluted to 1X), and NuPAGE antioxidant (250 µl per 100ml of buffer) to prevent reoxidation of reduced proteins. The outer buffer chamber was filled with 600ml of buffer for heat dissipation. Electrophoresis was carried out at 200V till the dye neared the base of the gels.

Protein electrophoresis using the BioRad system

An alternative system of gel electrophoresis was employed to check the purification of recombinant cofilin, using the BioRad Mini-Protean II™ Cell (Part II.IV, Page 81). 12 % polyacrylamide separating gel was made by pouring the liquid gel mix into a glass-plate sandwich, leaving approximately 1.5cm short of the top end of sandwich for the

stacking gel. This gel was overlaid with 150 µl of water saturated isobutanol to smoothen the top edge of the gel. The gel was allowed to set for 5 – 10 minutes, the butanol layer poured off and the excess blotted off. The stacking gel was then poured over the separating gel, and a comb inserted to create wells. This was allowed to set for 10 minutes before the comb was removed. Wells were cleaned of excess gel by scraping with a fine needle. Protein samples were denatured as described above using similar reducing conditions. Electrophoresis was performed with 300ml of 1X SDS electrophoresis buffer at 150V.

Western blotting and protein detection

The XCell™ Blot Module (Invitrogen Life Technologies) was used to electroblot the gel onto a PDVF membrane. The gel and PDVF membrane were sandwiched between a piece of filter paper and 2 blotting sponges on either side, which had been presoaked in transfer buffer. The PDVF membrane was orientated towards the anode, and transfer was effected overnight at 50mA, 4°C, in transfer buffer containing 20% methanol and NuPAGE antioxidant (250 µl per 100ml buffer). The membrane was then stained with Ponceau S solution (Sigma) to check for effectiveness of transfer, rinsed in water, then blocked in blocking buffer (TBS-0.1% (v/v) Tween-5% (v/v) in Marvel trade mark TM milk powder dissolved in ddH_2O) for 1 hour at room temperature. Incubation with the primary antibody was carried out with 1:500 dilution of anti-cofilin antibody in 3-5 ml of blocking buffer, contained in a 50ml tube, at 4°C overnight. The tube was continuously rolled on the Spiramix 5 (Denley) to ensure that the antibody contacted the entire surface of the membrane throughout the period of incubation. This was followed by 3 washes with TBS-0.1% Tween (v/v), and a 1 hour incubation with the secondary antibody (anti-rabbit horseradish peroxidase conjugate),

diluted to 1:500 in blocking buffer. Chemiluminescent detection of the cofilin immunoreaction was by the ECL Western blotting analysis system (Amersham Pharmacia Biotech), and exposure to X-ray film in a dark room.

The same PDVF membrane was then probed for actin and tubulin proteins, after the membrane was washed in TBS-0.1% Tween (v/v). The primary antibodies, anti-β-actin (Sigma) and anti-β-tubulin (Developmental Biology Hybridoma bank) at 1:400 dilution, were added sequentially, incubating either for 2 hours at room temperature, or overnight at 4°C. Anti-mouse horseradish peroxidase (1:500 dilution) was used as the secondary antibody, and chemiluminescent detection performed as before.

Western blot quantitation by densitometry

The X-ray films were scanned using the GS-710 Calibrated Imaging Densitometer (BioRad), and the immunoblots quantified using the Quantity One program (BioRad). A volume rectangle was drawn around each spot, and the total pixel intensity within this was calculated as the 'volume'. The background pixel noise was subtracted from this to obtain the 'adjusted volume'. This reflected the intensity of the immunoreaction, and hence was taken to be an estimate of the quantity of a specific protein in the sample (cofilin, actin or tubulin). Proteins from the stably-transfected cells were measured against untransfected cells.

Timelapse confocal microscopy of U373 MG cells

Timelapse imaging of cells was performed to track cell movement, using the Leica TCS NT confocal system attached to the Leica DM IRBE Inverted microscope (Figure

Tracking cell movement

(37 degrees Celsius, 5% CO2)

Fig. 2.5 Timelapse confocal imaging of U373 glioma cells and analysis of cell movement

Transfected (green fluorescent) and untransfected cells were imaged in the same field for at least 2 hours. Controlled conditions of 37°C and 5% CO2 were maintained throughout. Cells were plated for 24-48 hours prior to imaging, and grown in 10% fetal calf serum, DMEM/F12 medium.

Movement analysis

Positions of cell nuclei at 5 minute intervals were tracked using the MacGap Debug (Dr. William Sellers) or Metamorph (Universal Imaging Corporation) programs. Distances travelled were calculated using Microsoft Excel analysis of the (x,y) coordinates of the nuclei.

(Bar: 100 μm)

2.5). Cells stably transfected with either the pCofilin-IRES2-EGFP or pEGFP-N1 were plated with untransfected cells in equal numbers on a single well (of a 6-well plate), and grown in standard medium a day before imaging. Transiently transfected cultures were imaged at least 1 day after transfection (1-8 days). Cells were imaged every 5 minutes in a single z series, for at least 2 hours, using the 10 X 0.3 NA dry HL Fluor lens. Controlled conditions were maintained in a climate chamber, at 37°C, 5% CO_2. Green fluorescence was detected by excitation at 488nm, with emission collected via the BP525/50 filter.

Movement analysis of U373 MG cells

The confocal images obtained were analysed using the MacGap Debug (Dr. William Sellers) or Metamorph (Universal Imaging Corporation) programs. Cell movement was determined by tracking the positions of cell nuclei at 5-minute intervals, over a period of at least 2 hours. Distances travelled by each cell was calculated using Microsoft Excel analysis of the (x,y) coordinates of its nucleus. The movement of at least 10 cells each from the transfected and untransfected groups were followed. Statistical analysis was performed using Microsoft Excel and SigmaStat programs.

II.IV PURIFICATION OF RECOMBINANT COFILIN BY ION-EXCHANGE CHROMATOGRAPHY

Cofilin was purified in order that it could be used as a positive control in Western blot detection of expression in U373 MG glioblastoma cells, together with protein derived from adult mouse brain. Recombinant cofilin was first produced in *E. coli* cells by transforming them with the pMW 172 plasmid (obtained from Dr. Michael Way, Imperial Cancer Research Fund, Lincoln's Inn Fields, London) encoding cofilin, then purified by eluting from an anion-exchange cellulose column, followed by adsorption onto a cation-exchange cellulose column. Finally, cofilin was retrieved by eluting off the cation-exchange column in a linear gradient of salt.

Production of recombinant cofilin in *E.coli*

Chemically-competent BL21 *E.coli* cells were transformed with the pMW 172 plasmid encoding cofilin by heat shock (as described in Part II.I, Molecular Biology). Cells were plated on selective LB agar plates with 50μg/ml ampicillin and grown overnight at 37°C. The following day, a loopful of colonies was picked up to inoculate 1 litre of 2XTY medium containing 50μg/ml ampicillin, and the transformed bacteria expanded by growing overnight at 37°C in a shaking incubator at 220 rpm. Induction of expression was encouraged by treating with 1mM isopropyl-β-D-thiogalactoside (IPTG) for approximately 4 hours. Cells were collected by centrifuging at 11,000g_{av} (10,000 rpm with the JA20 rotor) for 5 minutes in a Beckman JLA centrifuge.

Cells were lysed by the following method:

Fig. 2.6 Purification of recombinant cofilin through DE 52 anion-exchange and CM 52 cation-exchange columns

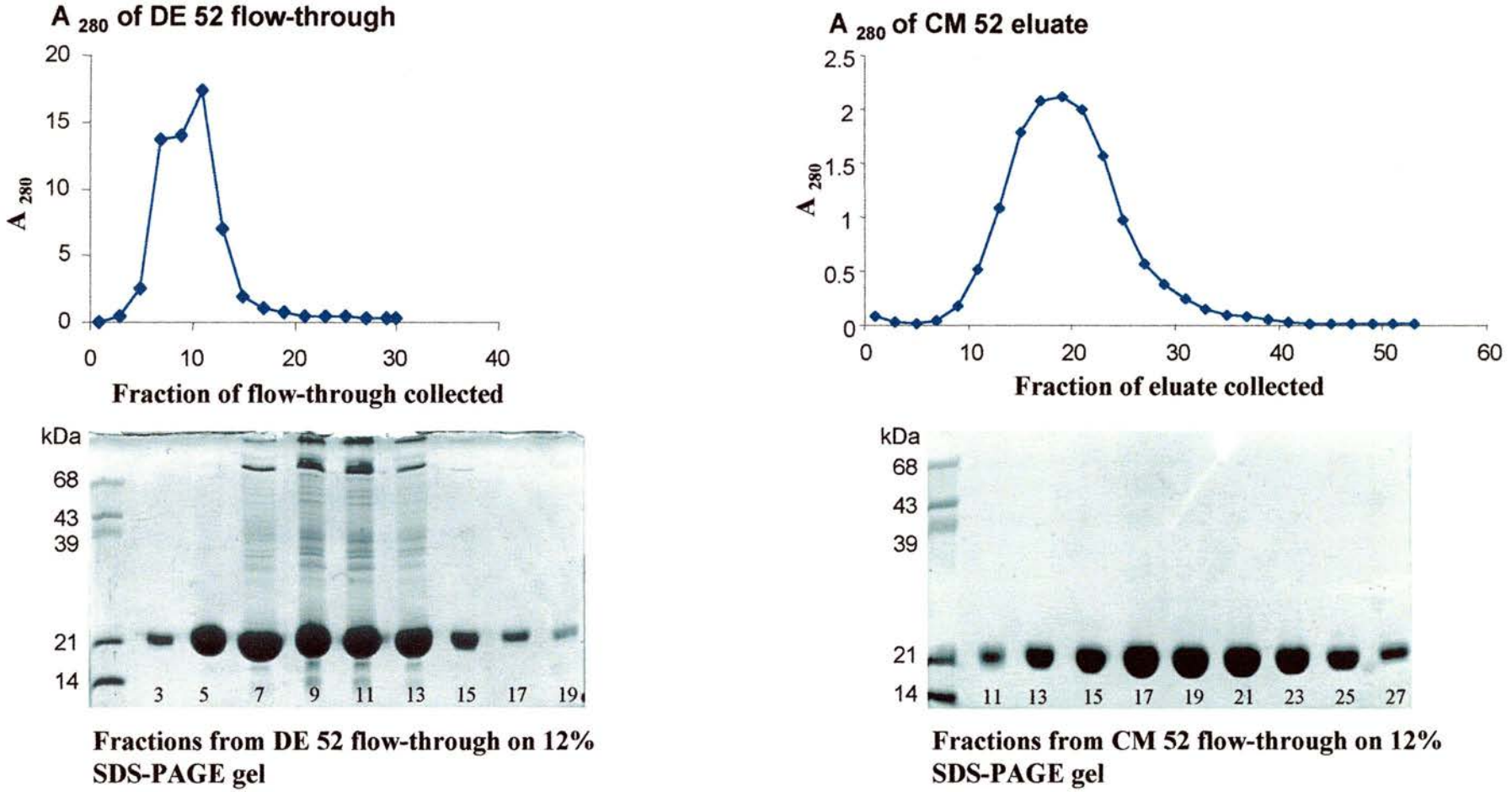

Fractions from DE 52 flow-through on 12% SDS-PAGE gel

Fractions from CM 52 flow-through on 12% SDS-PAGE gel

Recombinant protein produced in *E. coli* was purified by ion-exchange chromatography through DE 52 and CM 52 cellulose columns. The eluate from both columns was collected in fractions, and checked for the presence of cofilin (21kDa) by electrophoresis under denaturing conditions. Fractions with peak absorbance at 280nm (A_{280}) were collected from the DE 52 column, and passed through the CM 52 column to bind cofilin. Cofilin was finally eluted off CM 52, and the amount eluted monitered by A_{280}. The purity of cofilin was confirmed by denaturing electrophoresis.

The pellet obtained by centrifugation was frozen at - 20°C for 30 minutes, then thawed and collected in 25ml of lysis buffer. Cells were mixed well to break up clumps and refrozen at -20°C for a few hours to overnight. This was followed by thawing and sonication for 2 - 3 minutes to lyse cells, followed by a final cycle of freezing and thawing to maximise lysis.

240µl of 1M $MgCl_2$, 24µl of 1M $MnCl_2$ and 20µl of 10µg/ml of DNAse 1 (Sigma) were added to the lysate and incubated at room temperature with stirring for 30 minutes. The lysate was cleared by centrifugation at $11,000g_{av}$ for 30 minutes, and 1mM DTT was added to the supernatant which contains recombinant cofilin.

Purification of cofilin by ion-exchange chromatography

The supernatant was dialysed against 1 litre of DE 52 buffer (pH 8.0) at 4°C, then added to a DE 52 anion-exchange column (Whatman Ltd.) which had been pre-equilibrated with DE52 buffer. This column bound most bacterial proteins with pI less than 8.0 as they were negatively charged at pH 8.0. The flow-through, which contained cofilin, was collected in aliquots by a fraction collector, and assayed for the presence of proteins by measuring the absorbance at 280nm (A_{280}) (Figure 2.6). Samples were obtained from fractions with A_{280} equal to or exceeding 0.5 and electrophoresed under denaturing conditions on 12% polyacrylamide gels (w/v) (prepared as described in Part II.III, Protein Electrophoresis Using the BioRad System) to check for cofilin content. These fractions were pooled together and added to the CM 52 cation-exchange column (Whatman Ltd.) which had been equilibrated with CM 52 buffer (pH 8.0). Cofilin was positively charged and thus bound to the CM 52 column at this pH. This initial eluate was discarded and the column was washed

with 200ml of CM 52 buffer. Finally, cofilin was eluted off the column using a linear gradient of increasing KCl concentration. This gradient was achieved by running two reservoirs in series – the first containing 80 ml of CM 52 buffer with 200mM KCl, flowing into the second reservoir containing 80 ml of CM 52 buffer that was connected to the column. The eluate was collected in fractions and the yield of cofilin was monitered by A_{280}. Samples derived from fractions with A_{280} equal to or exceeding 0.5 were electrophoresed on 12% polyacrylamide gel (w/v) as before to determine the purity of extraction. The pooled fractions encompassing the peak range of A280 and hence containing high concentrations of cofilin were dialysed overnight at 4°C in 1 litre of 10mM Tris-Cl, pH 8.0 with 1mM sodium azide (as preservative) and 1mM DTT. DTT was added to retain the cysteine residues in the reduced state as oxidation causes cofilin to precipitate out of solution. Finally, purified cofilin was stored at 4°C.

Fig. 2.7 Generation of pBluescript KS II (-) vectors bearing coding sequences of human ADF, cofilin 1, and profilin 1

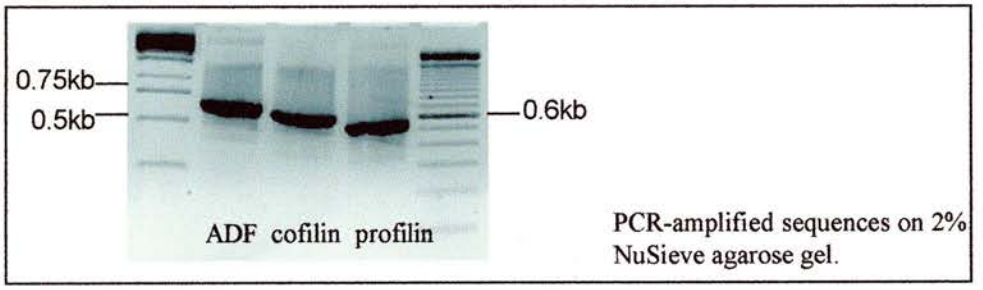

The coding sequences of ADF, cofilin and profilin were PCR-amplified from pMW172 vectors (obtained from Michael Way), digested with *Eco*R1 and *Xba*1, then subcloned into the EcoR1 and Xba1 sites in pBluescript II KS (Stratagene).

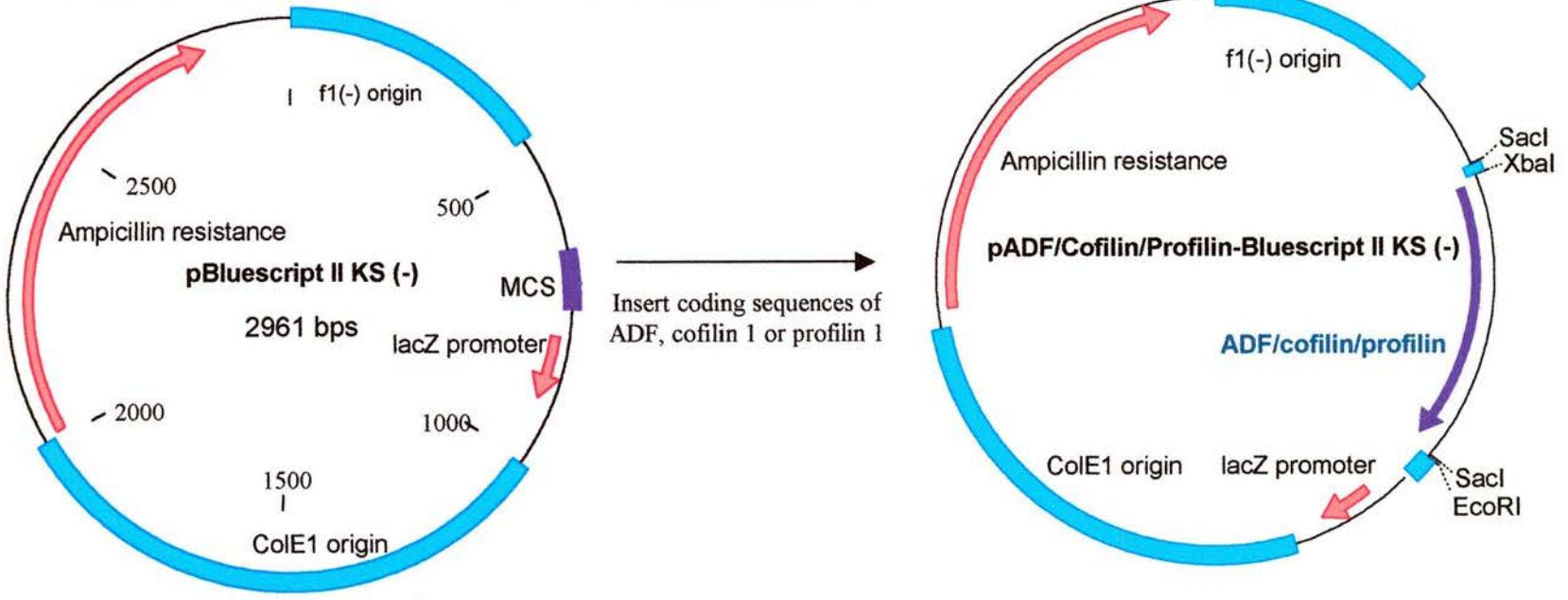

II.V RESULTS FROM MOLECULAR BIOLOGY PROCEDURES: CLONING THE CODING SEQUENCES OF COFILIN, ADF (ACTIN DEPOLYMERIZING FACTOR) AND PROFILIN INTO PLASMID EXPRESSION VECTORS

Construction of pBluescript II KS (-) vectors

The original pMW 172 plasmids encoding cofilin, ADF and profilin were designed for protein expression and contained the T7 promoter driving transcription in the sense direction only. In order to generate antisense riboprobes that could be used in in-situ hybridisation to detect expression of these genes, the coding sequences were subcloned into pBluescript II KS (-) (Stratagene). The inserts were orientated such that the T7 and T3 promoters drove the transcription of the sense and antisense probes respectively. Cloning was achieved by PCR amplification of the cDNAs in pMW 172, using the primers pMW 172 forwards (5'-AGG GAG ACC ACA ACG GT-3') and pMW 172 reverse (5'-GCT CAG CGG TGG CAG CAG-3'). These primers annealed to sites flanking the genes and were common to all the pMW 172 vectors used. The cDNAs were inserted into the *Xba*1 and *EcoR*1 restriction sites in the multiple cloning region of pBluescript II KS (-) (Figure 2.7). Recombinant plasmids were introduced into competent *E.coli* (DH5α strain) by heat shock, and plated onto ampicillin and X-gal-coated LB agar plates. This enabled the selection of transformed bacteria on the basis of ampicillin resistance and loss of β-galactosidase activity. Resistant white colonies were picked, and the recombinant plasmids obtained were checked for the presence of DNA inserts by restriction digests with *Xba*1 and *EcoR*1 (Figure 2.8). The sequences of the cofilin, ADF and profilin inserts were confirmed by fluorescent-

Fig. 2.8 Restriction digests of pBluescript plasmids with inserts obtained from transformed DH5α clones, electrophoresed on 1% agarose gel. 2 clones were tested for presence of each insert. Inserts were excised by double digests with *Eco*R1 and *Xba*1 (arrowed). Insert sizes: 608bp, ADF insert; 552bp, cofilin insert; 471bp, profilin insert.

The sequences of the inserts were confirmed by sequencing using the ABI Prism BigDye Terminator Cycle Sequencing Kit (Perkin-Elmer Applied Biosystems).

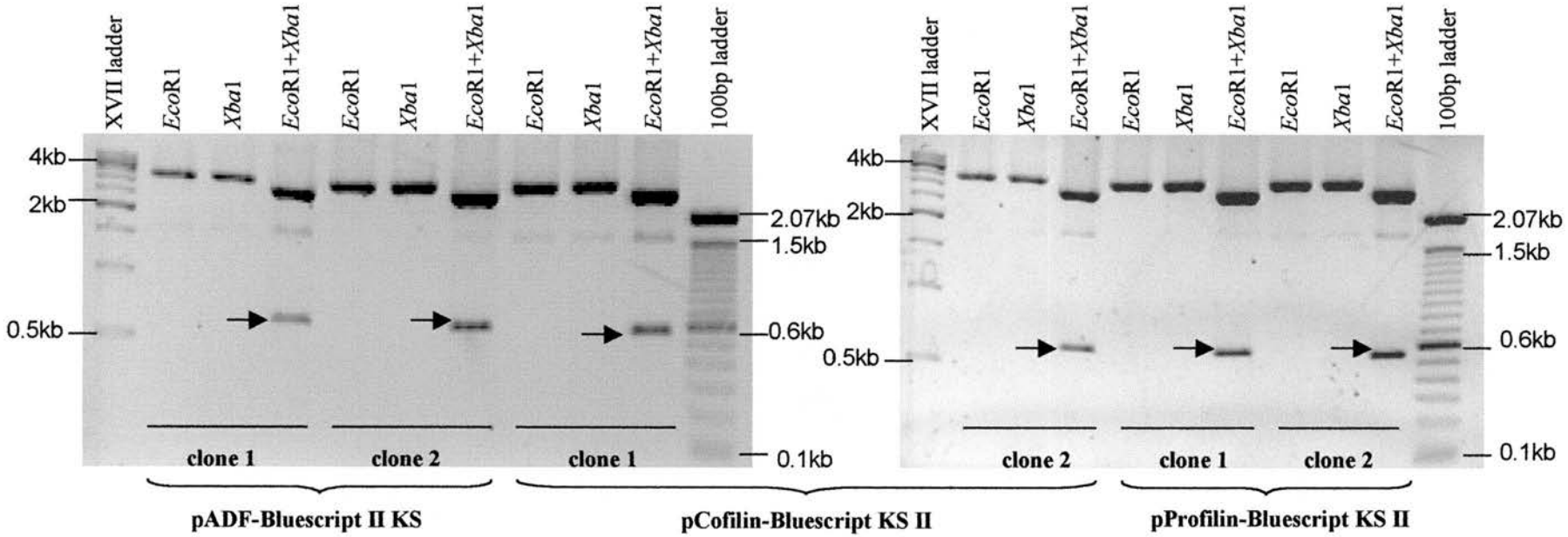

based cycle sequencing using the pUC-18R primer (5'-TGT TGT GTG GAA TTG TGA GC-3') and T7 primer (5'-ATT TAG GTG ACA CTA TAG-3'), which amplify from the regions outlying *Xba*1 and *EcoR*1 sites. The coding sequences inserted into pBluescript II KS (-) were identical to the published sequences of cofilin (Ogawa et al., 1990), ADF/destrin (Hawkins et al., 1993) and profilin (Kwiatkowski and Bruns, 1988). Comparisons of the cloned sequences with published data are displayed in Appendix F.

Construction of pIRES2-EGFP vectors

The pIRES2-EGFP vector contains the internal ribosome entry site (IRES) between the multiple cloning region and the enhanced green fluorescent protein (EGFP) coding region. This enables the cloned gene and EGFP to be translated from a single bicistronic mRNA in mammalian cells. The transcription of the cloned gene and EGFP is driven by a cytomegaloviral promoter (P_{CMV}). The detection of EGFP in U373 MG glioma cells which had been transfected by the recombinant plamids was used as a marker of gene expression. The vector carries a kanamycin/neomycin resistance gene, allowing stably transformed mammalian cells to be selected using the antibiotic, geneticin sulphate (G418).

The coding sequences of cofilin, ADF and profilin were subcloned from the pBluescript II KS (-) vectors into pIRES2-EGFP plasmids (Clontech laboratories Inc.), by ligating into *Sac*1 and *EcoR*1 restriction sites of the multiple cloning region (Figure 2.9). The recombinant plasmids were introduced into competent *E.coli* (SCS 110 strain) by heat shock, and transformed bacteria was selected in the presence of

Fig. 2.9 Generation of pIRES2-EGFP vectors bearing coding sequences of human ADF, cofilin 1 and profilin 1

The coding sequences for ADF, cofilin 1 and profilin 1 were subcloned from pADF/cofilin/profilin-Bluescript II KS (-) vectors into the pIRES2-EGFP vector (Clontech laboratories, Inc.), by ligation into *Eco*R1 and *Sac*1 restriction sites.

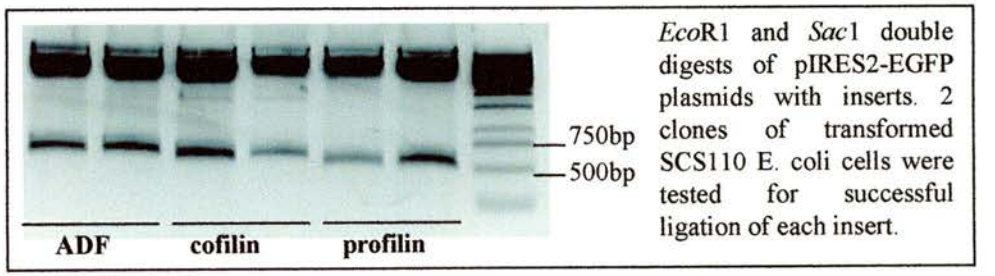

*Eco*R1 and *Sac*1 double digests of pIRES2-EGFP plasmids with inserts. 2 clones of transformed SCS110 E. coli cells were tested for successful ligation of each insert.

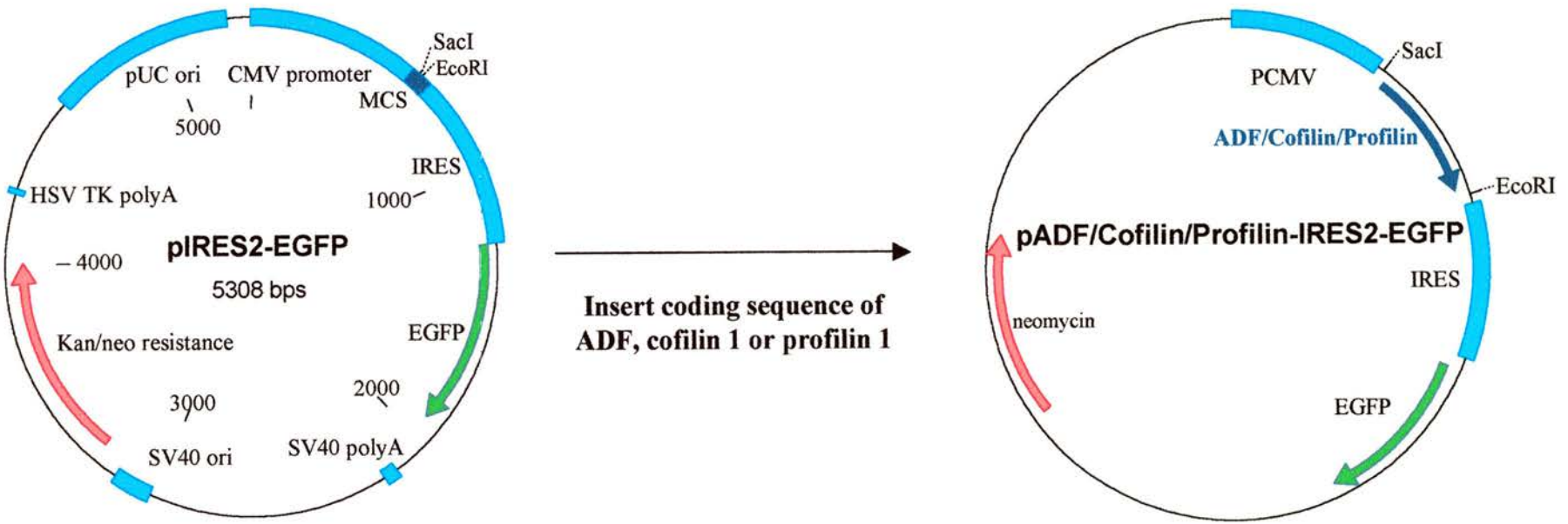

kanamycin at 100μg/ml. The identities of the DNA inserts obtained from resistant colonies were confirmed by restriction mapping (Figure 2.10).

Construction of pTRE vectors

pTRE is a response plasmid that is used to express the cloned gene in the inducible mammalian expression system, the Tet-Off Gene Expression System (Clontech laboratories Inc.). The Tet-Off system enables gene expression to be regulated under the influence of the antibiotic tetracycline, or its derivatives such as doxycycline (Gossen and Bujard, 1992). Gene expression is repressed more severely as the concentration of tetracycline/doxycycline increases (Clontech Tet Systems User Manual, protocol PT3001-1). By cloning the cofilin, ADF and profilin coding sequences into pTRE, it would be possible to examine the effects of different levels of protein expression in U373 MG cells transfected with these plasmids.

The coding sequences of cofilin, ADF and profilin were subcloned from pIRES2-EGFP vectors into the *Xba*1 restriction site of pTRE, together with the IRES-EGFP sequence (Figure 2.11). The IRES-EGFP sequence was included in order to identify gene expression in transfected U373 MG cells. The *Xba*1-cut pTRE vector was treated with calf intestinal phosphatase to dephosphorylate its 5' ends, before ligating with *Xba*1-restricted coding sequences. The ligation mix was desalted by ethanol precipitating the DNA and resuspending in water. This was then used to transform competent SCS 110 cells by electroporation, and transformed cells were selected in the presence of 50μg/ml ampicillin. *Xba*1 digests of recombinant plasmids confirmed the presence of the DNA inserts. Since the cloning had been non-directional, sense

Fig. 2.11 Generation of pTRE vectors bearing coding sequences of human ADF, cofilin 1, and profilin 1

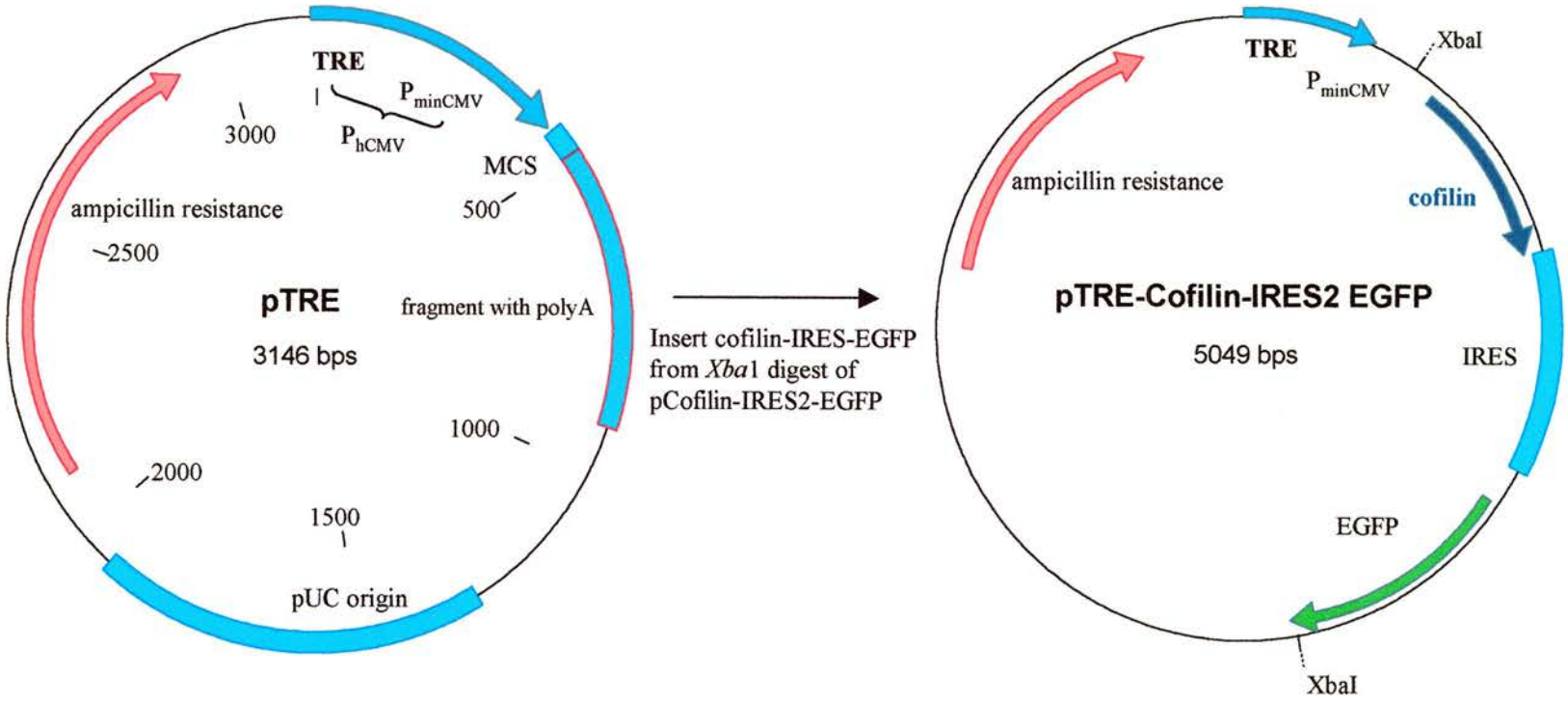

Fig. 2.12 Identification of pTRE constructs with cloned genes orientated in the sense direction

Sense constructs were identified by the sizes of the restriction fragments obtained using specific enzymes. The main identifying fragments are indicated below, with other expected fragments as bracketed. Arrowed digests indicate presence of sense constructs.

pTRE-ADF-IRES2-EGFP *Sac*1 digest:

Sense	617bp
	(53, 104, 617, 4331bp)
Antisense	1384bp
	(53, 104, 1384, 3564bp)

pTRE-Cofilin-IRES2-EGFP *Eco*R1 digest:

Sense	573bp
	(573,4476bp)
Antisense	1384bp
	(1384, 3665bp)

pTRE-Profilin-IRES2-EGFP *Eco*R1 digest:

Sense	492bp
	(492, 4476bp)
Antisense	1384bp
	(1384, 3584bp)

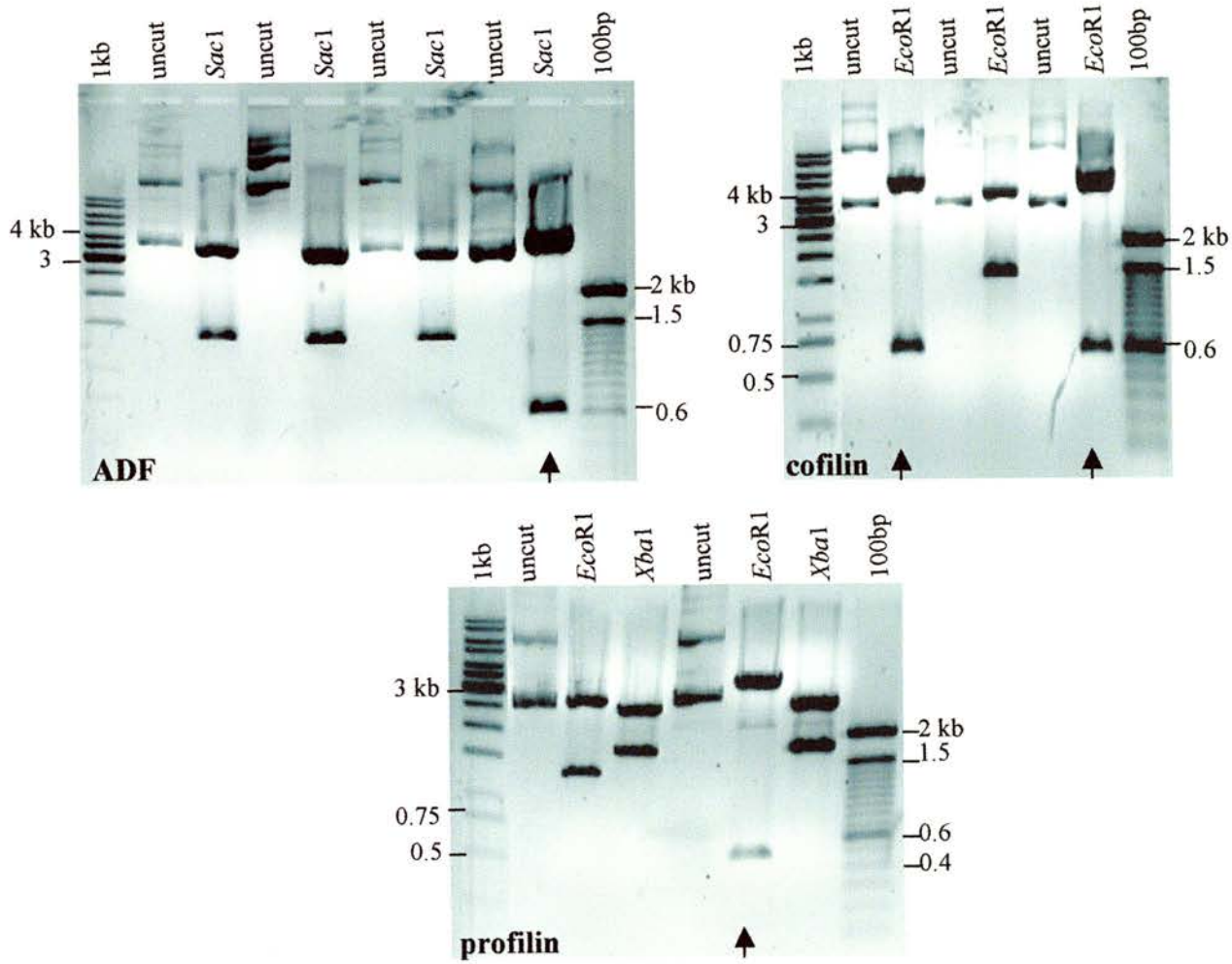

constructs were identified using other restriction enzymes: *EcoR*1 for cofilin and profilin constructs, and *Sac*1 for the ADF construct. These cut the cloned sequences into differently-sized fragments that were unique to either the sense or antisense orientation (Figure 2.12).

CHAPTER 3

EXPRESSION OF COFILIN AND OTHER ACTIN-BINDING PROTEINS IN THE EMBRYONIC MOUSE BRAIN AND U373 MG GLIOBLASTOMA CELLS

This chapter consists of two main parts. Part III.I is concerned with the expression of cofilin and actin depolymerizing factor (ADF) in the late embryonic mouse brain, determined using *in situ* hybridization. Part III.II characterises the expression of actin, cofilin and other actin-binding proteins in the U373 MG glioblastoma cell line used in the overexpression studies. Each part is written and discussed separately.

III.I EXPRESSION OF COFILIN AND ACTIN DEPOLYMERIZING FACTOR IN EMBRYONIC MOUSE BRAIN

INTRODUCTION AND SUMMARY OF METHODS USED

The transcription of cofilin and actin depolymerizing factor (ADF) genes was studied in the cortex of a wild-type mouse at embryonic day 17 (E17) by *in situ* hybridization. This relatively late age of gestation was chosen in order to investigate expression of these genes in the cortex at the final stages of embryonic development. It has been shown that ADF levels are highest in the central nervous system of embryonic chicks (Bamburg and Bray, 1987), suggesting that it is involved in the development of the nervous system. The activities of ADF and cofilin are required to reorganise the actin cytoskeleton during the formation of neuronal connections (Kuhn *et al.*, 2000; Meberg and Bamburg, 2000).

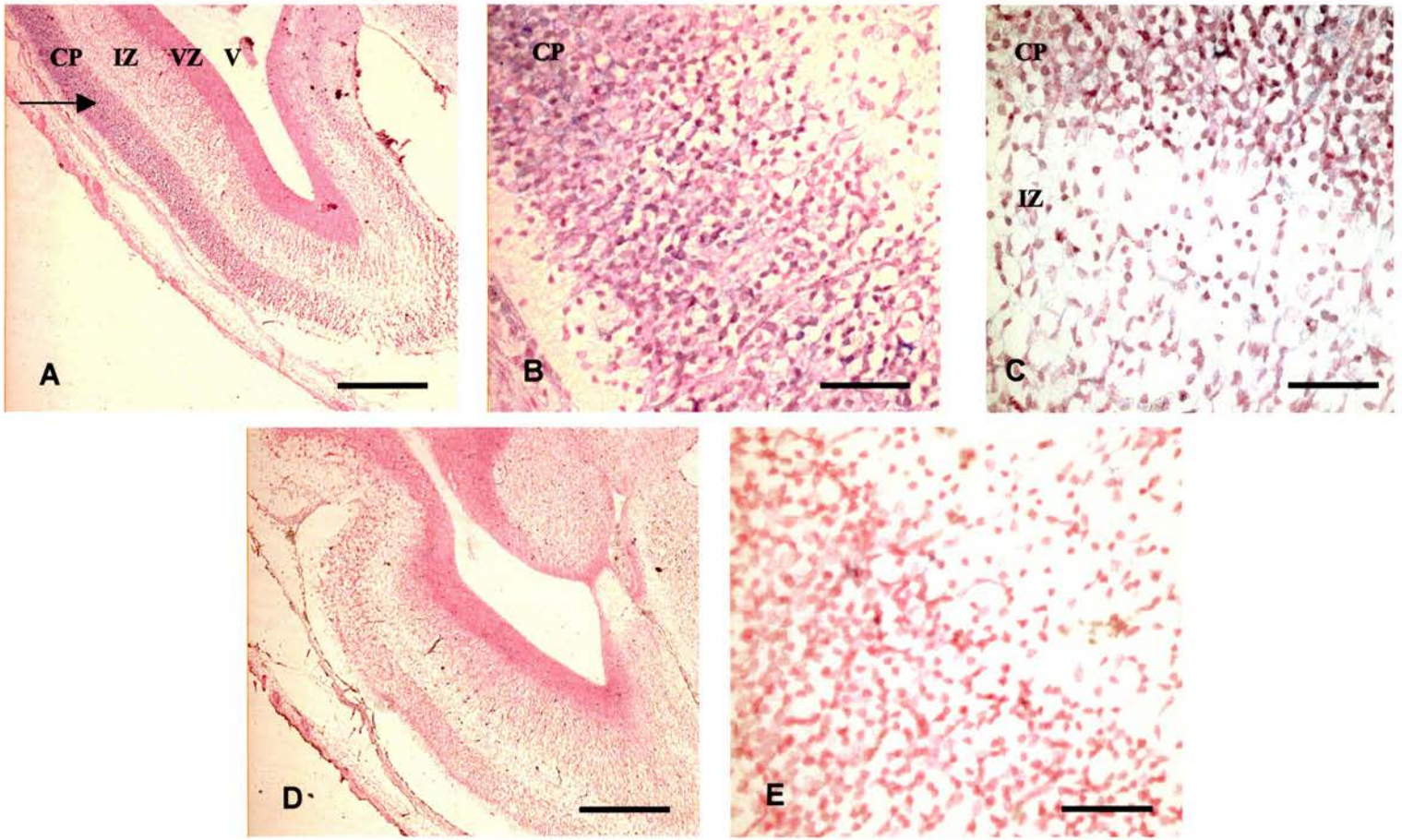

Fig. 3.1 In situ hybridization to detect expression of cofilin in embryonic mouse brain at age E17

DIG-labeled antisense riboprobe was used to detect cofilin expression in embryonic mouse brain by in situ hybridization. Positively stained cells appear dark purple when detected using NBT/BCIP substrate. Cells were counterstained with Nuclear fast red dye, so that negative populations appear pink. A & B: Cofilin was shown to be expressed mainly in the cortical plate of the embryonic cortex (arrowed). C: Cofilin expression in the intermediate zone. D & E: Control experiment using sense riboprobe showing negative staining. The cortical plate is shown at higher magnification in E. CP: cortical plate; IZ: intermediate zone; VZ: ventricular zone; V: ventricle. Bar: A,D: 500μm; B, C, E: 62.5μm.

RNA probes were generated from pBluescript KS II (-) vectors encoding these genes. The construction of these vectors are discussed in the Results section of Chapter 2. Sagittal sections of 10μm thickness were obtained from the E17 embryo which had been fixed in 4% paraformaldehyde (w/v) and embedded in paraffin. Prior to hybridization, sections were dewaxed in xylene, rehydrated in a graded ethanol series and permeabilized with Proteinase K. Sections were incubated with Digoxegenin (DIG)-labeled antisense riboprobes. DIG-labeled sense riboprobes were used to control for non-specific hybridization. Secondary detection of hybridization was achieved by treating with anti-DIG antibody conjugated to alkaline phosphatase. The chromogenic substrate NBT/BCIP (Nitroblue tetrazolium chloride/5-bromo-4-chloro-3-indoyl-phosphate) was used to detect alkaline phosphatase activity. The development of a deep purple colour indicated that the riboprobes had hybridized with the mRNA. Sections were counterstained with Nuclear fast red dye, so that cells in the cortex would be more easily visualized by the pink staining of their nuclei. The methods are recorded in detail in Chapter 2, Part II.II.

III.Ia Results of *in situ* hybridization using RNA probes for cofilin and ADF

Expression of cofilin and ADF in the cortex

mRNA expression of cofilin was present mainly in the cortical plate of the E17 cortex (Figure 3.1). Many of the cells in this region were positively stained, compared to the relative paucity in the intermediate and ventricular zones. However, the intermediate

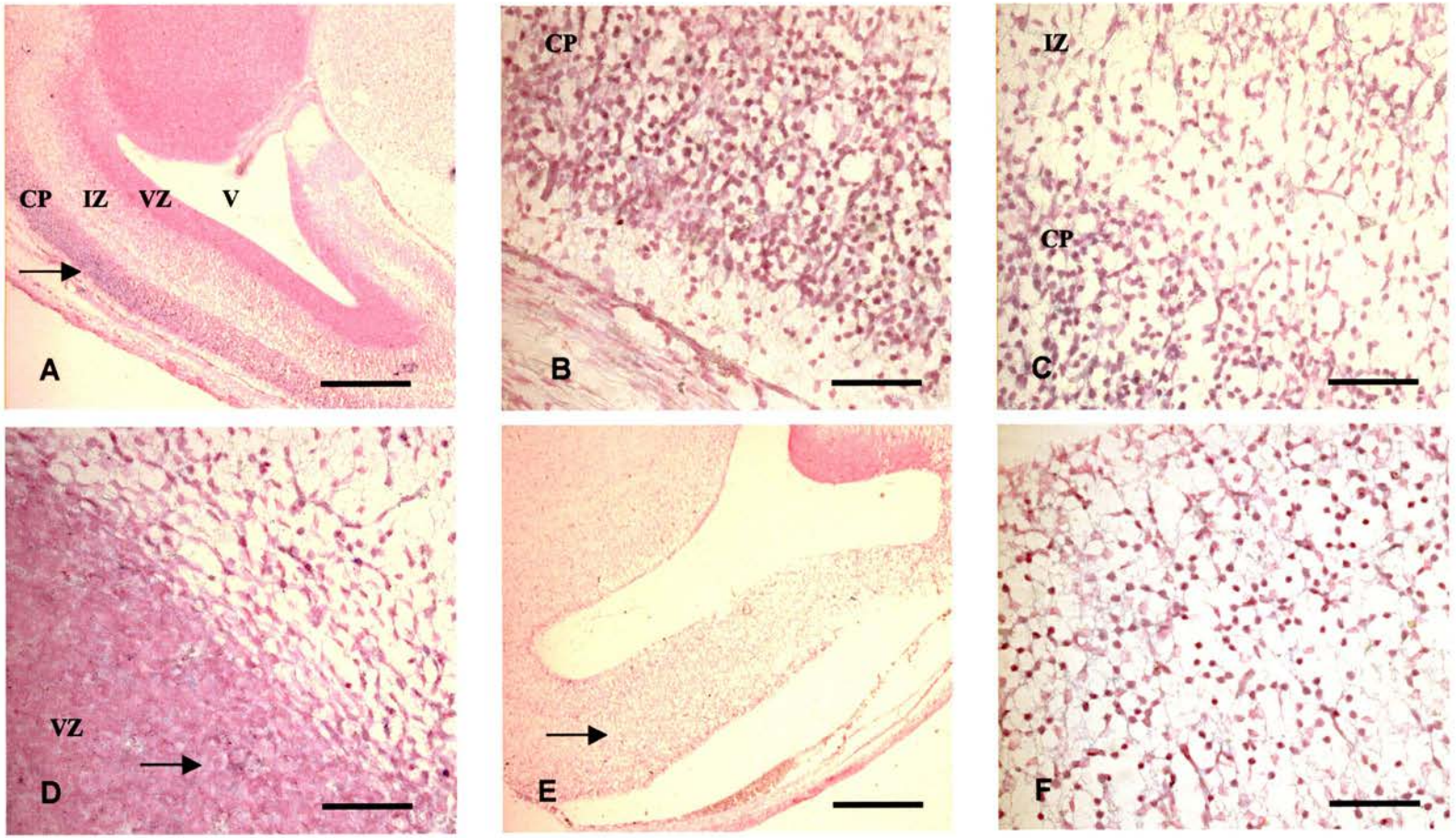

Fig. 3.2 In situ hybridization to detect expression of ADF (actin depolymerzing factor) in embryonic mouse brain at age E17

DIG-labeled antisense riboprobe was used to investigate ADF expression in embryonic mouse brain by in situ hybridization. Detection of hybridisation was by the NBT/BCIP substrate. Slides were counterstained with Nuclear fast red dye. A & B: ADF was expressed mainly in the cortical plate of the embryonic cortex (arrowed). ADF was also expressed in the intermediate zone (C) and ventricular zone (D) (arrowed). E & F: ADF expression in the midbrain. CP: cortical plate; IZ: intermediate zone; VZ: ventricular zone; V: ventricle. Bar: A, E: 500μm; B, C, D, F: 62.5μm.

zone also contained some positively stained cells. In the control experiment using the sense riboprobe, no hybridization was detected and cells stained pink with Nuclear fast red. Like cofilin, mRNA expression of ADF was concentrated mainly to the cortical plate, with fewer positively stained cells present in the ventricular and intermediate zones (Figure 3.2). In addition, cells in the midbrain expressed ADF. Hence, it appears that both cofilin and ADF colocalise to the cortex of the embryonic mouse in late gestation.

III.Ib Discussion

In situ hybridization indicates that cofilin and ADF are actively transcribed throughout the embryonic mouse cortex at E17. Transcripts were detected in high concentrations in the region of neuronal differentiation (cortical plate), and were present in some cells in the migratory zone (intermediate zone) and proliferative region (ventricular zone). The cortex develops by the generation of neuronal precursors at the ventricular zone, their migration outwards to the pial surface through the intermediate zone, and differentation in the outer cortical plate (Price and Willshaw, 2000).

Cytoskeletal remodeling is important in the development of the nervous system, and neuronal extensions appear to be dependent on actin assembly at the growth cones (Lin and Forscher, 1993). The activities of cofilin and ADF have been shown to be regulated during the formation of neuronal extensions (neurites) in response to growth factors (Meberg *et al.*, 1998). When the rat phaeochromocytoma cell line PC-12 is induced to differentiate into neurons by nerve growth factor (NGF), lamellipodia form

initially, which then extend as neurites. Both cofilin and ADF colocalise with actin filaments at the lamellipodia, accompanied by transient increases in the activated (dephosphorylated) forms of cofilin and ADF. Another supportive piece of evidence for the active roles of cofilin and ADF in neuronal growth comes from the observation that the overexpression of ADF in rat neurons increased the growth of neurites (Meberg and Bamburg, 2000). These findings suggest that these actin-binding proteins might be crucial to the differentiation of neurons, and possibly in the formation of neuronal connections that depend on growth cones.

Cell migration is an integral feature of cortical development. Neuronal precursors migrate from their sites of birth in the ventricular zone along the processes of glial cells, to reach the outer layers of the cortex (reviewed by Price and Willshaw, 2000). Cofilin and ADF are crucial for normal cell migration, as loss of the *Drosophila* ADF/cofilin results in the failure of migration in ovarian cells (Chen *et al.*, 2001). This is accompanied by accumulation of actin filaments, due to lack of ADF/cofilin-induced depolymerization. The finding that neuronal precursors in the intermediate zone actively transcribe cofilin and ADF reflects the requirement for these proteins in the turnover of the actin cytoskeleton as cells migrate.

High levels of ADF (Bamburg and Bray, 1987) have been identified in the brains of chick embryos. Cofilin is also present in relatively large amounts in the adult mouse brain (Moriyama *et al.*, 1990). It is known that cofilin and ADF are required in early embryonic development for cytokinesis. Moreover, tissues derived from the neuroectoderm in *Xenopus laevis* embryos express large amounts of ADF/cofilin (Abe *et al.*, 1996). These observations are consistent with the view that cofilin and ADF

have important roles in the development of the nervous system. The *in situ* detection of cofilin and ADF in the stratified layers of the E17 mouse cortex suggest that these actin-binding proteins function not only in early development, but also in the late embryonic stages of brain development. It is postulated that cofilin and ADF are important mediators of the actin filament dynamics in growth cones and neuronal extensions, necessary for the establishment of the neuronal network within the brain.

III.II EXPRESSION OF ACTIN, COFILIN AND OTHER ACTIN-BINDING PROTEINS IN U373 MG GLIOBLASTOMA CELLS

INTRODUCTION

The actin cytoskeleton and associated proteins involved in actin filament treadmilling were studied in glioblastoma cells. These studies elucidated some of the cytoskeletal components that operate in the motility of these tumour cells. The actin-binding proteins cofilin, ADF and profilin were shown to be expressed in U373 MG glioblastoma cells by reverse transcription-PCR, using primers specific to the cDNAs. Immunofluorescent microscopy was performed to characterise the distribution of cofilin in untransfected cells, as well as cells that had been transfected with either pCofilin-IRES2-EGFP or pEGFP-N1. These cells were immunostained for cofilin after growing in standard culture conditions using a polyclonal rabbit anti-human cofilin antibody (Cytoskeleton Inc.). The biological activity of cofilin was also investigated following stimulation of serum-starved cells with the addition of fetal calf serum. Immunodetection of actin in untransfected cells displayed the cytoskeletal pattern of motile and spreading cells plated on plastic culture dishes. The results

Fig. 3.3 Reverse transcription-PCR reveals innate expression of ADF, cofilin and profilin in the U373 MG glioblastoma cell line

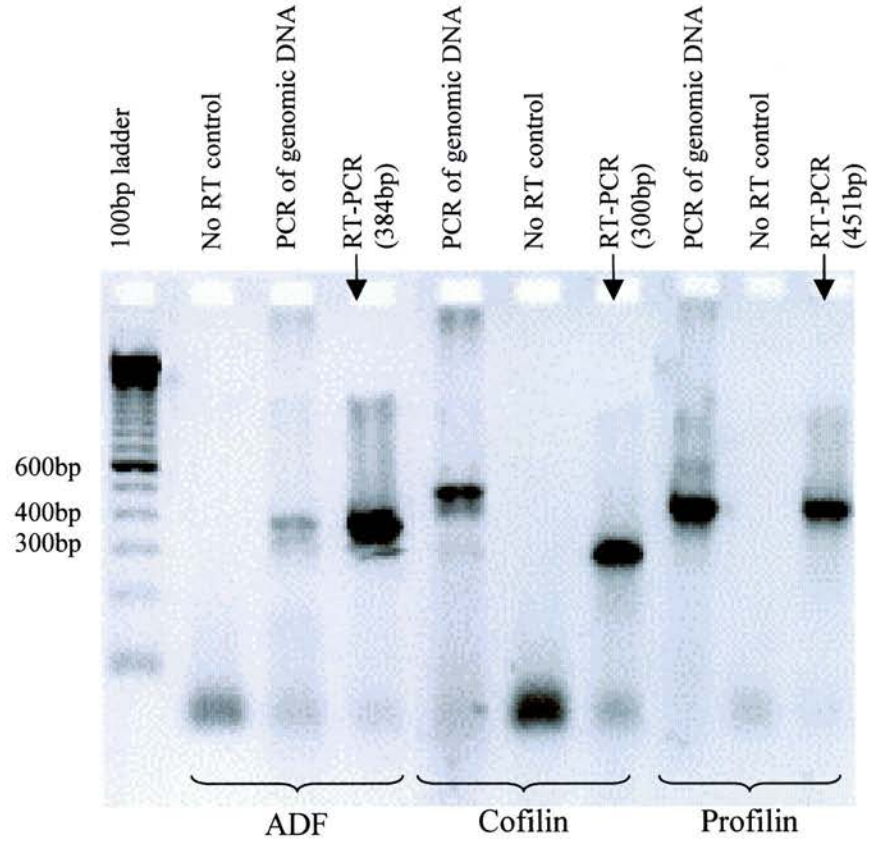

PCR products electrophoresed on 2% NuSieve GTG agarose gel.

RNA was treated with DNAse 1 before reverse transcription to remove contaminating DNA.

suggest that cofilin plays an active role at the ruffling membrane and leading lamellipodia of glioblastoma cells.

III.IIa Reverse transcription-PCR (RT-PCR) to detect expression of cofilin, ADF and profilin in U373 MG cells

Summary of methods in RT-PCR

RT-PCR was performed on total RNA extracted from untransfected U373 MG glioblastoma cells by the procedure described in Materials and Methods, Part II.I. PCR was carried out using primers that were specific for the cDNAs of cofilin 1, ADF and profilin 1. These primers were designed using the Primer3 Output program, with the following input: Pubmed accession numbers D00682 (cofilin 1), NM_006870 (ADF), J03191.1 (profilin 1). The PCR products were electrophoresed on a 2% NuSieve GTG agarose gel (w/v) alongside a 100bp molecular weight ladder. Control RNA samples contained no reverse transcriptase and were otherwise subjected to the same procedure. This was to ensure that the PCR products obtained had not been amplified from any contaminating genomic DNA. The sequences of the primers used are listed in Appendix G.

Results of RT-PCR detection of gene expression

RT-PCR revealed that U373 MG glioblastoma cells express cofilin, ADF and profilin. The PCR products obtained were of the expected sizes for cofilin at 300bp, ADF at 384bp, and profilin at 451bp (Figure 3.3). These products were absent in the control

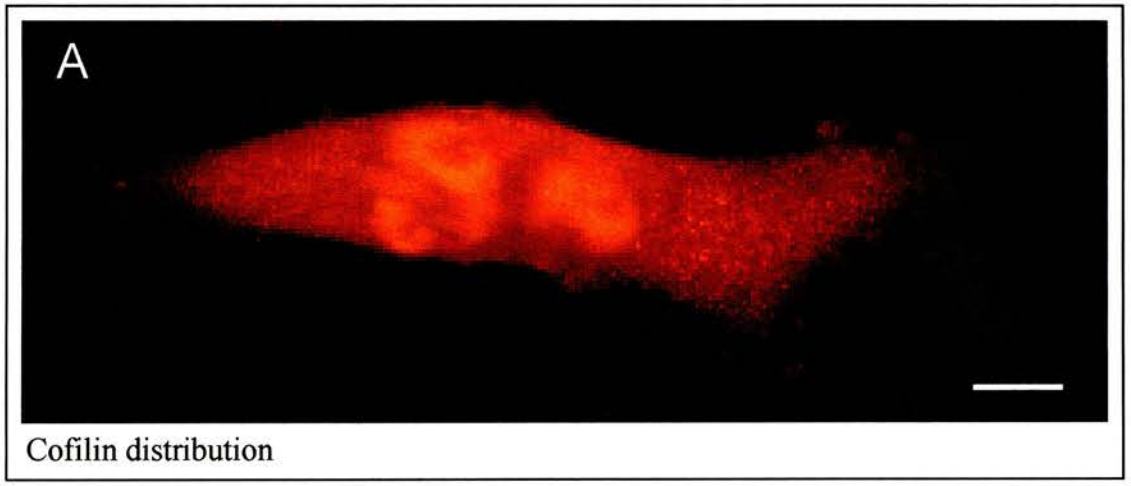

Cofilin distribution

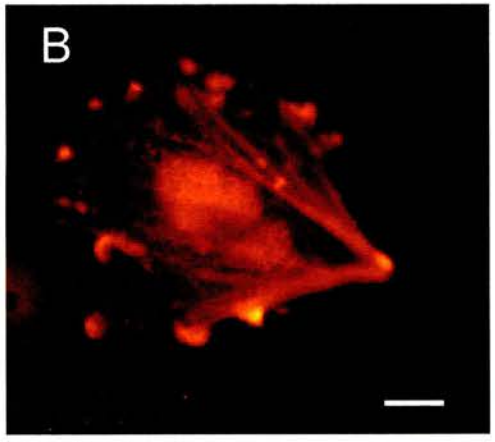

β-actin distribution

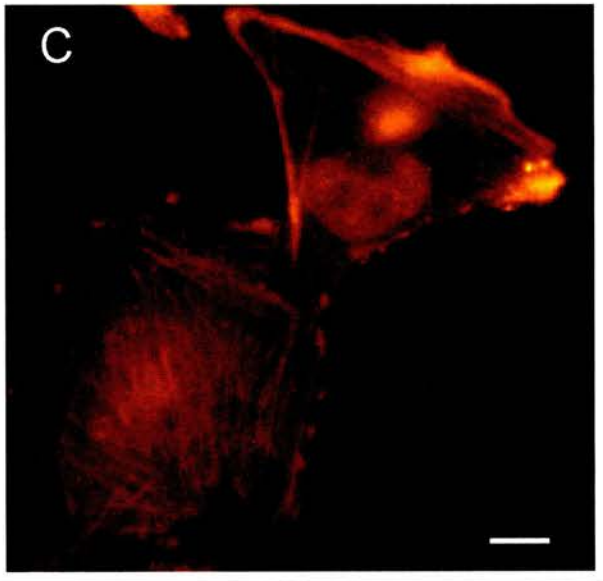

Fig. 3.4 Distribution of cofilin and β-actin in U373 glioma cells

Immunochemistry to locate cofilin and β-actin in U373 glioma cells was performed on cells fixed in 4% paraformaldehyde, and permeabilised with 0.1% Triton X-100. TRITC-conjugated secondary antibody was used for detection. Images were obtained with the Leica DC 200 digital camera connected to the Leica DMRB microscope.

A.Cofilin is detected in membrane ruffles, and diffusely distributed in the cytoplasm and nucleus.

B. & C. Actin is distributed in stress fibres, ruffling membranes, cortex and nucleus.

(Bar: 10μm)

samples, confirming that they had been amplified from the cDNA of these cells. This indicated that active transcription of these genes occurs in glioblastoma cells grown in standard culture conditions. Hence these cells possess the actin-binding proteins which are known to be crucial to actin filament dynamics in moving cells (see Introduction, Part II).

III.IIb Immunodetection of cofilin and β-actin in U373 MG cells

Summary of immunocytochemistry methods

Monolayer cultures of U373 MG cells were grown on chamber slides and fixed in 4% paraformaldehyde (w/v). Cells were permeabilised with 0.1% Triton X-100 (v/v) before incubation with anti-cofilin or anti-β-actin antibodies. TRITC or Alexa Fluor 546 secondary antibodies were used for fluorescent detection of the immunoreaction. Control reactions excluded the primary antibody so that background fluorescence arising from non-specific binding of the secondary antibody could be detected. Images were obtained using the Leica DMRE confocal microscope or the Leica DMRB microscope fitted with a digital camera. Detailed protocols can be found in Materials and Methods, Part II.III (Immunocytochemistry).

Results

Cofilin was shown to be localised to the ruffling membrane of U373 MG cells. It was also diffusely distributed within the cytoplasm and nucleus (Figure 3.4A). A similar pattern of distribution was observed when cofilin was overexpressed in cells which

Fig. 3.5 Distribution of cofilin in stable transfectants with pCofilin-IRES2-EGFP

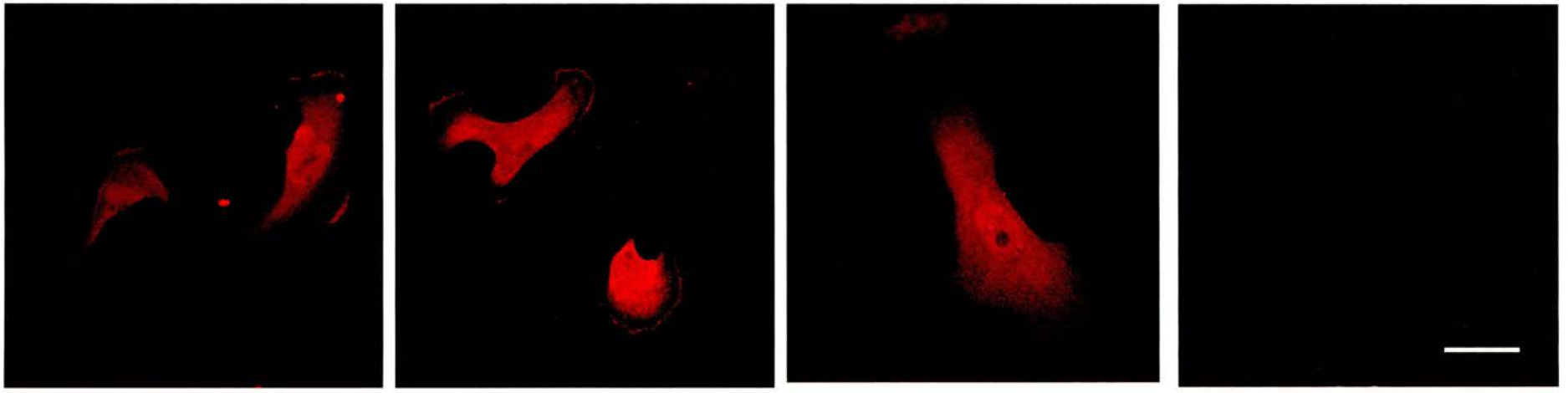

A B C D

A - C. Immunochemistry to detect cofilin expression in cells stably transfected with pCofilin-IRES2-EGFP (Cof 8 clone), grown in standard culture medium (DMEM/F12, 10% fetal calf serum). A & B. Cells displaying motile morphology. C. Spreading cell.

D. Negative control omitting the primary antibody (anti-human cofilin IgG).

Images were obtained using the Leica DMRE confocal microscope. (Bar: 50μm.)

had been stably transfected with pCofilin-IRES2-EGFP (Figure 3.5). In cells which presented a motile morphology, cofilin was especially pronounced at the leading lamellipodium, compared to the generalised cytoplasmic distribution in a spreading cell (Figure 3.5). Actin was distributed as stress fibres extending the length of the cytoplasm, at the ruffling membrane (Figure 3.4B), along the cortex of the cell (Figure 3.4C) and in the nucleus.

III.IIc Distribution of cofilin after serum stimulation of U373 MG cells

Serum stimulation of cells

U373 MG cells were grown in chamber slides under standard culture conditions for 24 – 72 hours. Cells were then serum-deprived for 24 hours, and stimulated by addition of 10% volume of fetal calf serum for up to 30 to 60 minutes. Cells were fixed and immunostained for cofilin using the methods described in Materials and Methods, Part II.III.

Results

When grown under standard conditions, cultures of glioblastoma cells exhibited heterogeneity of morphology. These consisted of cells with ruffling membranes, polarised cells with leading lamellipodia and spreading cells. Serum deprivation resulted in the withdrawal of ruffles and lamellipodia, and a large proportion of cells assumed a spindle-shaped appearance (data not shown). Addition of serum stimulated the formation of ruffles, and many cells appeared to regain a motile morphology with

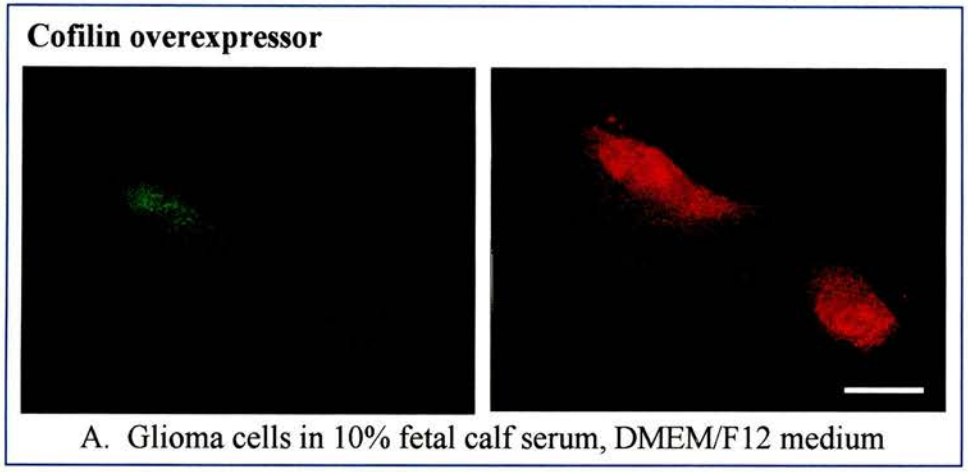

A. Glioma cells in 10% fetal calf serum, DMEM/F12 medium

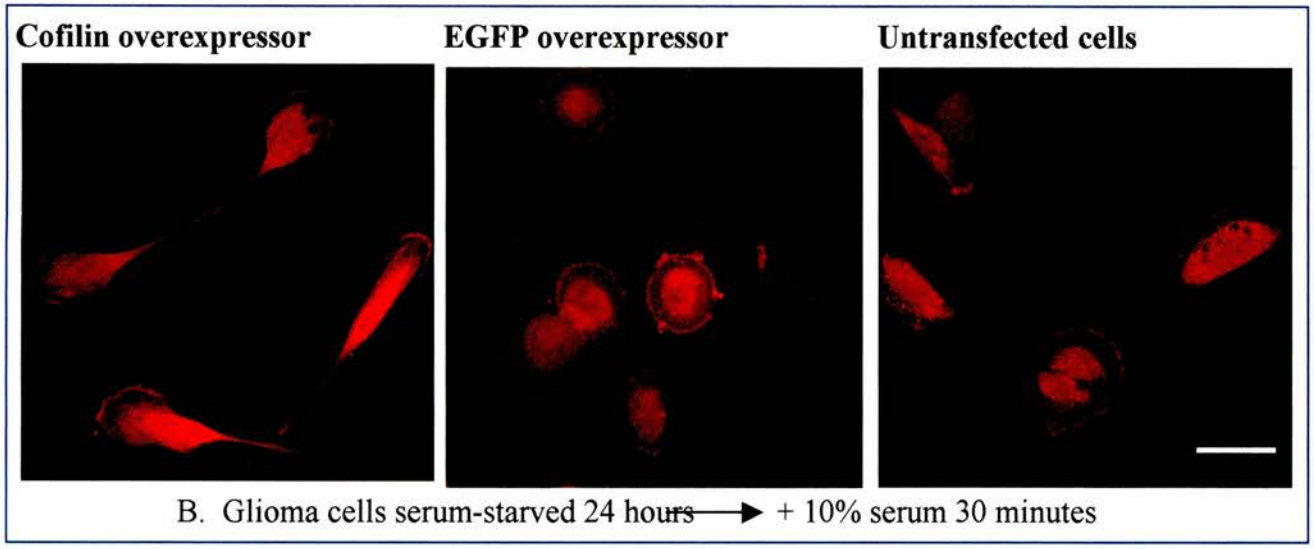

B. Glioma cells serum-starved 24 hours ⟶ + 10% serum 30 minutes

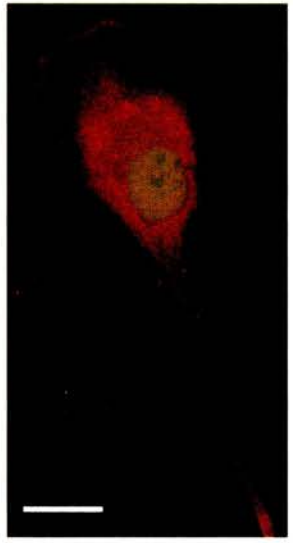

C. Overlay of GFP and TRITC images in a cofilin-overexpressing cell

Fig. 3.6 Recruitment of cofilin to the ruffling edge of U373 glioma cells

Untransfected U373 cells and cells stably overexpressing cofilin or EGFP were derived of fetal calf serum for 24 hours, then exposed to 10% serum for 30 minutes. Cells were fixed in 4% paraformaldehyde, permeabilised with 0.1% Triton X-100, and immunostained for cofilin (TRITC-conjugated secondary antibody). Confocal images were obtained using the Leica DMRE microscope. Bars: A: 25μm; B: 50μm; C: 20μm.

leading lamellipodia. Ruffles and lamellipodia stained intensely for cofilin (Figure 3.6). This was observed in untransfected cells, as well as cells that overexpressed cofilin and EGFP.

III.IId Discussion

The experiments demonstrated that U373 MG glioblastoma cells express the actin-binding proteins cofilin, ADF and profilin, which are necessary in motility driven by actin polymerization. Actin was distributed in stress fibres, membrane ruffles, along the cell cortex and in the nucleus. Cofilin was observed to be concentrated in the ruffling membrane and lamellipodia, and was also diffusely distributed in the cytoplasm and nucleus.

The dynamics of β-actin has been studied in live mammalian cells, using fluorescence microscopy of EGFP-β-actin fusion proteins in mouse melanoma cells (Ballestrem *et al.*, 1998). In stationary cells, actin was localised mainly to stress fibres and ruffles. In migrating cells, actin was concentrated in the lamellipodia, and also arranged in fibres running parallel to the leading edge. These actin-containing structures were observed in glioblastoma cells by fluorescent immunochemistry.

Nuclear colocalisation of actin and cofilin in glioblastoma cells is consistent with previous observations that cofilin can translocate to the nuclei and associate with actin in cells such as fibroblasts (Nishida *et al.*, 1987) and myotubes (Abe *et al.*, 1993). Intranuclear actin-cofilin rods were induced when these cells were heat-shocked or treated with dimethyl sulfoxide. However, cofilin is also present in the nuclei of

certain cells cultured under normal conditions, including fibroblasts (Iida *et al.*, 1992) and tumour cells (Samstag *et al.*, 1996). Malignant human T lymphoma cell lines and freshly recovered leukemic cells were found to constitutively harbour cofilin and actin in their nuclei. It has been suggested that nuclear localisation of cofilin might be important in the growth and survival of these tumour cells. The inactive, phosphorylated form of cofilin failed to localise within the nucleus, and a predominance of inactive cofilin induced apoptosis of cells. A nuclear localisation signal has been identified in cofilin, and consists of a stretch of five basic amino acids, KKRKK (Lys-Lys-Arg-Lys-Lys) (Iida *et al.*, 1992). It is postulated that this signal operates when cofilin and actin enter the nucleus as a complex. The experiments showed that cofilin and actin accumulate in the nuclei of glioblastoma cells under normal culture conditions, compatible with the observations reported in malignant lymphoma cells.

Localisation of cofilin to ruffling membranes and lamellipodia in glioblastoma cells reflects its activity in the formation of these structures. It has been shown that cofilin is recruited to motile regions in several cells, including *Dictyostelium discoideum* (Aizawa *et al.*, 1995) and mammalian cells (Bamburg and Bray, 1987; Chan *et al.*, 2000; Svitkina and Borisy, 1999; Yonezawa *et al.*, 1987). As discussed in the Introduction, cofilin participates in reorganising the actin cytoskeleton in these structures by depolymerizing and severing actin filaments.

Serum deprivation of glioblastoma cells caused the withdrawal of the motile structures, which re-emerged with the addition of 10% fetal calf serum (v/v). Serum starvation is known to alter actin cytoskeletal organisation. Serum-starved fibroblasts

lose stress fibres, focal adhesions and membrane ruffles (Ridley and Hall, 1992). This may be related to the loss of factors that stimulate actin assembly, including growth factors and phospholipids (such as lysophosphatidic acid). These factors appear to act via the Rho GTPases, Rho and Rac, to activate pathways leading to actin polymerization (Ridley and Hall, 1992; Ridley *et al.*, 1992).

Cofilin was recruited to ruffling membranes and lamellipodia following serum stimulation, in untransfected cells and cells which overexpressed cofilin and EGFP. Besides introducing growth factors, serum addition also induced an increase in the pH of the cytoplasm, and the increased intracellular pH stimulates cofilin activity (Bernstein *et al.*, 2000). Recruitment of cofilin to lamellipodia was observed when wounds were created in confluent cultures of serum-deprived fibroblasts, which introduced rapid transient increases in intracellular pH.

The precise localisation of cofilin at the lamellipodium appears to vary with cell type (Svitkina and Borisy, 1999). Cofilin is excluded from the most peripheral 0.3 - 0.7μm zone in *Xenopus laevis* keratocytes, whilst in fibroblasts cofilin is distributed throughout the entire leading edge. In keratocytes, cofilin has been shown to depolymerize and sever actin filaments mainly at the rear of the lamellipodium, where the pointed (slow-growing) ends of filaments are orientated towards the cell body (Svitkina and Borisy, 1999). At the front of the lamellipodium, the actin filament network (dendritic brush) is protected from disassembly by cofilin, possibly by Arp2/3 which caps pointed ends (Mullins *et al.*, 1998). The lack of cofilin activity at the extreme front of keratocytes is also consistent with its preferential binding to ADP-bound actin, present mainly towards the pointed ends of filaments (Maciver and

Weeds, 1994). Although cofilin is detected throughout the fibroblast lamellipodium, it is postulated that its activity might be limited by the association of Arp2/3 with filaments. The relative inactivity of cofilin away from the lamellipodia can perhaps be attributed to the protection of actin filaments from depolymerization within the cell body, by the presence of other filament-binding proteins such as tropomyosin (Bernstein and Bamburg, 1982). The binding of muscle-derived tropomyosin to actin filaments has been shown to prevent its disassembly caused by actin depolymerizing factor (ADF). Depolymerization by ADF/cofilin is therefore directed to filaments at the ruffling membrane as they lack tropomyosin (Wehland and Weber, 1980).

The distribution of cofilin in cells that had been transfected with pCofilin-IRES2-EGFP or pEGFP-N1 was similar to that in untransfected cells, when grown under normal conditions and after serum stimulation. This suggests that cofilin exhibited normal activity in the transfected populations, and was most likely regulated in a similar fashion as in wildtype cells. This information is relevant in interpreting the results of cofilin overexpression induced in U373 MG glioblastoma cells in Chapter 4.

CHAPTER 4

QUANTITATION OF COFILIN EXPRESSION IN U373 MG GLIOBLASTOMA CELLS STABLY TRANSFECTED WITH pCofilin-IRES2-EGFP AND pEGFP-N1 EXPRESSION VECTORS

INTRODUCTION

Cofilin expression in U373 MG human glioma cells which had been stably transfected with pCofilin-IRES2-EGFP and pEGFP-N1 was compared to untransfected cells by immunodetection. Preliminary data from Western blot analysis showed that stable transfectants with pCofilin-IRES2-EGFP overexpressed cofilin, and the anti-cofilin antibody used in immunodetection identified cofilin specifically. The levels of cofilin overexpression in the stable clones were quantified using flow cytometry. The methods employed are discussed in Chapter 2 (Part II.III).

In this study, flow cytometry afforded simultaneous measurements of both EGFP and Spectral Red fluorescence (for immunodetection of cofilin) in each glioma cell. The rapid measurements enabled a large number of cells to be analysed at a time, so that populations of cells could be compared against each other. The data that was derived from each population included the percentage of positively immunostained cells, and the intensity of fluorescence.

The intensity of immunofluorescence has been widely used to reflect the level of antigen expression in cells. This has proved useful, for example, in the characterization

of haematological malignancies, based on quantifying the density of specific antigens in tumour cells (Almasri et al., 1992; Caldwell and Patterson, 1991; Lavabre-Bertrand, 1996). A similar approach was taken to quantify cofilin expression in stably transfected and untransfected U373 MG glioma cells, where the mean intensities of cofilin immunofluorescence were compared.

IV.I Determination of cofilin expression by Western blotting

Summary of methods used in Western blotting

Cells were harvested and their proteins were extracted and quantified. Cellular proteins were electrophoresed under reducing and denaturing conditions and blotted onto PDVF membranes. Blots were probed for cofilin using rabbit anti-human cofilin IgG, and a secondary antibody conjugated to horseradish peroxidase. The immunoreaction was detected on X-Ray films by chemiluminescence, in the presence of luminol, which emits light following oxidation by horseradish peroxidase (ECL Western blotting detection system, Amersham Pharmacia, manufacturer's notes). Protein loading was compared between lanes by standardizing against relative amounts of β-actin and β-tubulin immunodetected on the same blot. Films were scanned using the GS-710 Calibrated Imaging Densitometer (BioRad), and quantified with the Quantity One™ program. The detailed methods are described in Chapter 2, Part II.III (Protein electrophoresis and Western blotting).

Fig 4.1 Specificities of anti-cofilin, anti-β-actin and anti-β-tubulin antibodies

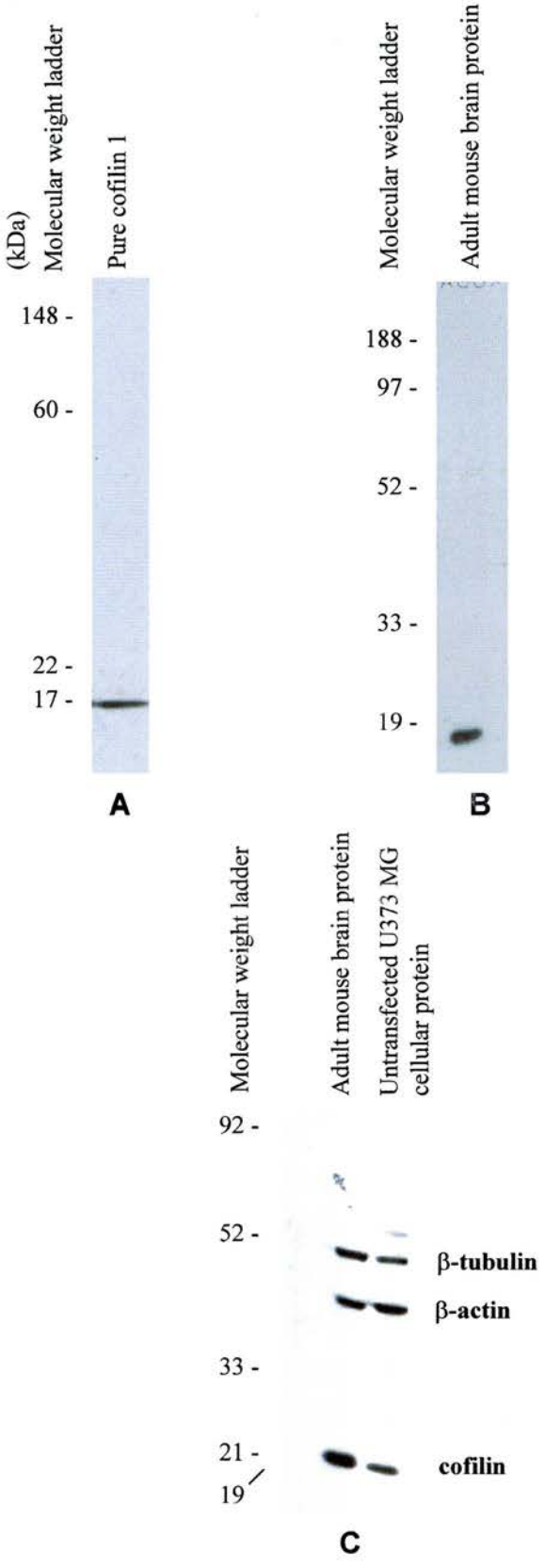

A, B. Immunoblots with anti-cofilin antibody, identifying single bands for pure cofilin 1 and adult mouse brain proteins.

C. Immunoblot with combined detection of b-actin, b-tubulin and cofilin in proteins extracted from adult mouse brain and untransfected U373 MG cells.

Positions of the molecular weight ladders are indicated. Weights are in kiloDaltons.

Results

Specificities of anti-cofilin, anti-β-actin and anti-β-tubulin antibodies

The specificities of the primary antibodies used were tested by immunoblotting aliquots of pure cofilin protein (prepared as described in Chapter 2, Part II.IV, Purification of Recombinant Cofilin by Ion-exchange Chromatography) and total protein from adult mouse brain, prepared by lysing the homogenate in TENT buffer (see Protein extraction, Chapter 2, Part II.III). The anti-cofilin antibody (rabbit anti-human cofilin IgG, Cytoskeleton Inc.) identified a single band in adult mouse brain protein at approximately 17 - 19kDa, similar to the band obtained by immunoblotiing pure cofilin. The anti-β-actin and anti-β-tubulin antibodies identified bands at about 42kDa and 55kDa respectively (Figure 4.1). These molecular weights are consistent with those reported in databases: cofilin 1, Swissprot accession number P23528 (18.5kDa); β-actin, Swissprot accession number P02570 (41.7kDa); β-tubulin, IPI accession number IPI00013475 (49.9kDa). The molecular weights of the proteins identified were calculated from linear graphs derived by plotting relative mobility and log molecular weight, based on the Multimark multi-coloured molecular weight standard (Invitrogen Life Technologies). (This method of molecular weight determination is discussed by Ausubel F. M. et al, 2000).

Expression of cofilin in stable clones as determined by Western blotting

Cofilin expression in stable clones was compared to untransfected cells, using the expression of β-actin and β-tubulin as loading controls. Data from Western blot

Fig. 4.2 Western blots on stable clones to detect cofilin expression

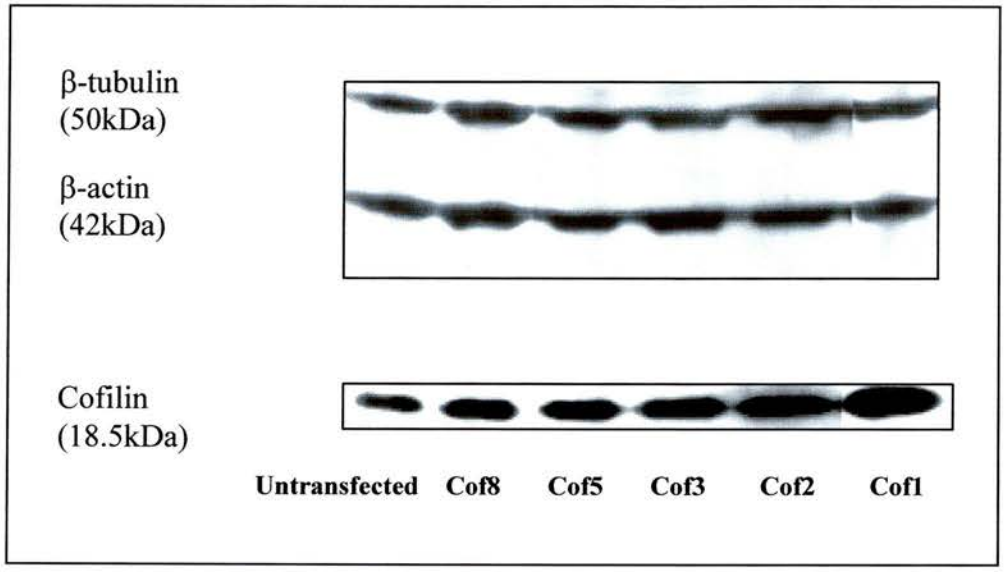

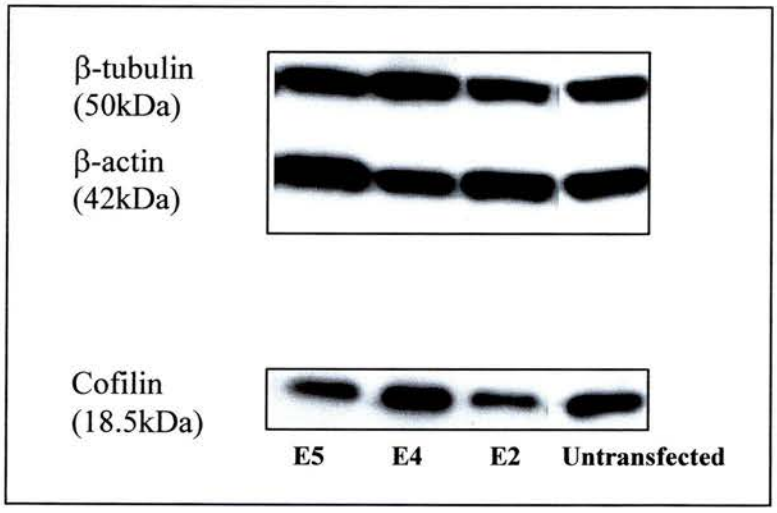

Cof1, 2 3,5, 8: stable clones transfected with pCofilin-IRES2-EGFP

E2, 4, 5: stable clones transfected with pEGFP-N1

analysis suggested that clones derived from transfection with pCofilin-IRES2-EGFP expressed higher levels of cofilin compared to untransfected cells. Cofilin expression in control clones transfected with pEGFP-N1 was similar to that in untransfected cells (Figure 4.2). In order to quantify the levels of cofilin expression in stable transfectants more precisely, flow cytometric analysis of cofilin immunofluorescence was performed.

IV.II. Quantitation of cofilin expression in stable clones by flow cytometry

Summary of methods used in flow cytometry

Cells were prepared for immunodetection of cofilin with rabbit anti-human cofilin IgG, as detailed in Chapter 2, Part II.III (Immunocytochemistry). The Coulter EPICS XL Cytometer was used, and results were analysed with the Expo^{TM} 32 ADC Analysis software. 10,000 cells were analysed for each sample, and the analysis was restricted to viable cells by gating on the basis of forward scatter (related to cell size) and side scatter (related to cell granularity) (Figure 4.4). These cells lay within gate A, and the data collected were displayed on logarithmic scales ($\log_{10}$).

In order to separate the green (EGFP) from the red fluorescent signals, an anti-rabbit Spectral Red-conjugated secondary antibody was selected to detect cofilin immunoreaction. Spectral Red is a phycoerythrin-cyanin 5 (PE-Cy5) fluorochrome derived from covalent coupling of R-phycoerythrin to the synthetic dye cyanine-5 (manufacturer's notes). Both EGFP and Spectral Red are excited at the same

Fig.4.3 Flow cytometry settings for fluorescence detection based on isotype negative control for untransfected U373 MG cells

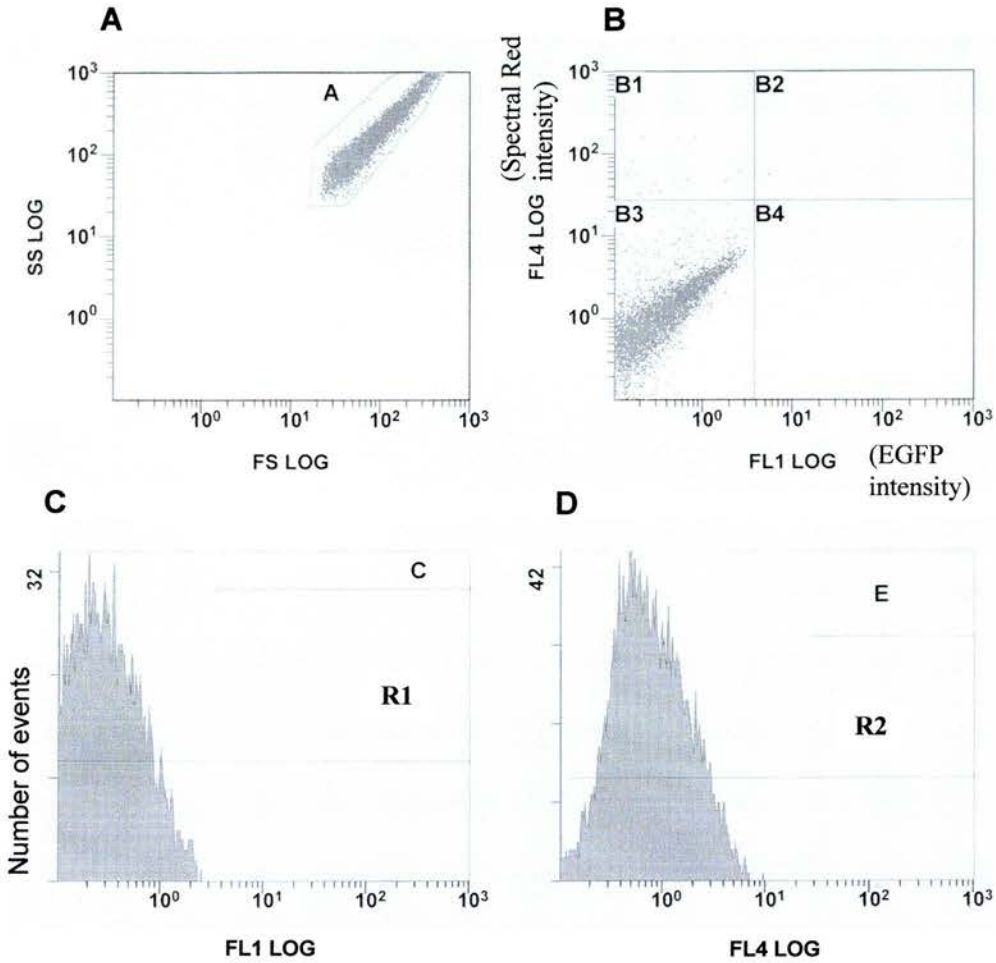

A. Viable cells were gated for analysis on the basis of forward scatter (FS log) and side scatter (SS log).

B. Background fluorescence for EGFP (FL1 log) and Spectral Red conjugate (FL4 log) were set below 10.

C. Histogram plot of number of cells distributed in the FL1 channel (EGFP). R1: 100% gated cells.

D. Histogram plot of number of cells distributed in the FL4 channel (Spectral Red conjugate). R2: 100% gated cells.

wavelength (488nm), but have different emission spectra. This allows the fluorochromes to be distinctly detected (Table 4.1), thus minimizing false positive signals arising from cross-detection of fluorescent emission. EGFP fluorescence was detected in the FL1 channel (plotted as FL1 log), whilst the Spectral Red fluorescence was detected in the FL4 channel (plotted as FL4 log).

Control experiments included cells which were not incubated with anti-cofilin antibody, as well as cells treated with an isotype control primary antibody (Chapter 2). Based on these controls, signal amplification was set so that the mean background Spectral Red fluorescence (mean FL4 log) was below 10. The mean background EGFP fluorescence (mean FL1 log) was also set below 10, based on detection in untransfected cells (Figure 4.3).

Results

Correlation between EGFP fluorescence and cofilin (Spectral Red) immunofluorescence

Simultaneous measurements of the intensities of EGFP and cofilin immunofluorescence (Spectral Red) in untransfected and transfected U373 MG cells are presented in Figure 4.4. Spectral Red intensity (FL4 log) was plotted against EGFP intensity (FL1 log). The distribution of fluorescence intensities in cells stably transfected with pCofilin-IRES2-EGFP suggests that levels of cofilin overexpression correlated with EGFP expression in a population of cells derived from the same clone.

Table 4.1 Determination of cofilin expression levels by immunochemistry: relative quantitation of fluorescence intensity by flow cytometry

Primary Ab: Polyclonal rabbit anti-human cofilin @ 1:100 (ie. 2.5mg/L) (Cytoskeleton Inc.)

Secondary Ab: Goat anti-rabbit IgG (H+L specific) Spectral Red conjugate @ 1:100 (Cambridge Bioscience)

Controls: 1. Isotype control: Rabbit anti-mouse immunoglobulins @ 1:100 (ie. 2.8mg/L) (Dako)

2. No primary antibody

	Peak excitation	Peak emission
EGFP	488nm	507nm
Spectral Red	488nm	667nm

} Minimal spectral overlap in detection

The data on fluorochromes was obtained from the manufacturers for EGFP (Clontech laboratories Inc.) and Spectral Red conjugate (Cambridge Bioscience).

Fig. 4.4 FL4 log (cofilin immunofluorescence) versus FL1 log (EGFP)

Untransfected cells

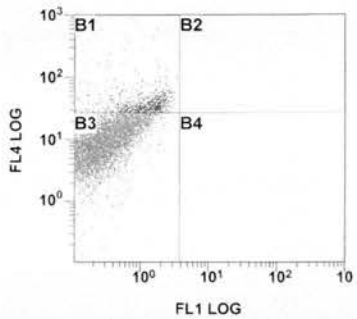

pEGFP-N1 transfected cells (E2 clone)

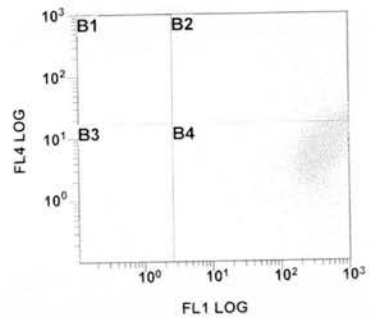

pEGFP-N1 transfected cells (E4 clone)

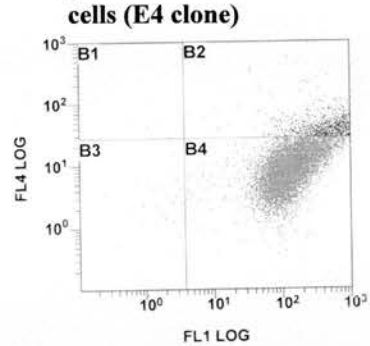

pEGFP-N1 transfected cells (E5 clone)

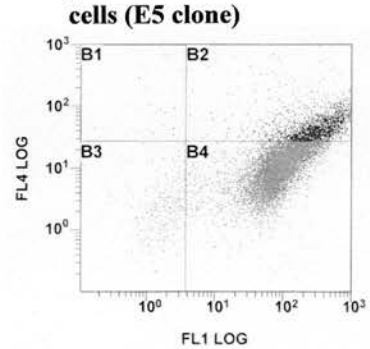

pCofilin-IRES2-EGFP transfected cells (Cof1 clone)

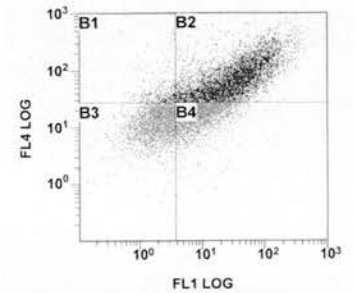

pCofilin-IRES2-EGFP transfected cells (Cof3 clone)

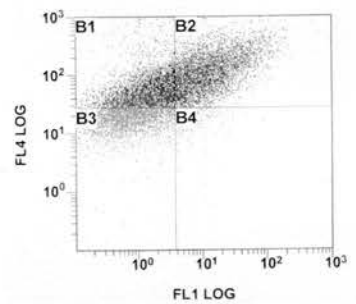

pCofilin-IRES2-EGFP transfected cells (Cof5 clone)

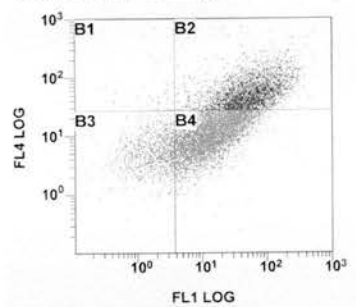

pCofilin-IRES2-EGFP transfected cells (Cof7 clone)

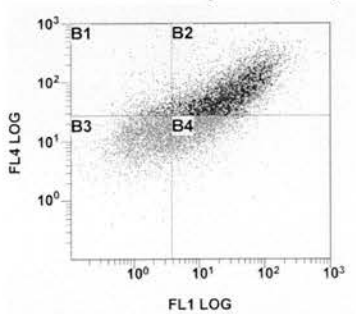

pCofilin-IRES2-EGFP transfected cells (Cof8 clone)

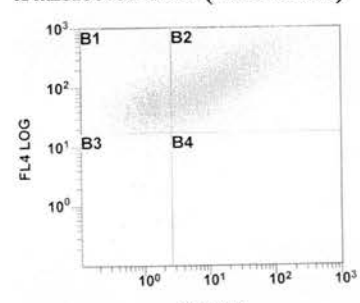

Table 4.2 Ratio of means of FL4 log (transfected:untransfected) calculated from two flow cytometry sessions, performed under similar experimental conditions

Stable Clones with pCofilin-IRES2-EGFP	Mean FL4 log of stable clones:untransfected cells (Experiment 1)	Mean FL4 log of stable clones:untransfected cells (Experiment 2)
Cof 5	2.3	-
Cof 7	4.4	3.4
Cof 1	4.5	4.9
Cof 8	-	7.0
Cof 3	7.2	-

Stable Clones with pEGFP-N1	Mean FL4 log of stable clones:untransfected cells	Mean FL4 log of stable clones:untransfected cells
E2	-	0.7
E4	1.1	0.6
E5	1.5	1.1

A ratio of 1 denotes that the mean FL4 log is equal to untransfected cells.

On average, cells expressing higher levels of cofilin were also expressing higher levels of EGFP.

Comparison of cofilin expression levels in stable clones

The mean Spectral Red fluorescent intensity, as indicated on the FL4 log axis of each transfected population of 10,000 cells, was compared against the untransfected population. This reflected the level of cofilin expression in the different populations, as detected by immunochemistry. EGFP fluorescence was recorded on the FL1 log axis. Comparisons of the mean FL4 intensities of the transfected and untransfected populations are shown in Figures 4.5 A-F.

Mean FL4 log intensities of cells in gate A confirmed that cells that had been stably transfected with pCofilin-IRES2-EGFP overexpressed cofilin. The average Spectral Red immunofluorescence in these cells ranged from approximately 2 – 7 times higher than untransfected cells. In contrast, the mean intensities of cofilin immunofluorescence in control cells stably transfected with pEGFP-N1 were comparable to untransfected cells (Table 4.2). This indicates that the overexpression of cofilin had not been induced in the control populations. The data is presented graphically in Figure 4.6.

IV.III Discussion

Flow cytometric measurements of the stable clones transfected with pCofilin-IRES2-EGFP enabled relative levels of cofilin overexpression to be quantified in several

Fig. 4.5A Fluorescence levels of EGFP (FL1 log) and Spectral Red conjugate (FL4 log) in untransfected cells

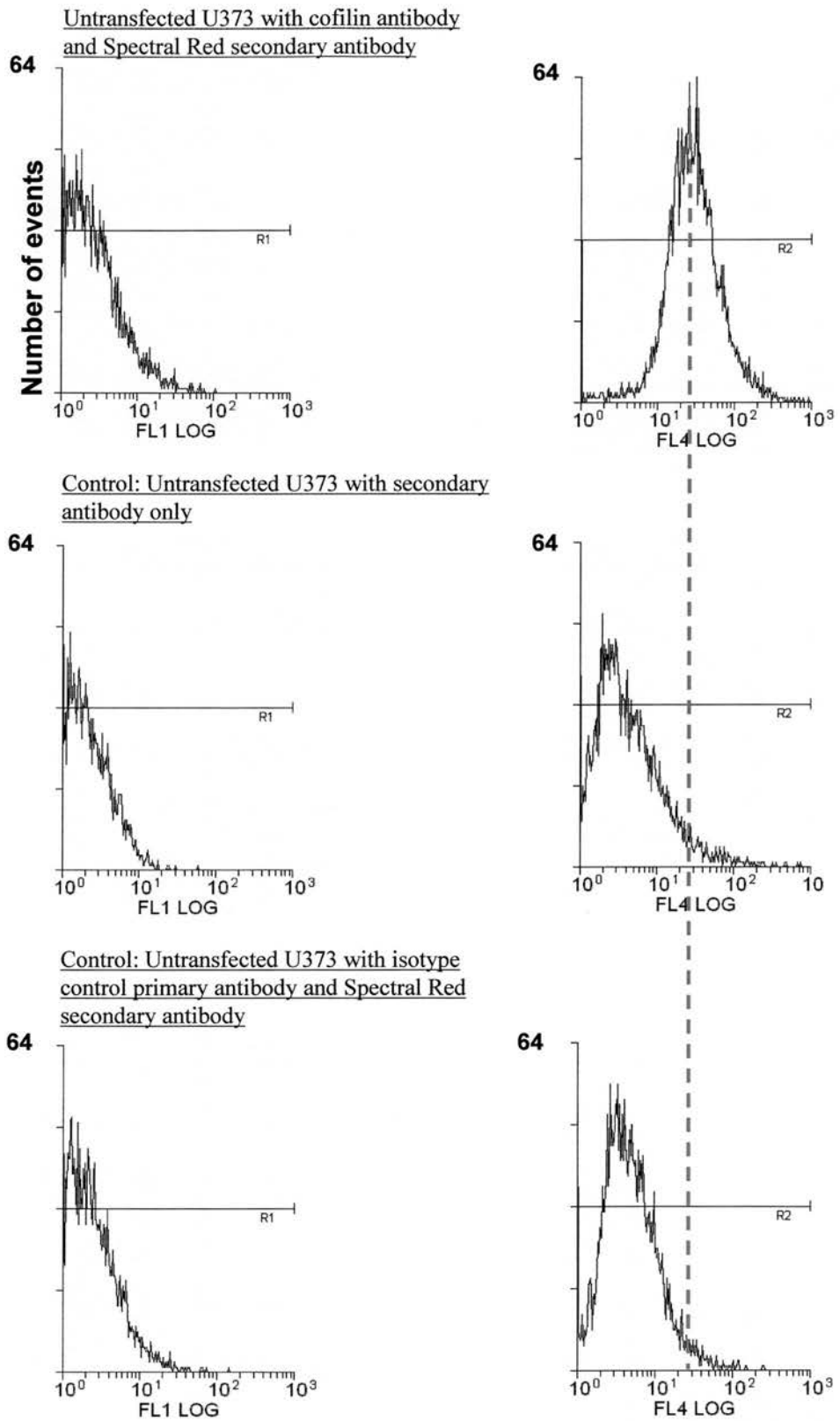

Dashed line indicates the mean Spectral Red intensity (FL4 log) of the untransfected population immunostained for cofilin and is compared to the mean intensities of the negative controls.

Fig. 4.5B Comparison between the mean intensities of EGFP (FL1 log) and Spectral Red conjugate (FL4 log) in untransfected and pCofilin-IRES2-EGFP-transfected cells immunostained for cofilin (Clones 1, 3)

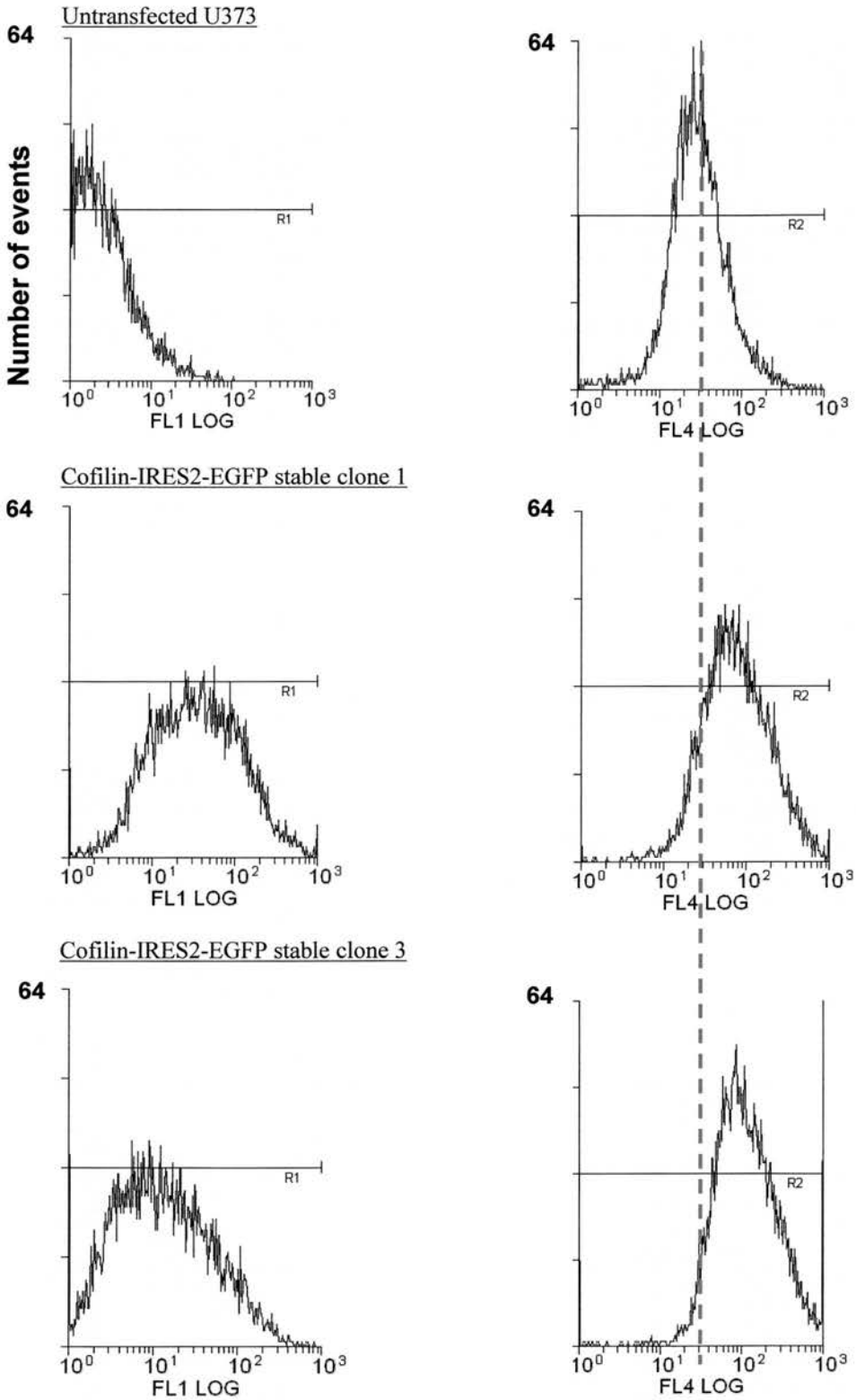

Dashed line indicates the mean Spectral Red intensity (FL4 log) of the untransfected population immunostained for cofilin. Clones stably transfected to overexpress cofilin show positive shifts along FL4 log, indicating increased intensities of cofilin immunofluorescence.

Fig. 4.5C Comparison between the mean intensities of EGFP (FL1 log) and Spectral Red conjugate (FL4 log) in untransfected and pCofilin-IRES2-EGFP-transfected cells immunostained for cofilin (Clones 5, 7)

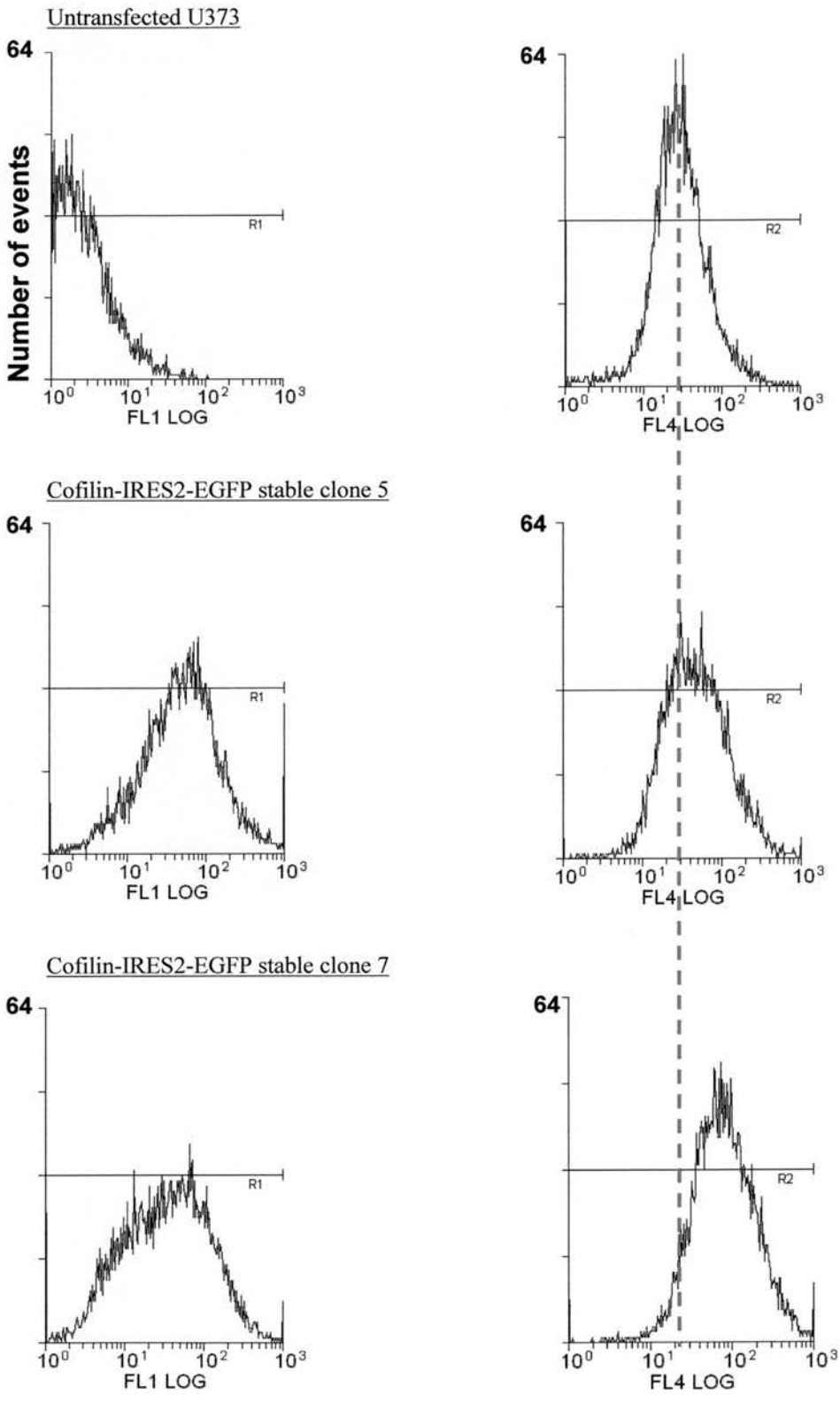

Fig. 4.5D Comparison between the mean intensities of EGFP (FL1 log) and Spectral Red conjugate (FL4 log) in untransfected and pCofilin-IRES2EGFP-transfected cells immunostained for cofilin (Clone 8)

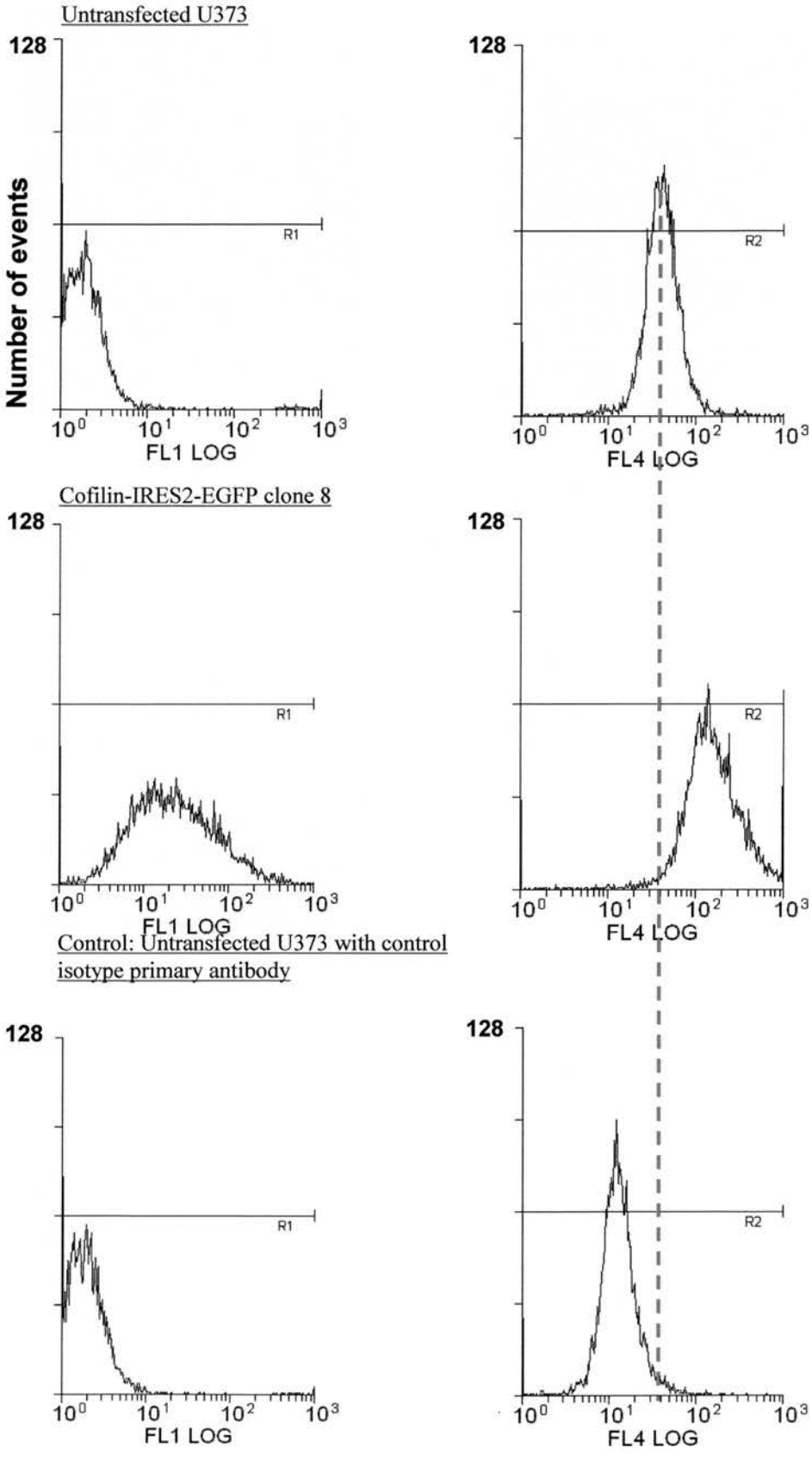

Fig. 4.5E Comparison between the mean intensities of EGFP (FL1 log) and Spectral Red conjugate (FL4 log) in untransfected and pEGFP-N1-transfected cells immunostained for cofilin (Clones 4,5)

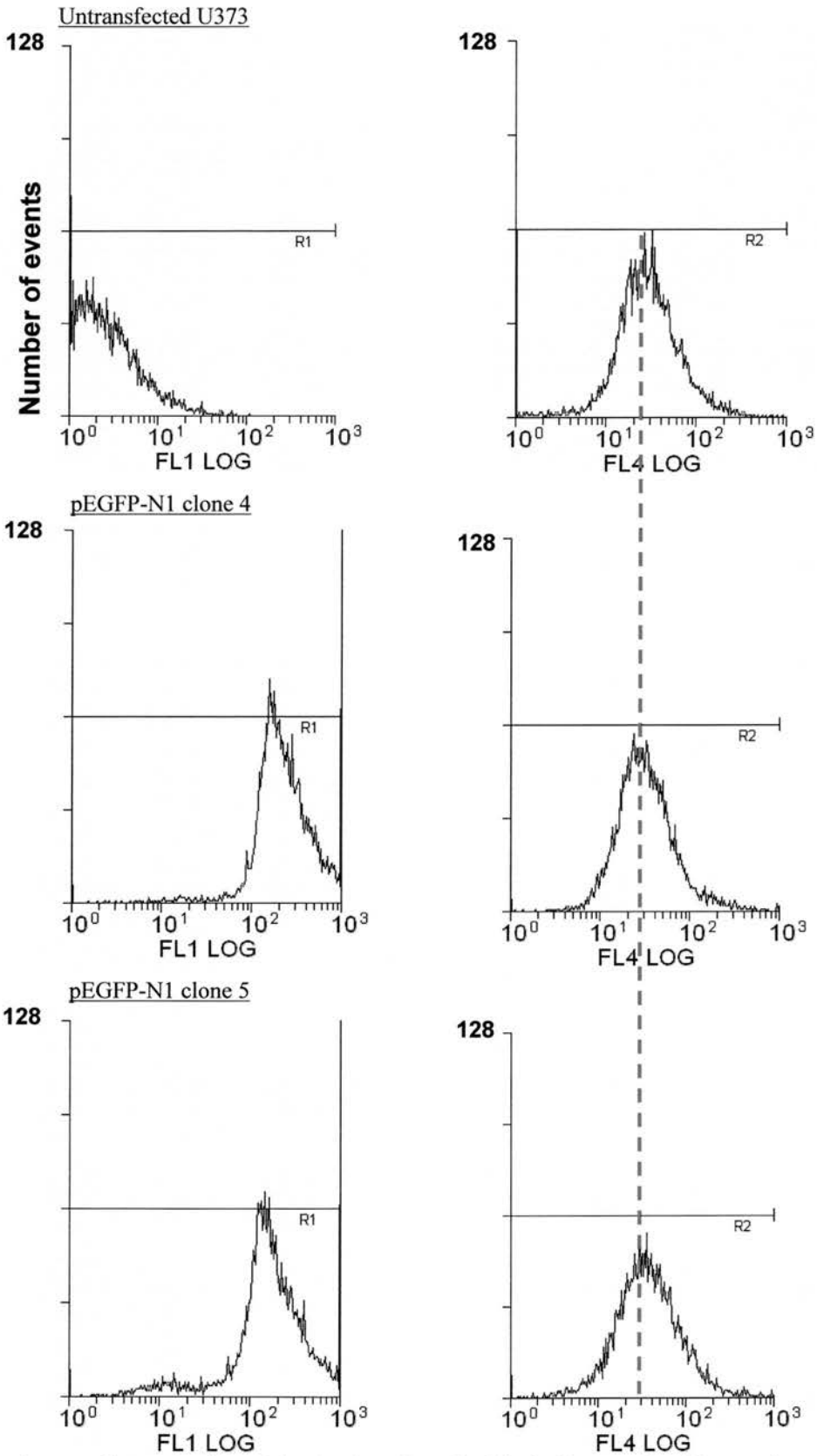

The mean immunofluorescent intensities for detection of cofilin in the control stable transfectants are similar to the untransfected population (dashed line).

Fig. 4.5F Comparison between the mean intensities of EGFP (FL1 log) and Spectral Red conjugate (FL4 log) in untransfected and pEGFP-N1-transfected cells immunostained for cofilin (Clone 2)

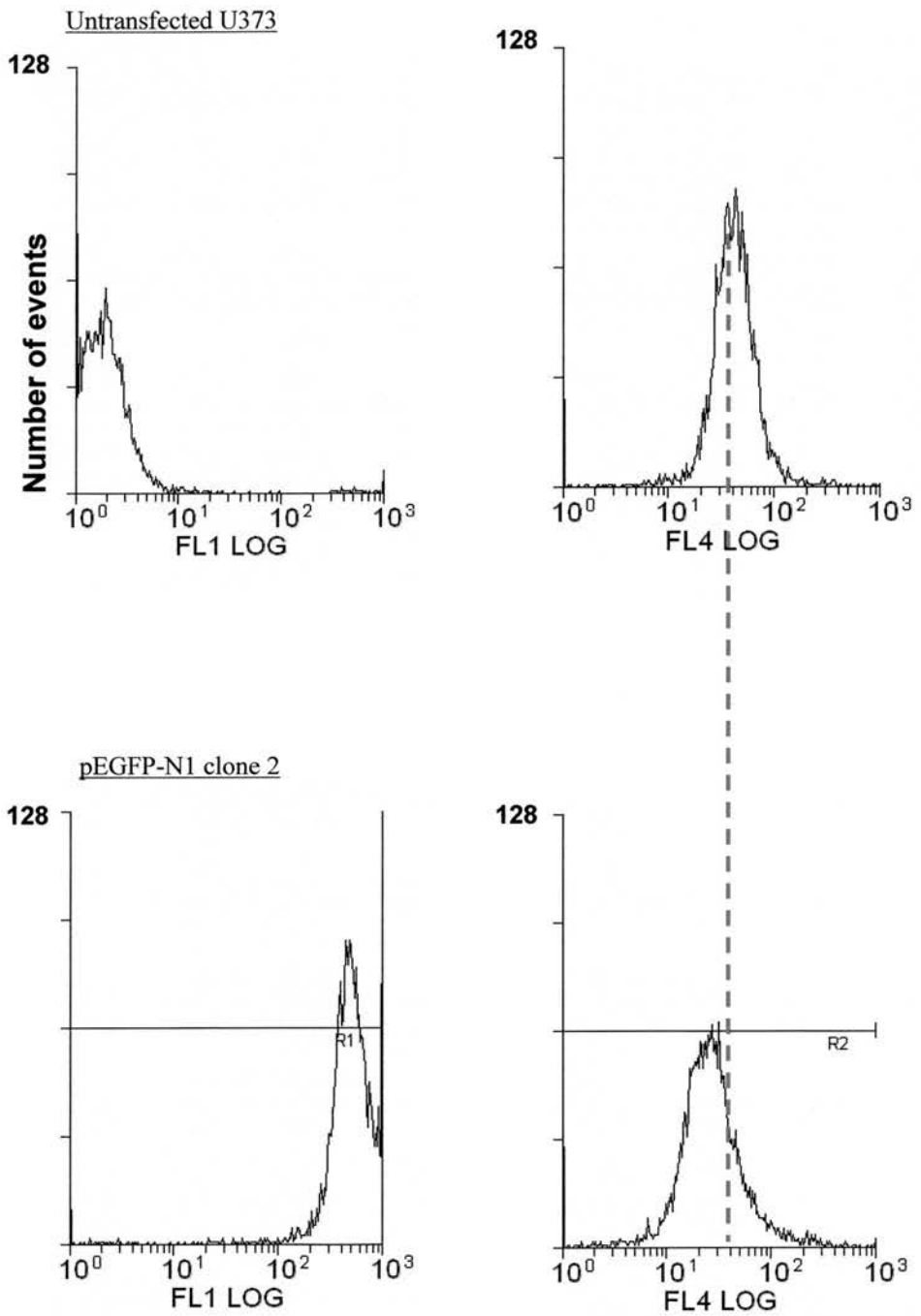

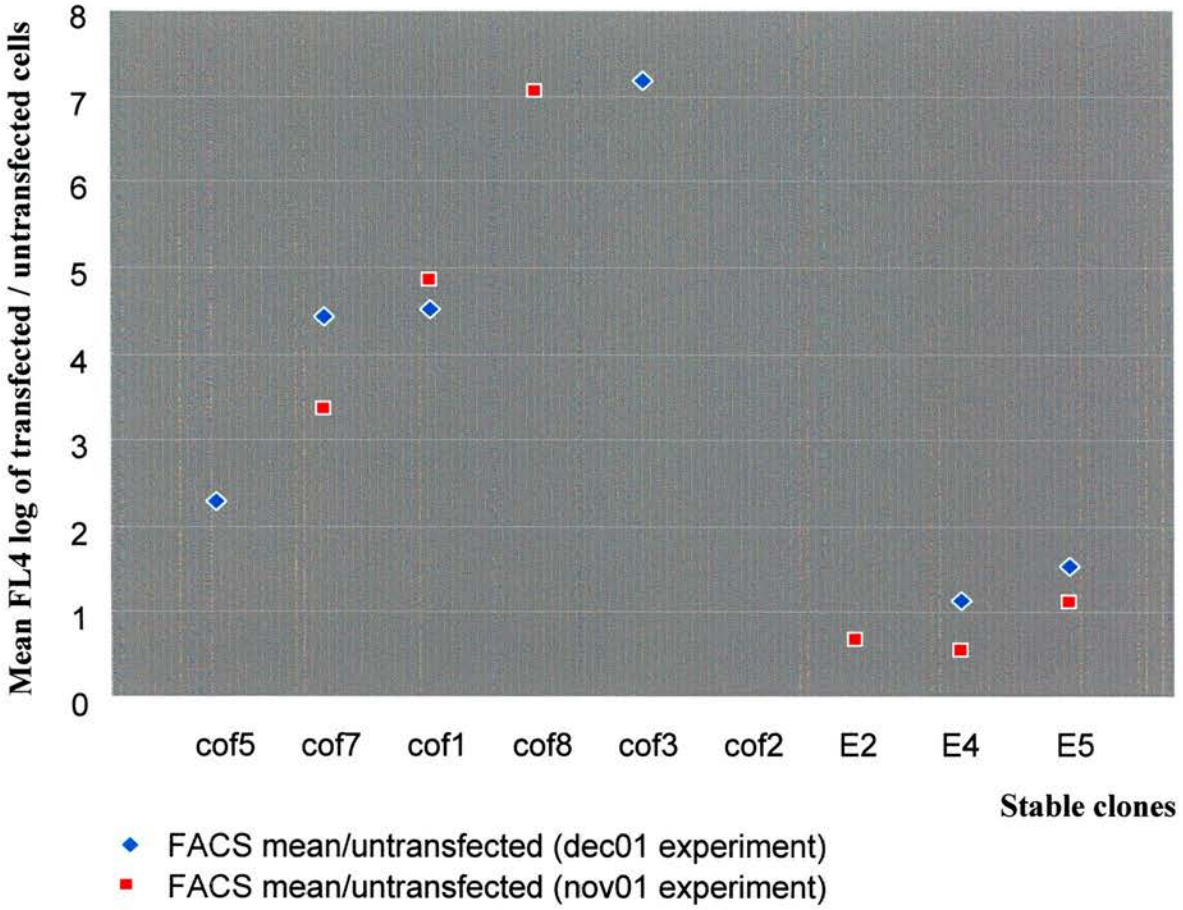

Fig. 4.6 Comparison of mean FL4 intensities (Spectral Red fluorescence) in stable transfectants by flow cytometry

The mean FL4 log of each population was compared with that of untransfected U373 MG cells. The ratio of mean FL4 log of transfected:untransfected is plotted for each of the stably-transfected populations. A ratio of 1 denotes that the mean FL4 log intensity of the transfected population is identical to that of untransfected cells. The graph is plotted on the basis of results obtained in two experiments (denoted as dec01 and nov01).

Cof 5,7,1,8,3,2: stable clones derived from transfections with pCofilin-IRES2-EGFP.

E2, 4, 5: stable clones derived from transfections with pEGFP-N1.

populations. It was possible to chart cofilin expression in a representative sample of at least 10,000 cells for each population examined, based on the immunofluorescence intensity recorded by each cell. Statistical analysis on the information derived from this large number of cells reflects the profile of cofilin expression in each stable clone.

Timelapse microscopy revealed that clones stably transfected with pCofilin-IRES2-EGFP exhibited different degrees of motility (discussed in Chapter 5). Whilst previous observations implicate cofilin overexpression in increased cell movement (Aizawa et al., 1996), it is as yet unknown how varying levels of overexpression might affect motility. Flow cytometric quantatition was performed not only to confirm cofilin overexpression, but also to quantify the extent of overexpression in the clones.

Flow cytometry was the preferred method of quantitation, over Western blot analysis. It has been suggested that cofilin expression might influence actin levels, as overexpressing cofilin in *Dictyostelium discoideum* induced increases in actin content (Aizawa et al., 1996). In addition, the relationship between cofilin and the expression of other cytoskeletal proteins, such as tubulin, remains unclear. Cytoskeletal proteins like actin are commonly used as loading controls in Western blots. However, the interpretation of results becomes complex because of these inter-relationships. The preliminary data obtained from Western blots was based on the assumption that expressions of β-actin and β-tubulin remained unchanged. If actin was indeed increased by cofilin overexpression, the data would underestimate the level of cofilin overexpression in stable clones. Flow cytometry quantitation allowed more direct measurements of the cofilin immunoreaction to be made, in the absence of assumptions regarding the expression of other proteins.

Flow cytometry also enabled cofilin immunodetection in individual cells, which reflected the profile of expression in each clonal population. This profile is relevant since gene expression is known to vary even in isogenic populations (McAdams, 1997). The range of cofilin expression in the untransfected and stably transfected populations was observed to be distributed normally (Figures 4.6 A-F). Thus the comparison of mean Spectral Red fluorescent intensities is a reasonable measure of the differences between levels of cofilin expression in the populations. Clones that overexpressed cofilin were found to differ in their average levels of cofilin. In Chapter 5, it will be shown that these variations in cofilin overexpression appeared to have significant influences on the motile behaviour of U373 MG glioblastoma cells.

CHAPTER 5

TIMELAPSE ANALYSIS OF U373 MG GLIOBLASTOMA CELLS TO INVESTIGATE THE EFFECTS OF COFILIN OVEREXPRESSION IN STABLE AND TRANSIENT TRANSFECTIONS

INTRODUCTION

U373 MG glioblastoma cells were imaged live using timelapse confocal microscopy, in a controlled environment that recapitulated standard culture conditions. Transfected and untransfected cells were mixed and plated onto plastic dishes. This enabled the two populations to be observed simultaneously under the same experimental setting. The motility of cells transfected with the cofilin overexpression vector, pCofilin-IRES2-EGFP, was compared to untransfected cells. In control experiments, the motility of cells transfected with pEGFP-N1 was compared to untransfected cells. Both transient and stable transfections were imaged with the Leica TCS NT confocal system. Preliminary experiments with transient transfections were analysed over periods ranging approximately 2 to 6 hours. Stable transfections were analysed over periods of at least 2 hours and up to 5 hours. The movement of at least 10 cells per population studied was tracked by following the positions of their nuclei, and the distances travelled were calculated using the Microsoft Excel program. Statistical analysis was performed using SigmaStat (SPSS Inc.). Only motile cells were chosen for analysis, hence cells that had rounded up, were dividing or spreading were excluded. In addition, the total number of cells observed in each field was manually counted to determine regional cell density. The methods are described in detail in

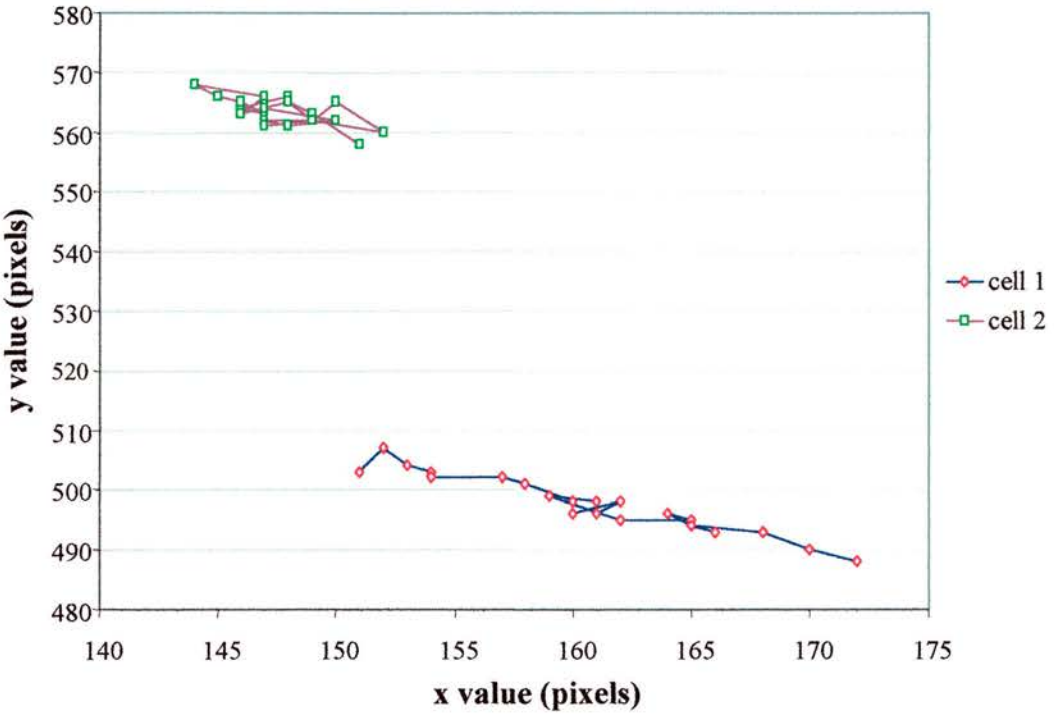

Fig. 5.1 Tracking the movement of cells

This graph shows the positions of two cells tracked over approximately 2 hours on the timelapse images. The positions are translated into (x,y) coordinates by the MacGap Debug and MetaMorph software programs.

Chapter 2, Part II.III (Timelapse confocal microscopy and Movement analysis of U373 MG cells), and a typical view obtained by timelapse confocal microscopy is shown in Figure 2.5.

V.I Timelapse analysis of transient transfections

Summary of methods used in analysing transient transfections

U373 MG cells were plated onto 6-well culture dishes and transfected with pCofilin-IRES2-EGFP using Fugene^{TM} 6 transfection reagent a day later. In separate wells, control transfections with pEGFP-N1 were performed. Cells were imaged by confocal microscopy at least 24 hours after transfection, when EGFP fluorescence was evident. The maximum transfection efficiency was 20%, and fields containing a combination of transfected and untransfected cells were observed every 5 minutes, for periods of about 2 to 16 hours. The timelapse pictures were analysed using the MacGap Debug program developed by Dr. William Sellers, which enabled the movement of cell nuclei to be recorded as changes in (x,y) coordinates on the Microsoft Excel program (Figure 5.1). Cell nuclei were tracked manually by positioning markers over them (Chapter 2, Figure 2.5).

The distance covered between adjacent points was calculated by the formula based on right-angled triangles (Pythagoras theorem):

Distance travelled between 2 points (pixels) = $\sqrt{(X_b - X_a)^2 + (Y_b - Y_a)^2}$

Where (X_a, Y_a) and (X_b, Y_b) are the coordinates of the points in pixels.

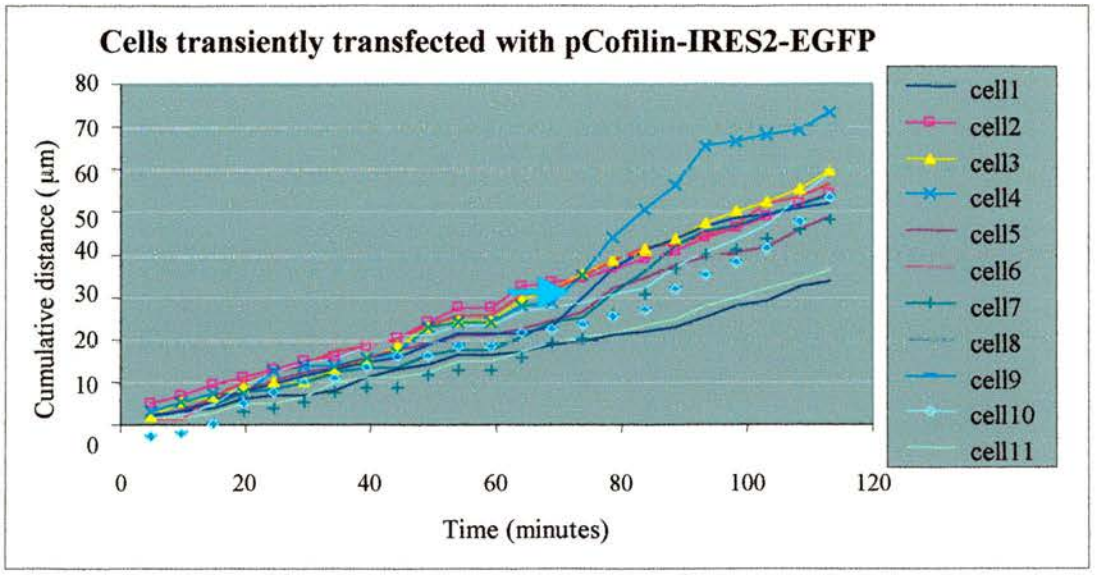

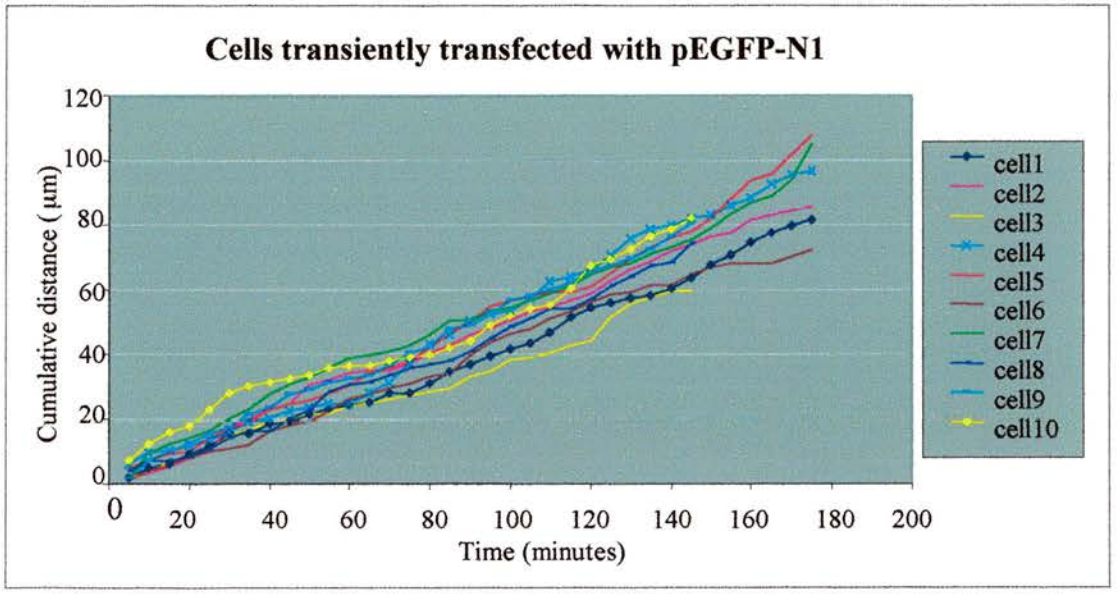

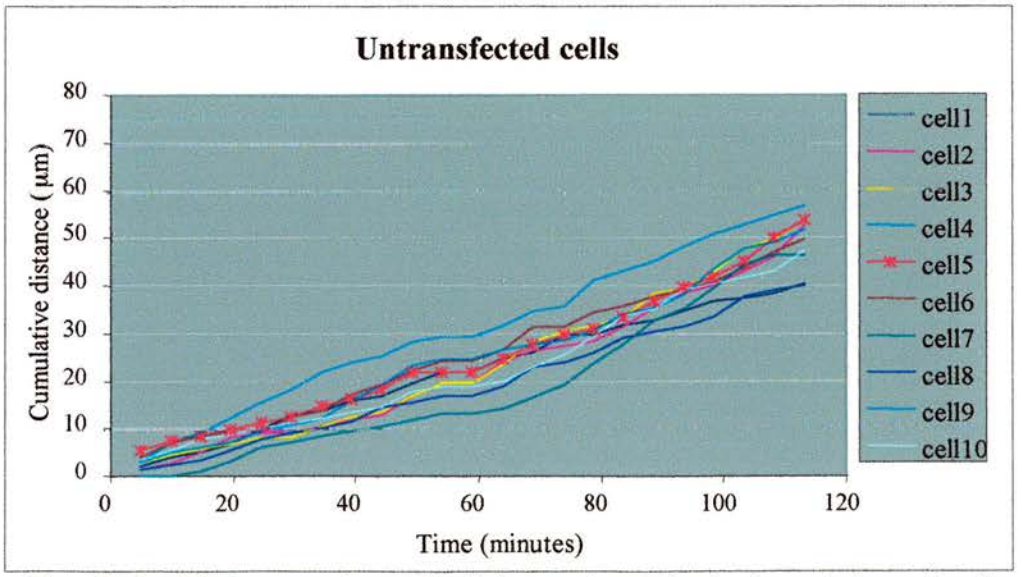

Fig. 5.2 Distances travelled by untransfected and transiently transfected cells over 113-175 minutes

The majority of cells appeared to move at constant speed, as indicated by the approximately linear pattern of the graphs. Only one cell (arrowed) showed a transient sharp gain in speed after 70 minutes, and resumed the initial locomotion rate after approximately 90 minutes.

The images acquired were scaled such that 1024 pixels on the screen represented 1000μm. Hence, the actual distance covered in micrometers was calculated by the formula:

Distance in μm = Distance in pixels ÷1024 × 1000.

The speed of individual cells was expressed as distance travelled per 5 minutes (μm / 5minutes). This was calculated by the formula:

Distance travelled per 5 minutes =

[Cumulative distance travelled (μm) ÷ Total time of analysis (minutes)] × 5

Statistical significance was tested using the Mann-Whitney Rank Sum test, computed by the SigmaStat software program. The t-test was also performed in populations that were determined to be distributed normally by SigmaStat.

Results obtained with transient transfections

Pattern of motility

There was a steady increase in the cumulative distances travelled by transfected and untransfected cells over time, suggesting that the majority of cells moved at roughly constant speed (Figure 5.2). This observation was made over the first 2 to 3 hours of imaging, when the density of cells remained somewhat unchanged. Thus, cells had settled in the climate chamber, and it would be reasonable to compare the motility of cells recorded in this time.

Fig. 5.3 Motility analysis of U373 cells transiently transfected with pCofilin-IRES2-EGFP

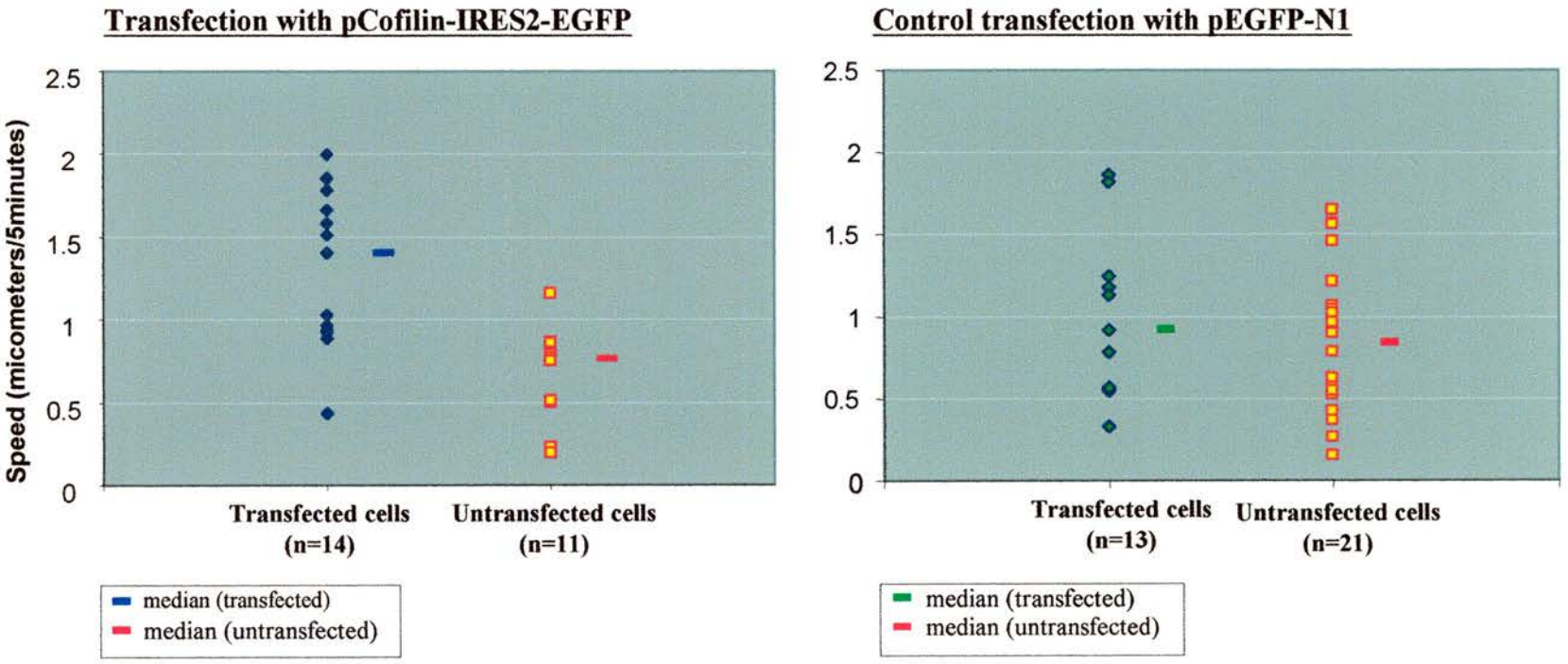

Timelapse confocal microscopy of U373 cells was performed at 37°C, 10% CO2, 26 hours after transfection. The cell density in the field observed was 139 cells/mm^2.

Left: There was a significant increase in the median speed of the cells transfected with pCofilin-IRES2-EGFP compared with untransfected cells (P = 0.001, MannWhitney Rank Sum test). Right: Control experiment. No detectable difference in median speeds was observed between cells transfected with pEGFP-N1 and untransfected cells (P = 0.448).

Effects of cofilin overexpression on motility

At imaging field densities of 120 cells/mm^2 and 139 cells/mm^2 , it was observed that cells that had been transiently transfected with pCofilin-IRES2-EGFP moved significantly faster than untransfected cells (P = 0.004 and 0.001 respectively, Mann-Whitney Rank Sum test). The distribution of speed of the populations at 139 cells/mm^2 is displayed in Figure 5.3. In this experiment, the median speed of cofilin-overexpressing cells was twice that of untransfected cells. In contrast, cells that had been transiently transfected with pEGFP-N1 in the control experiment did not move significantly faster than untransfected cells, at a comparable cell density of 130 cells/mm^2 (P > 0.050). This suggested that motility was enhanced in cells that overexpressed cofilin.

Effects of cell density on motility

Analysis of transient transfections showed that the motility of cells in culture was influenced by cell density (Figure 5.4). At moderate density, there was a marked increase in the speed of cells overexpressing cofilin. However, the motility of these cells was similar to untransfected cells at high densities above 250 cells/mm^2, where cultures approached confluence. Hence, close contact between cells obliterated the effects of cofilin overexpression observed when cells were more widely spaced.

Preliminary experiments with stable transfections also suggested at low density, the effects of cofilin overexpression on motility were lost. Although the mean and median

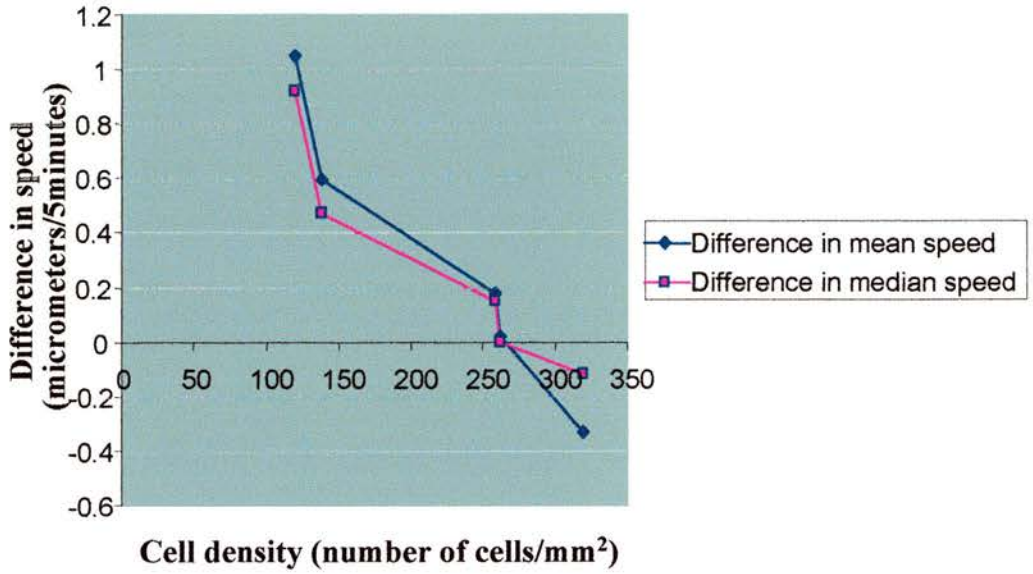

Cell density (cells/mm^2)	Mann-Whitney Rank Sum test	T-test
120	P = 0.004	P = 0.002
139	P = 0.001	P = 0.001
259	P = 0.130	P = 0.323
262	P = 0.89	Test not appropriate
320	P = 0.198	P = 0.142

Fig. 5.4 Speed of U373 MG cells overexpressing cofilin over a range of cell densities

The differences in mean and median speed between cells transfected with pCofilin-IRES2-EGFP and untransfected cells were determined for 5 experiments. Transfected cells moved significantly faster at cell densities below 250 cells/mm^2. At higher densities approaching confluence, speed did not differ significantly between transfected and untransfected cells. The p values for tests of significance were obtained using Sigmastat (SPSS Inc.).

speed of cofilin-overexpressing cells were faster than untransfected cells, the differences were not statistically significant.

V.II Timelapse analysis of stable transfections

Summary of methods used in timelapse experiments

6 stable clones transfected with pCofilin-IRES2-EGFP and 3 stable clones transfected with pEGFP-N1 were derived by methods described in Chapter 2, Part I.III, by G-418 antibiotic selection. Flow cytometric analysis confirmed that the stable clones obtained with pCofilin-IRES2-EGFP transfections overexpressed cofilin, but not the EGFP-overexpressing controls (Chapter 4). Equal numbers of stably-transfected cells and untransfected cells were plated onto each well of a 6-well dish and allowed to settle for 24 – 48 hours before timelapse imaging. The imaging was conducted in the same manner as for transient transfections. Motility analysis was performed using either the MacGap Debug or the Metamorph programs, which work similarly to transform positions of cell nuclei into (x,y) coordinates on the images.

Results of timelapse analysis on stable transfections

The motility of cells was analysed in fields containing ~ 70 – 140 cells/mm^2. 6 experiments using different stable clones were carried out to investigate the effects of cofilin overexpression on movement, and compared against 2 control experiments using stable EGFP-expressing clones. At least 10 cells each from the transfected and untransfected populations were tracked at 5-minute intervals over periods lasting 3 hours or longer, except one timelapse which lasted 100 minutes (Cof 5 clone). The

Fig. 5.5 Motility analysis of U373 cells stably-transfected with pCofilin-IRES2-EGFP

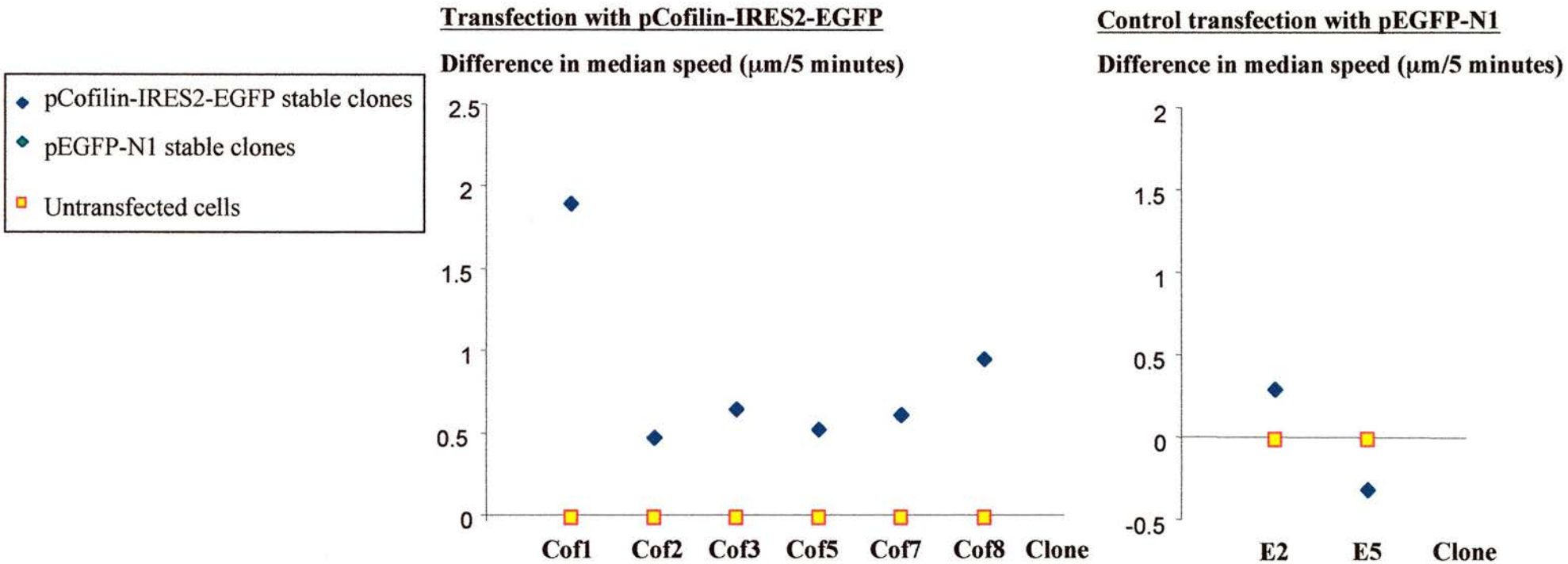

Timelapse microscopy was performed with 6 stable clones that overexpressed cofilin (Cof 1, 2, 3, 5, 7, 8), and 2 control stable clones that overexpressed only EGFP. Each experiment consisted of cells from a stable clone mixed with untransfected cells. The median speed of each stable clone is paired with that of the untransfected cells present in the same field. P values are obtained using the Mann-Whitney Rank Sum test. T-tests were performed where appropriate to compare the mean speed.

results from motility analysis are shown in Figure 5.5 and summarised in Table 5.1. The median (and mean) speed of the cofilin-overexpressing stable clones were consistently higher than untransfected cells. The results were statistically significant at the 5% level for the majority of cofilin-overexpressing clones. In contrast, control clones did not move faster than untransfected cells. Hence, the observations with stable transfections confirm the preliminary findings in transient transfections that cofilin overexpression enhances the motility of U373 MG glioblastoma cells.

Effects of cofilin overexpression levels on motility of glioblastoma cells

Cofilin expression in stable transfectants was determined by fluorescence immunochemistry and measured using flow cytometry. The data presented in Chapter 4 show that stable clones transfected with pCofilin-IRES2-EGFP overexpressed cofilin to different extents, as reflected by the variations in mean fluorescence intensity (Figure 4.6). In order to investigate the relationship between cofilin levels and motility, the magnitude of increase in mean speed was analysed against level of overexpression for each clone. The results are shown in Figure 5.6. The relative level of cofilin overexpression of each stable clone is calculated by:

Mean intensity of cofilin immunofluorescence of stable clone ÷ untransfected cells

It appears that motility was most enhanced when cofilin was expressed 4 – 5 times above that of untransfected cells. The increase in motility was less pronounced at relatively high levels of cofilin overexpression (more than 7 times normal), as well as at lower levels (below 3 times normal). This suggests that the degree of motility varies

Clones	Median speed	Mean speed	Median speed (untransfected cells)	Mean speed (untransfected cells)	Cell density (cells/mm2)	Time of analysis	P (Mann-Whitney Rank Sum test)	P (t-test)
Cof 1	2.803	2.93	1.243	1.026	74	185	0.001	< 0.001
Cof 2	2.676	2.464	2.035	1.978	140	180	0.042	0.025
Cof 3	1.615	1.572	1.052	0.917	72	185	0.031	0.024
Cof 5	1.223	1.148	0.707	0.615	102	100	0.089	0.050
Cof 7	1.494	1.319	0.767	0.696	72	180	0.015	-
Cof 8	2.313	2.309	1.721	1.349	81	180	0.050	0.053
E 2	1.082	1.113	0.761	0.810	88	320	0.345	0.126
E 5	0.692	0.332	0.739	0.638	104	185	0.678	0.869

Table 5.1 Motility analysis of stable clones

Cof 1,2, 3, 5, 7, 8 have been stably transfected with pCofilin-IRES2-EGFP. E2, 5 are controls stably transfected with pEGFP-N1. The table includes the mean and median speed of the untransfected population imaged together with the stable clone during each timelapse experiment.

Fig. 5.6 Effect of cofilin expression levels on U373 cells stably-transfected with pCofilin-IRES2-EGFP

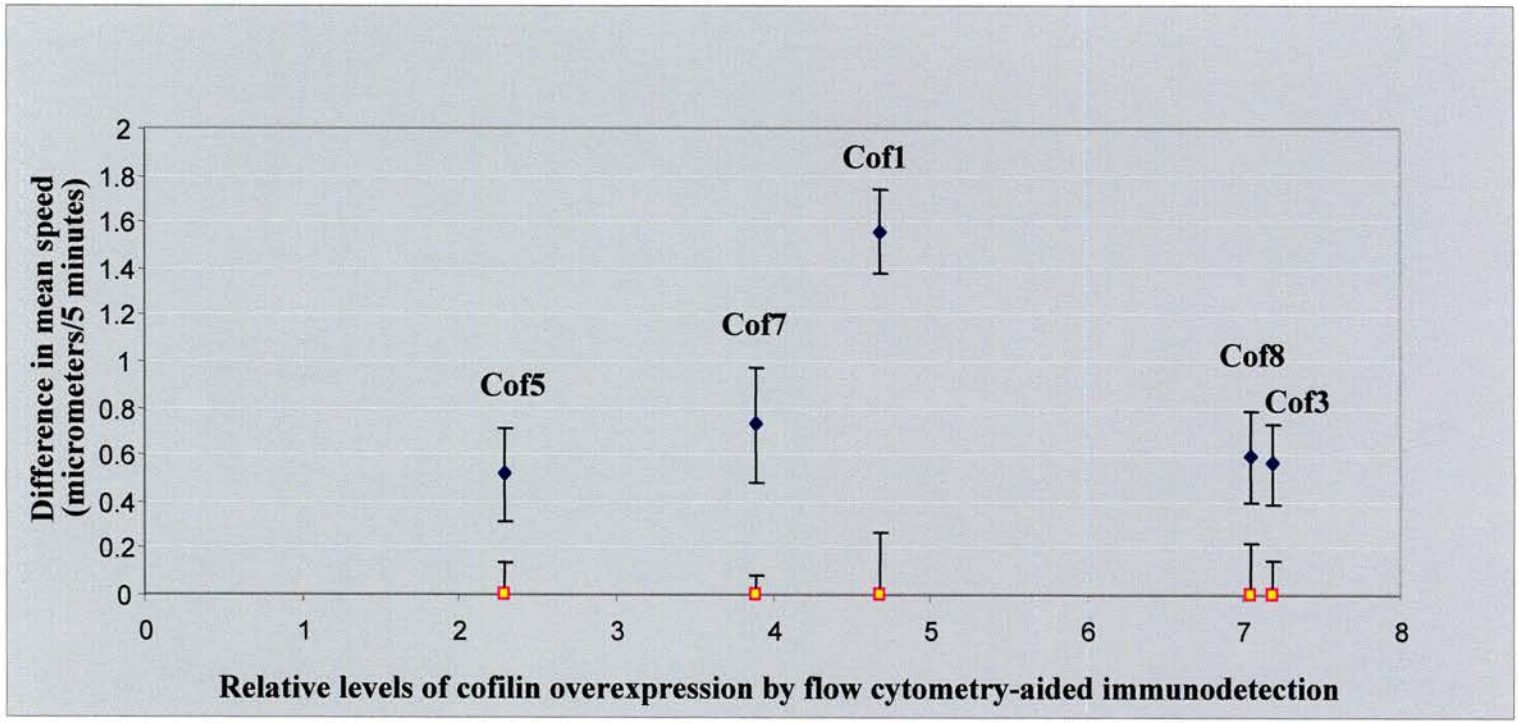

with changes in the intracellular content of cofilin, such that the fastest speed is attained at an optimal level of overexpression.

V.III. DISCUSSION

Transient transfections of U373 MG glioblastoma cells which were plated at moderate cell density suggested that overexpression of cofilin promotes motility. The experiments were therefore extended to examine the effects of cofilin overexpression in stable transfections. As it was possible to isolate clones of stably-transfected cells, this method allowed the selection of separate populations that overexpressed cofilin to different extents. Chapter 4 discusses how relative levels of cofilin overexpression were determined in stable clones by flow cytometry. The complemetary results of transient and stable transfections indicated that glioblastoma cells moved faster when cofilin was overexpressed. In addition, the increase in motility could be influenced by the extent of cofilin overexpression in cells, as well as by variations in regional cell density. The interpretation of these findings is elaborated in the final Discussion chapter.

The IRES-EGFP-containing vector was used for cofilin overexpression, to enable cofilin and EGFP to be produced as separate proteins from a single bicistronic mRNA. EGFP identified cells that overexpressed cofilin. This method was selected in preference to tagging overexpressing cells with a cofilin-EGFP fusion protein. There is biochemical evidence that disrupting the carboxyl-terminal portion of cofilin decreases its ability to bind actin filaments at alkaline pH (Moriyama et al., 1992), and it is unknown if cofilin activity might be altered in the presence of an EGFP tag. Hence the

IRES-EGFP vector provided a means to ensure that cells overexpressed wild-type cofilin in its native form.

Care was taken in the experimental design to ensure that conditions were standardised to minimise experimental variation and optimise data comparability. Consistent methods of cell culture and timelapse recording were employed. Controls were included in each experiment to account for systematic errors of measurement, as well as correct for other confounding factors that might have been accidentally introduced. The Mann-Whitney Rank Sum test was used as the main test of significance, as this is a non-parametric method suitable for analysing small samples with variable distribution. The experimental conditions and controls used are explained below.

To account for any effects that might arise from the introduction of EGFP into cells, transfections with pEGFP-N1 were used as controls. As an additional control, mixed populations of transfected and untransfected cells were imaged and analysed in the same field for each timelapse experiment. This ensured that the comparisons between the transfected and untransfected populations were made under identical conditions, and minimised errors arising from variability between experiments.

Several factors that could potentially affect cell motility irrespective of cofilin expression were identified and standardised in experiments as best possible. This was necessary in order to compare the results of experiments performed on different occasions. Cells were plated 24 to 48 hours before timelapse microscopy in fresh medium to allow them to settle and adhere. 6-well Iwaki plastic dishes were used in all the timelapse experiments, so that cells moved on a similar type of substratum. This was to control for motility differences arising from movement on different surfaces

(Hartmann-Petersen et al., 2000). Cells were imaged in a climate chamber set at 37°C with 5% CO_2, in the presence of 10% fetal calf serum (v/v). This maintained them in regulated conditions of temperature, pH and serum content, which may otherwise affect the motility of cells. pH variation is known to be crucial to cofilin activity, as it severs actin filaments more readily at increased pH (Hawkins et al., 1993). pH and temperature have been shown to critically affect the motility of fibroblasts, becoming more sluggish in acidic conditions and at lower temperatures (Hartmann-Petersen et al., 2000). Serum content affects the movement of cells by altering their ability to form motile protrusions, as discussed in Chapter 3.

Immotile cells such as those that had rounded up, dividing cells and large spreading cells were excluded from the analysis on motility. This was to prevent any bias in the interpretation of the results. Cell nuclei were chosen as reference points for movement as they were clearly identifiable and translocated along with cell bodies when cells moved. They were more reliable indicators of movement than the leading lamellipodia, which were difficult to follow as they were often retracted and reformed as cells probed around and changed directions.

Transient transfections indicated that a possible confounding factor in motility analysis could arise from differences in cell density of the observed field. This observation was consistent with findings that plating density could affect the motility of fibroblasts (Hartmann-Petersen et al., 2000). To ensure that the data obtained from stable transfections were comparable, fields were chosen to cover a narrow spectrum of densities, between 70 – 140 cells/mm^2, and well below confluence levels. As shown in the data, the manifestation of cofilin overexpression on motility is most evident at

moderate cell density. Hence this was a reasonable range within which one might optimally observe the effects resulting from changes in cofilin levels.

In conclusion, the experiments have been conducted under rigorous conditions in order to ensure the validity of the observations. The effects on motility induced by the overexpression of cofilin in U373 MG glioblastoma cells are discussed in Chapter 7.

Fig. 6.1 Transfection of stable Tet-off U373 cells with pTre-cofilin-IRES2-EGFP plasmid to demonstrate inducibility of gene expression

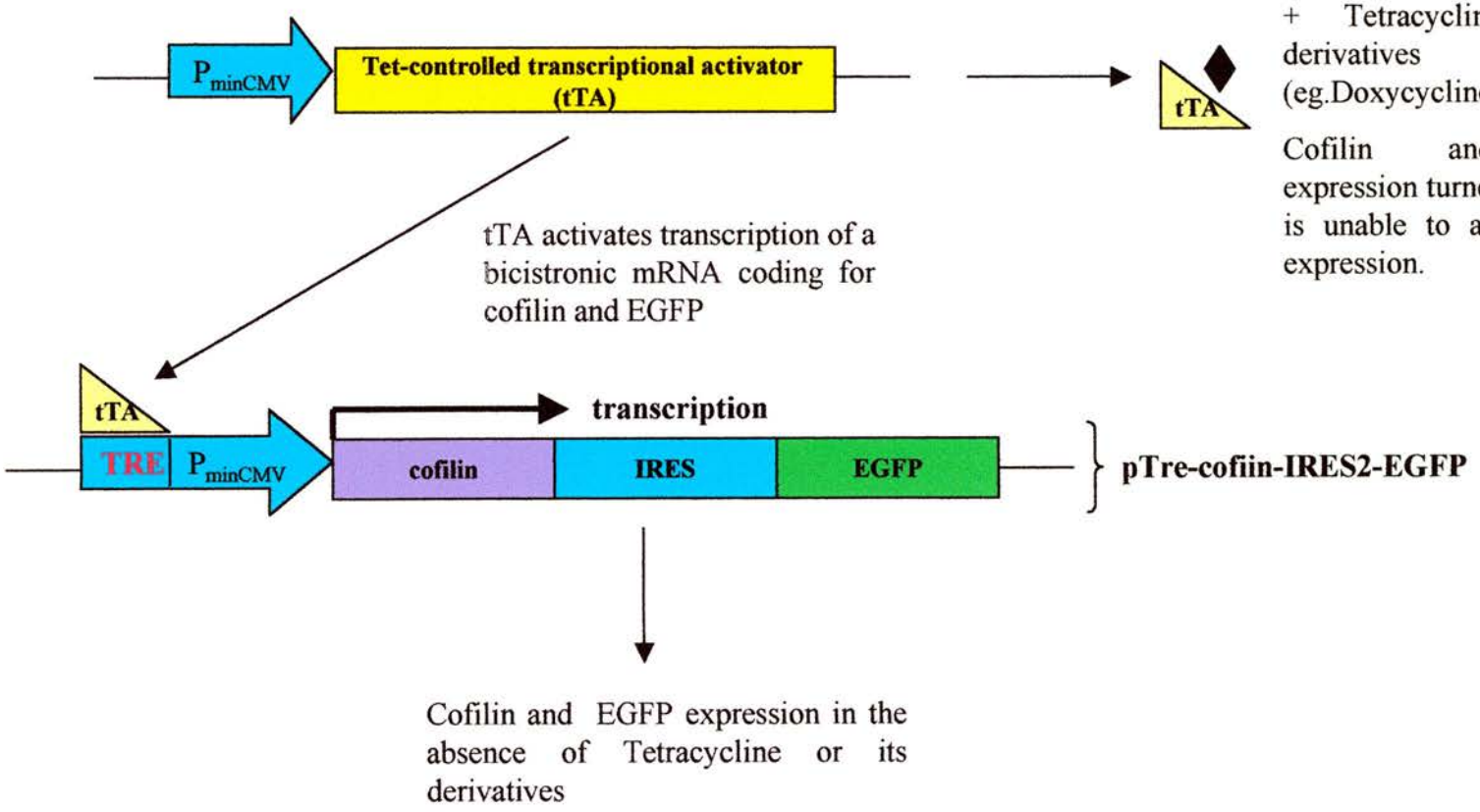

CHAPTER 6

PROSPECTIVE WORK: CORRELATING THE MOTILITY OF U373 MG GLIOBLASTOMA CELLS WITH COFILIN OVEREXPRESSION LEVELS USING THE TET-OFF SYSTEM

INTRODUCTION

A precise investigation into how the motility of glioblastoma cells might vary with cofilin levels may be achieved by using a tetracycline-based inducible system, the Tet-Off system (Clontech laboratories Inc.). This system was developed by Gossen and Bujard (1992). It uses a tetracycline-controlled transactivator (tTA) to drive the expression of the gene of interest, by stimulating transcription from a minimal promoter sequence derived from the human cytomegalovirus promoter. This system allows transcription to be regulated in the presence of the tetracycline antibiotic or its derivatives such as doxycycline. Transcription is increasingly reduced as antibiotic dose rises in the culture medium, and turned off at high concentrations. This system requires double-stable transfectants to be developed. The first stable transfection introduces tTA to the cell line, the second introduces the gene of interest cloned into the tetracycline-responsive plasmid pTRE. An illustration into how the Tet-Off system may be adapted to study the effects of cofilin expression is shown in Figure 6.1.

Fig. 6.2 Reverse transcription-PCR to detect expression of tet-controlled transcriptional activator (tTA) in stable Tet-off U373 clones

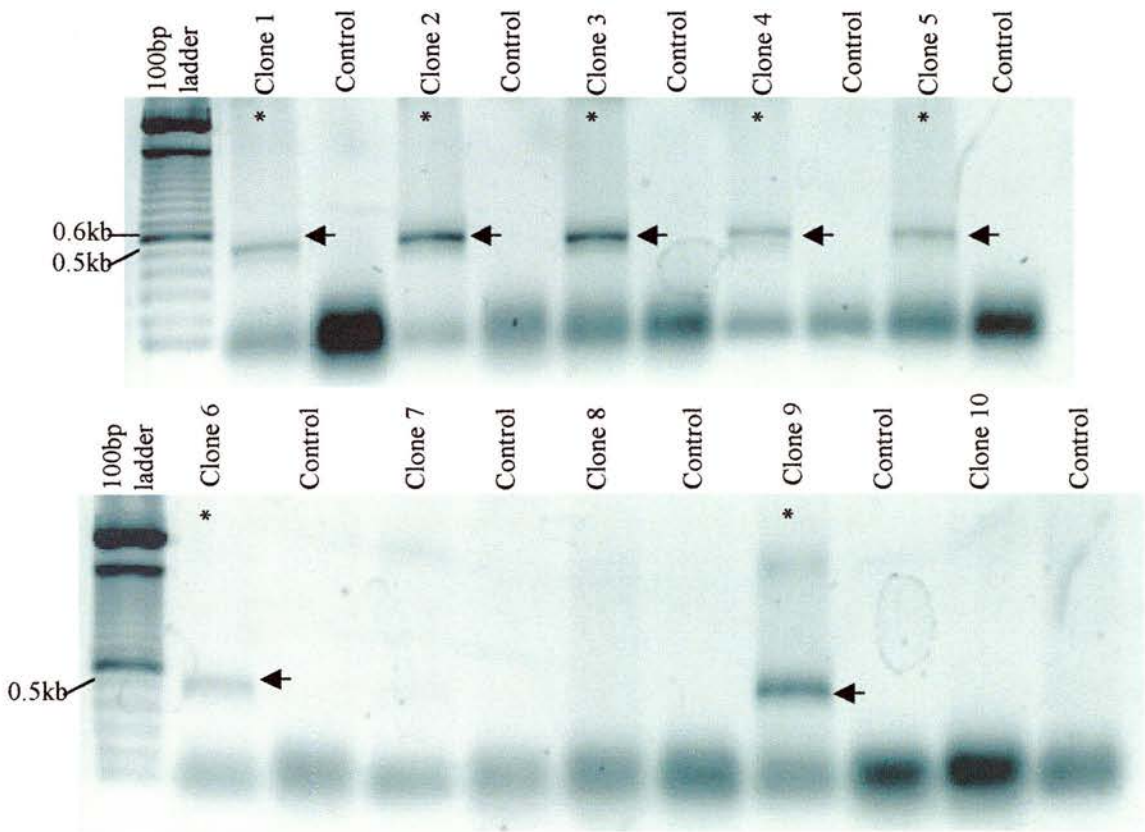

10 U373 clones were tested for stable expression of tTA. The 7 clones expressing tTA are marked with *. These are positive for the 0.5kb PCR product that identifies tTA. Negative controls were derived from corresponding RNA preparations subjected to PCR, without RT (reverse transcriptase).

VI.I Methods used in developing the Tet-Off system to investigate the effects of cofilin overexpression

The coding sequence of human cofilin 1, together with the IRES2-EGFP sequences, were excised from the pCofilin-IRES2-EGFP vector and subcloned into the pTRE vector (Clontech laboratories Inc.). This generated the pTRE-Cofilin-IRES2-EGFP, as reported in the Results section of Chapter 2. To obtain stable transfectants expressing the tetracycline-controlled transactivator (tTA), U373 MG cells were transfected with the pTet-Off plasmid that codes for tTA (Clontech laboratories Inc.) using FuGene^{TM} 6 transfection reagent, and selected in the presence of G-418 antibiotic (see Chapter 2, Part II.III). Clones were obtained and tested for the expression of tTA by RT-PCR using specific primers (Figure 6.2). The primer sequences were: forward primer 5'– GCT TAA TGA GGT CGG AAT CG -3'; reverse primer 5'- TAA GAA GGC TGG CTC TGC AC -3'. 7 clones were positively identified, and one of these (Clone 9) was selected to develop the double-stable cell line. This clone was cotransfected with pTRE-Cofilin-IRES2-EGFP and pTK-Hyg, so that double-stable clones could be selected using hygromycin. Controls were cotransfected with pEGFP-N1 and pTK-Hyg. Transfected cells were grown in selective medium containing 100μg/ml hygromycin with 10% Tet System approved fetal bovine serum (v/v), which lacks traces of tetracycline and its derivatives (Clontech laboratories Inc.). Hygromycin-resistant cells were flow-sorted using the Beckson Dickinson FACS Vantage SE to separate EGFP-expressing cells, and returned to grow under standard culture conditions. The detailed protocols employed for cloning the pTRE vector and obtaining stable clones are recorded in Chapter 2, Parts II.I and II.III.

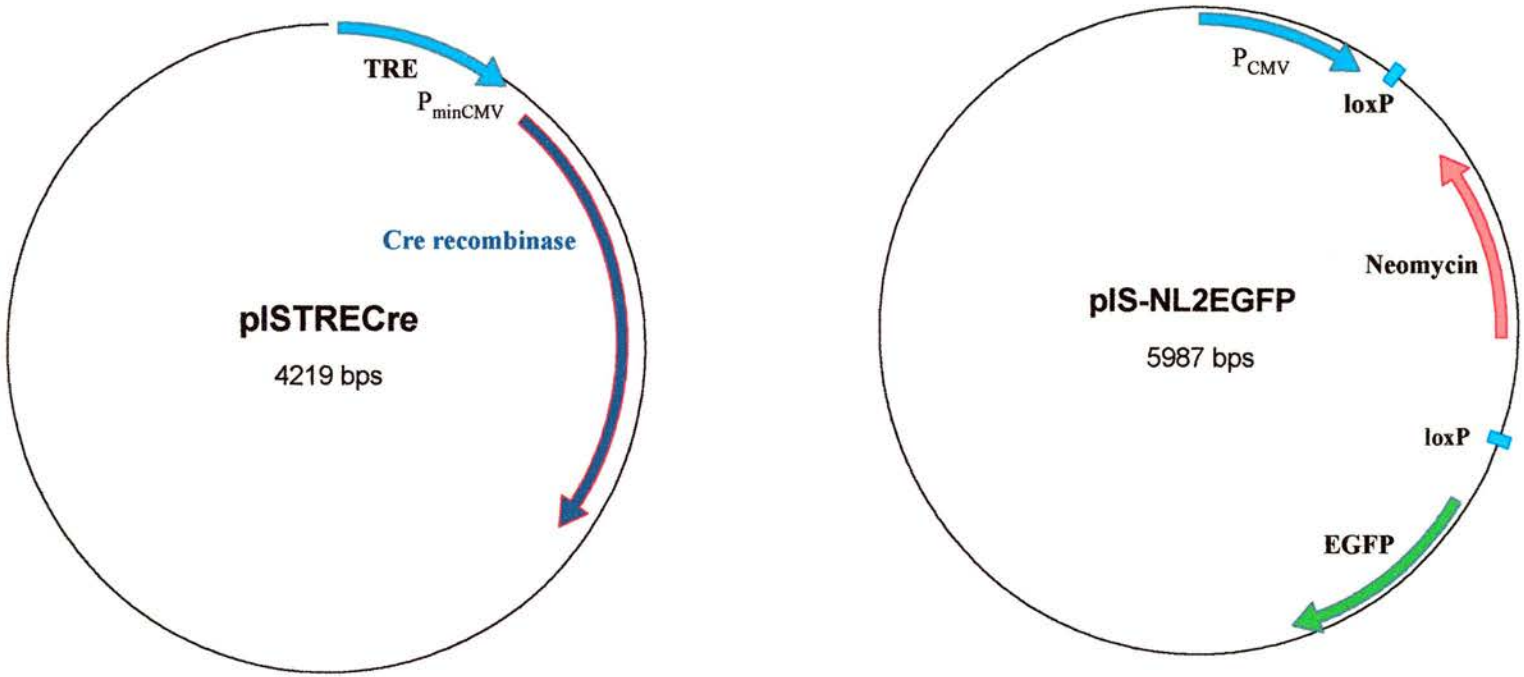

Fig. 6.3 Vectors used to test inducibility of the Tet-off system in U373 glioma cells

These plasmids were developed by Dr T.I. Simpson, Biomedical Sciences, University of Edinburgh.

VI.II Testing the inducibility of gene expression in stable transfectants expressing tTA

A tTA-expressing clone stably transfected with pTet-Off (Clone 9, Figure 6.2) was selected for establishing double-stable cell lines and tested for its ability to respond to doxycycline. This was achieved by cotransfecting with a pTRE plasmid encoding Cre recombinase (pISTreCre), and a pEGFP-N1 plasmid encoding neomycin flanked by *loxP* sites (floxed neomycin cassette in pIS-NL2EGFP). Both plasmids were created by Dr T.I. Simpson and the plasmid maps are shown in Figure 6.3. An explanation of how this system might test the functional status of tTA in the clone as well as the inducibility of the system is shown in Figure 6.4. The expression of Cre recombinase is dependent on transcriptional activation by tTA, and the activity of this enzyme results in excision of the floxed neomycin cassette. This allows the translation of EGFP, which is otherwise suppressed by the interposition of neomycin adjacent to the cytomegaloviral promoter. Thus the detection of green fluorescent cells indicates the activity of tTA. Figure 6.5 shows that EGFP was expressed in a cotransfected cell derived from the stable clone, indicating that tTA was functional in this clone.

The Tet-Off system was also tested for inducibility of cofilin expression. The tTA stable clone was transiently transfected with pTRE-Cofilin-IRES2-EGFP. tTA would induce the expression of both cofilin and EGFP. However, in the presence of doxycycline, tTA activity is inhibited and EGFP expression should be undetectable. Transient transfections were observed for 24 hours up to a week after transfection for EGFP fluorescence. It was

Fig. 6.4 Cotransfection of stable Tet-off U373 cells with pIS-NL2EGFP and pISTreCre plasmids to demonstrate inducibility of gene expression

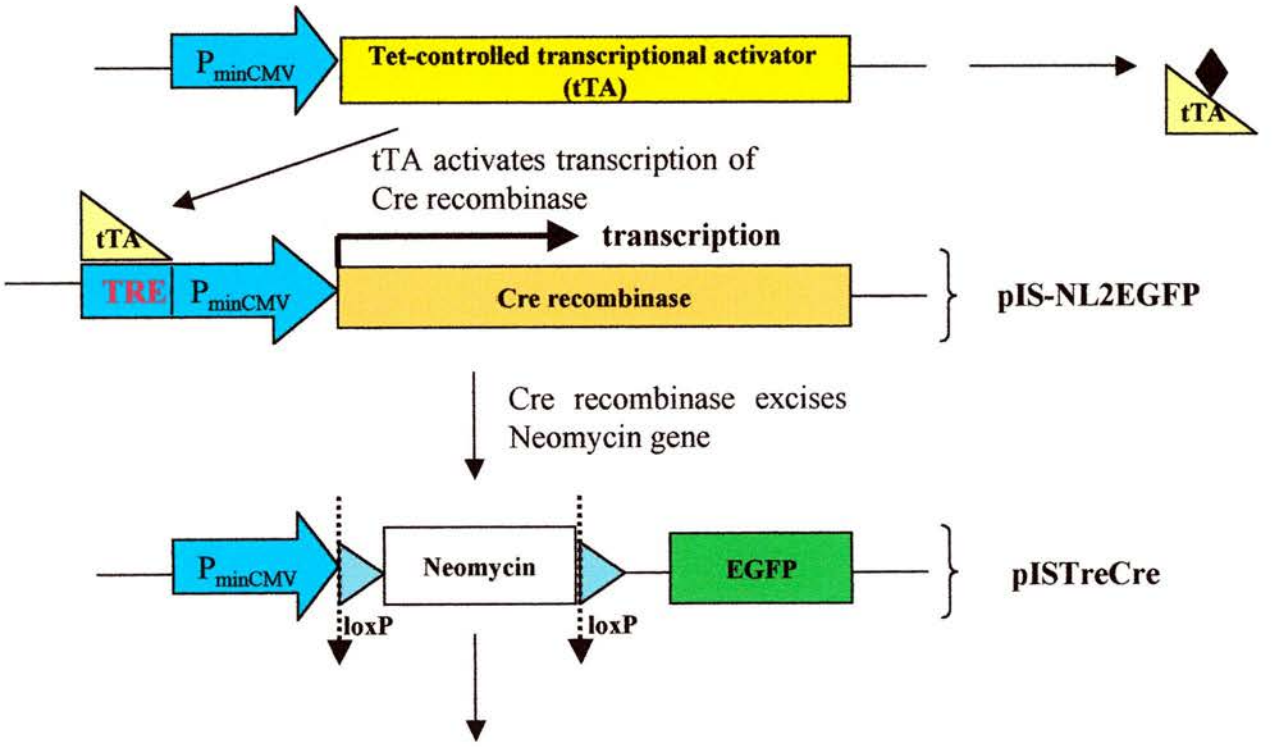

Fig. 6.5 Testing the function of the tetracycline-controlled transactivator in a stable tTA-expressing clone

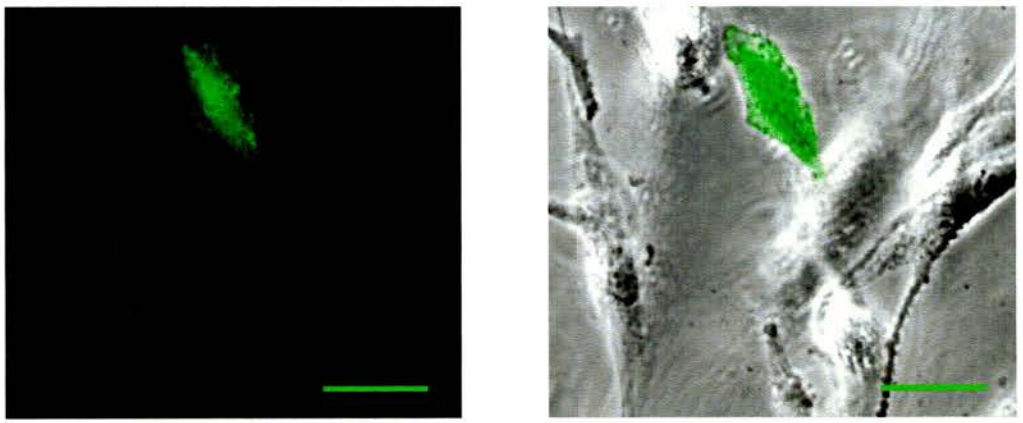

A green fluorescent Tet-off U373 glioma cell cotransfected with pIS-NL2EGFP and pISTreCre plasmids, in the absence of tetracycline. Expression of Cre recombinase has been induced by the tetracycline-controlled transactivator (tTA). (Confocal imaging with Leica TCS NT. Bar: 50μm.)

Fig. 6.6 Transfection of stable Tet-off U373 glioma cells with pTre-cofilin-IRES2-EGFP showing inducible expression of EGFP responsive to Doxycycline administration in representative fields

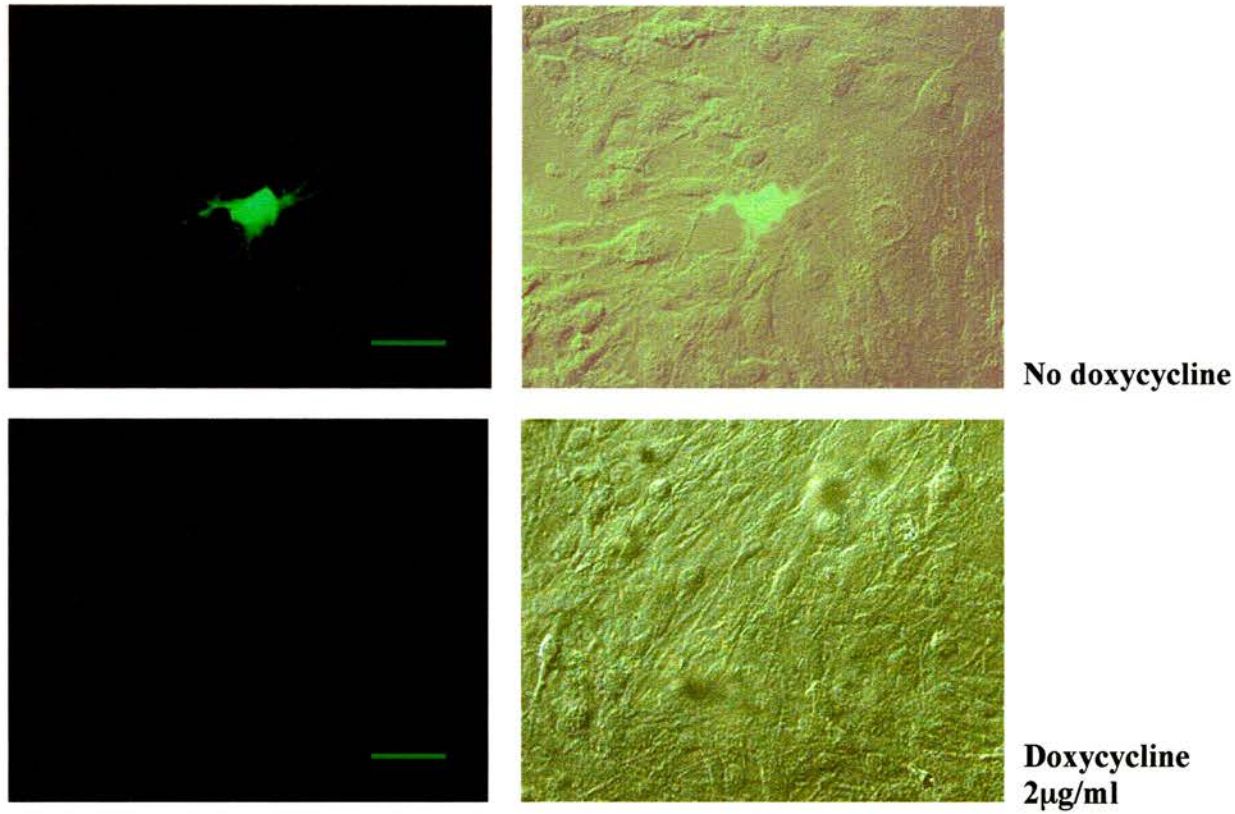

Stable Tet-off U373 glioma cells were transfected with pTre-Cofilin-IRES2 –EGFP and cultured for 72 hours in the presence or absence of Doxycycline, then fixed with 4% paraformaldehyde. Digital images were obtained using the Leica DC 200 camera mounted on the Leica DMRB microscope. Left panels: fluorescence with FITC filter. Right panels: DIC (differential interference contrast) optics and fluorescent overlay. Bar: 50μm.

observed that no green cells could be detected in the presence of doxycycline at 2μg/ml. In comparison, cultures grown in the absence of doxycycline contained EGFP-expressing cells (Figure 6.6). These experiments suggest that cofilin overexpression could potentially be modulated by the Tet-Off system.

VI.III Selecting double-stable cells using fluorescence activated cell sorter (FACS)

The tTA-expressing clone that had been tested for inducibility was cotransfected with pTRE-Cofilin-IRES2-EGFP and the plasmid that confers hygromycin resistance, pTK-Hyg. Ratios of 10:1 and 20:1 of pTRE-Cofilin-IRES2-EGFP to pTK-Hyg were used in cotransfections. To control for effects of EGFP, tTA-expressing cells were also cotransfected with pEGFP-N1 and pTK-Hyg. Cotransfected cells were enhanced in selective medium containing 100μg/ml hygromycin, since this concentration induced massive cell death in untransfected cells (Chapter 2, Part II.III). Culture of cells over several weeks continued to yield a mixture of green fluorescent and non-green cells, despite the use of medium containing only hygromycin, penicillin and streptomycin and was otherwise antibiotic-free. Hence cells were flow-sorted by the Beckson Dickinson FACS Vantage SE to isolate the double-stable EGFP-expressing cells. Viable cells were selected on the basis of forward (FSC) and side scatter (SSC), and these were sorted into 2 groups comprising relatively high EGFP-expressors and low-EGFP expressors. Figures 6.7 and 6.8 show how cells transfected with pTRE-Cofilin-IRES2-EGFP and pEGFP-N1 were sorted respectively. A negative control population of cells containing untransfected

Fig. 6.7 Selection of double-stable Tet-off U373 cells expressing pTre-cofilin-IRES2-EGFP by FACs sorting of green fluorescent cells (Becton Dickinson FACsVantage SE)

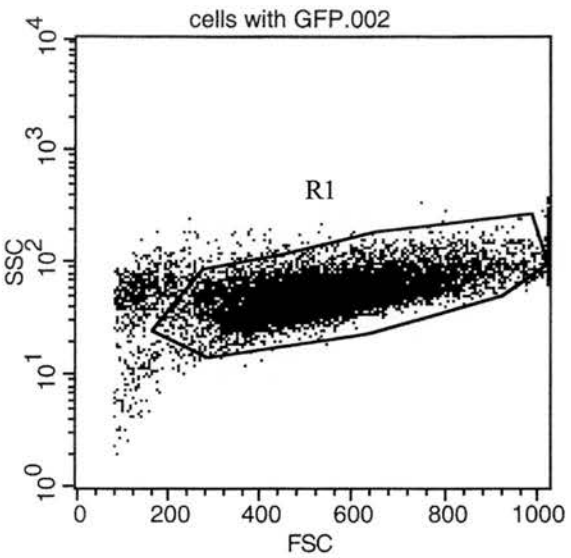

Cells were sorted into a low green population (R2 gate) and a high green population (R3 gate). In the FL1 channel, M1 denotes the gate for all EGFP-expressing cells (bottom histogram).

Legend SSC: Side scatter

FSC: Forward scatter

FL1: Green fluorescence

FL3: Red fluorescence

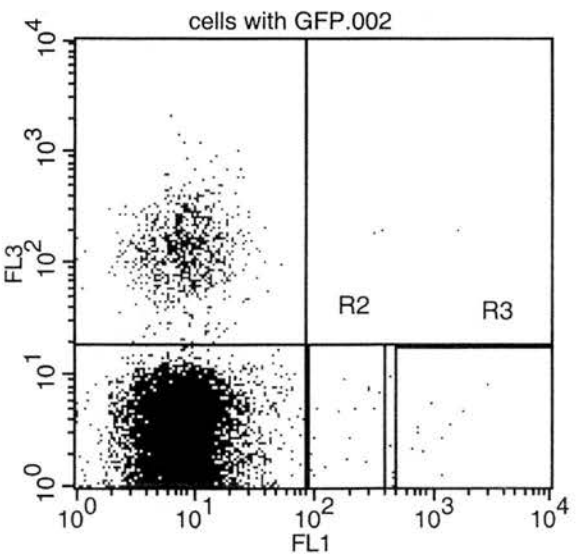

Gated Events: 11045
Total Events: 11045

Region	Events	% Gated	% Total
R1	10000	90.54	90.54
R2	31	0.28	0.28
R3	11	0.10	0.10

Quad	Events	% Gated	% Total
UL	856	8.56	7.75
UR	3	0.03	0.03
LL	9106	91.06	82.44
LR	35	0.35	0.32

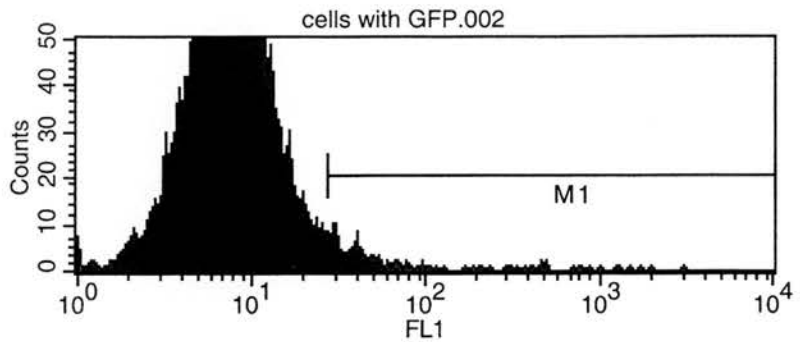

Marker	Events	% Gated	% Total
All	10000	100.00	90.54
M1	246	2.46	2.23

Fig. 6.8 Selection of double-stable Tet-off U373 cells expressing pEGFPN1 by FACs sorting of green fluorescent cells (Becton Dickinson FACsVantage SE)

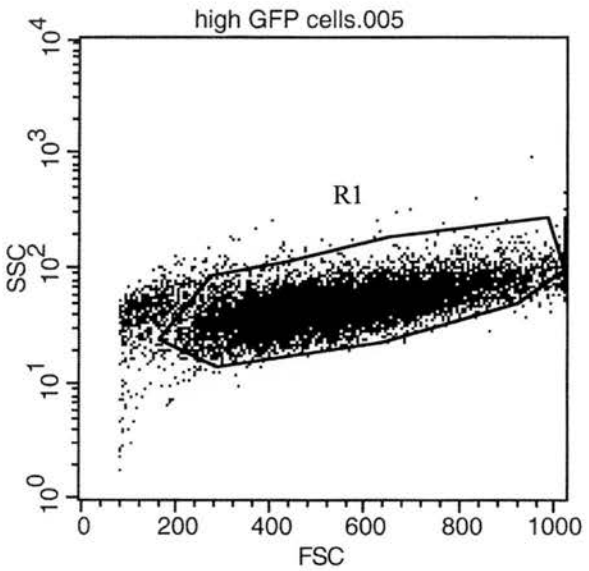

Cells were sorted into a low green population (R2 gate) and a high green population (R3 gate). The M1 gate in the FL1 channel denotes all EGFP-expressing cells.

Legend SSC: Side scatter

FSC: Forward scatter

FL1: Green fluorescence

FL3: Red fluorescence

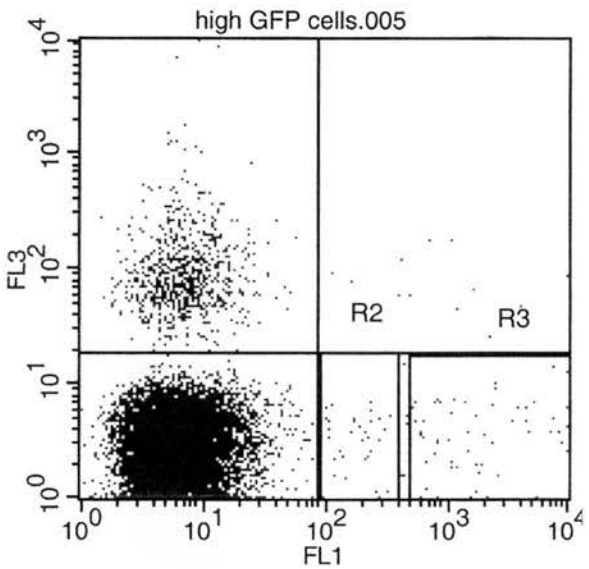

Gated Events: 11027
Total Events: 11027

Region	Events	% Gated	% Total
R1	10000	90.69	90.69
R2	43	0.39	0.39
R3	68	0.62	0.62

Quad	Events	% Gated	% Total
UL	747	7.47	6.77
UR	13	0.13	0.12
LL	9140	91.40	82.89
LR	100	1.00	0.91

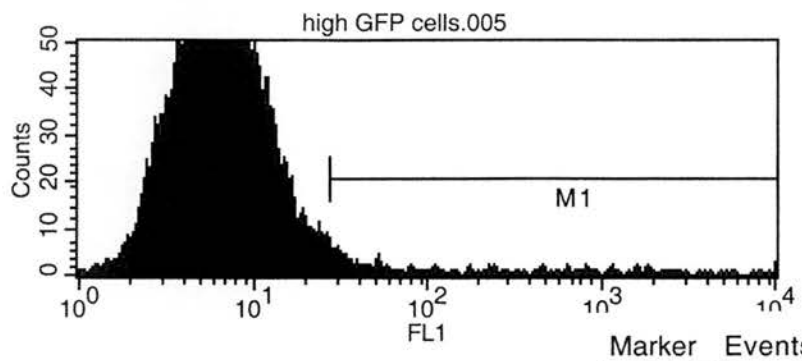

Marker	Events	% Gated	% Total
All	10000	100.00	90.69
M1	249	2.49	2.26

Fig. 6.9 Control Tet-off U373 cells expressing only the tet-controlled transcriptional activator (tTA) as detected by the Becton Dickinson FACsVantage SE

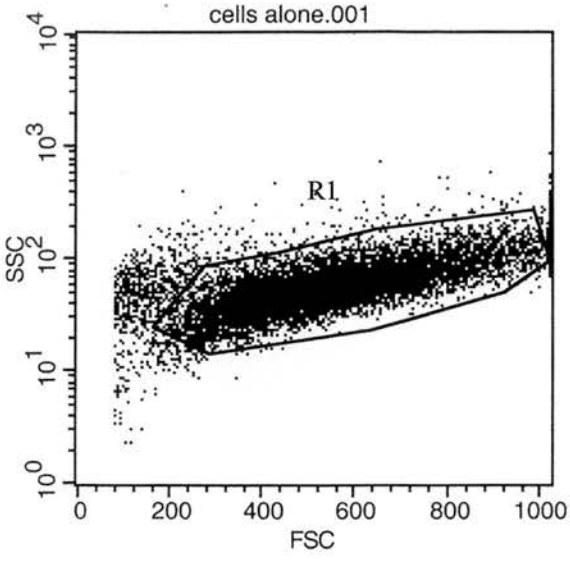

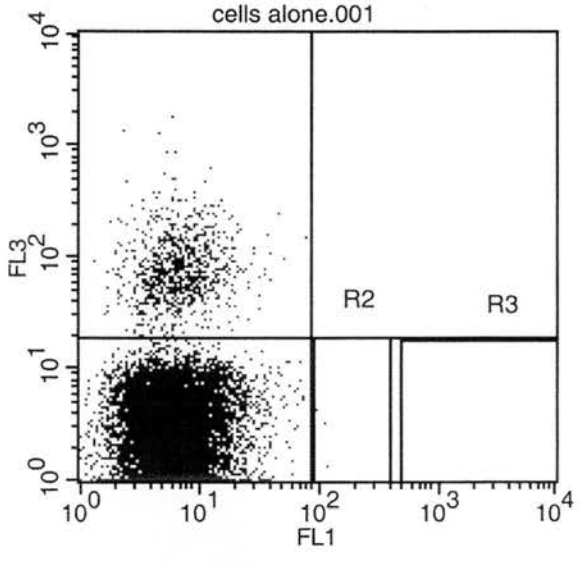

Gated Events: 11366
Total Events: 11366

Region	Events	% Gated	% Total
R1	9991	87.90	87.90
R2	15	0.13	0.13
R3	0	0.00	0.00

Quad	Events	% Gated	% Total
UL	805	8.06	7.08
UR	0	0.00	0.00
LL	9183	91.91	80.79
LR	3	0.03	0.03

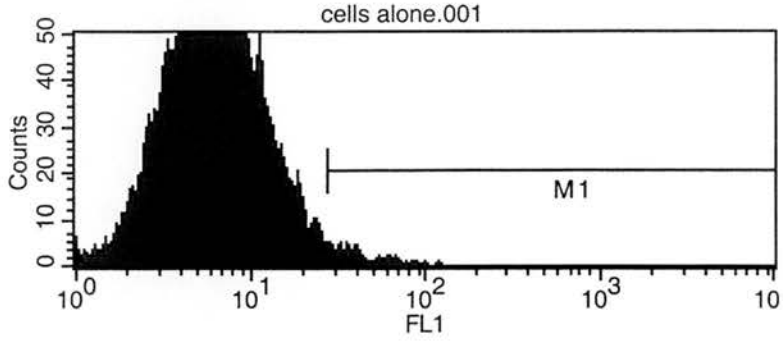

Marker	Events	% Gated	% Total
All	9991	100.00	87.90
M1	149	1.49	1.31

Figure. 6.10 Sample check for purity of sorted 'high' green cells collected from the tTA-expressing clone transfected with pTRE-Cofilin-IRES2-EGFP

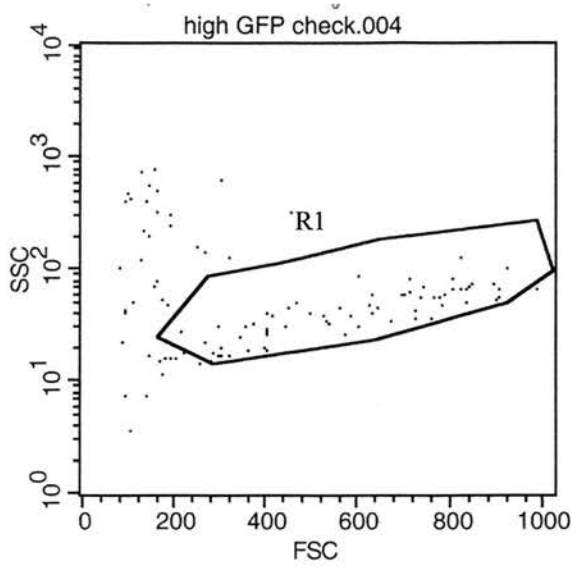

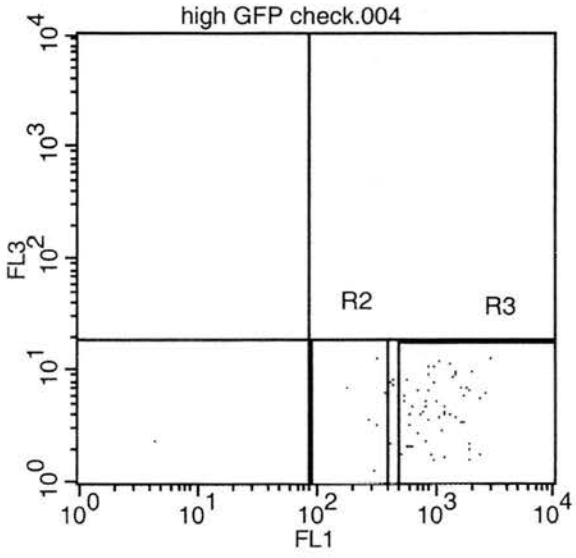

Gated Events: 105
Total Events: 105

Region	Events	% Gated	% Total
R1	64	60.95	60.95
R2	14	13.33	13.33
R3	57	54.29	54.29

Quad	Events	% Gated	% Total
UL	0	0.00	0.00
UR	0	0.00	0.00
LL	1	1.56	0.95
LR	63	98.44	60.00

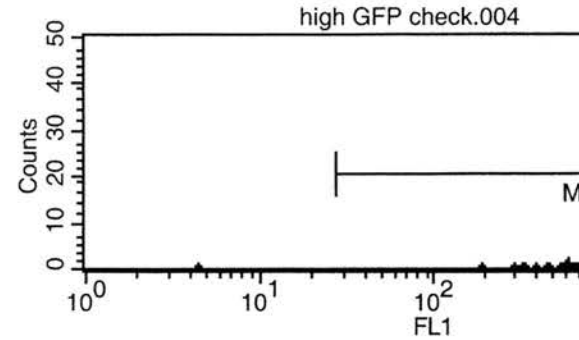

Marker	Events	% Gated	% Total
All	64	100.00	60.95
M1	63	98.44	60.00

Figure. 6.11 Sample check for purity of sorted 'low' green cells collected from the tTA-expressing clone transfected with pTRE-Cofilin-IRES2-EGFP

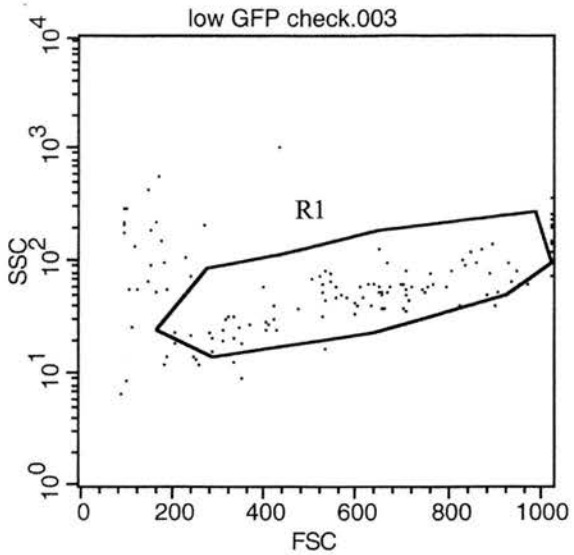

A number of autofluorescing cells (LL quadrant) have been collected together with the EGFP-expressing cells (LR quadrant, R2 region).

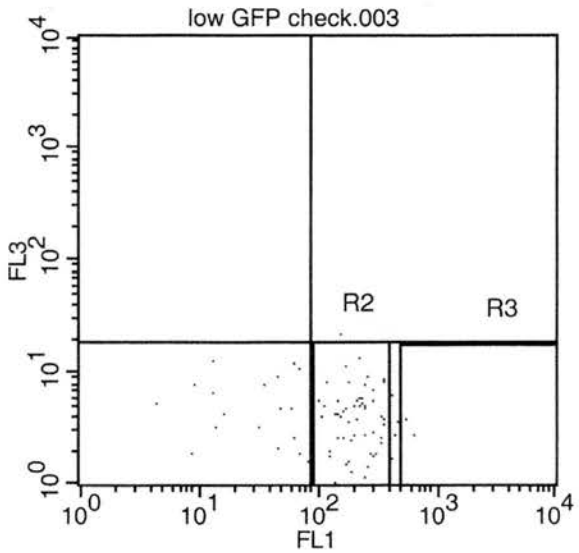

Gated Events: 135
Total Events: 135

Region	Events	% Gated	% Total
R1	83	61.48	61.48
R2	68	50.37	50.37
R3	6	4.44	4.44

Quad	Events	% Gated	% Total
UL	0	0.00	0.00
UR	1	1.20	0.74
LL	18	21.69	13.33
LR	64	77.11	47.41

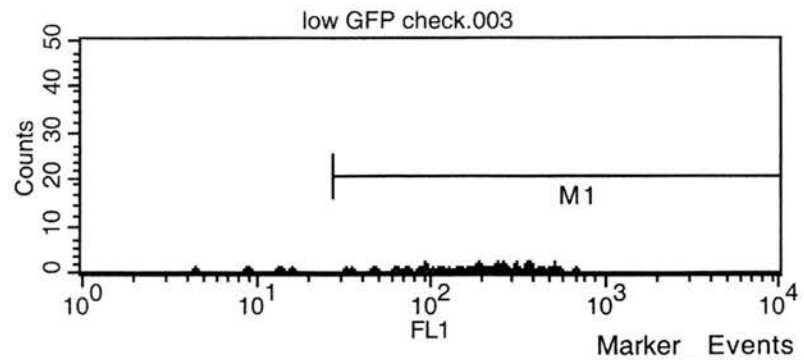

Marker	Events	% Gated	% Total
All	83	100.00	61.48
M1	76	91.57	56.30

tTA-expressing stable clone was used to detect the level of autofluorescence, so that only green fluorescent cells were collected (Figure 6.9). At various intervals samples were taken from the collected populations and analysed with the flow sorter to check for accuracy of sorting (Figures 6.10 and 6.11). Prophylactic treatment with a combination of antibiotics (plasmocin, streptomycin and penicillin) before and after sorting reduced the risk of bacterial infection acquired during flow cytometry (Chapter 2, Part II.III, Selection of Stable Cell Lines).

VI.IV Discussion

The Tet-Off system was initiated to extend an insight into how sensitive the motility machinery is to levels of cofilin overexpression. The results from timelapse experiments on stable clones that overexpressed cofilin from the pCofilin-IRES2-EGFP vector suggested that a more complex relationship might exist between the amount of cofilin in cells and their motility, although overexpression generally increased the speed of cells. The stable clones were found to differ in the degrees of cofilin overexpression and locomotion (Chapter 4). However, investigations into the nature of the correlation were limited by the number of stable clones that could be obtained and maintained in the period of study. If it was possible to regulate cofilin levels in each of the stable clones, one could explore cellular responses over a more comprehensive spectrum of expression.

In order that cofilin expression could be induced by tTA, the pTRE-Cofilin-IRES2-EGFP vector was created and used to establish double-stable cell lines from the tTA-expressing

stable clone. This tetracycline-responsive vector contained the coding sequence of cofilin and the IRES-EGFP sequence. Activation of gene expression by tTA would lead to the transcription of a bicistronic mRNA encoding cofilin and EGFP. This enabled double-stable cells with inducible cofilin expression to be identified by EGFP fluorescence, when grown in the absence of tetracycline or doxycycline.

RT-PCR revealed the expression of the tetracycline-controlled transactivator (tTA) in stable clones transfected with pTet-Off. It was also necessary to test the functional ability of tTA. This was established in two different assays, utilising the Cre recombinase system as well as the pTRE system encoding cofilin and EGFP. Both assays confirmed that tTA could induce the expression of genes cloned into the tetracycline-responsive plasmid (pTRE).

It has been reported that the tetracycline inducible system could regulate gene expression up to five orders of magnitude in a luciferase assay (Gossen and Bujard, 1992). Theoretically, this system would be able to dissect in more detail how cofilin influences motility. Preliminary experiments involving transient transfections of the tTA-expressing clone with pTRE-Cofilin-IRES2-EGFP indicated that gene expression was sensitive to levels of doxycycline in the culture medium. EGFP expression was undetectable with fluorescence microscopy at a concentration of 2μg/ml, reflecting the potential for cofilin expression to be regulated in a similar manner.

Hygromycin-resistant double-stable cells were obtained from a tTA-expressing clone cotransfected with pTRE-Cofilin-IRES2-EGFP and pTK-Hyg. These cells had to be flow-sorted to isolate the EGFP-expressing cells as a mixture of green and non-green fluorescent cells persisted in selective medium, in the absence of tetracycline. The non-green fluorescent cells might represent the population in which the Cofilin-IRES2-EGFP sequence had integrated into genomic loci in regions were the chromatin is condensed and silenced (reviewed by Bishop J., 1999). An alternative explanation might be that only the hygromycin resistance gene had stably integrated, but not the Cofilin-IRES2-EGFP sequence as the culture conditions only selected for hygromycin resistance. There is evidence to suggest that integrated plasmid DNA could be excised from the host genome (McBurney *et al.*, 1994). A third possibility is that some cells were not successfully cotransfected with both vectors, and had acquired only hygromycin resistance. A degree of inefficiency in cotransfections has been observed in transient transfections using flow cytometric analysis (Ducrest *et al.*, 2002).

The sorting of double-stable cells into groups of low- and high-expressors of EGFP proved to be especially useful in eliminating non-green cells that appeared to contaminate the low-expressing group. Figure 6.11 shows that the sample retrieved from the low EGFP-expressing group to check accuracy of sorting also contained a number of non-green cells. This problem was encountered when green fluorescent cells were sorted together in the same group at a separate session. The resultant culture contained a small number of cells that did not fluoresce green.

The main problems encountered during the development of the system included the isolation of hygromycin-resistant double-stable cells that expressed pTRE-Cofilin-IRES2-EGFP and pEGFP-N1 and infection acquired after FACS sorting. As mentioned, hygromycin-resistant cells consisted of both green and non-green fluorescent cells. Isolation of double-stable cells was initially attempted by plating at low density so that clonal growth would be encouraged. However, this proved to be laborious and time-consuming as growth at low density was slow, and 'colonies' derived were still heterogeneous. These colonies were thus expanded and FACS sorted to select the green fluorescent cells. The major setbacks that arose were post-sorting infection, and contamination with non-green cells in the populations in which the green fluorescent cells had been sorted in a single group to include 'low' EGFP expressors.

In summary, the Tet-off system was developed to induce variable and potentially regulatable levels of cofilin overexpression. The inducibility of gene expression in the system was tested, and it was evident that gene expression could be switched off in the presence of doxycycline. Double-stable cells expressing tTA, cofilin and EGFP were established and selected by FACS. Future work will involve clonal expansion of these double-stable cells and investigating how the motility of cells might vary with the quantitative control of cofilin overexpression using doxycycline.

CHAPTER 7

DISCUSSION ON THE EFFECTS OF COFILIN OVEREXPRESSION IN U373 MG GLIOBLASTOMA CELLS

It has been demonstrated that overexpression of cofilin in U373 MG glioblastoma cells increases their motility. This was established in both transient and stable transfections with pCofilin-IRES2-EGFP. The extent of motility appears to be sensitive to levels of cofilin, so that an optimum level that confers the highest increase in speed could be defined. Furthermore, the effects of cofilin overexpression were most distinct at moderate regional cell density. At high density approaching confluence, glioblastoma cells that overexpressed cofilin did not move faster than untransfected cells. This suggests that close contact between cells limited their locomotion, irrespective of cofilin activity. Cofilin overexpression therefore does not affect normal contact inhibition of locomotion.

There is much evidence that advocates the essential role of cofilin in actin-based cell motility. Actin filament dynamics, characterised mainly by cycles of polymerization and depolymerization, are necessary for the formation of lamellipodia during locomotion. A rate-limiting step in the turnover of filaments is actin depolymerization at the pointed (slow-growing) ends, catalysed by ADF/cofilin proteins which increase the off rate of filaments (Carlier *et al.*, 1997; Maciver *et al.*, 1998) and also sever filaments (Maciver and Weeds, 1994). ADF, together with the Arp2/3 complex, capping protein and N-WASP, were found to be essential components driving actin-based bacterial motility (Loisel *et al.*, 1999). Several studies have shown that cofilin is

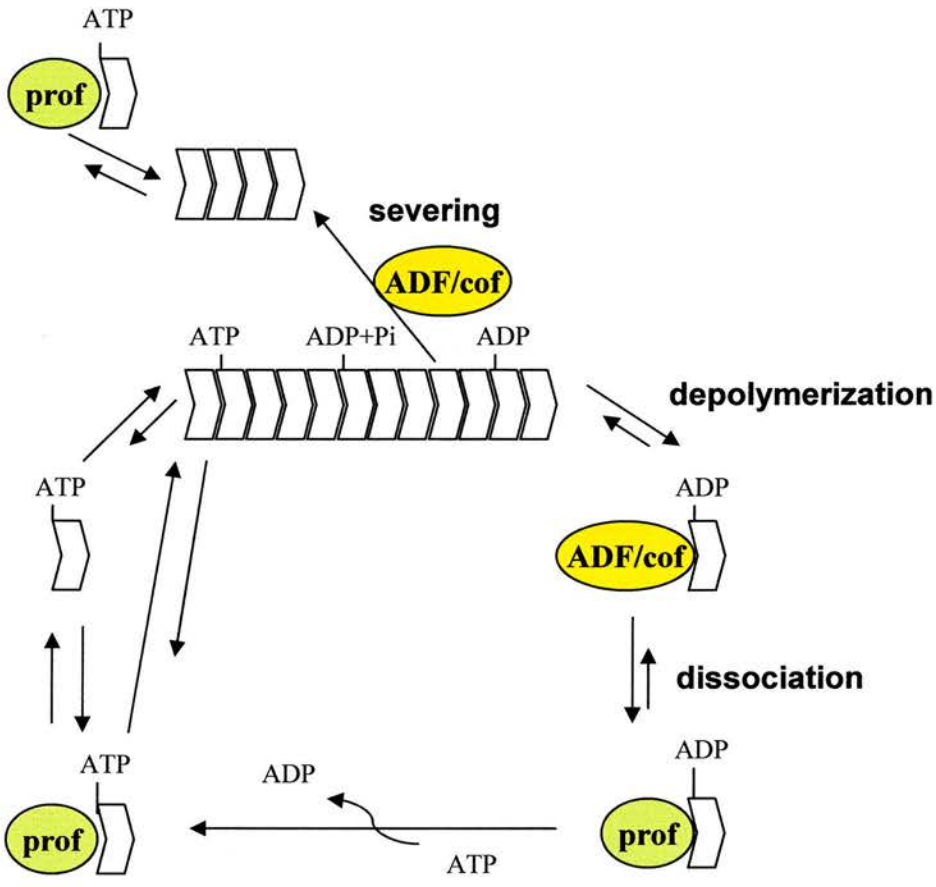

Fig. 7.1 How ADF/cofilin overexpression may increase the motility of glioblastoma cells

The rate-limiting step in actin filament treadmilling is depolymerization at the pointed ends of filaments. An increase in cofilin activity promotes depolymerization and generates a larger pool of actin monomers which can polymerize to the barbed ends. Cofilin dissociates from ADP-actin monomers after depolymerizatin and allows nucleotide exchange to form ATP-actin monomers. Profilin binds preferentially to ATP-actin monomers, shifting the equilibrium to enhance the amount of ATP-actin, as well as selectively adding ATP-actin to barbed ends (Didry et al, 1998). Profilin also increases nucleotide exchange catalytically (Nishida, 1985). In this way, cofilin synergises with profilin to produce ATP-actin monomers and accelerate filament treadmilling. The severing activity of cofilin also generates shorter filaments that can be recruited to the leading edge and participate in treadmilling.

recruited to just behind the leading edge of moving cells and motile structures such as ruffling membranes and lamellipodia (Aizawa *et al.*, 1997; Bamburg and Bray, 1987; Chan *et al.*, 2000; Kuhn *et al.*, 2000; Quirk *et al.*, 1993; Suzuki *et al.*, 1995), and the growth cones of neurons (Kuhn *et al.*, 2000). In glioblastoma cells, fluorescent immunodetection of cofilin localised its presence in similar structures, indicating an active role in remodelling the actin cytoskeleton in response to motility-inducing signals (Chapter 3, Part III.II).

It has been observed that cofilin levels in cells can influence their locomotory ability. Lack of functional cofilin leads to impaired movement. Cell migration is defective in the ovaries of *Drosophila* larvae with a loss-of-function mutation in the *twinstar* (*tsr*) gene encoding the *Drosophila* homologue of ADF/cofilin (Chen *et al.*, 2001). In contrast, overexpression of cofilin in *Dictyostelium discoideum* facilitates increased movement (Aizawa *et al.*, 1996).

Cofilin overexpression increases the motility of glioblastoma cells

The increased motility associated with cofilin overexpression might be explained by several mechanisms that ultimately result in enhanced actin filament treadmilling, a major force-producing event in movement (see Introduction, Part II). The depolymerizing activity of cofilin frees actin subunits from the pointed ends of filaments, generating a pool of monomers which can participate in filament assembly (Carlier *et al.*, 1997). Since depolymerization is rate-limiting, an increase in cofilin activity, such as that resulting from overexpression, would be expected to favour filament treadmilling (Figure 7.1). In addition, cofilin synergises with profilin to

increase the ATP-actin monomer pool, which adds preferentially to the barbed (fast-growing) ends of filaments. ATP-actin also associates with profilin and the profilin-actin complex elongates filaments by binding selectively to the barbed ends (Pring *et al.*, 1992). Hence actin polymerization is accelerated in the presence of cofilin and profilin (Didry *et al.*, 1998). ADF/cofilin alone can generate increased amounts of ATP-actin from depolymerization, which results in the formation of the ADF/cofilin-bound ADP-actin monomer complex, dissociation of ADF/cofilin from the complex and subsequent exchange of ADP for ATP (Didry *et al.*, 1998). Another mechanism that could contribute to increased motility is severing of actin filaments by cofilin (Maciver *et al.*, 1991). It has been suggested that severing produces shorter filaments with free barbed ends that can be recruited to the leading edge and act as nuclei for polymerization (Theriot, 1997). Actin nucleation induced by the severing activity of cofilin has been shown to be fundamental to lamellipodial protrusion in metastatic melanoma cells stimulated by epidermal growth factor (Zebda *et al.*, 2000). In these cells, inactivation of cofilin by phosphorylation abolished the appearance of free barbed ends associated with actin nuclei and cellular protrusion.

An interesting finding in the overexpression studies in U373 MG glioblastoma cells was that the greatest increase in motility occurred at an optimum level of cofilin. Enhancement of motility was less marked when cofilin was expressed both above and below this level. There is a precedence for such an influence of cytoskeletal protein levels on motility. In vitro experiments show that the motility of the *Listeria* bacteria in reconstituted medium varies with the concentration of actin depolymerizing factor (ADF) in a bell shaped curve (Loisel *et al.*, 1999), and the effect of cofilin is likely to be similar. In biochemical assays, the rate of actin polymerization is affected by ADF

concentration in a similar manner, climbing to a maximum then decreasing with rising ADF concentration (Didry *et al.*, 1998).

The decrease in treadmilling rate at high levels of cofilin might be explained by a few possible mechanisms. In cells, ADP-actin monomers exist as free entities, or complexed with proteins including ADF/cofilin. In the presence of excess ADF/cofilin, its high affinity for ADP-actin monomers (Maciver and Weeds, 1994) might shift the equilibrium and result in a predominance of ADF/cofilin-bound ADP-actin. Since cofilin reduces the rate of nucleotide exchange on actin (Nishida, 1985), this limits the regeneration of ATP-actin monomers and therefore the rate of polymerization. Competition between cofilin and profilin for actin binding (Blanchoin and Pollard, 1998) implies that production of ATP-actin is further hindered with excess cofilin, since profilin promotes nucleotide exchange (Nishida, 1985). This hypothesis is supported by the finding that the steady-state concentration of ATP-actin diminishes at high concentrations of ADF (Didry *et al.*, 1998). Furthermore, ADF-bound ADP-actin repolymerizes to the pointed ends of filaments when present in excess, potentially retarding treadmilling.

Excessive severing and depolymerization in the presence of large amounts of cofilin could be counter-productive to treadmilling. In Chapter 3, it was discussed that cofilin activity is confined to the inner zone of the lamellipodium, leaving the outermost lamellipodium free from depolymerization (Svitkina and Borisy, 1999). This was proposed to be due partly to the protection of pointed ends by the Arp2/3 complex, and presumably the 'fresh' filaments in the outer zone are largely ATP-bound. Thus, the polymerization of filaments occurs mainly at the extreme front, with the supply of

actin monomers generated by cofilin activity towards the cellular interior. It is possible that an excess of cofilin displaces Arp2/3 from the pointed ends, so that depolymerization and severing occurs throughout the lamellipodium. The Arp2/3 complex has been shown to bind ADP-actin (present at the pointed ends) with less affinity then ATP-actin (at barbed ends). The binding of cofilin (actophorin) to the Arp2/3 complex, although weak, may further reduce its association with pointed ends, exposing them to cofilin (Blanchoin *et al.*, 2000). Widespread activity of cofilin might induce ectopic sites of polymerization on severed filaments, leading to a reduction in directional treadmilling and motility.

The effects of regional cell density on cofilin activity

Plating density has been shown to affect both cell motility (Hartmann-Petersen *et al.*, 2000) and cell morphology (Berezin *et al.*, 1997). At low densities, fibroblasts appear relatively rounded, whilst increasing density promotes the appearance of cellular extensions. These morphological alterations have been attributed to higher levels of growth factors and matrix proteins secreted when more cells are present. On the other hand, high plating density causes a significant decrease in fibroblast motility, attributable to contact inhibition of movement.

The activity of cofilin in overexpressing cells appears to be influenced by cell density, possibly arising from interactions with the environment which are mediated by intercellular signals and matrix adhesions. This might explain the differences in outcome observed over a range of regional cell density. The stimulation of motility by cofilin overexpression was revealed at moderate cell density. In contrast, changes in

motility were insignificant at low cell densities below 70 cells/mm^2, and also at high cell densities above 200 cells/mm^2 (Chapter 5, Effects of Cell Density on Motility). This suggests that cells that overexpressed cofilin were regulated by mechanisms underlying contact stimulation and contact inhibition of movement, as well as other extracellular factors that influence locomotion.

Cell-cell contact has been observed to stimulate migration of cells in culture and isolated cells are poorly motile (Thomas and Yamada, 1992). This contact stimulation of movement was observed in human melanocytes and melanoma cells, as well as primary neural crest cells from quail embryos. Cells may also be stimulated to move in the presence of neighbouring cells by the secretion of growth factors and matrix proteins. Glioblastoma cells express growth factors such as fibroblast growth factor (FGF) and platelet-derived growth factor (PDGF). The epidermal growth factor receptor (EGFR) is also often amplified (Rasheed and Bigner, 1991). In vitro experiments show that the migratory and invasive capacities of glioblastoma cells increase in the presence of growth factors such as EGF and FGF (Engebraaten *et al.*, 1993). Since cofilin is recruited to the lamellipodia and leading edges to effect actin filament treadmilling when tumour cells are activated by these factors (Chan *et al.*, 2000), its overexpression can be expected to potentiate the response to motility-inducing stimuli.

In addition to growth factors, glioblastoma cells secrete extracellular matrix components (Bouterfa *et al.*, 1999). The effects of matrix proteins on motility are complex, as tumour cells secrete a variety of matrix proteins and it is unclear which proteins contribute significantly to glioblastoma invasion. However, glioblastoma cells

appear to migrate faster on fibronectin and collagen-coated substrata (Bouterfa *et al.*, 1999). These observations suggest that the secretion of growth factors and matrix proteins can alter the degree of motility. Critical concentrations of these proteins might be required to maximise the locomotory ability of cells, so that the effects of cofilin overexpression are predominantly observed at moderate but not low cell densities. In support of this, it has been noted that in fibroblasts an optimal concentration of fibronectin coating induced maximum movement, with reduced motility at lower and higher concentrations (Hartmann-Petersen *et al.*, 2000).

At high cell density, both cofilin-overexpressing and untransfected glioblastoma cells were observed to exhibit contact inhibition of movement. Contact inhibition in motile cells (Abercrombie, 1970) describes a common conduct of cells which contact each other during movement. Contact-inhibited cells halt movement in directions that would result in crawling over or under other cells, and tend to translocate into free spaces. It has been observed that some tumour cells exhibit reduced contact inhibition, but do not completely lose this property which characterises the behaviour of untransformed cells (Abercrombie, 1979; Guelstein *et al.*, 1973). The pathways activated by contact inhibition and leading to cytoskeletal reorganisation with changes in motility are not fully dissected. They are likely to involve signalling via cell surface molecules such as integrins and cadherins. Integrins and cadherins are transmembrane glycoproteins mediating cell-matrix and cell-cell adhesions respectively (Hynes, 1992; Takeichi, 1993). Some integrins also function in intercellular adhesions. It appears that integrins and cadherins synergise to achieve contact inhibition of movement, although the moleular intersections are unknown (Huttenlocher *et al.*, 1998). Timelapse analysis of U373 MG glioblastoma cells suggests that cofilin overexpression per se is not

sufficient to overcome contact inhibition. This is perhaps a consequence of regulatory activities on several other components of the cytoskeletal machinery to retard movement. The activity of cofilin itself might be subject to downregulation.

Conclusion: cofilin activity in tumour cells

The proposition that regulation of cofilin might be implicated in the spread of tumours arises from observations that its activity is altered in several tumours, and that this potentially affects migration. Growth factor-induced tumour cell migration has been shown to be dependent on actin polymerization at the leading edges of cells, facilitated by ADF/cofilin. Inactivation of cofilin by phosphorylation critically hinders this response to growth factors (Zebda *et al.*, 2000). Interestingly, several tumour cell types have been shown to harbour an excess of active (dephosphorylated) cofilin (Nebl *et al.*, 1996). This includes freshly acquired tumours (T-lymphoma cells), as well as tumour cell lines such as T-lymphoma cells (Jurkat), cervical carcinoma cells (HeLa), colon (KM12), liver (HepG2) and kidney (COS1). The rat glioblastoma cell line (C6), which is also highly invasive, is known to overexpress cofilin (Gunnersen *et al.*, 2000).

The experiments demonstrate that human glioblastoma cells harness cofilin to locomote, and their motility is sensitive to cofilin levels. The influence of cell density on motility induced by cofilin overexpression implies that the magnitude of its effects is dictated by interactions within the cellular environment. In conclusion, cofilin overexpression enhances glioblastoma motility, and its activity can be modulated in response to variations in the extracellular precincts. These findings are indicative that

cofilin could be an important downstream effector of signalling events that mediate tumour migration. It would be enlightening to study the expression and regulation of cofilin in primary brain tumour specimens, as this might reveal if differences exist in vivo between tumours of varying invasiveness. An understanding of the control of cofilin and its cytoskeletal partners in the motile machinery of cancers would be invaluable in addressing the limitations that continue to elude modern therapy – tumour dissemination.

APPENDIX A

MATERIALS FOR MOLECULAR BIOLOGY

Solutions

TBE (10X)

0.9M Tris-Cl, pH 7.5
0.9M Boric acid
20mM EDTA, pH8.0

TAE (50X)

2M Tris-Cl, pH 7.5
50mM EDTA, pH 8.0
5.7% (v/v) glacial acetic acid

PBS(10X)

1.37M NaCl
27.6mM KCl
81mM Na_2HPO_4
14.7mM KH_2PO_4

TE buffer (pH 7.4, 7.6,.8.0)

10mM Tris-Cl, pH 7.4, 7.6, 8.0
1mM EDTA, pH 8.0

Tail tip lysis buffer

0.1M Tris-Cl, pH 8.0
0.2M NaCl
0.005M EDTA
0.2% SDS (w/v) (sodium dodecyl sulphate)

Bacterial culture: media and antibiotics

LB medium

LB tablets: 1 tablet dissolved in 50ml water and autoclaved to sterilise.
(Sigma, L-7275)

2XTY

1L of medium:
16g tryptone
10g yeast extract
5g NaCl

Autoclave.

SOB medium

2% (w/v) tryptone
0.5% (w/v) yeast extract
0.05% (w/v) NaCl
2.5mM KCl
pH 7.0 with NaOH

Autoclave, then add MgCl2 to 10mM.

SOC medium

SOB medium
20mM glucose
Filter sterilise (0.2μm filter) and store at -20°C.

LB-agar

35g of LB-agar dissolved in 1L water and autoclaved to sterilise.
Kept liquid in a 60°C oven till just before pouring onto plates.
(Sigma, L-2897)

Ampicillin

50mg/ml stock dissolved in 50% ethanol (v/v) and stored at -20°C.
To use, dilute 1000-fold to 50μg/ml in media, at temperatures not exceeding 50°C.
(Roche, 835 242)

Kanamycin

100mg/ml stock, stored at -20°C. Working concentration 30 – 100μg/ml.

Competent cell freezing mix

100mM KCl, 50mM $CaCl_2$, 10mM potassium acetate pH 7.5, 10% glycerol (v/v)

Glycerol freezing storage mix

65% (v/v) glycerol
0.1M $MgSO_4$
25mM Tris-HCl, pH8.0

X-Gal stock

X-gal 30mg/ml in N,N'-dimethylformamide
Store at -20°C in the dark. Allow to dry before plating cells on LB agar.

IPTG stock

0.1M IPTG in ddH_2O
Filter sterilise (0.2μm filter) and store at 4°C.

E. coli bacterial strains

DH5α
(Clontech laboratories Inc.)

SCS110
(Clontech laboratories Inc.)

Vectors used for cloning

pMW 172
(Dr. Michael Way)

pBluescript II KS (-)
(Stratagene, GenBank accession X52329)

pIRES$_2$-EGFP
(Clontech laboratories Inc.)

pTRE
(Clontech laboratories Inc., GenBank accession U89931)

Agarose gel electrophoresis

Agarose

NuSieve GTG agarose
(FMC BioProducts)

Agarose
(Sigma, A-9539)

Molecular weight ladders

100bp DNA ladder
(GibcoBrl, 15628-019)

500bp DNA ladder (DNA molecular weight marker XVII)
(Roche, 1 855 646)

GeneRuler™ 1kb DNA ladder
(MBI Fermentas, SM 0312)

Loading buffer

Orange G (BDH, 43725)
10ml buffer

Glycerol	5ml
0.5M EDTA pH8.0	40µl
Double-distilled water	5ml

Add a few grains of Orange G dye and mix.

Molecular biology enzymes

DNA restriction enzymes

These were manufactured by Boehringer Mannheim (Roche) or New England Biolabs and used with the appropriate buffers according to the manufacturers' instructions.

DNA modifying enzymes

T4 DNA ligase
(Roche, 481 220)

Taq DNA polymerase in storage buffer B
(Promega, M2661)

Calf intestinal alkaline phosphatase
(Roche, 713 023)

Other enzymes

Proteinse K
(Roche, 745 723)

DNase 1, RNase-free (Deoxyribonuclease 1, 10U/µl)
(Roche)

Molecular biology kits

Plasmid DNA extraction and purification

Ultraclean mini plasmid prep kit
(Mo Bio laboratories, 12300-100)

QIAprep Spin Miniprep kit
(Qiagen, 27106)

Plasmid midi kit
(Qiagen, 12143)

Qiaex II gel extraction kit
(Qiagen, 20021)

QIAquick gel extraction kit
(Qiagen, 28704)

RNA extraction from U373 MG glioma cells

RNeasy Mini kit
(Qiagen, 74104)

RT (reverse transcription)-PCR of U373 MG cells

Superscript™ preamplification system for first strand cDNA synthesis
(GibcoBrl, 18089-011)

Plasmid DNA sequencing

ABI Prism BigDye terminator cycle sequencing ready reaction kit, with Amplitaq DNA polymerase, FS
(Perkin-Elmer Applied Biosystems)

Equipment and accessories for molecular biology

Bacterial transformation by electroporation

BioRad gene pulser/E. coli pulser cuvette

Electroporator
(BioRad)

Bacterial incubator

Gallenkamp shaking incubator

Centrifuges

Biofuge stratos
(Heraeus instruments)

Beckman Avanti™ J-25

Biofuge pico
(Heraeus instruments)

Polymerase chain reaction

PTC-225 Peltier Thermal Cycler

Spectrophotometer

Jenway 6105 U.V./Vis. spectrophotometer

Gel electrophoresis

Dual intensity ultraviolet transilluminator
(Ultra-Violet Products)

Computer software

Primer design

Primer3 Output
(Whitehead Institute, MIT)

Gel electrophoresis imaging and DNA quantitation

Alphaimager 1220
(Alpha Innotech Corporation)

APPENDIX B

MATERIALS FOR IN SITU HYBRIDIZATION

DIG RNA Labeling Kit (SP6/T7):
Includes 10X transcription buffer; 10X NTP labeling mixture with 10mM ATP, CTP, GTP, 6.5mM UTP, 3.5mM DIG-11-UTP (pH 7.5); T7 RNA polymerase 20units/µl.
(Roche, 1 175 025)

T3 RNA polymerase (20units/µl)
(Roche, 1 031 163)

RNase A (make 10mg/ml stock)
(Roche)

Proteinase K
(Roche, 745 723)

Total RNA (10mg/ml from yeast)
(Roche, 109 223)

Anti-Digoxigenin-AP, fab fragments (sheep)
(Roche, 1 093 274)

NBT/BCIP Stock solution (18.75mg/ml NBT; 9.4mg/ml BCIP)
(Roche, 1681451)

TESPA (amino-propyltriethoxysilane)
(Sigma, A-3648)

DPX mountant for microscopy
(BDH, 360294H)

Stock Solutions

0.5M EDTA, pH 8.0

10X phosphate buffered saline (PBS stock)

PBS-0.1%Tween (v/v)

4M NaCl

1M $MgCl_2$

2M Tris-Cl, pH 9.5
3M sodium acetate, pH 5.5

0.01% Diethyl pyrocarbonate (DEPC) in double-distilled water (v/v)

10% sodium dodecyl sulphate (w/v) (SDS)

50% Dextran sulphate (v/v)

4% paraformaldehyde (w/v)

Xylene

2M Triethanolamine in ddH_2O (w/v)

2X SSC in 50% formamide (v/v)

Maleic acid buffer, pH 7.5
100mM maleic acid (w/v)
150mM NaCl
ddH_2O

Blocking buffer
10% Blocking reagent (w/v) (Roche, 1 096 176)
Dissolve in maleic acid buffer and store aliquots of 15ml at -20°C.

20X SSPE, pH 7.4
0.02M EDTA, pH 8.0
3.6M NaCl
0.2M NaH_2PO_4

20X phosphate buffer, pH 7.5
1M Tris-Cl
0.1M EDTA, pH 8.0
ddH_2O, pH to 7.5

20X SSC, pH 7.0
3M NaCl
0.3M sodium citrate

10X salts
3M NaCl
0.1M Tris-Cl (pH 6.8)
NaH_2PO_4.H2O 7.8g/L (MW 138)
Na_2HPO_4 7.1g/L (MW 142)
50mM EDTA

Alkaline phosphatase buffer, pH 9.5 (per L)
12.5ml of 4M NaCl
25ml of 1M $MgCl_2$
25ml 2M Tris-Cl (pH 9.5)
750µl Tween
2-3 flakes Levamisole (Sigma, L-9756)

Hybridization mix
10ml:
5ml formamide
1ml 20X SSPE
500ml 10% SDS (w/v)
2ml 50% Dextran sulphate (v/v)
200µl total RNA (10mg/ml stock)
500µl 100X Denharts solution

Frozen in 700µl aliquots at -20°C.

100X Denharts solution
250ml:
5g Ficoll (Sigma, F2375)
5g polyvinylpyrrolidone
5g bovine serum albumin
200ml DECP-water
Stir overnight in a baked beaker, make up to the final volume of 250ml.
Store in aliquots of 15ml at -20°C (stable for several years).

Anti-DIG immunoreaction buffer
150ml:
15ml 10% blocking buffer (@1%) (w/v)
15ml 10X PBS (@1X)
3ml sheep serum (Diagnostics Scotland)
150µl Tween
30µl anti-Digoxigenin-AP (@1:5000 final dilution)

APPENDIX C

MATERIALS FOR CELL BIOLOGY

Cell Culture

Cell line

U373 MG human glioblastoma-astrocytoma:
Epithelial morphology; derived from a malignant tumour by explant technique.
(European Collection of Cell Cultures (ECACC), number 89081403)

Standard culture medium

Dulbecco's Modified Eagle Medium/ Nutrient Mix F12 (1:1), without L-glutamine (DMEM/F12, GibcoBrl)

10% fetal bovine serum (v/v)

2mM L-glutamine
(stock: 100X (200mM) L-glutamine, GibcoBrl)

100 units/ml penicillin + 100µg/ml streptomycin
(stock: 10 000 units of penicillin + 10000µg of streptomycin, GibcoBrl)

Fetal bovine serum for Tet-Off system

Tet System approved fetal bovine serum
(Clontech laboratiores Inc., 8630-1)

Trypsinization

Trypsin-EDTA (0.25% trypsin (v/v), 1mM EDTA.4Na) (1X), liquid
(GibcoBrl)

Dulbecco's Phosphate Buffered Saline,1X, liquid
(GibcoBrl)

Freezing Medium

95% Fetal bovine serum (v/v)

5% DMSO (dimethyl sulfoxide) (v/v)

Antibiotic for prophylaxis against Mycoplasma and related bacterial contamination

Plasmocin™
(InvivoGen)

Plastic ware

1.8 ml Nunc cryotubes
(Nalge Nunc International)

Flasks

25cm^2 culture area flasks (T25)
(Iawki, 3100-025)

75cm^2 culture area flasks (T75)
(Iwaki, 3110-075)

Plates

6 well (9.4cm^2 culture area/well) plate
(Iwaki, 3810-006)

24 well (2.0cm^2 culture area/well) plate
(Iawki, 3820-024)

Sterile plastic pipettes

5ml pipette
(Iwaki, LX5ML)

10ml pipette
(Iwaki, LX10ML)

25ml pipette
(Iwaki, LX25ML)

Transfection of U373 MG cells

Plasmids

@ 300 ng/µl (0.02-2.0 µg/µl

pCofilin-IRES2-EGFP

pTet-Off
(Clontech laboratories Inc., catalogue K1620-A)

pTRE-Cofilin-IRES2-EGFP

pISTRECre and pIS-NL2EGFP
(Dr. T. I. Simpson)

pEGFP-N1
(Clontech laboratories Inc., GenBank accession U55762)

pTK-Hyg
(Clontech laboratories Inc., GenBank accession U40398)

Transfection reagents

FuGene™ 6 transfection reagent
(Roche)

Serum-free medium (DMEM/F12)
(GibcoBrl)

Antibiotic selection for stable cell lines

50mg/ml Geneticin sulphate (G-418) in 0.1M HEPES buffer pH 7.3
(GibcoBrl)

Hygromycin B
(Calbiochem-Novabiochem Corporation)

HEPES buffer (1M)
(Sigma, H0887)

APPENDIX D

MATERIALS FOR IMMUNOCHEMISTRY

Immunocytochemistry

A. Immunostaining on slides

Fixation

4% paraformaldehyde (w/v)

Phosphate buffered saline (PBS) or distilled water

Permeabilisation

0.1% Triton X-100 (v/v)
(Sigma)

Phosphate buffered saline

Blocking serum

20% serum (v/v) in phosphate buffered saline (PBS):
serum of same species from which the secondary antibody is derived.
(serum from Diagnostics Scotland)

Primary antibodies

Cofilin polyclonal antibody (250 μg/ml rabbit anti-human)
(Cytoskeleton Inc., ACFL02)

Monoclonal anti-β-actin clone AC-74 (1.2 mg/ml):
Mouse IgG2a isotype, cross reacts with several species including humans.
(Sigma, A5316)

Fluorescent secondary antibodies

Alexa Fluor 546 goat anti-rabbit IgG (H+L) (2 mg/ml)
(Molecular Probes)

TRITC-conjugated swine anti-rabbit immunoglobulins
(tetramethyl-rhodamine isothiocyanate R isomer, DAKO)

TRITC-conjugated rabbit anti-mouse immunoglobulins
(DAKO)

Aqueous slide mountant

Vectashield
(Vector laboratories Inc.)

Moviol-488 (Harco)

DABCO (1,4-diazabicyclo-[2.2.2]octane) as antifade
(Sigma)

Chamber slides

Lab-Tek II chamber slide with cover (8 well)
(Nalge Nunc International)

B. Immunochemistry for flow cytometry (Immunocytometry)

Fixation

4% paraformaldehyde (w/v)
(prepared from 10% stock with PBS or H_2O)

Permeabilisation

70% cold ethanol (v/v)
(stored at -20°C)

Washes and cell suspension

PBS – 1% BSA (w/v): 1g bovine albumin in 100ml PBS
(Bovine albumin fraction V, Sigma)

PBS-1% BSA (w/v)-1% formalin (v/v)

Blocking serum

20% goat serum in PBS (v/v)
(Goat serum from Diagnostics Scotland)

Primary antibody

Cofilin polyclonal antibody (250 µg/ml rabbit anti-human)
(Cytoskeleton Inc., ACFL02)

Isotype control primary antibody

Rabbit anti-mouse immunoglobulins
(Dako)

Secondary antibody

Goat anti-rabbit IgG (H+L specific) Spectral Red conjugate
(Southern Biotechnology Associates Inc., Cambridge Bioscience catalogue number 4050-13)

Protein electrophoresis and Western blotting

Protein extraction

TENT buffer

Stock:
20mM Tris, pH 8.0
2mM EDTA
150mM NaCl
1% Triton-X100 (v/v)

Add protease inhibitors to TENT buffer before use:

	Frozen Stock	Volume for 1200µl (1180.6ml TENT)
1mM Pefabloc	0.1M	12.0µl
10µg/ml aprotinin	10mg/ml	1.2µl
2µg/ml leupeptin	1mM	5.0µl
1µg/ml pepstatin	1mM	1.2µl

Cold PBS (in 4°C fridge)

Determination of protein concentration

BCA Protein Assay Reagent kit
(Pierce, catalogue number 23227)

Protein electrophoresis using NuPAGE system

NuPAGE 10% Bis-Tris precast gel (12well)
(Invitrogen Life Technologies, NP 0302)

NuPAGE MOPS SDS running buffer 20X
(Invitrogen Life Technologies, NP 0001)

NuPAGE antioxidant
(Invitrogen Life Technologies, NP 0005)

NuPAGE sample reducing agent 10X (0.5M DTT in stabilized liquid form)
(Invitrogen Life Technologies, NP 0004)

NuPAGE 4X sample buffer
(Invitrogen Life Technologies, NP 0007)

Multimark multi-coloured standard
(Invitrogen Life Technologies, LC 5725)

1-100 microliter filter tips for loading samples
(Alpha laboratories, LW 1285)

Protein electrophoresis using BioRad system

12% Polyacrylamide separating gel (w/v)

10ml (1gel)	Amount
30% acrylamide mix	4ml
1.5M Tris (pH8.8)	2.5ml
10% SDS	100µl
ddH_2O	3.36ml
10% ammonium persulfate (1g/10ml, fresh)	100µl
TEMED	100µl
(*add last just before pouring : gel sets quickly*)	

0.5% Stacking gel (coloured to distinguish from separating gel) (w/v)

8 ml (1 gel)	Amount
30% acrylamide mix	1.32ml
0.5M Tris (pH 6.8)	2.00ml
10% SDS	80µl
ddH_2O	4.6ml
10% ammonium persulfate (fresh)	100µl
TEMED (tetramethylethylenediamine)	100µl
(*add last just before pouring*)	
(+/- Bromophenol blue	0.1%)

5X SDS running buffer, pH 8.3

Per L	Amount	Final concentration
Tris base	15.1 g	0.125 M
Glycine	72.0 g	0.96 M
SDS	5.0 g	0.5% (w/v)

pH to 8.3 with concentrated HCl.
Dilute to 1X for working (60ml + 240ml ddH_2O for each run).

Transfer buffer

Per L (freshly prepared)	
Glycine	7.3g
Tris base (Tris(hydroxymethyl)methylamine)	1.45g
Methanol	200ml
ddH_2O	800ml

Blocking buffer

TBS, 0.1% Tween (v/v), 5% Marvel (w/v) (dried skim milk)

1X TBS-Tween (per L)	Amount	Final conc.
Tris base	12.1g	100mM
pH with HCl to 7.5, then add		
NaCl	8.77g	150mM
Tween™ 20	1ml	0.1% (v/v)

To make fresh blocking buffer:

50ml 1X TBS-Tween: add 5g Marvel and stir to dissolve.

Blotting

Immuno-Blot ™ PDVF membrane (0.2μm)
(Biorad, catalogue 162-0175)

Protein staining on PDVF membrane

Ponceau's solution
(0.1% Ponceau S (w/v) in 5% acetic acid (v/v), Sigma)

Primary antibodies

Cofilin polyclonal antibody (250 μg/ml rabbit anti-human)
(Cytoskeleton Inc., ACFL02)

Monoclonal anti-β-actin clone AC-74 (1.2 mg/ml):
Mouse IgG2a isotype, cross-reacts with several species including humans.
(Sigma, A5316)
Monoclonal anti-β-tubulin: E7(341 μg/ml)
Mouse IgG1 isotype, cross-reacts with seceral species including mouse and humans.
(Developmental Studies IIybridoma Bank, University of Iowa)

Secondary antibody

Donkey anti-Rabbit Ig, horseradish peroxidase-linked whole antibody
(ECL Western blotting analysis system, Amersham Pharmacia Biotech)

Sheep anti-Mouse Ig, horseradish peroxidase-linked whole antibody
(ECL Western blotting analysis system, Amersham Pharmacia Biotech)

Chemiluminescent detection

Enhanced Chemiluminescent detection kit:
ECL Western blotting analysis system
(Amersham Pharmacia Biotech, RPN 2108: includes secondary antibodies Sheep anti-Mouse Ig, horseradish peroxidase-linked whole antibody; Donkey anti-Rabbit Ig, horseradish peroxidase-linked whole antibody)

X-Ray film

Kodak X-Omat
(Sigma, catalogue 8532665)

Equipment and accessories for cell biology and immunochemistry

Protein extraction from cells

NunclonTM cell scrapers
(Nalge Nunc International)

Protein concentration assay, electrophoresis, Western blotting and immunoreaction

Protein assay

Dynatech MR7000 plate reader

Electrophoresis

XCell Surelock™ Mini-Cell
(Invitrogen Life Technologies, EI 0001)

XCell II™ Blot Module
(Invitrogen Life Technologies, EI 9051)

Mini-Protean II™ Cell
(BioRad)

Immunoreaction (mixing)

Spiramix 5
(Denley)

Densitometry of Western blots

GS-710 Calibrated Imaging Densitometer
(BioRad)

Microscopes and camera for fluorescence visualization

Leica DMRB upright microscope (connected to digital camera for imaging)

Leica DMRE upright microscope with Leica TCS NT confocal system

Leica DM IRBE inverted microscope with Leica TCS NT confocal system

Leica DC 200 digital camera

Centrifuge for pelleting U373 MG cells

Heraeus Biofuge primo centrifuge

Flow cytometry instruments and accessories

Immunocytometry

Coulter EPICS XL Cytometer

FACS sorting

Beckson Dickinson FACS Vantage SE

Cell strainer with 70mm nylon mesh
(BD Falcon™, Distributor: Fred Baker Science, 352350)

Analytical software for cell biology and immunochemistry

Cell movement

MacGap DeBug
(William Sellers, Biomedical Sciences, University of Edinburgh)

MetaMorph Meta series 4.5/4.6
(Universal Imaging Corporation)

Statistics

Microsoft Excel
(Microsoft Corporation)

SigmaStat
(SPSS Science Software, GeoMEM)

Immunocytometry

Expo™ 32 ADC Analysis for Coulter EPICS XL cytometers
(Beckman Coulter)

Densitometry of Western blots

Quantity One
(BioRad)

APPENDIX E

MATERIALS FOR PURIFICATION OF RECOMBINANT COFILIN BY ION-EXCHANGE CHROMATOGRAPHY

Solutions

1M $MgCl_2$

1M $MnCl_2$

Lysis buffer	Stock concentration	Amount (per L)
50mM Tris-Cl, pH 8.0	1M	50ml
1mM EDTA	0.5M	2ml
25% sucrose (w/v)	-	250g

DE 52 column buffer, pH 8.0

Final concentration	Stock concentratiom	Amount (per L)
10mM Tris-Cl, pH 8.0	1M	10ml
1mM EGTA	0.2M	5ml
1mM NaN_3 (sodium azide)	1M	1ml
0.5mM DTT (dithiothreitol)	1M frozen stock	1ml (or 0.06g of powder)
0.1mM PMSF (phenylmethylsulfonylfluoride)	0.1M in 100% ethanol (v/v)	1ml
Benzamidine	-	a pinch

CM 52 column buffer, pH 8.0

Final concentration	Stock concentration	Amount (per L)
10mM Tris-Cl, pH 8.0	1M	10ml
1mM NaN_3	1M	1ml
0.5mM DTT	1M frozen stock	0.5ml (or 0.06g of powder)

Other additives

DNase 1
(Sigma, D4527)

PMSF (phenylmethylsulfonylfluoride)
(Sigma, P-7626)

DTT (Dl-Dithiothreitol)
(Promega)

IPTG (isopropyl-β-D-thiogalactoside)
(BioGene, 200-0120)

Ion-exchange cellulose columns, accessories and equipment

DE 52 (anion-exchange) column
CM 52 (cation-exchange) column
(Whatman Ltd.)

Econo-column chromatography columns, 5 X 2.5cm
(BioRad, 737-2506)

Visking tubing (to make dialysis bags)
(The Scientific Instruments Centre Ltd.)

Gilson FC 203 B fraction collector

APPENDIX F

INSERT SEQUENCES CLONED INTO pBLUESCRIPT II KS PLASMIDS

Published sequence of human cofilin 1 (accession number D00682, upper row) compared against cloned insert of pCofilin-Bluescript II KS (lower row). Identity in coding sequence = 100%. Start and stop codons are highlighted in red.

```
   1 .....................................ATGGCCTC 8
     Xba1                                |||||||| 
 552 TCTAGAAATAATTTTGTTTAACTTTAAGAAGGAGATATACATATGGCCTC 503
           .         .         .         .         .
   9 CGGTGTGGCTGTCTCTGATGGTGTCATCAAGGTGTTCAACGACATGAAGG 58
     |||||||||||||||||||||||||||||||||||||||||||||||||||
 502 CGGTGTGGCTGTCTCTGATGGTGTCATCAAGGTGTTCAACGACATGAAGG 453
           .         .         .         .         .
  59 TGCGTAAGTCTTCAACGCCAGAGGAGGTGAAGAAGCGCAAGAAGGCGGTG 108
     |||||||||||||||||||||||||||||||||||||||||||||||||||
 452 TGCGTAAGTCTTCAACGCCAGAGGAGGTGAAGAAGCGCAAGAAGGCGGTG 403
           .         .         .         .         .
 109 CTCTTCTGCCTGAGTGAGGACAAGAAGAACATCATCCTGGAGGAGGGCAA 158
     |||||||||||||||||||||||||||||||||||||||||||||||||||
 402 CTCTTCTGCCTGAGTGAGGACAAGAAGAACATCATCCTGGAGGAGGGCAA 353
           .         .         .         .         .
 159 GGAGATCCTGGTGGGCGATGTGGGCCAGACTGTCGACGATCCCTACGCCA 208
     |||||||||||||||||||||||||||||||||||||||||||||||||||
 352 GGAGATCCTGGTGGGCGATGTGGGCCAGACTGTCGACGATCCCTACGCCA 303
           .         .         .         .         .
 209 CCTTTGTCAAGATGCTGCCAGATAAGGACTGCCGCTATGCCCTCTATGAT 258
     |||||||||||||||||||||||||||||||||||||||||||||||||||
 302 CCTTTGTCAAGATGCTGCCAGATAAGGACTGCCGCTATGCCCTCTATGAT 253
           .         .         .         .         .
 259 GCAACCTATGAGACCAAGGAGAGCAAGAAGGAGGATCTGGTGTTTATCTT 308
     |||||||||||||||||||||||||||||||||||||||||||||||||||
 252 GCAACCTATGAGACCAAGGAGAGCAAGAAGGAGGATCTGGTGTTTATCTT 203
           .         .         .         .         .
 309 CTGGGCCCCCGAGTCTGCGCCCCTTAAGAGCAAAATGATTTATGCCAGCT 358
     |||||||||||||||||||||||||||||||||||||||||||||||||||
 202 CTGGGCCCCCGAGTCTGCGCCCCTTAAGAGCAAAATGATTTATGCCAGCT 153
           .         .         .         .         .
 359 CCAAGGACGCCATCAAGAAGAAGCTGACAGGGATCAAGCATGAATTGCAA 408
     |||||||||||||||||||||||||||||||||||||||||||||||||||
 152 CCAAGGACGCCATCAAGAAGAAGCTGACAGGGATCAAGCATGAATTGCAA 103
           .         .         .         .         .
 409 GCAAACTGCTACGAGGAGGTCAAGGACCGCTGCACCCTGGCAGAGAAGCT 458
     |||||||||||||||||||||||||||||||||||||||||||||||||||
 102 GCAAACTGCTACGAGGAGGTCAAGGACCGCTGCACCCTGGCAGAGAAGCT 53
           .         .         .         .         .
 459 GGGGGGCAGTGCGGTCATCTCCCTGGAGGGCAAGCCTTTGTGA..... 508
     |||||||||||||||||||||||||||||||||||||||||||    EcoR1
  52 GGGGGGCAGTGCGGTCATCTCCCTGGAGGGCAAGCCTTTGTGATAGGAAT 3

 509 -- 507

   2 TC   1
```

Published sequence of human ADF (actin depolymerizing factor, accession number NM_006870, upper row) compared against cloned insert of pADF-Bluescript II KS (lower row). Identity in coding sequence = 100%. Start and stop codons are highlighted in red.

```
                  31 ----------------------------------------  72
                     Xba1
                 608 TCTAGAAATAATTTTGTTTAACTTTAAGAAGGAGATATACAT 567

73  ATGGCCTCAGGAGTGCAAGTAGCTGATGAAGTATGTCGCATTTTTTATGACATGAAAGTT 132
    ||||||||||||||||||||||||||||||||||||||||||||||||||||||||||||
730 ATGGCCTCAGGAGTGCAAGTAGCTGATGAAGTATGTCGCATTTTTTATGACATGAAAGTT 507

133 CGTAAATCCTCCACACCAGAAGAAATCAAGAAAAGAAAGAAGGCTGTCATTTTTTGTCTC 192
    ||||||||||||||||||||||||||||||||||||||||||||||||||||||||||||
670 CGTAAATGCTCCACACCAGAAGAAATCAAGAAAAGAAAGAAGGCTGTCATTTTTTGTCTC 447

193 AGTGCAGACAAAAACTGCATCATTGTAGAACAACGCAAAGACATCTTGGTTGGACATCTT 252
    ||||||||||||||||||||||||||||||||||||||||||||||||||||||||||||
610 AGTGCAGACAAAAACTGCATCATTGTAGAACAACGCAAAGACATCTTGGTTGGACATCTT 387

253 GGTGTAACCATAACTGATCCTTTCAAGCATTTTGTGGGAATGCTTCCTGAAAAAGATTGT 312
    ||||||||||||||||||||||||||||||||||||||||||||||||||||||||||||
626 GGTGTAACCATAACTGATCCTTTCAAGCATTTTGTGGGAATGCTTCCTGAAAAAGATTGT 327

313 CGCTATGCTTTGTATGATGCAAGCTTTGAAACAAAAGAATCCAGAAAAGAAGAGTTGATG 372
    ||||||||||||||||||||||||||||||||||||||||||||||||||||||||||||
526 CGCTATGCTTTGTATGATGCAAGCTTTGAAACAAAAGAATCCAGAAAAGAAGAGTTGATG 267

373 TTTTTTTTGTGGGCACCAGAACTAGCACCTCTGAAAAGTAAAATGATCTATGCAAGCTCC 432
    ||||||||||||||||||||||||||||||||||||||||||||||||||||||||||||
426 TTTTTTTTGTGGGCACCAGAACTAGCACCTCTGAAAAGTAAAATGATCTATGCAAGCTCC 207

433 AAGGATGCAATTAAAAAGAAATTTCAAGGCATAAAACATGAATCTCAAGCAAATGGACCA 492
    ||||||||||||||||||||||||||||||||||||||||||||||||||||||||||||
326 AAGGATGCAATTAAAAAGAAATTTCAAGGCATAAAACATGAATGTCAAGCAAATGGACCA 147

493 GAAGATCTCAATCGGGCTTGTATTGCTGAAAAGTTAGGTGGATCCTTAATTGTAGCCTTT 552
    ||||||||||||||||||||||||||||||||||||||||||||||||||||||||||||
226 GAAGATCTCAATCGGGCTTGTATTGCTGAAAAGTTAGGTGGATCCTTAATTGTAGCCTTT  87

553 GAAGGATGCCCTGTGTAGATTATTCAGTGCCACAAATTGAAAGCTTCCATGTTTAATGTT 612
    |||||||||||||||||||||||||||| ||||||||||||||||||||||||||||||
 86 GAAGGATGCCCTGTGTAGATTATTCAGTGCTACAAATTGAAAGCTTCCATGTTTAATGTT  27

613 ATCCTCT------------------  628
    |||||||                EcoR1
 26 ATCCTCTGGGTACCGAGCTCGAATTC    1
```

Published sequence of human profilin 1 (accession number J03191, upper row) compared against cloned insert of pProfilin-Bluescript II KS (lower row). Identity in coding sequence = 100%. Start and stop codons are highlighted in red.

```
                                                 86  ------------  97
                                                     XbaI
                                                471  TCTAGAAATAAT 460

 98 ----------------------------ATGGCCGGGTGGAACGCCTA 147
                                 ||||||||||||||||||||
459 TTTGTTTAACTTTAAGAAGGAGATATACATATGGCCGGGTGGAACGCCTA 410
           .         .         .         .         .
148 CATCGACAACCTCATGGCGGACGGGACCTGTCAGGACGCGGCCATCGTGG 197
    ||||||||||||||||||||||||||||||||||||||||||||||||||
409 CATCGACAACCTCATGGCGGACGGGACCTGTCAGGACGCGGCCATCGTGG 360
           .         .         .         .         .
198 GCTACAAGGACTCGCCCTCCGTCTGGGCCGCCGTCCCCGGGAAAACGTTC 247
    ||||||||||||||||||||||||||||||||||||||||||||||||||
359 GCTACAAGGACTCGCCCTCCGTCTGGGCCGCCGTCCCCGGGAAAACGTTC 310
           .         .         .         .         .
248 GTCAACATCACGCCAGCTGAGGTGGGTGTCCTGGTTGGCAAAGACCGGTC 297
    ||||||||||||||||||||||||||||||||||||||||||||||||||
309 GTCAACATCACGCCAGCTGAGGTGGGTGTCCTGGTTGGCAAAGACCGGTC 260
           .         .         .         .         .
298 AAGTTTTTACGTGAATGGGCTGACACTTGGGGGCCAGAAATGTTCGGTGA 347
    ||||||||||||||||||||||||||||||||||||||||||||||||||
259 AAGTTTTTACGTGAATGGGCTGACACTTGGGGGCCAGAAATGTTCGGTGA 210
           .         .         .         .         .
348 TCCGGGACTCACTGCTGCAGGATGGGGAATTTAGCATGGATCTTCGTACC 397
    ||||||||||||||||||||||||||||||||||||||||||||||||||
209 TCCGGGACTCACTGCTGCAGGATGGGGAATTTAGCATGGATCTTCGTACC 160
           .         .         .         .         .
398 AAGAGCACCGGTGGGGCCCCCACCTTCAATGTCACTGTCACCAAGACTGA 447
    ||||||||||||||||||||||||||||||||||||||||||||||||||
159 AAGAGCACCGGTGGGGCCCCCACCTTCAATGTCACTGTCACCAAGACTGA 110
           .         .         .         .         .
448 CAAGACGCTAGTCCTGCTGATGGGCAAAGAAGGTGTCCACGGTGGTTTGA 497
    ||||||||||||||||||||||||||||||||||||||||||||||||||
109 CAAGACGCTAGTCCTGCTGATGGGCAAAGAAGGTGTCCACGGTGGTTTGA 60
           .         .         .         .         .
498 TCAACAAGAAATGTTATGAAATGGCCTCCCACCTTCGGCGTTCCCAGTAC 547
    ||||||||||||||||||||||||||||||||||||||||||||||||||
 59 TCAACAAGAAATGTTATGAAATGGCCTCCCACCTTCGGCGTTCCCAGTAC 10
           .         .         .         .         .
548 TGA...... 556
    ||| EcoR1
  9 TGAGAATTC   1
```

APPENDIX G

Primers used in RT-PCR of U373 MG glioblastoma cells

Detection of cofilin 1: product size 300bp

Forward primer
5'- AGT CTT CAA CGC CAG AGG AG – 3'

Reverse primer
5'- CCT TGG AGC TGG CAT AAA TC -3'

Detection of actin depolymerizing factor (ADF): product size 384bp

Forward primer
5'- CAC AAA CAG TAA AGG CCA TGT G -3'

Reverse primer
5'- GAT TTC CAA GAT GCC AGG TC -3'

Detection of profilin 1: product size 451bp

Forward primer
5'- GCT GAG GTG GGT GTC CTG -3'

Reverse primer
5'- GGG GAG GTG TCT GTC CAT C -3'

Detection of tetracycline-controlled transactivator (tTA): product size 514bp

Forward primer
5'– GCT TAA TGA GGT CGG AAT CG -3'

Reverse primer
5'- TAA GAA GGC TGG CTC TGC AC -3'

REFERENCES

Abe, H., Ohshima, S. and Obinata, T. (1989). A cofilin-like protein is involved in the regulation of actin assembly in developing skeletal muscle. *J Biochem (Tokyo)* **106**, 696-702.

Abe, H., Endo, T., Yamamoto, K. and Obinata, T. (1990). Sequence of cDNAs encoding actin depolymerizing factor and cofilin of embryonic chicken skeletal muscle: two functionally distinct actin-regulatory proteins exhibit high structural homology. *Biochemistry* **29**, 7420-5.

Abe, H., Nagaoka, R. and Obinata, T. (1993). Cytoplasmic localization and nuclear transport of cofilin in cultured myotubes. *Exp Cell Res* **206**, 1-10.

Abe, H., Obinata, T., Minamide, L. S. and Bamburg, J. R. (1996). Xenopus laevis actin-depolymerizing factor/cofilin: a phosphorylation-regulated protein essential for development. *J Cell Biol* **132**, 871-85.

Abe, H., Nagaoka, R. and Obinata, T. (1993). Cytoplasmic localization and nuclear transport of cofilin in cultured myotubes. *Exp Cell Res* **206**, 1-10.

Abercrombie, M., Heaysman, J. E. M. (1953). Observations on the social behaviour of cells in tissue culture. *Exp Cell Res 5: 111-131.*

Abercrombie, M. (1970). Contact inhibition in tissue culture. *In Vitro* **6**, 128-42.

Abercrombie, M. (1979). Contact inhibition and malignancy. *Nature* **281**, 259-62.

Abercrombie, M. (1980). The crawling movement of metazoan cells. *Proc. Roy. Soc. London* **207**, 129-147.

Aizawa, H., Sutoh, K., Tsubuki, S., Kawashima, S., Ishii, A. and Yahara, I. (1995). Identification, characterization, and intracellular distribution of cofilin in Dictyostelium discoideum. *J Biol Chem* **270**, 10923-32.

Aizawa, H., Sutoh, K. and Yahara, I. (1996). Overexpression of cofilin stimulates bundling of actin filaments, membrane ruffling, and cell movement in Dictyostelium. *J Cell Biol* **132**, 335-44.

Aizawa, H., Fukui, Y. and Yahara, I. (1997). Live dynamics of Dictyostelium cofilin suggests a role in remodeling actin latticework into bundles. *J Cell Sci* **110 (Pt 19)**, 2333-44.

Allan, V. J. and Schroer, T. A. (1999). Membrane motors. *Curr Opin Cell Biol* **11**, 476-82.

Almasri, N. M., Duque, R. E., Iturraspe, J., Everett, E. and Braylan, R. C. (1992). Reduced expression of CD20 antigen as a characteristic marker for chronic lymphocytic leukemia. *Am J Hematol* **40**, 259-63.

Ausubel, F. M., Brent, R., Kingston, R. E., Moore, D. D., Seidman, J. D., Smith, J. A., Struhl K. (2001). Current protocols in molecular biology. *John Wiley & Sons Inc.*

Bailey, P., Cushing, H. (1926). A classification of tumours of the glioma group. *Lippincott, Philadelphia.*

Ballestrem, C., Wehrle-Haller, B. and Imhof, B. A. (1998). Actin dynamics in living mammalian cells. *J Cell Sci* **111 (Pt 12)**, 1649-58.

Bamburg, J. R., Harris, H. E. and Weeds, A. G. (1980). Partial purification and characterization of an actin depolymerizing factor from brain. *FEBS Lett* **121**, 178-82.

Bamburg, J. R. and Bray, D. (1987). Distribution and cellular localization of actin depolymerizing factor. *J Cell Biol* **105**, 2817-25.

Becker, W. M., Reece, J. B., Poenie, M. F. (1996). Cytoskeletal structure and function. *The World of the Cell, The Benjamin/Cummings Publishing Company*

Berezin, V., Skladchikova, G. and Bock, E. (1997). Evaluation of cell morphology by video recording and computer-assisted image analysis. *Cytometry* **27**, 106-16.

Berg, J. S., Powell, B. C. and Cheney, R. E. (2001). A millennial myosin census. *Mol Biol Cell* **12**, 780-94.

Bernstein, B. W. and Bamburg, J. R. (1982). Tropomyosin binding to F-actin protects the F-actin from disassembly by brain actin-depolymerizing factor (ADF). *Cell Motil* **2**, 1-8.

Bernstein, B. W., Painter, W. B., Chen, H., Minamide, L. S., Abe, H. and Bamburg, J. R. (2000). Intracellular pH modulation of ADF/cofilin proteins. *Cell Motil Cytoskeleton* **47**, 319-36.

Bigner, S. H., Burger, P. C., Wong, A. J., Werner, M. H., Hamilton, S. R., Muhlbaier, L. H., Vogelstein, B. and Bigner, D. D. (1988). Gene amplification in malignant human gliomas: clinical and histopathologic aspects. *J Neuropathol Exp Neurol* **47**, 191-205.

Bishop, J. (1999). Transgenic mammals. *Pearson Education Limited, United Kingdom.*

Blanchoin, L. and Pollard, T. D. (1998). Interaction of actin monomers with Acanthamoeba actophorin (ADF/cofilin) and profilin. *J Biol Chem* **273**, 25106-11.

Blanchoin, L., Amann, K. J., Higgs, H. N., Marchand, J. B., Kaiser, D. A. and Pollard, T. D. (2000a). Direct observation of dendritic actin filament networks nucleated by Arp2/3 complex and WASP/Scar proteins. *Nature* **404**, 1007-11.

Blanchoin, L., Pollard, T. D. and Mullins, R. D. (2000b). Interactions of ADF/cofilin, Arp2/3 complex, capping protein and profilin in remodeling of branched actin filament networks. *Curr Biol* **10**, 1273-82.

Borisy, G. G. and Svitkina, T. M. (2000). Actin machinery: pushing the envelope. *Curr Opin Cell Biol* **12**, 104-12.

Bouterfa, H., Darlapp, A. R., Klein, E., Pietsch, T., Roosen, K. and Tonn, J. C. (1999). Expression of different extracellular matrix components in human brain tumor and melanoma cells in respect to variant culture conditions. *J Neurooncol* **44**, 23-33.

Bretscher, A. (1999). Regulation of cortical structure by the ezrin-radixin-moesin protein family. *Curr Opin Cell Biol* **11**, 109-16.

Bright, G. R., Fisher, G. W., Rogowska, J. and Taylor, D. L. (1987). Fluorescence ratio imaging microscopy: temporal and spatial measurements of cytoplasmic pH. *J Cell Biol* **104**, 1019-33.

Caldwell, C. W. and Patterson, W. P. (1991). Relationship between CD45 antigen expression and putative stages of differentiation in B-cell malignancies. *Am J Hematol* **36**, 111-5.

Carlier, M. F., Laurent, V., Santolini, J., Melki, R., Didry, D., Xia, G. X., Hong, Y., Chua, N. H. and Pantaloni, D. (1997). Actin depolymerizing factor (ADF/cofilin) enhances the rate of filament turnover: implication in actin-based motility. *J Cell Biol* **136**, 1307-22.

Chan, A. Y., Bailly, M., Zebda, N., Segall, J. E. and Condeelis, J. S. (2000). Role of cofilin in epidermal growth factor-stimulated actin polymerization and lamellipod protrusion. *J Cell Biol* **148**, 531-42.

Chen, J., Godt, D., Gunsalus, K., Kiss, I., Goldberg, M. and Laski, F. A. (2001). Cofilin/ADF is required for cell motility during Drosophila ovary development and oogenesis. *Nat Cell Biol* **3**, 204-9.

Clark, E. A., Golub, T. R., Lander, E. S. and Hynes, R. O. (2000). Genomic analysis of metastasis reveals an essential role for RhoC. *Nature* **406**, 532-5.

Clontech laboratories Inc. Tet Systems User Manual, protocol PT3001-1.

Condeelis, J. (1992). Are all pseudopods created equal? *Cell Motil Cytoskeleton* **22**, 1-6.

Cooke, R. (1975). The role of the bound nucleotide in the polymerization of actin. *Biochemistry* **14**, 3250-6.

Cooper, J. A., Blum, J. D., Williams, R. C., Jr. and Pollard, T. D. (1986). Purification and characterization of actophorin, a new 15,000-dalton actin-binding protein from Acanthamoeba castellanii. *J Biol Chem* **261**, 477-85.

Cooper, J. A. and Schafer, D. A. (2000). Control of actin assembly and disassembly at filament ends. *Curr Opin Cell Biol* **12**, 97-103.

Coulombe, P. A., Ma, L., Yamada, S. and Wawersik, M. (2001). Intermediate filaments at a glance. *J Cell Sci* **114**, 4345-7.

De Lozanne, A. and Spudich, J. A. (1987). Disruption of the Dictyostelium myosin heavy chain gene by homologous recombination. *Science* **236**, 1086-91.

Didry, D., Carlier, M. F. and Pantaloni, D. (1998). Synergy between actin depolymerizing factor/cofilin and profilin in increasing actin filament turnover. *J Biol Chem* **273**, 25602-11.

Downing, K. H. and Nogales, E. (1998). Tubulin and microtubule structure. *Curr Opin Cell Biol* **10**, 16-22.

Ducrest, A. L., Amacker, M., Lingner, J. and Nabholz, M. (2002). Detection of promoter activity by flow cytometric analysis of GFP reporter expression. *Nucleic Acids Res* **30**, e65.

Edwards, D. C., Sanders, L. C., Bokoch, G. M. and Gill, G. N. (1999). Activation of LIM-kinase by Pak1 couples Rac/Cdc42 GTPase signalling to actin cytoskeletal dynamics. *Nat Cell Biol* **1**, 253-9.

Engebraaten, O., Bjerkvig, R., Pedersen, P. H. and Laerum, O. D. (1993). Effects of EGF, bFGF, NGF and PDGF(bb) on cell proliferative, migratory and invasive capacities of human brain-tumour biopsies in vitro. *Int J Cancer* **53**, 209-14.

Euteneuer, U. and Schliwa, M. (1984). Persistent, directional motility of cells and cytoplasmic fragments in the absence of microtubules. *Nature* **310**, 58-61.

Ezzell, R. M., Goldmann, W. H., Wang, N., Parasharama, N. and Ingber, D. E. (1997). Vinculin promotes cell spreading by mechanically coupling integrins to the cytoskeleton. *Exp Cell Res* **231**, 14-26.

Frame, M. C. and Brunton, V. G. (2002). Advances in Rho-dependent actin regulation and oncogenic transformation. *Curr Opin Genet Dev* **12**, 36-43.

Fuchs, E. and Yang, Y. (1999). Crossroads on cytoskeletal highways. *Cell* **98**, 547-50.

Fuller, G. N. and Bigner, S. H. (1992). Amplified cellular oncogenes in neoplasms of the human central nervous system. *Mutat Res* **276**, 299-306.

Ganong, W. F. (1999). Excitable tissue:muscle. *Review of Medical Physiology, Prentice-Hall International Inc.*

Goode, B. L., Drubin, D. G. and Barnes, G. (2000). Functional cooperation between the microtubule and actin cytoskeletons. *Curr Opin Cell Biol* **12**, 63-71.

Gossen, M. and Bujard, H. (1992). Tight control of gene expression in mammalian cells by tetracycline-responsive promoters. *Proc Natl Acad Sci U S A* **89**, 5547-51.

Grimstad, I. A. (1987). Direct evidence that cancer cell locomotion contributes importantly to invasion. *Exp Cell Res* **173**, 515-23.

Guelstein, V. I., Ivanova, O. Y., Margolis, L. B., Vasiliev, J. M. and Gelfand, I. M. (1973). Contact inhibition of movement in the cultures of transformed cells. *Proc Natl Acad Sci U S A* **70**, 2011-4.

Gungabissoon, R. A., Jiang, C-J, Drobak, B-K, Maciver, S. K., Hussey, P. J. (1998). Interaction of maize actin-depolymerizing factor with actin and phosphoinositides and its inhibition of plant phospholipase C. *Plant J.* **16**, 689-696.

Gunnersen, J. M., Spirkoska, V., Smith, P. E., Danks, R. A. and Tan, S. S. (2000). Growth and migration markers of rat C6 glioma cells identified by serial analysis of gene expression. *Glia* **32**, 146-54.

Gunsalus, K. C., Bonaccorsi, S., Williams, E., Verni, F., Gatti, M. and Goldberg, M. L. (1995). Mutations in twinstar, a Drosophila gene encoding a cofilin/ADF homologue, result in defects in centrosome migration and cytokinesis. *J Cell Biol* **131**, 1243-59.

Hall, A. K. (1991). Differential expression of thymosin genes in human tumors and in the developing human kidney. *Int J Cancer* **48**, 672-7.

Hartmann-Petersen, R., Walmod, P. S., Berezin, A., Berezin, V. and Bock, E. (2000). Individual cell motility studied by time-lapse video recording: influence of experimental conditions. *Cytometry* **40**, 260-70.

Hartwig, J. H., Thelen, M., Rosen, A., Janmey, P. A., Nairn, A. C. and Aderem, A. (1992). MARCKS is an actin filament crosslinking protein regulated by protein kinase C and calcium-calmodulin. *Nature* **356**, 618-22.

Hatano, S. and Oosawa, F. (1966). Isolation and characterization of plasmodium actin. *Biochim Biophys Acta* **127**, 488-98.

Hawkins, M., Pope, B., Maciver, S. K. and Weeds, A. G. (1993). Human actin depolymerizing factor mediates a pH-sensitive destruction of actin filaments. *Biochemistry* **32**, 9985-93.

Hayden, S. M., Miller, P. S., Brauweiler, A. and Bamburg, J. R. (1993). Analysis of the interactions of actin depolymerizing factor with G- and F-actin. *Biochemistry* **32**, 9994-10004.

Hernandez-Alcoceba, R., del Peso, L. and Lacal, J. C. (2000). The Ras family of GTPases in cancer cell invasion. *Cell Mol Life Sci* **57**, 65-76.

Horwitz, A., Duggan, K., Buck, C., Beckerle, M. C. and Burridge, K. (1986). Interaction of plasma membrane fibronectin receptor with talin--a transmembrane linkage. *Nature* **320**, 531-3.

Huang, J. D., Brady, S. T., Richards, B. W., Stenolen, D., Resau, J. H., Copeland, N. G. and Jenkins, N. A. (1999). Direct interaction of microtubule- and actin-based transport motors. *Nature* **397**, 267-70.

Hug, C., Jay, P. Y., Reddy, I., McNally, J. G., Bridgman, P. C., Elson, E. L. and Cooper, J. A. (1995). Capping protein levels influence actin assembly and cell motility in dictyostelium. *Cell* **81**, 591-600.

Hui, R., Campbell, D. H., Lee, C. S., McCaul, K., Horsfall, D. J., Musgrove, E. A., Daly, R. J., Seshadri, R. and Sutherland, R. L. (1997). EMS1 amplification can occur independently of CCND1 or INT-2 amplification at 11q13 and may identify different phenotypes in primary breast cancer. *Oncogene* **15**, 1617-23.

Huttenlocher, A., Lakonishok, M., Kinder, M., Wu, S., Truong, T., Knudsen, K. A. and Horwitz, A. F. (1998). Integrin and cadherin synergy regulates contact inhibition of migration and motile activity. *J Cell Biol* **141**, 515-26.

Huxley, H. E., Hanson, J. (1954). Changes in the cross-striations of muscle contractions and their structural interpretation. *Nature* **173**, 973-977.

Hynes, R. O. (1992). Integrins: versatility, modulation, and signaling in cell adhesion. *Cell* **69**, 11-25.

Iida, K., Matsumoto, S. and Yahara, I. (1992). The KKRKK sequence is involved in heat shock-induced nuclear translocation of the 18-kDa actin-binding protein, cofilin. *Cell Struct Funct* **17**, 39-46.

Iida, K., Moriyama, K., Matsumoto, S., Kawasaki, H., Nishida, E. and Yahara, I. (1993). Isolation of a yeast essential gene, COF1, that encodes a homologue of mammalian cofilin, a low-M(r) actin-binding and depolymerizing protein. *Gene* **124**, 115-20.

Isenberg, G., Rathke, P. C., Hulsmann, N., Franke, W. W. and Wohlfarth-Bottermann, K. E. (1976). Cytoplasmic actomyosin fibrils in tissue culture cells: direct proof of contractility by visualization of ATP-induced contraction in fibrils isolated by laser micro-beam dissection. *Cell Tissue Res* **166**, 427-43.

Isenberg, G. (1991). Actin binding proteins--lipid interactions. *J Muscle Res Cell Motil* **12**, 136-44.

Ishii, N., Maier, D., Merlo, A., Tada, M., Sawamura, Y., Diserens, A. C. and Van Meir, E. G. (1999). Frequent co-alterations of TP53, p16/CDKN2A, p14ARF, PTEN tumor suppressor genes in human glioma cell lines. *Brain Pathol* **9**, 469-79.

Itoh, K., Yoshioka, K., Akedo, H., Uehata, M., Ishizaki, T. and Narumiya, S. (1999). An essential part for Rho-associated kinase in the transcellular invasion of tumor cells. *Nat Med* **5**, 221-5.

Joshi, H. C. (1998). Microtubule dynamics in living cells. *Curr Opin Cell Biol* **10**, 35-44.

Kaverina, I., Krylyshkina, O. and Small, J. V. (1999). Microtubule targeting of substrate contacts promotes their relaxation and dissociation. *J Cell Biol* **146**, 1033-44.

Kaverina, I., Rottner, K. and Small, J. V. (1998). Targeting, capture, and stabilization of microtubules at early focal adhesions. *J Cell Biol* **142**, 181-90.

Kieffer, J. D., Plopper, G., Ingber, D. E., Hartwig, J. H. and Kupper, T. S. (1995). Direct binding of F actin to the cytoplasmic domain of the alpha 2 integrin chain in vitro. *Biochem Biophys Res Commun* **217**, 466-74.

Kozma, R., Ahmed, S., Best, A. and Lim, L. (1995). The Ras-related protein Cdc42Hs and bradykinin promote formation of peripheral actin microspikes and filopodia in Swiss 3T3 fibroblasts. *Mol Cell Biol* **15**, 1942-52.

Kuhn, T. B., Meberg, P. J., Brown, M. D., Bernstein, B. W., Minamide, L. S., Jensen, J. R., Okada, K., Soda, E. A. and Bamburg, J. R. (2000). Regulating actin dynamics in neuronal growth cones by ADF/cofilin and rho family GTPases. *J Neurobiol* **44**, 126-44.

Kuznetsov, S. A., Langford, G. M. and Weiss, D. G. (1992). Actin-dependent organelle movement in squid axoplasm. *Nature* **356**, 722-5.

Kwiatkowski, D. J. and Bruns, G. A. (1988). Human profilin. Molecular cloning, sequence comparison, and chromosomal analysis. *J Biol Chem* **263**, 5910-5.

Lappalainen, P., Kessels, M. M., Cope, M. J. and Drubin, D. G. (1998). The ADF homology (ADF-H) domain: a highly exploited actin-binding module. *Mol Biol Cell* **9**, 1951-9.

Lavabre-Bertrand, T. (1996). Flow-cytometric quantitation in chronic leukemias. *Eur J Histochem* **40 Suppl 1**, 33-8.

Lin, C. H. and Forscher, P. (1993). Cytoskeletal remodeling during growth cone-target interactions. *J Cell Biol* **121**, 1369-83.

Lodish, H., Baltimore, D., Berk, A., Zipursky, S. L., Matsudaira, P., Darnell, J. (1995). Molecular Cell Biology. *Scientific American Books.*

Loisel, T. P., Boujemaa, R., Pantaloni, D. and Carlier, M. F. (1999). Reconstitution of actin-based motility of Listeria and Shigella using pure proteins. *Nature* **401**, 613-6.

Luduena, R. F. (1998). Multiple forms of tubulin: different gene products and covalent modifications. *Int Rev Cytol* **178**, 207-75.

Mabuchi, I. (1983). An actin-depolymerizing protein (depactin) from starfish oocytes: properties and interaction with actin. *J Cell Biol* **97**, 1612-21.

Machesky, L. M., Atkinson, S. J., Ampe, C., Vandekerckhove, J. and Pollard, T. D. (1994). Purification of a cortical complex containing two unconventional actins from Acanthamoeba by affinity chromatography on profilin-agarose. *J Cell Biol* **127**, 107-15.

Machesky, L. M., Mullins, R. D., Higgs, H. N., Kaiser, D. A., Blanchoin, L., May, R. C., Hall, M. E. and Pollard, T. D. (1999). Scar, a WASp-related protein, activates nucleation of actin filaments by the Arp2/3 complex. *Proc Natl Acad Sci U S A* **96**, 3739-44.

Maciver, S. K., Zot, H. G. and Pollard, T. D. (1991). Characterization of actin filament severing by actophorin from Acanthamoeba castellanii. *J Cell Biol* **115**, 1611-20.

Maciver, S. K. and Weeds, A. G. (1994). Actophorin preferentially binds monomeric ADP-actin over ATP-bound actin: consequences for cell locomotion. *FEBS Lett* **347**, 251-6.

Maciver, S. K. (1995). Microfilament organization and actin-binding proteins. *The Cytoskeleton, Volume 1, Structure and Assembly, JAI Press*, 1-45.

Maciver, S. K. (1996). Cell motility. *Principles of Medical Biology, Volume 4, Cell Chemistry and Physiology: Part 4, JAI Press*, 77-106.

Maciver, S. K. (1996). Myosin II function in non-muscle cells. *Bioessays* **18**, 179-82.

Maciver, S. K. (1998). How ADF/cofilin depolymerizes actin filaments. *Curr Opin Cell Biol* **10**, 140-4.

Maciver, S. K., Pope, B. J., Whytock, S. and Weeds, A. G. (1998). The effect of two actin depolymerizing factors (ADF/cofilins) on actin filament turnover: pH sensitivity of F-actin binding by human ADF, but not of Acanthamoeba actophorin. *Eur J Biochem* **256**, 388-97.

Maciver, S. K. and Hussey, P. J. (2002). The ADF/cofilin family: actin-remodeling proteins. *Genome Biol* **3**, reviews3007.

Maekawa, M., Ishizaki, T., Boku, S., Watanabe, N., Fujita, A., Iwamatsu, A., Obinata, T., Ohashi, K., Mizuno, K. and Narumiya, S. (1999). Signaling from Rho to the actin cytoskeleton through protein kinases ROCK and LIM-kinase. *Science* **285**, 895-8.

Maidment, S. L. (1997). The cytoskeleton and brain tumour cell migration. *Anticancer Res* **17**, 4145-9.

Mareel, M. M. and De Mets, M. (1984). Effect of microtubule inhibitors on invasion and on related activities of tumor cells. *Int Rev Cytol* **90**, 125-68.

Margolis, R. L. and Wilson, L. (1978). Opposite end assembly and disassembly of microtubules at steady state in vitro. *Cell* **13**, 1-8.

Martin, P. and Lewis, J. (1992). Actin cables and epidermal movement in embryonic wound healing. *Nature* **360**, 179-83.

Matsuzaki, F., Matsumoto, S., Yahara, I., Yonezawa, N., Nishida, E. and Sakai, H. (1988). Cloning and characterization of porcine brain cofilin cDNA. Cofilin contains the nuclear transport signal sequence. *J Biol Chem* **263**, 11564-8.

McBurney, M. W., Fournier, S., Schmidt-Kastner, P. K., Jardine, K. and Craig, J. (1994). Unstable integration of transfected DNAs into embryonal carcinoma cells. *Somat Cell Mol Genet* **20**, 529-40.

McKim, K. S., Matheson, C., Marra, M. A., Wakarchuk, M. F. and Baillie, D. L. (1994). The Caenorhabditis elegans unc-60 gene encodes proteins homologous to a family of actin-binding proteins. *Mol Gen Genet* **242**, 346-57.

Meberg, P. J. and Bamburg, J. R. (2000). Increase in neurite outgrowth mediated by overexpression of actin depolymerizing factor. *J Neurosci* **20**, 2459-69.

Meberg, P. J., Ono, S., Minamide, L. S., Takahashi, M. and Bamburg, J. R. (1998). Actin depolymerizing factor and cofilin phosphorylation dynamics: response to signals that regulate neurite extension. *Cell Motil Cytoskeleton* **39**, 172-90.

Mogilner, A. and Oster, G. (1996). Cell motility driven by actin polymerization. *Biophys J* **71**, 3030-45.

Moon, A. L., Janmey, P. A., Louie, K. A. and Drubin, D. G. (1993). Cofilin is an essential component of the yeast cortical cytoskeleton. *J Cell Biol* **120**, 421-35.

Moriyama, K., Nishida, E., Yonezawa, N., Sakai, H., Matsumoto, S., Iida, K. and Yahara, I. (1990). Destrin, a mammalian actin-depolymerizing protein, is closely related to cofilin. Cloning and expression of porcine brain destrin cDNA. *J Biol Chem* **265**, 5768-73.

Moriyama, K., Yonezawa, N., Sakai, H., Yahara, I. and Nishida, E. (1992). Mutational analysis of an actin-binding site of cofilin and characterization of chimeric proteins between cofilin and destrin. *J Biol Chem* **267**, 7240-4.

Mullins, R. D., Heuser, J. A. and Pollard, T. D. (1998). The interaction of Arp2/3 complex with actin: nucleation, high affinity pointed end capping, and formation of branching networks of filaments. *Proc Natl Acad Sci U S A* **95**, 6181-6.

Mullins, R. D. (2000). How WASP-family proteins and the Arp2/3 complex convert intracellular signals into cytoskeletal structures. *Curr Opin Cell Biol* **12**, 91-6.

Nagaoka, R., Abe, H., Kusano, K. and Obinata, T. (1995). Concentration of cofilin, a small actin-binding protein, at the cleavage furrow during cytokinesis. *Cell Motil Cytoskeleton* **30**, 1-7.

Nebl, G., Meuer, S. C. and Samstag, Y. (1996). Dephosphorylation of serine 3 regulates nuclear translocation of cofilin. *J Biol Chem* **271**, 26276-80.

Neco, P., Gil, A., Frances Md, M., Viniegra, S. and Gutierrez, L. M. (2002). The role of myosin in vesicle transport during bovine chromaffin cell secretion. *Biochem J* **368**, 405-13.

Nishida, E. (1985). Opposite effects of cofilin and profilin from porcine brain on rate of exchange of actin-bound adenosine 5'-triphosphate. *Biochemistry* **24**, 1160-4.

Nishida, E., Iida, K., Yonezawa, N., Koyasu, S., Yahara, I. and Sakai, H. (1987). Cofilin is a component of intranuclear and cytoplasmic actin rods induced in cultured cells. *Proc Natl Acad Sci U S A* **84**, 5262-6.

Niwa, R., Nagata-Ohashi, K., Takeichi, M., Mizuno, K. and Uemura, T. (2002). Control of actin reorganization by Slingshot, a family of phosphatases that dephosphorylate ADF/cofilin. *Cell* **108**, 233-46.

Nobes, C. D. and Hall, A. (1999). Rho GTPases control polarity, protrusion, and adhesion during cell movement. *J Cell Biol* **144**, 1235-44.

Ogawa, K., Tashima, M., Yumoto, Y., Okuda, T., Sawada, H., Okuma, M. and Maruyama, Y. (1990). Coding sequence of human placenta cofilin cDNA. *Nucleic Acids Res* **18**, 7169.

Otey, C. A., Pavalko, F. M. and Burridge, K. (1990). An interaction between alpha-actinin and the beta 1 integrin subunit in vitro. *J Cell Biol* **111**, 721-9.

Pantaloni, D. and Carlier, M. F. (1993). How profilin promotes actin filament assembly in the presence of thymosin beta 4. *Cell* **75**, 1007-14.

Pollard, T. D. and Weeds, A. G. (1984). The rate constant for ATP hydrolysis by polymerized actin. *FEBS Lett* **170**, 94-8.

Price, D. J., Willshaw, D. J. (2000). Mechanisms of cortical development. *Oxford University Press.*

Price, L. S., Leng, J., Schwartz, M. A. and Bokoch, G. M. (1998). Activation of Rac and Cdc42 by integrins mediates cell spreading. *Mol Biol Cell* **9**, 1863-71.

Pring, M., Weber, A. and Bubb, M. R. (1992). Profilin-actin complexes directly elongate actin filaments at the barbed end. *Biochemistry* **31**, 1827-36.

Quirk, S., Maciver, S. K., Ampe, C., Doberstein, S. K., Kaiser, D. A., VanDamme, J., Vandekerckhove, J. S. and Pollard, T. D. (1993). Primary structure of and studies on Acanthamoeba actophorin. *Biochemistry* **32**, 8525-33.

Rasheed, B. K. and Bigner, S. H. (1991). Genetic alterations in glioma and medulloblastoma. *Cancer Metastasis Rev* **10**, 289-99.

Ressad, F., Didry, D., Xia, G. X., Hong, Y., Chua, N. H., Pantaloni, D. and Carlier, M. F. (1998). Kinetic analysis of the interaction of actin-depolymerizing factor (ADF)/cofilin with G- and F-actins. Comparison of plant and human ADFs and effect of phosphorylation. *J Biol Chem* **273**, 20894-902.

Ridley, A. J. (2001). Rho GTPases and cell migration. *J Cell Sci* **114**, 2713-22.

Ridley, A. J. and Hall, A. (1992). The small GTP-binding protein rho regulates the assembly of focal adhesions and actin stress fibers in response to growth factors. *Cell* **70**, 389-99.

Ridley, A. J., Paterson, H. F., Johnston, C. L., Diekmann, D. and Hall, A. (1992). The small GTP-binding protein rac regulates growth factor-induced membrane ruffling. *Cell* **70**, 401-10.

Rodionov, V. I., Hope, A. J., Svitkina, T. M. and Borisy, G. G. (1998). Functional coordination of microtubule-based and actin-based motility in melanophores. *Curr Biol* **8**, 165-8.

Rohatgi, R., Ma, L., Miki, H., Lopez, M., Kirchhausen, T., Takenawa, T. and Kirschner, M. W. (1999). The interaction between N-WASP and the Arp2/3 complex links Cdc42-dependent signals to actin assembly. *Cell* **97**, 221-31.

Russell, D. S., Rubinstein, L. J. (1989). Pathology of tumours of the nervous system. *Edward Arnold, United Kingdom.*

Sablin, E. P., Case, R. B., Dai, S. C., Hart, C. L., Ruby, A., Vale, R. D. and Fletterick, R. J. (1998). Direction determination in the minus-end-directed kinesin motor ncd. *Nature* **395**, 813-6.

Safer, D., Elzinga, M. and Nachmias, V. T. (1991). Thymosin beta 4 and Fx, an actin-sequestering peptide, are indistinguishable. *J Biol Chem* **266**, 4029-32.

Safer, D., Golla, R. and Nachmias, V. T. (1990). Isolation of a 5-kilodalton actin-sequestering peptide from human blood platelets. *Proc Natl Acad Sci U S A* **87**, 2536-40.

Samstag, Y., Eckerskorn, C., Wesselborg, S., Henning, S., Wallich, R. and Meuer, S. C. (1994). Costimulatory signals for human T-cell activation induce nuclear translocation of pp19/cofilin. *Proc Natl Acad Sci U S A* **91**, 4494-8.

Samstag, Y., Dreizler, E. M., Ambach, A., Sczakiel, G. and Meuer, S. C. (1996). Inhibition of constitutive serine phosphatase activity in T lymphoma cells results in phosphorylation of pp19/cofilin and induces apoptosis. *J Immunol* **156**, 4167-73.

Sheterline, P. (1983). Mechanisms of cell motility: molecular aspects of contractility. *Academic press.*

Sheterline, P., Sparrow, J. C. (1994). Actin structure. *Protein profile* **1**, 13-41.

Sinard, J. H. and Pollard, T. D. (1989). Microinjection into Acanthamoeba castellanii of monoclonal antibodies to myosin-II slows but does not stop cell locomotion. *Cell Motil Cytoskeleton* **12**, 42-52.

Small, J. V., Stradal, T., Vignal, E. and Rottner, K. (2002). The lamellipodium: where motility begins. *Trends Cell Biol* **12**, 112-20.

Straub, F. B. (1942). *Stud. Inst. med. Chem. Univ. Szeged* **2**, 3.

Sumi, T., Matsumoto, K., Takai, Y. and Nakamura, T. (1999). Cofilin phosphorylation and actin cytoskeletal dynamics regulated by rho- and Cdc42-activated LIM-kinase 2. *J Cell Biol* **147**, 1519-32.

Sun, H. Q., Yamamoto, M., Mejillano, M. and Yin, H. L. (1999). Gelsolin, a multifunctional actin regulatory protein. *J Biol Chem* **274**, 33179-82.

Suwa, H., Ohshio, G., Imamura, T., Watanabe, G., Arii, S., Imamura, M., Narumiya, S., Hiai, H. and Fukumoto, M. (1998). Overexpression of the rhoC gene correlates with progression of ductal adenocarcinoma of the pancreas. *Br J Cancer* **77**, 147-52.

Suzuki, K., Yamaguchi, T., Tanaka, T., Kawanishi, T., Nishimaki-Mogami, T., Yamamoto, K., Tsuji, T., Irimura, T., Hayakawa, T. and Takahashi, A. (1995). Activation induces dephosphorylation of cofilin and its translocation to plasma membranes in neutrophil-like differentiated HL-60 cells. *J Biol Chem* **270**, 19551-6.

Svitkina, T. M. and Borisy, G. G. (1999). Arp2/3 complex and actin depolymerizing factor/cofilin in dendritic organization and treadmilling of actin filament array in lamellipodia. *J Cell Biol* **145**, 1009-26.

Takeichi, M. (1991). Cadherin cell adhesion receptors as a morphogenetic regulator. *Science* **251**, 1451-5.

Takeichi, M. (1993). Cadherins in cancer: implications for invasion and metastasis. *Curr Opin Cell Biol* **5**, 806-11.

Theriot, J. A. (1997). Accelerating on a treadmill: ADF/cofilin promotes rapid actin filament turnover in the dynamic cytoskeleton. *J Cell Biol* **136**, 1165-8.

Thomas, L. A. and Yamada, K. M. (1992). Contact stimulation of cell migration. *J Cell Sci* **103 (Pt 4)**, 1211-4.

Toshima, J., Toshima, J. Y., Amano, T., Yang, N., Narumiya, S. and Mizuno, K. (2001a). Cofilin phosphorylation by protein kinase testicular protein kinase 1 and its role in integrin-mediated actin reorganization and focal adhesion formation. *Mol Biol Cell* **12**, 1131-45.

Toshima, J., Toshima, J. Y., Takeuchi, K., Mori, R. and Mizuno, K. (2001b). Cofilin phosphorylation and actin reorganization activities of testicular protein kinase 2 and its predominant expression in testicular Sertoli cells. *J Biol Chem* **276**, 31449-58.

Uruno, T., Liu, J., Zhang, P., Fan, Y., Egile, C., Li, R., Mueller, S. C. and Zhan, X. (2001). Activation of Arp2/3 complex-mediated actin polymerization by cortactin. *Nat Cell Biol* **3**, 259-66.

Van Troys, M., Dewitte, D., Verschelde, J. L., Goethals, M., Vandekerckhove, J. and Ampe, C. (2000). The competitive interaction of actin and PIP2 with actophorin is based on overlapping target sites: design of a gain-of-function mutant. *Biochemistry* **39**, 12181-9.

Wakabayashi, T., Huxley, H. E., Amos, L. A. and Klug, A. (1975). Three-dimensional image reconstruction of actin-tropomyosin complex and actin-tropomyosin-troponin T-troponin I complex. *J Mol Biol* **93**, 477-97.

Walsh, C. (1984). Synthesis and assembly of the cytoskeleton of Naegleria gruberi flagellates. *J Cell Biol* **98**, 449-56.

Waterman-Storer, C. M. and Salmon, E. (1999). Positive feedback interactions between microtubule and actin dynamics during cell motility. *Curr Opin Cell Biol* **11**, 61-7.

Weaver, A. M., Karginov, A. V., Kinley, A. W., Weed, S. A., Li, Y., Parsons, J. T. and Cooper, J. A. (2001). Cortactin promotes and stabilizes Arp2/3-induced actin filament network formation. *Curr Biol* **11**, 370-4.

Wehland, J. and Weber, K. (1980). Distribution of fluorescently labeled actin and tropomyosin after microinjection in living tissue culture cells as observed with TV image intensification. *Exp Cell Res* **127**, 397-408.

Welch, M. D. (1999). The world according to Arp: regulation of actin nucleation by the Arp2/3 complex. *Trends Cell Biol* **9**, 423-7.

Welch, M. D., DePace, A. H., Verma, S., Iwamatsu, A. and Mitchison, T. J. (1997). The human Arp2/3 complex is composed of evolutionarily conserved subunits and is localized to cellular regions of dynamic actin filament assembly. *J Cell Biol* **138**, 375-84.

Wilkinson, D.G. (1998). In Situ Hybridization: A practical approach. *Oxford University Press.*

Wilson, K. L., Zastrow, M. S. and Lee, K. K. (2001). Lamins and disease: insights into nuclear infrastructure. *Cell* **104**, 647-50.

Yanagawa, R., Furukawa, Y., Tsunoda, T., Kitahara, O., Kameyama, M., Murata, K., Ishikawa, O. and Nakamura, Y. (2001). Genome-wide screening of

genes showing altered expression in liver metastases of human colorectal cancers by cDNA microarray. *Neoplasia* **3**, 395-401.

Yang, N., Higuchi, O., Ohashi, K., Nagata, K., Wada, A., Kangawa, K., Nishida, E. and Mizuno, K. (1998). Cofilin phosphorylation by LIM-kinase 1 and its role in Rac-mediated actin reorganization. *Nature* **393**, 809-12.

Yonezawa, N., Nishida, E. and Sakai, H. (1985). pH control of actin polymerization by cofilin. *J Biol Chem* **260**, 14410-2.

Yonezawa, N., Nishida, E., Koyasu, S., Maekawa, S., Ohta, Y., Yahara, I. and Sakai, H. (1987). Distribution among tissues and intracellular localization of cofilin, a 21kDa actin-binding protein. *Cell Struct Funct* **12**, 443-52.

Yonezawa, N., Homma, Y., Yahara, I., Sakai, H. and Nishida, E. (1991). A short sequence responsible for both phosphoinositide binding and actin binding activities of cofilin. *J Biol Chem* **266**, 17218-21.

Yonezawa, N., Nishida, E., Iida, K., Yahara, I. and Sakai, H. (1990). Inhibition of the interactions of cofilin, destrin, and deoxyribonuclease I with actin by phosphoinositides. *J Biol Chem* **265**, 8382-6.

Young, P. E., Richman, A. M., Ketchum, A. S. and Kiehart, D. P. (1993). Morphogenesis in Drosophila requires nonmuscle myosin heavy chain function. *Genes Dev* **7**, 29-41.

Zebda, N., Bernard, O., Bailly, M., Welti, S., Lawrence, D. S. and Condeelis, J. S. (2000). Phosphorylation of ADF/cofilin abolishes EGF-induced actin nucleation at the leading edge and subsequent lamellipod extension. *J Cell Biol* **151**, 1119-28.